CHARACTERIZATION AND IMMUNOMODULATION OF THE INFANT IMMUNE RESPONSE TO RESPIRATORY SYNCYTIAL VIRUS

by

Katherine Marie Eichinger

Bachelor of Science, University of Michigan, 2004

Master of Science, University of Michigan, 2008

Doctor of Pharmacy, University of Michigan, 2009

Submitted to the Graduate Faculty of

School of Pharmacy in partial fulfillment

of the requirements for the degree of

Doctor of Philosophy

University of Pittsburgh

2019

UNIVERSITY OF PITTSBURGH

SCHOOL OF PHARMACY, CLINICAL AND TRANSLATIONAL SCIENCE GRADUATE PROGRAM

This dissertation was presented

by

Katherine Marie Eichinger

It was defended on

March 18, 2019

and approved by

Robert B. Gibbs, Ph.D., Professor, Pharmaceutical Sciences

Philip E. Empey, PharmD, Ph.D., Assistant Professor, Pharmacy and Therapeutics

John F. Alcorn, Ph.D., Associate Professor, Department of Pediatrics

R. Stokes Peebles, Jr., M.D., Professor, Department of Medicine

Dissertation Advisor: **Kerry M. Empey, PharmD, Ph.D.**, Assistant Professor, Pharmacy and Therapeutics

CHARACTERIZATION AND IMMUNOMODULATION OF THE INFANT IMMUNE RESPONSE TO RESPIRATORY SYNCYTIAL VIRUS

Katherine Marie Eichinger, PharmD, Ph.D.

University of Pittsburgh, 2019

Respiratory syncytial virus (RSV) is a single-stranded, negative sense RNA virus that is the leading viral cause of serious respiratory tract infections in infants and young children worldwide. The virus is highly infectious and a majority of children are infected during their first RSV season. Decades of research has provided critical information detailing mechanisms of viral pathogenesis and host immune subversion however, a regretfully incomplete understanding of the infant RSV immune response still exists. Generally, infants are heavily reliant on innate immunity to respond to pathogens and they divert normal, pro-inflammatory responses to allergy-inducing innate immune responses, making them particularly vulnerable to intracellular pathogens like RSV. While this diversion can protect infants from over-exuberant immunopathology, allergic responses can potentiate mucus production and airway obstruction acutely as well as increase the predisposition towards atopy and asthma later in life. Clinical observations have noted an inverse relationship between increased pro-inflammatory RSV immune responses and reduced RSV disease severity in children, but the acute and long-term effects of pro-inflammatory immunomodulation during primary, infant RSV infection are not well understood. In this dissertation, we hypothesized that pro-inflammatory immunomodulation during primary infant RSV infection alters acute and memory RSV immune responses.

We demonstrate that both innate and adaptive infant RSV immunity is less robust when compared to adult responses. Alveolar macrophages (AMs), critical innate immune cells, were less activated and had fewer differentially expressed genes (DEGs) in response to RSV infection than

adults. Administration of the pro-inflammatory cytokine, interferon gamma (IFNγ), during primary RSV infection reduced viral titers, increased AM activation, and increased RSV-specific $CD8^+$ T cell responses. Not only did IFNγ treatment have an effect on primary RSV immune responses, it also increased RSV-specific memory $CD8^+$ T cell responses, reduced airway hyperresponsiveness, and contributed to signals of innate trained immunity upon secondary infection. We also demonstrated that passive immunization with RSV-neutralizing maternal antibodies resulted in heightened innate immune activation and increased mucus production. Our data suggests that immunomodulation of the primary infant RSV immune response can have beneficial acute and long-term effects but must be properly balanced to avoid immunopathology.

TABLE OF CONTENTS

LIST OF TABLES

LIST OF FIGURES

LIST OF ABBREVIATIONS

RSV	Respiratory Syncytial Virus
IFNγ	Interferon gamma
AMs	Alveolar Macrophages
DEGs	Differentially Expressed Genes
DC	Dendritic Cells
Th1	T helper type 1
Th2	T helper type 2
TLR	Toll-Like Receptor
APC	Antigen Presenting Cell
FI-RSV	Formalin-Inactivated RSV
FBS	Fetal Bovine Serum
P/S	Penicillin/Streptomycin
PBS	Phosphate Buffered Saline
H&E	Hematoxylin & Eosin
RSV L19	RSV Line 19
BSA	Bovine Serum Albumin
DPSPX	1,3-Dipropyl-8-(P-Sulfophenyl)Xanthine
CLip	Clodronate Liposomes
CFSE	Carboxyfluorescein succinimidyl Ester
HBSS	Hank's Balanced Salt Solution

IFNγR1KO	IFNγ Receptor 1 Knock Out
WT	Wild Type
i.n.	Intranasal
FACS	Fluorescence Activated Cell Sorting
BAL	Bronchoalveolar Lavage
MSLN	Mediastinal Lymph Node
URL	Upper Right Lung
LD	Lung Digest
MNC	Mononuclear Cells
CPE	Cytopathic Effect
Pfu	Plaque Forming Units
PND	Post-Natal Day
ml	Milliliter
mcl	Microliter
mcg	Microgram
ng	Nanogram
μM	Micromolar
mM	Millimolar
gm	gram
DPI	Days Post-Infection
TUNEL	Terminal deoxynucleotidyl transferase dUTP Nick End Labeling
PAS	Periodic Acid-Schiff
FW	First Wash

AUC	Area Under the Curve
i.m.	Intramuscular
RT	Room Temperature
nm	nanometer
OD	Optical Density
ANOVA	Analysis of Variance
LRTI	Lower Respiratory Tract Infection
AEC	Airway Epithelial Cells
MHCII	Major Histocompatibility Complex II
SR-A	Scavenger Receptor-A (CD204)
MR	Mannose Receptor (CD206)
MRT	Mean Residence Time
Cpk	Peak Concentration
FSC	Forward Scatter
SSC	Side Scatter
NK	Natural Killer
1^0	Primary
2^0	Secondary
MFI	Mean/Median Fluorescence Intensity
VED	Vaccine Enhanced Disease
AHR	Airway Hyperresponsiveness

ACKNOWLEDGEMENTS

The pursuit of a Ph.D. is a lengthy, and at times exhausting process. My Ph.D. journey has been supported by a number of wonderful people that I would like to recognize and to whom I would like to dedicate this dissertation.

First, I have valued the support and encouragement of my advisor, Dr. Kerry Empey. You have always nurtured my development as an independent scientist and supported my research objectives even when they have diverged from your own. I admire your dedication to the lab while always maintaining your children as your first priority.

Secondly, satisfaction in my personal and professional lives dramatically improved when Jessica Kosanovich joined the lab three and a half years ago. It is hard to imagine a better or closer working relationship and I hope/wish I never have to.

Lastly, I would not have been able to complete this program without the support of my family. I want to thank my parents for providing me with a balanced perspective on life and fostering a strong sense of independence from an early age. Both my parents and in-laws helped care for my children when our two career household went in different directions. My children inspired me to work harder and also kept me humble. Finally, none of what I accomplished would have been possible without my husband, Dan. You are a wonderful husband and father and work tirelessly for more equal justice in this world. Your sense of humor kept me laughing in times of despair and I am grateful for you every day.

1.0 INTRODUCTION

Since the discovery of RSV in the late 1950's, it was quickly recognized as the most important viral cause of severe respiratory tract infections in infants and children worldwide. Decades of research have given us a more complete understanding of RSV pathogenesis but most of the data generated from preclinical RSV studies have relied on adult animal models. Our lab has worked extensively to characterize RSV pathogenesis using an infant model of RSV infection (1) to better identify age-specific therapeutic opportunities. Data in this dissertation continues the work in characterizing infant RSV immune responses as well as investigates two therapeutic immunomodulatory agents; IFNγ and anti-RSV maternal antibodies. Evidence from the studies detailed in the following chapters will demonstrate that infant RSV immune responses are dramatically different from those of adults and that immunomodulation of primary infant RSV results in acute and long-term changes in RSV immunity.

1.1.1 Viral structure and function

RSV is a member of the Paramyxoviridae family of viruses, which includes viruses responsible for measles, mumps, and a number of viruses causing respiratory tract infections (2). There are animal versions of RSV, suggesting that as the virus evolved it jumped between species, but there is no animal reservoir for human RSV (3). The virus is a non-segmented, negative-sense, single-

stranded, enveloped RNA virus that has 10 genes that encode 11 proteins. Approximately half of RSV's proteins are involved in the nucleocapsid structure and/or RNA synthesis, including the N, L, P, M2-1, and M2-2 proteins (4). The encapsidation of genomic RNA, as well as, the positive-sense replicative intermediate, is performed by the nucleocapsid N protein. The large L protein and P phosphoprotein are the major polymerase subunit and co-factor in RNA synthesis, respectively (3-5). M2 proteins are involved in transcription and maintaining the balance between transcription and RNA replication (3), with the M2-1 protein being essential for viral viability (6).

Two non-structural proteins, NS1 and NS2, are small nonessential proteins that modulate the host immune response to RSV infection. These accessory proteins act as virulence factors for the virus and have been shown to alter the host immune response in a number of ways. NS1 and NS2 are known to antagonize the type I and III interferon responses, and inhibit type I interferon receptor signaling (7-13). The proteins have also demonstrated the ability to inhibit apoptosis, allowing the virus to continue to replicate within airway epithelial cells (14). Additional effects of these accessory proteins include, decreased maturation of dendritic cells (DCs), skewed T cell responses, and decreased nuclear factor kappa-light-chain-enhancer of activated B cells (NF-κB) activation (13, 15-17).

The four remaining viral proteins associate with the lipid bilayer and form the viral envelope. Viron morphogenesis is influenced by the M matrix protein, which lines the inner envelope surface. The small hydrophobic SH proteins are transmembrane surface glycoproteins, while the heavily glycosylated G and F proteins are the two major protective antigens eliciting neutralization (4). Although RSV has a single serotype, it has two subgroups, A and B, which are distinguished primarily by variations in the G protein. The G protein is critical for infection and plays a major role in viral attachment (18). Interestingly, this protein is also expressed in a secreted

form that acts as an antigen decoy and inhibits the antibody-mediated effects of innate leukocytes bearing Fc receptors (19, 20). The G protein has also been found to reduce respiratory rates through the induction of substance P (21), which may be a factor in apneic episodes that can occur in infants with severe RSV bronchiolitis. Finally, the fusion F protein is the surface glycoprotein that directs viral penetration through membrane fusion and mediates the formation of syncytia by directing the fusion of an infected cell with neighboring cells (3).

The F protein is unique in that it is a major target of vaccine development because its sequence is highly conserved between RSV subgroups and it is required for viral entry (22). Recent atomic structure analyses of the F protein have demonstrated that it exists in two distinct conformations, pre-fusion and post-fusion (23-25). Mediation of viral-cell membrane fusion requires an irreversible transition from the metastable pre-F to a stable post-F conformation. While pre- and post-F have unique shapes, they share approximately 50% of their surface area and two antigenic sites (II and IV) that are moderately sensitive to neutralization. On the surface unique to pre-F, at least three highly neutralization sensitive antigenic sites have been reported (Ø, III, and V), with site Ø having the highest neutralization potential (22). The neutralizing activity of antibodies in the sera of naturally RSV infected individuals (> 7 years of age) are primarily derived from pre-F specific antibodies (26). Therefore, effective neutralization of RSV requires that RSV F-specific antibodies must recognize and interrupt pre-F prior to the conformational change to its post-F structure (27).

1.1.2 Epidemiology, clinical symptoms, pathogenesis

In 1956, RSV was isolated from a laboratory chimpanzee with symptoms of a cold and subsequently determined to be of human origin (4). Since the time of its discovery, RSV was

quickly recognized as the leading viral cause of serious respiratory tract disease in the pediatric population. Recently, global RSV burden has been estimated to cause 33 million annual, acute lower respiratory tract infections, resulting in 3.2 million hospital admissions, and approximately 60,000 in-hospital deaths in children (< 5 years). Infants (< 6 months of age) accounted for nearly half of all hospitalizations and in-hospital deaths (28). Overall estimates of annual RSV mortality could be as high as 120,000.

The risk of severe RSV disease increases according to factors that are known to compromise an individual's ability to control a respiratory infection, including the following: young age (<6 months of age), premature birth (< 35 week gestation), bronchopulmonary dysplasia, congenital heart disease, immunodeficiency or immunosuppression, narrow airways, low birth weight, and old age (3, 29). While these factors play an important role in the development of severe disease, the overwhelming majority (80%) of children hospitalized for severe RSV were previously healthy (30).

In the United States, RSV infections typically begin in November and end in May with both A and B strains circulating concurrently (31). Although the two strains maintain a high degree of antigenic relatedness, epidemics usually involve multiple circulating strains and the strains may alternate in dominance every 1 or 2 years (3). This alternation is thought to play a role in the potential for RSV to re-infect its hosts, but strain differences do not seem to play a role in disease variability. RSV is a highly contagious human pathogen, rivaling the measles virus (3). It is readily introduced and spreads with ease in settings with close contact such as, daycares, hospitals, nursing homes, and within families. For example, natural introduction of RSV into a daycare setting resulted in infection of more than 90% of infants and children (32) and approximately 50% of

families became infected when RSV was introduced during an outbreak, usually by an older child (33).

Primary RSV infection is thought to almost always be symptomatic. Inoculation typically occurs via large particle aerosol or through direct contact via the eyes or nose. Over the next 4 to 5 days, the virus replicates in the nasopharynx, which can be followed by spreading to the lower respiratory tract (31). Symptoms of upper airway disease include rhinorrhea, cough, otitis media, and low grade fever. The most common form of lower airway disease is bronchiolitis, characterized by airway resistance, air trapping, and wheezing, but can also include pneumonia and croup (3, 31, 34).

RSV produces a very superficial infection and is restricted to the ciliated cells of the small bronchioles and type 1 pneumocytes in the alveoli. Compared to the rapid and extensive cytopathology induced by influenza infection, RSV infection has demonstrated a minimally cytopathic effect within the first 48 hours (35, 36). However, as the infection progresses and through the action of NS2, infected columnar, ciliated epithelial cells become rounded and are extruded from intact epithelium (37). Extruded epithelial cells mix with increased mucus and infiltrating immune cells in the lumen of an edematous airway to create an occlusion. Airway obstructions produce many of the clinical characteristics of bronchiolitis mentioned previously. Histologically, evidence of recovery begins in a matter of days but reconstitution of sloughed, ciliated epithelial cells takes at least two weeks. Complete restoration of epithelial integrity takes four to eight weeks, correlating with clinical symptoms of prolonged coughing, wheezing, and altered pulmonary function (31, 38). Approximately half of infants and children hospitalized with severe RSV have subsequent episodes of wheezing, asthma, and decreased lung function well into early adolescence (39, 40). Pre-clinical (41) and clinical data (42) have supported the association

between severe RSV infection, elevated concentrations of Th2 and Th17 cytokines, and the development of recurrent wheeze or asthma. Prevention of RSV through the administration of palivizumab in otherwise healthy preterm infants during RSV season significantly reduced the number of wheezing days in the first year of life, but had no effect on the incidence of asthma later in childhood (43, 44). This likely indicates that the association between RSV infection and increased risk of asthma continues well past infancy when children are at highest risk of severe RSV disease.

1.1.3 Characteristics of infant immunity

RSV has been primarily recognized as a problematic virus for children, as it infects individuals at an earlier age with greater consequences than other respiratory viruses. Rhinovirus is another respiratory virus common in the first year of life and has been associated with wheezing, but much less commonly infects infants less than six months of age (45). In contrast, the peak age of RSV hospitalization occurs at 2 months of age (3). The very young age of severe RSV increases the impact of the infectious process, as younger infants are less resilient to the effects of respiratory illnesses due to the narrow diameter of their airway, making them more susceptible to obstruction.

In addition to the anatomical vulnerabilities of the infant airway, infants mount biased immune responses to pathogens like RSV that set in motion poor immunological memory that likely contributes to recurrent RSV infections throughout life. In utero, the fetus is an allograft of their mother, so pro-inflammatory/T helper type 1 (Th1) cytokine responses must be avoided/limited to reduce the risk of rejection, resulting in abortion and/or pre-term delivery (46). This risk of fetal rejection is likely the reason why fetal immune systems are heavily biased towards T helper type 2 (Th2) cytokine responses (47). Lack of Th1 cytokine production in response to

stimulus was originally thought to be due to an impairment of neonatal immunity, but production of certain cytokines (IL-6, IL-10, IL-23, etc.) by innate immune cells in response to stimuli sometimes exceeded that of adults (48, 49). However, this bias away from Th1 polarizing cytokines leaves neonates vulnerable to intracellular pathogens and compromises their responses to vaccination.

In utero, infants have very limited antigen exposure required to induce adaptive immunity, thereby making infants heavily reliant on the innate immune system for protection from infections. One mechanism of pathogen recognition involves toll-like receptors (TLRs), whereby components of microbes are recognized by innate immune cells, stimulating anti-microbial defenses. Many neonatal TLR responses from antigen presenting cells (APCs), like macrophages and dendritic cells, are altered when compared to adult responses. These age-dependent changes may be due to differences in TLR expression or because of altered cytokine responses (50, 51). Generally, infant APCs have reduced Th1 cytokine responses following TLR stimulation and instead favor production of Th2 and Th17 cytokines (**Table 1.1**). Although RSV stimulates TLR4, TLR2, and the intracellular sensors, retinoic acid-induced gene I (RIG-I) and TLR3 (52-56), infants have reduced levels of IL-12, IL-18, and IFNγ in response to infection (57). Other studies have demonstrated qualitative and quantitative defects in neonatal DC responses that subsequently lead to compromised $CD8^+$ T cell function (58). Epigenetic studies have begun to shed light on a mechanism behind the propensity of infant APCs to respond to stimuli with a Th2 bias. Hypomethylation of cytokine loci contributes to the expression of cytokine genes, while hypermethylation can silence other cytokine genes. The Th2 locus in $CD4^+$ T cells is

hypomethylated in both human and murine infants compared to adults (59, 60), which correlates with increased Th2 cytokine responses in infants.

Table 1.1 Cytokine responses of the newborn

Cytokine	Relative expression in neonates	General function
TNFα	↓	Pro-inflammatory; Th1-cell response
IFNα	↓	Antiviral; influences vaccine responses
IFNγ	↓	Activates macrophages; ↑ IL-12; Th1-cell response
IL-12	↓	Promotes growth and differentiation of T cells and stimulates NK cells; Th1-cell response
IL-1β	↓	Fever; acute-phase response
IL-6	↑	Acute-phase response; inhibits tissue neutrophilia; inhibits T regulatory (Tregs) cells and promotes Th17 development
IL-8	↑	Neutrophil chemoattractant
IL-10	↑	Anti-inflammatory; inhibits TNFα, IL-1, and IFNγ production
IL-23	↑	Promotes Th17 development

***Adapted from its original form**: Levy O. Innate immunity of the newborn: basic mechanisms and clinical correlates. Nature reviews Immunology. 2007;7(5):379-90.*

Innate immunity provides the critical link between non-specific pathogen recognition and activation of adaptive immunity, which offers targeted pathogen-specific immunity. The ability to strike the right balance in overcoming Th2 biases and activating Th1 innate responses plays an important role in the differentiation of naïve T cells, which are critical in the clearance of RSV (61). While there is some evidence to suggest that robust cytotoxic $CD8^+$ T cells responses can lead to immunopathology (62), other studies have demonstrated the importance of $CD8^+$ T cells in ameliorating Th2-related pathology and affiliated eosinophil recruitment (63-65). Age at primary infection is critical in the establishment of memory T cell responses as evidenced by infant, primary RSV infections resulting in Th2 memory T cell development accompanied by eosinophilia (66). In fact, infection at a young age can divert the normal anti-inflammatory role of T regulatory

cells (Tregs) into promoting Th2 responses that lead to asthma (41). Additionally, T cells that recently emigrated from the thymus, termed recent thymic emigrants (RTEs), are present in a high frequency in the periphery of human infants (67) and infant mice (68). RTEs are impaired in the acquisition of Th1 functionality making infants vulnerable to intracellular pathogens (67).

Antibodies are an additional correlate of protection against RSV infection but protection from infection is usually short-lived. Maternal anti-RSV antibodies can offer neonates some protection but maternal antibody levels are highly variable and largely dependent on the time since last RSV exposure. Maternal antibodies can also further complicate the generation of active immunity in infants because of their role in epitope blocking and other immunosuppressive effects (69). Generally, infant antibody responses have compromised efficacy because of a shorter half-life, higher IgG1/IgG2a ratio, a delayed onset, and are of lower affinity than adult antibodies (70). Elicitation of antibody production is also reduced in infants because of delayed germinal center maturation (71).

1.1.4 State of therapy/prevention

Currently, severe RSV infections are treated with supportive care as there is no effective treatment. Ribavirin is the only drug licensed to treat patients with severe RSV infection but due to unproven effectiveness and teratogenicity, it is not a part of routine clinical use. Infants at high-risk of severe disease can receive passive immunoprophylaxis during the RSV season through monthly injections of the RSV-neutralizing monoclonal antibody, palivizumab (Synagis). Prophylaxis with palivizumab reduces RSV-related hospitalization by 55% (72) but is costly and is only approved for use in high-risk infants. The limited utility of palivizumab emphasizes the importance of more universal approaches, including vaccination.

In the 1960s, a formalin inactivated RSV vaccine (FI-RSV) that was combined with the adjuvant alum was tested in children. In the following RSV season, 80% of FI-RSV immunized children were hospitalized with severe, vaccine enhanced RSV disease, resulting in the deaths of two toddlers (73). The failure of the FI-RSV vaccine hampered RSV vaccine development for 40 years, but as researchers investigated the mechanisms behind FI-RSV immunopathology and with the discovery of highly neutralization sensitive epitopes on RSV pre-F, progress towards a RSV vaccine has been made. There are currently a number of RSV vaccine approaches that span pre-clinical testing to Phase III clinical trials (74). Direct infant RSV immunization has been challenging because of biased/immature neonatal immune responses (75), the risk of vaccine-enhanced disease (73, 76), and the short time frame between birth and first RSV exposure. An alternative to direct infant vaccination is maternal immunization, which can produce high levels of neutralizing antibodies in mothers that are subsequently transferred to their offspring. A maternal vaccination approach is being tested by Novavax in Phase III clinical trials and being pursued by a number of other entities, including preclinical testing performed by our lab and discussed in **Chapter 6**.

In addition to new vaccine approaches and monoclonal antibodies undergoing preclinical or clinical testing, there are a number of antivirals being developed. The four types of RSV antivirals under development include: immunoglobulins, nucleoside analogues, small interfering RNAs (siRNA)-interference (anti-sense), and fusion inhibitors (77). All of the treatments are administered orally or through inhalation but all are therapies given once an infection has already been established. Their effectiveness is dependent on administration early in infection, which limits their utility based on the fact that most people present to healthcare providers at a time when viral replication has peaked (78).

In summary, the infant immune response must perform a delicate balancing act. On one hand, infants must learn to recognize and become tolerant of commensal microorganisms that play critical roles in maintaining homeostasis. On the other hand, they must learn to identify pathogenic organisms and develop an immune response that can eliminate the organism while preventing immunopathology that may compromise further development of organ systems, such as the lungs. As researchers, we must develop a deep understanding of, not only baseline age-dependent differences in immunity, but also age-specific host-pathogen interactions. Recognition of RSV as a leading cause of morbidity in the *very young* has come easily in a clinical sense, but research into RSV pathogenesis as well as, host-pathogen interaction studies have been less willing to adopt "infant-centric" models. By recognizing and understanding age-dependent RSV immune responses, we may be able to better identify therapeutic opportunities without disrupting the delicate balancing act between eliminating pathogens and preventing immunopathology.

2.0 MATERIALS AND METHODS

2.1 MATERIALS

2.1.1 Cell culture and reagents

The immortalized human epithelial HEp-2 cell line was purchased from American Type Culture Collection (ATCC, Catalog number: ATCC CCL-23) and cultured in MEM Earles (Life Technologies, Catalog number: 11095098) supplemented with 10% fetal bovine serum (FBS; Atlanta Biologicals, Catalog number: S12450), 5,000 U penicillin/streptomycin (P/S, Fisher Scientific, Catalog number: 30-002-CI), and amphotericin B 125mcg (Fungizone, Life Technologies, Catalog number: 15290018). HEp-2 cells were washed with 1X phosphate buffered saline (PBS, Fisher Scientific, Catalog number: BW17517Q) and harvested with 0.25% trypsin EDTA (Life Technologies, Catalog number: 25200056).

The immortalized human lung epithelial A549 cell line was purchased from ATCC (Catalog number: ATCC CCL-185) and cultured in DMEM (Fisher Scientific, Catalog number: BW12604Q) supplemented with 10% FBS, 5,000 U P/S, and 2mM L-glutamine (Fisher Scientific, Catalog number: MT25005CI). A549 cells were grown in flasks, washed with 1X PBS, and harvested with trypsin.

2.1.2 Viral strains

Line 19 RSV (RSV L19) subtype A virus was used exclusively in our studies and was provided by Dr. Martin Moore (originally at Emory University, Atlanta, GA; now at Meissa Vaccines, San Francisco, CA).

2.1.3 Cytokines and other pulmonary treatments

Recombinant murine interferon gamma (IFNγ; Peprotech, Catalog number: 315-05) was reconstituted in PBS containing carrier protein (0.1% bovine serum albumin (BSA)). Recombinant human IFNγ (Life Technologies, Catalog number: PHC4031) was reconstituted in PBS containing carrier protein (0.1% BSA). The pan-adenosine receptor antagonist 1,3-Dipropyl-8-(P-Sulfophenyl)Xanthine (DPSPX) was reconstituted in PBS (Sigma Aldrich, Catalog number: A022). Clodronate liposomes (CLip) were acquired from Liposoma B.V. (The Netherlands, Catalog number: C-005). Lyophilized carboxyfluorescein succinimidyl ester (CFSE) was prepared by dissolving the contents of the vial in dimethyl sulfoxide (DMSO, VWR, Catalog number: EM-2951) to a concentration of 5mM. The solution was further diluted to a concentration of 1μM using Hank's Balanced Salt Solution (HBSS, Fisher Scientific, Catalog number: SH30268LS).

2.1.4 Animals

Mice were maintained under pathogen-free conditions at the University of Pittsburgh Division of Laboratory Animal Resources (Pittsburgh, PA) and handled according to University of Pittsburgh

Institutional Animal Care and Use Committee approved protocols. For most experiments pathogen-free 6-10 week old Balb/c mice (The Jackson Laboratory, Bar Harbor, ME) were purchased and used experimentally or bred to obtain timed pregnancies. Timed pregnancies were obtained by co-housing female mice for 5-7 days to synchronize estrus and then were bred (1:1) for a minimum of 3 days. Some studies used IFNγ receptor-1 knock out mice (IFNγR1KO, The Jackson Laboratory) which were either on a Balb/c or C57BL6 background. Wild-type (WT) C57BL6 mice (The Jackson Laboratory) were used as controls in experiments that used IFNγR1KO mice on a C57BL6 background. Animals were anesthetized with isoflurane (Henry Schein, Catalog number: 50033) for intranasal (i.n.) infections and treatments.

2.1.5 RNA isolation

RNA was isolated from fluorescence-activated cell sorting (FACS) using the MagMAX-96 Total RNA Isolation Kit (Fisher Scientific, Catalog number: AM1830).

2.1.6 Flow cytometry materials and antibodies

Bronchoalveolar lavage (BAL) cells were collected via washes with HBSS + EDTA (30μM, Invitrogen, Catalog number: 15575-020). Mediastinal lymph nodes (MSLN) were collected in HBSS. Lung cells (URL, LD) used for flow cytometry were isolated following collection in RPMI 1640 media (Life Technologies, Catalog number: 11875093) supplemented with 3% FBS and enzyme treated with collagenase A (1mg/mL, Sigma Aldrich, C9891). Red blood cells were eliminated from all tissue types using ACK (ammonium chloride potassium) solution (Fisher Scientific, Catalog number: A1049201).

BAL and lung cells analyzed for intracellular cytokine production by innate immune cells were resuspended in 0% RPMI (RPMI 1640 media, HEPES (25mM, Fisher Scientific, Catalog number: 155630), L-glutamine (Mediatech, Catalog number: MT25005CI), 5,000U P/S, 50μM β-mercaptoethanol (Sigma Aldrich, Catalog number: M6250)) supplemented with 10% FBS and brefeldin A (Biolegend, Catalog number: 420601). BAL and lung cells analyzed for intracellular cytokine production by T cells were resuspended in 0% RPMI supplemented with 10% FBS and purified anti-mouse CD28 (Biolegend, Catalog number: 102101) and placed in a plate coated with purified anti-mouse CD3ε (Biolegend, Catalog number: 100301). Following CD3/CD28 stimulation, T cells were re-stimulated in 0% RPMI supplemented with 10% FBS, phorbol 12-myristrate 13-acetate (PMA, Sigma Aldrich, Catalog number: P8139-1MG), and ionomycin (Sigma Aldrich, Catalog number: I0634).

Cells were typically fixed prior to analysis (one exception: alveolar macrophages isolated for RNA sequencing) and one of the following agents were used: 1% paraformaldehyde (Alfa Aesar, Catalog number: 43368), BD Cytofix (BD Biosciences, Catalog number: 554655), Biolegend True Nuclear Fixative (Biolegend, Catalog number: 424401), or FoxP3/Transcription Staining Buffer Fixative (eBioscience, Catalog number: 00-5523-00). Note: If intracellular cell staining occurred then the permeabilization buffer from the respective kit (listed previously) was used.

The antibodies and isotype controls used for flow cytometry are listed in **Table 2.1**. Cells were resuspended prior to flow cytometry in staining buffer (PBA: 1X PBS, 0.1% BSA, 0.02% sodium azide). Samples were run on a BD LSRFortessa or BD LSR II managed by the University of Pittsburgh United Flow Core or Children's Hospital of Pittsburgh Rangos Research Center Flow

Cytometry Core Laboratory. Data was analyzed using FlowJo V10 software (FLOWJO, LLC, OR).

Table 2.1. Murine flow cytometry antibodies

Antibodies for surface antigens	Clone	Company	Antibodies for intracellular antigens	Clone	Company
Siglec F	E50-2440	BD Biosciences	CD206	C068C2	Biolegend
F4/80	T45-2342	BD Biosciences	Tbet	4B10	Biolegend
CD200R	OX-110	Biolegend	GATA3	16E10A23	Biolegend
CD11c	HL3	BD Biosciences	IL-5	TRFK5	Biolegend
CD11b	M1/70	BD Biosciences	TNFα	MP6-XT22	Biolegend
Ly6G	1A8	Biolegend	IL-4	11B11	Biolegend
MHCII	AMS-32.1	BD Biosciences	IFNγ	XMG1.2	Biolegend
CD80	16-10A1	Biolegend	Ki-67	B56	BD Biosciences
CD86	GL1	BD Biosciences	Isotype Controls	Clone	Company
CD204 (SR-A)	REA148	Miltenyi	Mouse IgG1	MOPC-21	Biolegend
CD103	2E7	Biolegend	Mouse IgG2b	MPC-11	Biolegend
CD27	LG.3A10	BD Biosciences	Rat IgG1	R3-34	BD Biosciences
CD73	TY/11.8	Biolegend	Rat IgG1	RTK2071	Biolegend
TCRβ	H57-597	Biolegend	Mouse IgG1	X40	BD Biosciences
CD4	GK1.5	BD Biosciences			
CD8	53-6.7	BD Biosciences			
CD44	IM7	BD Biosciences			
CD62L	MEL-14	Biolegend			
CD25	PC61	BD Biosciences			
KLRG1	2F1	BD Biosciences			
CD127 (IL-7Rα)	A7R34	Biolegend			
CD19	6D5	Biolegend			
CD16/32	2.4G2	BD Biosciences			
RSV F_{85-93} MHCI pentamer	H-2kd KYKNAVTEL	Proimmune			

2.1.7 Monocyte isolation

Blood samples were diluted (1:1) with PBS supplemented with 2% FBS. Mononuclear cells (MNCs) were enriched through the use of the density gradient medium, Lymphoprep (STEMCELL, Catalog number: 07801) and SepMate-50 tubes (STEMCELL, Catalog number: 85450). Enriched MNCs were resuspended in RPMI 1640 media supplemented with 10% FBS, 1% P/S, and 1% L-glutamine (10% MDM media). The EasySep Human Monocyte Isolation Kit (STEMCELL, Catalog number: 19359) was used to isolate monocytes using an EasySep Magnet (STEMCELL, Catalog number: 18000). The antibodies used to determine monocyte purity are listed in **Table 2.2**. Enriched monocytes were differentiated into macrophages with 10% MDM media supplemented with recombinant, human GM-CSF (Peprotech, Catalog number: 300-03-100UG).

Table 2.2 Human flow cytometry antibodies

Antibodies for surface antigens	Clone	Company
CD14	367107	Biolegend
CD16	3G8	Biolegend
HLA-DR	L243	Biolegend
CD36	5-271	Biolegend
CD11b	M1/70	Biolegend
Antibodies for intracellular antigens	**Clone**	**Company**
CD68	Y1/82A	Biolegend

2.1.8 RSV neutralizing and RSV-specific antibodies

Serum was collected in Gel-Z Serum Separator Tubes (Sarstedt, Catalog number: 41.1500.005). Purified RSV L19 was adhered to high-binding microtiter plate (Fisher Scientific, Catalog number: 14245153) in binding buffer (Na2CO3, NaHCO3, diH2O). The plate was blocked with blocking buffer (3% BSA; 3% bovine serum albumin in PBS). Primary and secondary antibodies used for the RSV neutralization assay and the RSV-specific IgG subtype analysis are listed in **Table 2.3**. TMB substrate (ThermoFisher Scientific, Catalog number: PI34021) was added and color was allowed to develop before being stopped with 1M sulfuric acid (Sigma Aldrich, Catalog number: 35276-1L). The optical density was read at 450 nm using the ELx800™ Plate Reader (BioTek, VT).

Table 2.3 Antibodies for neutralizing and RSV-specific antibody assays

	Antibody	Dilution	Company
RSV Neutralizing Antibody Assay	Anti-RSV polyclonal (1^{o})	1:4000	Abcam
	Goat anti-mouse IgG-HRP (2^{o})	1:4000	BioRad
RSV-specific IgG subtype Antibody Assay	Goat anti-mouse IgG2a-HRP	1:2500	Abcam
	Goat anti-mouse IgG1-HRP	1:5000	Abcam

2.1.9 Cytokine measurements

Cytokine measurements from blood, lung tissue, or BAL were performed using the Bio-Plex Pro™ Mouse Cytokine 23-plex Assay (BioRad, Catalog number: m60009rdpd) or the Th1/Th2 8-plex

Assay (BioRad, Catalog number: M6000003J7), per manufacturer's protocol or as outlined in the following methods. Plates were read using a Luminex® 200 Total System machine (Luminex Corp, Austin, TX) located and maintained by the lab of Dr. John Alcorn at Rangos Research Facility at Children's Hospital of Pittsburgh.

2.2 METHODS

2.2.1 RSV propagation and purification

RSV L19 was passed through four rounds of plaque purification for generation of master stocks; working stocks were propagated in HEp-2 cells. Briefly, working stocks were created by growing flasks of HEp-2 cells to 80% confluency, removing all but 3mls of media and infecting with 1ml of RSV L19 master stock for 1 hour on a rocker at 37° C. After incubation, the cells were supplemented with additional media and monitored for cytopathic effect (CPE; 80-90%), which occurred in approximately 36-48 hours. Once the desired CPE was reached, the cells were scraped and the entire contents of the flask harvested and then sonicated. Following centrifugation to remove cellular debris, aliquots of virus were quickly frozen in a dry ice/2-propanol (Fisher Scientific, Catalog number: A426P4) bath.

Purified RSV L19 was used in RSV-specific ELISA assays detailed below. It was prepared by growing HEp-2 cells to 80% confluency, which were then washed twice with PBS. Then 6mls of OptiMEM (Life Technologies, Catalog number: 31985070) supplemented with 2% FBS was added to the flask. Master stock RSV L19 was then added to the flask and incubated on a rocker for 2 hours. Following incubation, additional 2% FBS-OptiMEM was added to the flask and the

flask was monitored for CPE. Similar to the working stock, cells were scraped and sonicated when there was 80-90% CPE. However, the viral solution was centrifuged in Amicon Ultra-15 centrifugal filter tubes (Millipore, Catalog number: UFC910024) until 1ml of viral retentate remained and was aliquoted. Purified RSV L19 was flash frozen in liquid nitrogen.

2.2.2 RSV infections and intranasal treatments

Balb/c (WT and IFNγR1KO) or C57BL/6 mice (WT and IFNγR1KO) were purchased from The Jackson Laboratory (Bar Harbor, ME) at 6-8 weeks of age and bred in-house, as previously described (1) or used experimentally. Mice were infected i.n. with 5×10^5 plaque forming units (pfu) of RSV L19 per gram of body weight at post-natal day (PND) 2-7 (infants, ~1.5×10^6pfu in 10mcl) or 6-10 weeks of age (adults, ~10^7pfu in 100mcl) under isoflurane anesthesia. Recombinant-murine IFNγ (16ng/gm or 60ng/gm) was administered i.n. to PND 2-7 (or 6-10 week old C57BL/6 IFNγR1KO mice, where indicated) on 1, 3, and 5 days post-infection (DPI).

To deplete AMs, clodronate liposomes (CLip) (5mcl/gm of 5mg/ml suspension) were administered i.n. to PND 2 mice under 2% isoflurane anesthesia beginning day -1 post-infection, then daily until the mice were culled via 100% isoflurane for sample collection. On days 1, 3, and 5 when IFNγ was co-administered, the doses of CLip and IFNγ were separated by ≥ 6 hours.

To block adenosine receptor signaling, the pan-adenosine receptor antagonist, DPSPX (1μM in PBS), was administered i.n. to PND 3 mice beginning -1 DPI and continued daily until the mice were culled (Note: DPSPX was not administered on the day of RSV infection).

For secondary RSV infection studies, animals were allowed to recover for 6 weeks in-between primary and secondary challenges. Animals were then challenged with RSV L19 (5×10^5pfu/gm) and samples collected at indicated time points.

2.2.3 RSV viral titers

RSV lung titers were quantified from left lung at the indicated time points using H&E plaque assay, as described previously (79). Lungs were snap-frozen in a dry ice bath and stored at -80 °C. Lungs were thawed and homogenized with glass beads using a mortar and pestle. Homogenized lung was centrifuged and serial dilutions made in HEp-2 media. Dilutions were placed on HEp-2 cells plated in 12-wells and grown to 80% confluency. After incubation at 37 °C on a rocker for 1 hour, infected cells were covered with methyl cellulose and left to incubate for 5 days before fixing with 10% formalin and H&E staining. H&E plaque assays were also used for titering of RSV L19 working stocks as well as other viral solutions in in-vitro studies.

2.2.4 FACS sorting and RNA isolation for RNA sequencing

Naïve and RSV-infected infants (PND 4-5) and adult Balb/c (8-10 weeks) mice were culled and BAL collected at 4 and 3 DPI, respectively. Cells were processed for flow cytometry and surface stained (Siglec F, CD11c, CD11b, CD200R, F4/80, MHCII, Ly6G). The cells were not fixed so that we could ensure the highest quality RNA after sorting. Samples were then sorted on a LSRII Aria and AMs (Sig F^+, $F4/80^+$ $CD200R^+$ $CD11c^{HI}$, $CD11b^{+/-}$, $MHCII^{-/lo}$, and $Ly6G^-$) were collected into PBS supplemented with 50% FBS. Isolated AMs were centrifuged and resuspended in lysis buffer and stored at -80 °C until RNA isolation.

RNA from sorted AMs was isolated using the MagMAX-96 Total RNA Isolation Kit according the manufacturer's instructions. RNA was eluted into 25mcl and sent the lab of Dr. William Janssen at National Jewish Health for RNA sequencing. RNA quality was tested and normalized prior to library development and sequencing.

2.2.5 Histology

At the indicated time point, right lungs were gravity filled (25cm from meniscus to catheter) with 10% formalin after flushing the respiratory system with PBS. Lungs were preserved for at least 48 hours in 10% formalin at 4 ^{0}C. The lungs were paraffin-embedded, stained, and processed at the histology core at the McGowan Institute for Regenerative Medicine (University of Pittsburgh, PA). Terminal deoxynucleotidyl transferase dUTP nick end labeling (TUNEL) and periodic acid-Schiff (PAS) stains were used to identify cells undergoing apoptosis and mucus accumulation, respectively. Hematoxylin and Eosin (H&E) stain was used to identify inflammation. Slides were examined and quantified by individuals blinded to treatment group. For quantification of TUNEL staining, images were captured at 40X magnification and the average number of apoptotic cells per lung section were quantified and graphed. PAS-staining of mucus was scored according to previously published methods (1). In short, all airways were scored for the percentage of the airway staining PAS+ (bright pink) in each tissue section according to the following scale: 0 = no PAS+ cells; 1 = 1-25% PAS+ cells; 2 = 26-50% PAS+ cells; 3 = 51-75% PAS+ cells; 4 = 76-100% PAS+ cells.

2.2.6 Measuring extracellular adenosine concentrations

Naïve infants (PND 4-5) and adults (8-10 weeks) were culled and first wash (FW; 200mcl) collected. Cells were removed via centrifugation and the supernatant collected and transferred to a clean Eppendorf tube. FW supernatant was boiled for 90 seconds to deactivate enzymes that may metabolize adenosine. Samples were then sent to the lab of Dr. Edwin Jackson for adenosine quantification via liquid chromatography-mass spectrometry/mass spectrometry.

2.2.7 Pharmacokinetics and cytokine measurements

For the pharmacokinetic study, a single dose of murine IFNγ was administered i.n. to RSV-naive infant (PND 4-7) and adult (8-10 weeks) mice. Following the single dose of IFNγ, infant and adult mice were culled and samples collected at 0, 0.5, 1, 2, 4, 6, 8, 12, 18, 24, and 48 hours post-dose. Right lungs were collected, weighed and immediately snap-frozen in liquid nitrogen. Samples were stored at -80 ^{0}C until they were processed for protein quantification and cytokine analysis as previously described (80). Briefly, frozen lungs were homogenized in cold Tissue Protein Extraction Reagent (T-PER, Thermo Scientific) and protease inhibitor (HALT Protease Inhibitor Cocktail, Thermo Scientific) (1ml T-PER + 10mcl HALT protease inhibitor cocktail used for every 100mcg of frozen lung tissue), then centrifuged at 9,000g for 10 minutes at 4 ^{0}C. The supernatant was collected and total protein was quantified by bicinchoninic acid assay (BCA assay, Thermo Scientific Pierce) per manufacturer's instructions. The remaining supernatant was stored at -80 ^{0}C for cytokine analysis. IFNγ concentrations in lung homogenate and blood were analyzed by a murine 23-plex multiplex cytokine kit (Bio-Rad, Hercules, CA). Homogenized lung samples were diluted to a total protein concentration of 500mcg/ml using a 1:1 mixture of T-PER and sample diluent (provided by manufacturer). Blood was collected following cardiac puncture (adults) or severing of the abdominal aorta (infants) and allowed to clot for 45 minutes prior to processing. Following clotting, blood samples were centrifuged at 1,000 x g for 15 minutes at 4 ^{0}C. Supernatants were transferred and centrifuged again at 10,000 x g for 10 minutes at 4 ^{0}C. Samples were analyzed using a Luminex® 200™ Total System machine (Luminex Corp, Austin, Tx).

Lung IFNγ concentration-time data after a single i.n. IFNγ dose was analyzed by non-compartmental analysis (NCA). The terminal elimination rate constant, k_{el}, was estimated by log-linear regression of at least three time points visually assessed to be in the terminal phase of each

lung concentration-time plot. The terminal phase (elimination) half-life, $t_{1/2}$, was calculated as ln_2/k_{el}. The area under the lung concentration versus time curve, $AUC_{0\rightarrow\infty}$, was also calculated. Using the linear trapezoidal rule (81), $AUC_{last\rightarrow\infty}$ was extrapolated to infinity by calculating C_{last}/k_{el}. The $AUC_{0\rightarrow\infty}$ was calculated as the sum of $AUC_{last\rightarrow\infty}$ and $AUC_{0\rightarrow t}$. Other pharmacokinetic parameters calculated include IFNγ total body clearance, estimated as dose/AUC. The estimated neonatal dose capable of achieving adult AUC values was calculated by dividing the adult $AUC_{0\rightarrow\infty}$ by neonatal total body clearance.

2.2.8 IFNγ treatment of A549 cells

12-well plates were seeded with A549 cells ($1.5x10^5$cells/ml) and incubated for 24 hours until the wells were 70-80% confluent. Cells were pre-treated with IFNγ (100ng) by removing conditioned media and replaced with A549 media supplemented with IFNγ and incubated for 1 hour. IFNγ A549 media was then aspirated and replaced with IFNγ A549 media spiked with RSV L19 (multiplicity of infection = 2) and incubated for 3 hours with rocking. At the end of infection, well volumes were brought to a total of 1 ml with IFNγ A549 media and the plates were incubated until the desired time point.

Extracellular (budded) virus was quantified by collecting the supernatant from each well and centrifuging samples. Clarified supernatant was serially diluted and plated onto pre-prepared HEp-2 cells in 12-well plates (70-80% confluent) for viral plaque quantification via standard H&E assay described previously.

In order to quantify intracellular virus, A549 cells were detached from the plate via trypsin. The trypsin was deactivated with media and the cells were transferred to snap-cap tubes and

centrifuged. The cell pellet was resuspended in HEp-2 media and placed at -80 °C for 1 hour. Tubes were removed from the freezer and allowed to equilibrate to room temperature before repeating the freeze thaw cycle. Then, tubes were centrifuged and serial dilutions made from supernatant. Serial dilutions were placed on pre-prepared 12-well plates seeded with HEp-2 cells (70-80% confluent) and standard H&E plaque assays performed to determine viral titer, as described previously.

2.2.9 Cell preparation, cytokine analysis, and flow cytometry

FW and BAL were collected by instilling HBSS+EDTA into the alveolar space (FW-100mcl, BAL-1.2ml). The right lung (RL or URL) was harvested and enzyme-digested into a single cell suspension, as previously described (82). FW samples were centrifuged, and the soluble fraction was separated and stored at -80 °C for cytokine analysis. For some experiments MSLNs were collected and processed into single cell suspensions for flow cytometry.

Cytokine concentrations were determined using the Bio-Plex Pro™ Mouse Cytokine 23-plex or Th1/Th2 8-plex Assay (BioRad, CA), per manufacturer's protocol. Measured cytokine concentrations from secondary RSV infection studies (2 and 4 days post-secondary challenge) were used by collaborators (Drs. Yoram Vodovotz and Ruben Zamora) to develop dynamic network analyses.

The cellular components of BAL and RL were processed for surface and intracellular flow cytometric analysis. For surface and intracellular marker detection, cells were surface stained for 25 minutes and fixed (20-30 minutes) with one of the fixatives previously mentioned. For intracellular marker detection, cells were permeabilized according to manufacturer recommendations with one of the kits mentioned previously and stained for intracellular markers

for 45 minutes. Intracellular staining occurred on the same day that samples were run on the flow cytometer. Where indicated, BAL samples were incubated with RSV A Strain F-protein $_{85\text{-}93}$ MHC I pentamer, which was stained for prior to surface staining.

Intracellular cytokine staining occurred in innate and T cells from the BAL and lung in some studies. For innate intracellular cytokine staining, cells were resuspended and incubated in 0% RPMI supplemented with 10% FBS and brefeldin A (1:1000) for 3 hours. T cell intracellular cytokine staining occurred following overnight CD3ε/CD28 stimulation. First, a 96-well flat-bottom plate was coated with 50mcl of a CD3ε/PBS solution (50mcg/ml) and incubated at 4 ºC overnight or at 37 ºC for 2 hours. Then, BAL or lung cells resuspended in 0% RPMI supplemented with 10% FBS and CD28 (2mcg/ml) were placed in the CD3ε coated plate and incubated at 37 ºC overnight. The next morning, the cells were restimulated with PMA (10ng/ml), brefeldin A (1:1000), and ionomycin (1mcg/ml) for 3 hours. Following stimulation, cells were washed and then surface stained, fixed, permeabilized, and intracellularly stained as described previously.

2.2.10 Human monocyte isolation and differentiation

Whole blood was diluted 1:1 with PBS supplemented with 2% FBS and added to a SepMate50 tube with 15ml of Lymphoprep. Tubes were centrifuged and the top layer containing enriched MNCs was poured into a new 50ml conical tube. The MNCs were washed and spun twice before being resuspended in 10% MDM media.

For the plating method of isolating monocytes, MNCs were enumerated and aliquoted into wells. The cells were incubated at 37 ºC for at least 90 minutes before non-adherent cells were washed away. The remaining adherent cells could then undergo differentiation into macrophages.

For column enrichment of $CD14^+$ $CD16^-$ monocytes, enriched MNCs were enumerated and aliquoted for magnetic separation according to manufacturer's instructions in RoboSep buffer. Briefly, MNCs in RoboSep buffer were mixed with Platelet Removal Cocktail, Isolation Cocktail, and magnetic particles. The sample was then placed within the EasySep magnet where unwanted cell types were bound by antibodies conjugated to the magnetic particles and removed from the sample by the magnet. Then, enriched monocytes ($CD14^+$ $CD16^-$) could be poured off into a new tube, counted and aliquoted for differentiation into macrophages.

Differentiation of monocytes was induced by resuspending monocytes into 10% MDM media supplemented with human GM-CSF (25ng/ml) for 7 days. Every 2-3 days, 50% of conditioned media was replaced by fresh GM-CSF supplemented 10% MDM media. After differentiation, cells were detached from the plate by incubating them with TrypLE (Fisher Scientific, Catalog number: 12604013) for 20-30 minutes following washing. The TrypLE was deactivated with 10% MDM media and the cells processed for flow cytometry as described previously.

Monocyte purity was evaluated visually by differential cell staining after affixing isolated cells onto microscope slides. First, 100mcl of cell suspensions were spun onto slides then fixed with methanol and stained with the HEMA3 Stain Set (Fisher Scientific, Catalog number: 122-911), according to manufacturer's instructions. Cell purity was then assessed microscopically.

2.2.11 Airway hyperresponsiveness

Pulmonary function testing was measured on a flexiVent machine (SCIREZ, Montreal, Quebec, Canada) in the lab of Dr. John Alcorn under the assistance of Dr. Michelle Manni, as previously described (83). Briefly, Balb/c mice underwent secondary RSV challenge and were transferred to

Rangos Research Facility 6 days after secondary challenge. Animals were anesthetized and pulmonary function measurements taken following methacholine administration (0, 3.125, 12.5, and 25mg/mL).

2.2.12 CFSE staining and adoptive transfer

Animals that underwent primary RSV infection and IFNγ treatments as infants were rested for 6 weeks, then culled and BAL collected. AMs collected from individual animals were combined within a group and resuspended (7.5 x 10 cells/ml) in warmed RPMI 1640 media supplemented with 5% FBS and plated in a 12-well culture plate. Cells were incubated at 37 °C for 2 hours to allow adherence. Once adhered, the media was aspirated and the AMs were washed thoroughly with HBSS. After washing, AMs were incubated with the CFSE solution (1μM/ml) at 37 °C for 20 minutes with gentle rocking. After CFSE staining, AMs were washed twice with 5% RPMI and incubated for 10 minutes in 5% RMPI to allow the CFSE to undergo acetate hydrolysis. Then, AMs were washed with HBSS and removed from the plate via gentle enzyme dissociation with TrypLE. AMs were collected, centrifuged, counted, and resuspended in HBSS+EDTA ($5x10^5$cells/100mcl). Finally, the CFSE-stained AMs were kept on ice, protected from light, and adoptively transferred i.n. into adult, naïve recipient mice ($5x10^5$cells/100mcl). One day after adoptive transfer, recipient mice were challenged with RSV L19 ($5x10^5$pfu/gm) and culled at 4 DPI for sample analysis. In this study, BAL was collected for flow cytometry and left lungs collected for viral titers.

2.2.13 Maternal Immunization

At time of co-housing, 7 week old female BALB/c were immunized (prime) via intramuscular (i.m.) injection with 50mcl of vehicle (PBS), DS-Cav1 alone (10mcg/mouse; a gift from Jason McClellan, Dartmouth College, NH; currently at University of Texas, Austin), or in combination with Advax-SM (DS-Cav1 + Advax-SM; Advax-SM™, 1mg/mouse; a gift from Vaxine Pty Ltd, Bedford Park, Australia). A week later, mice were bred in-house and in the second week of gestation (21 days post-prime), female mice were boosted i.m. with their respective vaccine. Dams were challenged at 15 weeks of age (53 days post-prime/32 days post-boost), infants challenged at PND 5-6, and weanlings were weaned at 3 weeks of age and challenged 2 weeks later.

2.2.14 Plaque reduction neutralization test (PRNT)

Pre-challenge blood was collected from dams at 50 days post-prime (3 days prior to RSV challenge) via submandibular bleeding. Pre-challenge serum was collected from weanling groups (PND 37) immediately prior to RSV challenge. Post-challenge blood was collected at 4 days-post RSV challenge via severing of abdominal aorta (infants) or cardiac puncture (weanling and dams) at time of sacrifice. Serum was separated using Gel-Z Serum Separator, heat-inactivated at 56 °C for 30 minutes, and stored at -80 °C until neutralizing titers were determined. The following protocol was adapted from a previously described RSV PRNT assay (84). Heat-inactivated antisera was initially diluted in 10% FBS-DMEM at 1:40 (pre-challenge serum) or 1:20 (post-challenge serum) dilutions, then 2-fold serially diluted in a 96-well plate. RSV L19 (1500 PFU/well) was added and the antisera/virus mixture was incubated at 37°C for 1 hour. Virus-antisera mixture (100mcl) was added to $1.5x10^4$ HEp2 cells in each well of a 96-well plate and incubated at 37 °C

for 3 days at 5% CO_2. Plates were washed with PBS and fixed with acetone at 4 °C for 20 minutes. Goat anti-RSV polyclonal antibody was added at a 1:4000 dilution and incubated at room temperature (RT) for 1 hour. HRP-conjugated donkey anti-goat IgG was then added at a 1:4000 dilution and incubated at RT for 1 hour. TMB substrate was added and color was allowed to develop for 5 to 7 minutes, at which time 1M sulfuric acid was added to stop the reaction. Optical density was measured at 450nm. Reciprocal serum dilutions at which 50% of RSV L19 was neutralized in relation to control wells was graphed.

2.2.15 RSV-specific IgG subtype assay

RSV-specific IgG subtypes were measured as previously described (85). Briefly, Immulon high-binding 96-well microtiter plates were coated with 100mcl of purified RSV L19 virus (3×10^5pfu) in binding buffer at 4 ^{0}C overnight. After washing steps and blocking for 2 hours at 37 ^{0}C with blocking buffer (3% BSA in PBS), antisera was diluted (dams, 1:100; weanlings, 1:20) in blocking buffer and incubated in triplicate overnight at 4 ^{0}C. The plates were then incubated with HRP-conjugated IgG1 or IgG2a goat anti-mouse secondary antibodies at 37 ^{0}C for 90 minutes. TMB substrate was added and color was allowed to develop for 30 minutes at 37 ^{0}C. The optical density was read at 450 nm. Optical densities (OD) were graphed after subtracting background OD from triplicate wells incubated with blocking buffer.

2.2.16 Statistical analysis

GraphPad Prism version 5.0 was used for all statistical analyses. Means were compared using a Student's t-test, or for multiple comparisons, a one-way analysis of variance (ANOVA) was used

with Tukey's or Bonferroni post hoc test to evaluate statistical significance between groups. For experiments where multiple groups were compared over multiple time points, a two-way ANOVA was used and a Bonferroni post hoc test used to evaluate statistical significance between groups. Repeated measures ANOVA was used to determine changes in weight over time between groups with a Bonferroni post hoc test. All data are shown as mean ± SD of biological replicates within individual experiments. Where indicated, 2-3 infant BAL samples within a group were combined to form a single sample. $\rho < 0.05$ was considered statistically significant.

3.0 INFANT VERSUS ADULT RESPONSES TO RSV

Sections of this chapter are adapted from the published manuscript:

Katherine M. Eichinger, Jessica L. Kosanovich, and Kerry M. Empey

Localization of the T-cell response to RSV infection is altered in infant mice. *Pediatric Pulmonology*, 2018. 53 (2): 145-153. (© Wiley Periodicals, Inc.)

3.1 INTRODUCTION

Respiratory tract infections represent the single largest disease burden worldwide (86) and are especially prominent in infants and young children. In 2015, lower respiratory tract infections (LRTI) were responsible for 15.3% of mortality in children < 5 years old (87). Globally, RSV is the most common cause of acute LRTI in children resulting in a significant number of hospital admissions (28, 88). Despite RSV's immense contribution to the global burden of lung disease, there are no effective treatments or licensed vaccines. The anti-RSV antibody, palivizumab, reduces the number of RSV-associated hospitalizations in *high-risk* infants when given

prophylactically (89), yet 80% of RSV-related hospitalizations consist of previously healthy infants and children who do not receive prophylaxis (30, 90). A more universal measure aimed at preventing primary RSV-related morbidity and mortality is a healthcare priority. Therefore, a more complete understanding of the infant immune response to RSV is necessary to guide the development of future vaccines and therapeutic interventions.

Innate immunity provides the critical link between pathogen detection and induction of an effective adaptive immune response capable of clearing the invading organism. Eliciting an adaptive immune response against RSV requires pathogen detection by airway epithelial cells (AECs) and AMs and activation of these cells. Typically, invading pathogens activate AECs and AMs through pattern-recognition receptors, such as TLRs. Once activated, AMs will increase expression of co-stimulatory markers and both cell types will produce inflammatory cytokines that will recruit and activate additional immune cells. In adults, activated mononuclear cells produce TNFα, IL-1β, and IL-12 and increase co-stimulatory marker expression, which work in concert to promote inflammation and engage adaptive immunity to combat pathogens (91, 92). However, infant mononuclear cells activated through TLR agonists are generally characterized by a high IL-6 to TNFα cytokine response, which is reflective of their bias away from Th1-type cytokine responses (TNFα, IL-12p70, and IFNγ) (48, 92, 93). In part, this reduced capacity to mount an effective Th1 response makes infants vulnerable to infection by intracellular pathogens (50), such as RSV, and compromises their ability to facilitate effective adaptive immunity.

The importance of T lymphocytes in clearing RSV has been well established in murine (61, 94-96) and human studies (97). However, debate still exists regarding the effectiveness of T-cell recruitment to the air space of RSV-infected infants (98, 99). Autopsy samples from infants infected with RSV revealed that T-cell infiltration into the lung was meager but importantly, the

small number of T-cells located within the alveolar space were highly activated, suggesting close proximity to RSV-infected airway epithelium increases activation (98). Similarly, BAL samples from RSV-infected infants showed massive neutrophil recruitment but relatively small increases in the frequency of T-cells (100, 101). The $CD8^+$ T-cells recovered from the BAL of these infants had a highly activated, effector phenotype, were proliferating, and produced Granzyme B (101). However, in an infant murine model of influenza, recovery of T-cells from the alveolar space was deficient when compared to adults (102). Collectively these studies indicate that T-cells exert their anti-viral effects proximal to RSV-infected AECs within the bronchoalveolar space but the accumulation of infant T-cells may be inefficient. Murine studies investigating the role of T lymphocytes in RSV disease have relied heavily on adult models and may therefore be missing important differences in infant T-cell accumulation and activation in the airway. Furthermore, there is a scarcity of data regarding the age-dependent differences that may exist in T-cell accumulation throughout the pulmonary architecture of RSV-infected adult and infant mice.

It is well appreciated that infants have higher concentrations of immunosuppressive/immunoregulatory factors (ex. IL-10, TGFβ, IL-27, and retinoic acid) in the lung environment (103-105). One such molecule that has not been investigated in the context of infant RSV infection is the purine nucleoside, adenosine. This molecule's profound effects on the modulation of nitric oxide production, suppression of TNFα and IL-12 production, and facilitation of IL-10 production by macrophages has been extensively reviewed (106). High adenosine concentrations in neonatal plasma have been found to divert a normal Th1 cytokine response following TLR stimulation to a Th2-biased response (92), but the role that it may play within the infant airway during RSV infection has never been investigated.

In order to determine age-dependent differences in innate RSV immunity, a kinetic examination of innate immune cells was conducted in RSV-infected infant and adult mice using flow cytometry. Given the importance of AMs in maintaining homeostatic lung conditions as well as their role in initiating inflammatory immune responses, transcriptional sequencing of AMs from naïve and RSV-infected infant and adult mice was performed, in order to identify specific age-based differences. We also identified key differences in T cell accumulation within the pulmonary architecture of infant and adult mice following RSV infection. Lastly, we examined the role of extracellular adenosine on infant RSV immunity, which provides new insight into a previously unrecognized immunoregulatory molecule within the lung, disproportionately affecting infants. We hypothesized that increased concentrations of extracellular adenosine in the airways of infant mice will result in reduced innate activation following RSV challenge and subsequently, T cell recruitment to the infant airway will be reduced compared to adults.

3.2 RESULTS

3.2.1 Adult versus infant innate responses

3.2.1.1 Phenotypic characterization of innate immune cells from BAL using flow cytometry in a murine model of RSV L19

In previous flow cytometry experiments, our lab relied on antibodies directed against CD11b (αM) and CD11c (αX) integrins to identify innate immune cells in the BAL responding to RSV infection (1). However, our ability to fully characterize the innate immune response was limited by the fact that CD11b and CD11c are expressed by numerous cell types from both the adaptive and innate

immune systems. Identification of cell populations accurately using CD11b is further complicated by the fact that AMs and other activated immune cells increase their expression of CD11b in response to stimuli (107-109). To discriminate innate cell populations in the BAL using flow cytometry, an expanded panel of antibodies was created using data from published reports (110) and tested in our Balb/c model of RSV L19. Specifically for AMs, we analyzed the expression of markers listed in **Table 3.1** and previously identified as distinguishing AM markers in a review by Hussell and Bell (110). Overall, AMs in our model were in agreement with those summarized by Hussell and Bell with the exceptions of F4/80 and CD11b. F4/80 has been widely used as a murine macrophage marker and was expressed by AMs harvested from the BAL. As previously mentioned, CD11b was not expressed by AMs in naïve mice but was quickly upregulated in response to RSV infection.

Table 3.1. AM marker expression

AM Surface Marker	Hussell, T. & Bell, T.J. *Nat. Rev. Immunol. 2014*	Balb/c RSV L19 model
Siglec F	High expression	High expression
F4/80	Low expression	High expression
CD206 (transmembrane mannose receptor)	High expression	High expression
CD200R	High expression	High expression
CD11c	High expression	High expression
CD11b	Not expressed	Not expressed (naïve)/ Intermediate expression (RSV)

In addition to the markers highlighted in **Table 3.1**, Ly6G and major histocompatibility complex II (MHCII) were added to the panel to aid in the identification of neutrophils and dendritic cells, respectively. For an illustrative example, cell discrimination was conducted using flow cytometry and the eight marker panel (Siglec F, F4/80, CD206, CD200R, CD11c, CD11b, MHCII, and Ly6G) in a BAL sample collected from an adult animal with complex cellular infiltrate, as a result of a secondary RSV infection (**Figure 3.1A**). This innate immunophenotyping flow cytometry panel allows for discrimination of six, well defined, innate immune cell types. Additionally, the complexity of innate cellular immunophenotyping is highlighted when a naïve BAL sample is compared to a BAL sample harvested from an adult mouse responding to a secondary RSV infection in the context of CD11b and CD11c expression (**Figure 3.1B**). From the BAL of a naïve mouse, the overwhelming majority of cells are $CD11c^{HI}$ $CD11b^{-}$ and with the use of the innate immunophenotyping panel, these cells were identified in the overlay panel as AMs (Sig F^{+} $F4/80^{+}$ MR^{HI} $CD200R^{+}$ $CD11c^{HI}$) (**Figure 3.1B**). The introduction of secondary RSV results in a massive infiltration of innate immune cells that cannot be identified with CD11c and CD11b alone, as illustrated in the secondary RSV panel of single cells (**Figure 3.1B**). However, when the secondary RSV sample is viewed in the overlay panel, AMs, eosinophils (Sig F^{+} $F4/80^{+}$ $CD206^{lo/-}$ $CD200R^{-}$ $CD11c^{-}$ $CD11b^{int}$), neutrophils (Sig F^{-} $Ly6G^{+}$ $CD11b^{HI}$ $CD11c^{-}$), Sig F^{-} AMs (Sig F^{-} $F4/80^{+}$ $CD206^{HI}$, $CD200R^{+}$ $CD11c^{HI}$), monocytes (Sig F^{-} $F4/80^{+}$ $CD206^{lo/-}$ $CD11c^{+}$ $CD11b^{+}$), and dendritic cells (Sig F^{-} $CD11c^{+}$ $MHCII^{HI}$) can be viewed as discrete populations (**Figure 3.1B**). This demonstrates the necessity of using a well-defined flow cytometry panel to accurately immunophenotype cells infiltrating the airway in response to RSV infection. Without accurate identification, the immune response of one cell type may be misappropriated to another and add confusion in the RSV literature.

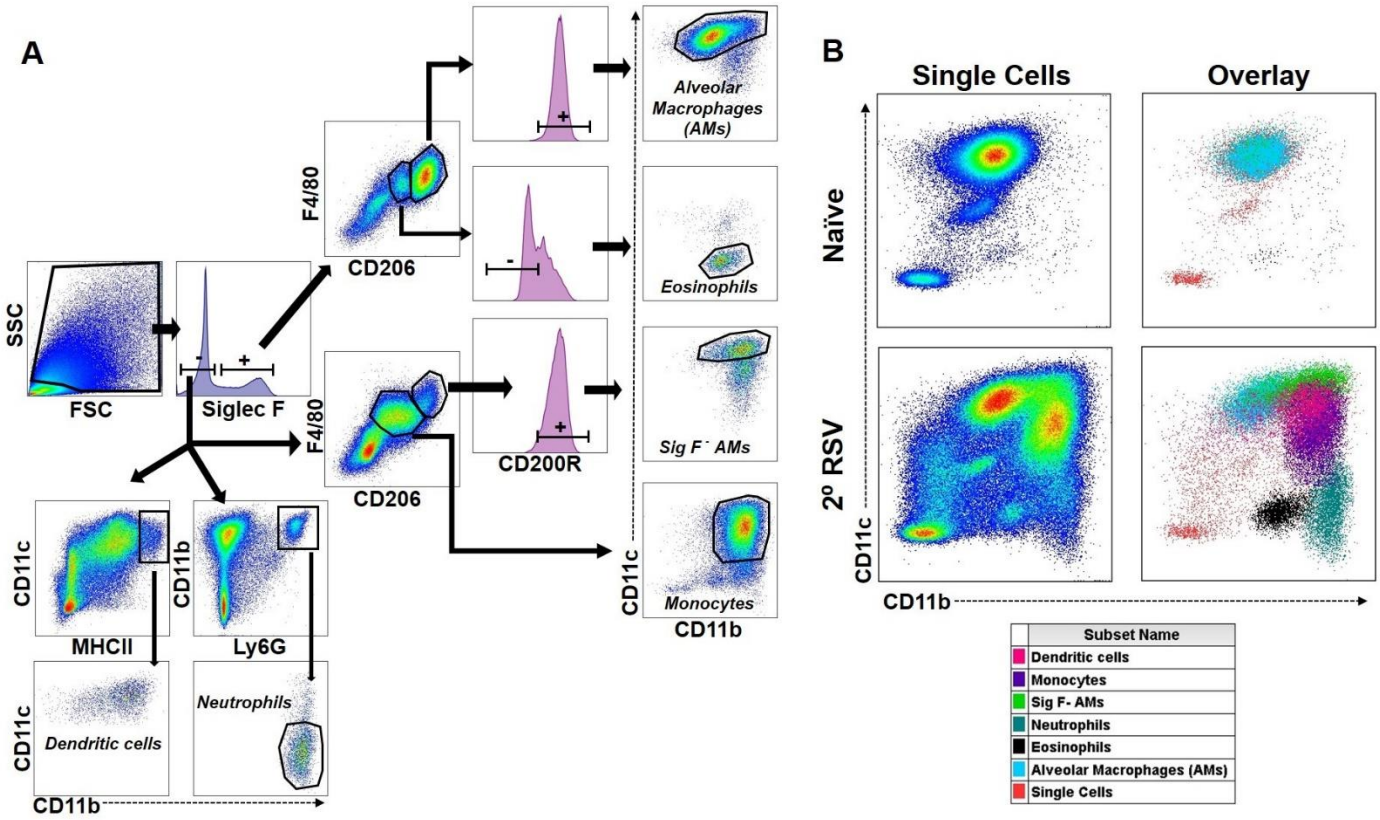

Figure 3.1. Innate BAL immunophenotyping using flow cytometry

Adult (6-8 week old) Balb/c mice were re-infected with RSV L19 after being initially challenged as infant mice (PND 4-6). At 4 days post-secondary challenge, BAL was collected and processed for flow cytometry. A representative example of the gating strategy used to identify innate immune cells is shown (A). Single cells analyzed via flow cytometry from a naïve and a 2^0 challenge sample were visualized according to their CD11b and CD11c expression (B). Then, using the gating strategy in (A), immunophenotyped innate immune cells were overlaid onto single cells (B).

3.2.1.2 Recruitment and activation of innate immune cells in response to RSV is decreased in infants compared to adults

To determine the recruitment kinetics of innate immune cell types following RSV infection, we analyzed the monocyte and DC frequency in the BAL of infant and adult Balb/c mice at multiple

time points following RSV infection. The frequency of monocytes (monos; Sig F^- $CD11c^+$ $CD11b^+$) rapidly rose in adult BAL, remained steady from 3 to 10 DPI, and began to decline slightly by 15 DPI (**Figure 3.2A**). Monocyte recruitment in RSV-infected infants was dramatically lower than that of adults, representing a negligible percentage of BAL cells (**Figure 3.2B**). Similar to adult monocytes, DCs (Sig F^- $CD11c^+$ MHCII ^{HI}) began increasing significantly in adult BAL as early as 3 DPI and peaked at 10 DPI (**Figure 3.2C**). In contrast, RSV-infected infants demonstrated significant increases in DC frequency at 7 and 10 DPI but in infants, DCs represented a very small percentage of BAL cells when compared to RSV-infected adults (**Figure 3.2D**).

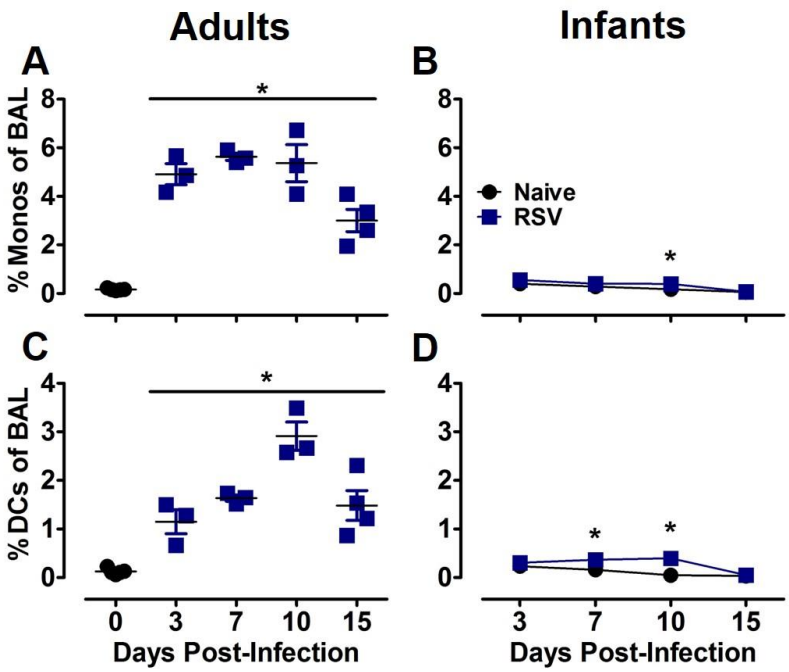

Figure 3.2. Reduced monocyte and DC recruitment in RSV-infected infants.

Adult (6-8 weeks) and infant (PND 4-5) Balb/c mice were infected with RSV L19. BAL was collected at 3, 7, 10, and 15 DPI and processed for flow cytometry. Frequencies of monocytes (monos) and DCs were calculated. The percentage of adult monos (A) and DCs (C) comprising the BAL were compared between naïve and RSV+ adult mice using ANOVA with a Bonferroni post-test. Naïve adult BALs ($n \geq 1$) were processed simultaneously with RSV+ samples at each time point to account for day to day variations in analysis. However, the data from all naïve adults were pooled and represented graphically as 0 DPI. The percentage of infant monos (B) and DCs (D) comprising the BAL were compared between naïve and RSV infants using 2-way ANOVA with Bonferroni post-test. Naïve, infant samples were analyzed at each time point to account for developmental changes. Data points represent individual mice (naïve adults) or the mean of $n \geq 3$-4 samples (2-3 infant BALs pooled per sample) per group ± SD; * ρ-value < 0.05. Data are representative of 2 independent experiments.

AMs make up the overwhelming majority of leukocytes in the airway (111). They must continually survey the lung environment and selectively identify pathogens vs. innocuous unfiltered debris, pollutants, etc. To determine age-based differences in AM responses following

RSV infection, the BALs of adult and infant RSV-infected mice were compared to naïve, age-matched controls using flow cytometry. Approximately 84% of naïve, adult BAL cells were AMs with the proportion of AMs decreasing significantly throughout the RSV infection time course as other cell types infiltrate the airway (**Figure 3.3A**). AMs represent a smaller percentage of cells found in infant BAL samples compared to adult mice, although the proportion of AMs steadily increases as the infants age (**Figure 3.3B**). However, the frequencies of AMs in infant BAL did not diverge between naïve and RSV infants, highlighting the lack of inflammatory cell recruitment to the infant airway following RSV challenge (**Figure 3.3B**). In adults, significant increases in markers of AM activation, including $CD11b^+$ (**Figure 3.3C**), $CD80^+$ (**Figure 3.3E**), $MHCII^+$ (**Figure 3.3G**), and the phagocytic scavenger receptor-A ($SR\text{-}A^+$, **Figure 3.3I**), occurred at different time points in response to RSV. Significant increases in markers of AM activation occurred in infants in response to RSV, however the peak or duration of increased activation was reduced when compared to adults. The duration and peak $CD11b^+$ expression (**Figure 3.3D**) was lower in infants compared to adults, while the peak of activation was reduced for $CD80^+$ (**Figure 3.3F**), $MHCII^+$ (**Figure 3.3H**), and $SR\text{-}A^+$ (**Figure 3.3J**) on infant AMs.

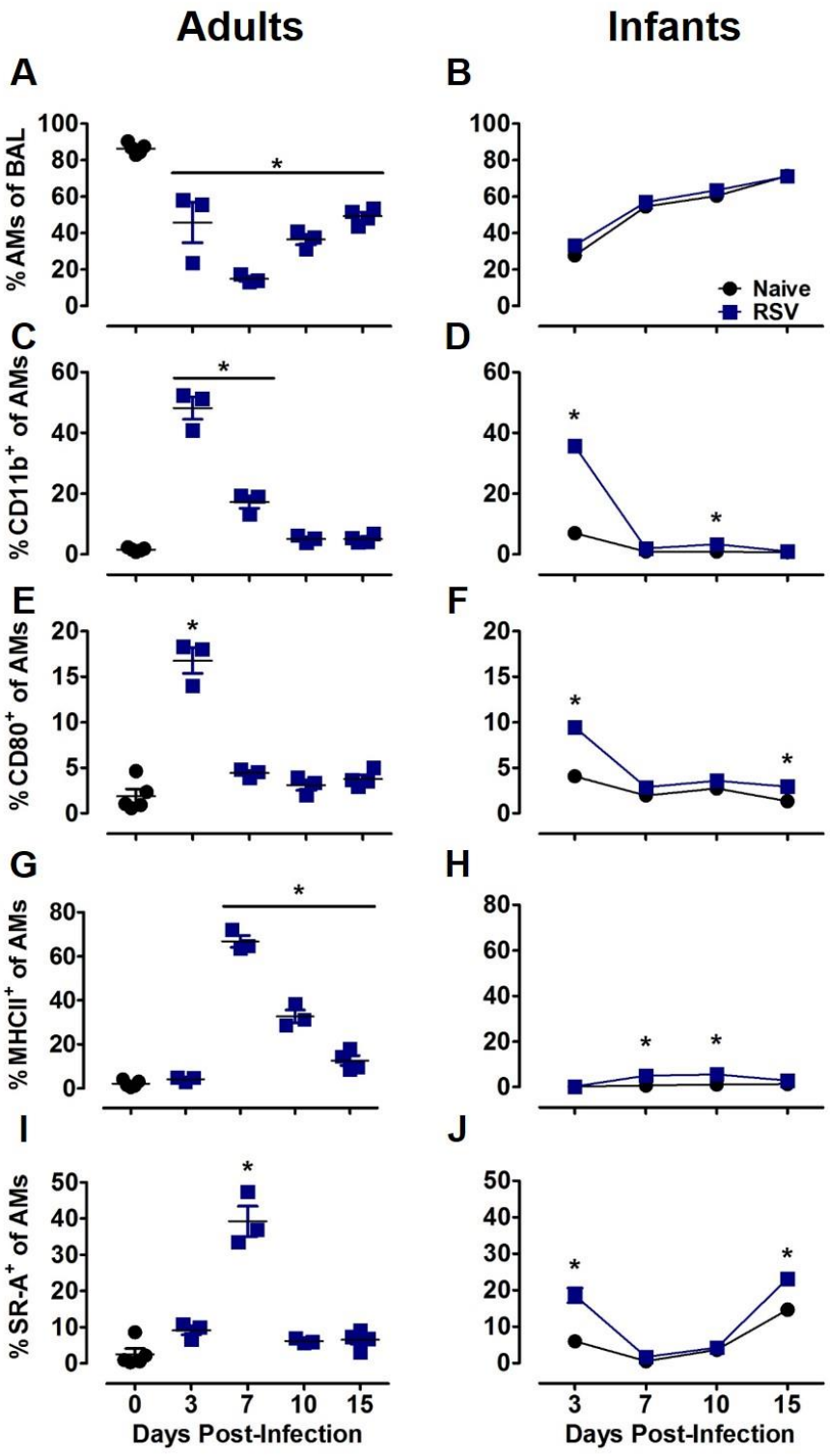

Figure 3.3. Age-dependent differences in AM activation in response to RSV.

Figure 3.3 (continued) Adult (6-8 weeks) and infant (PND 4-5) Balb/c mice were infected with RSV L19. BAL was collected at 3, 7, 10, and 15 DPI and processed for flow cytometry. The frequency of adult AMs (A) and their expression of $CD11b^+$ (C), $CD80^+$ (E), $MHCII^+$ (G), and $SR\text{-}A^+$ (I) were compared between naïve and RSV+ adult mice using ANOVA with a Bonferroni post-test; time points under bar indicate significantly different means compared to 0 DPI. Naïve adult BALs ($n \geq 1$) were processed simultaneously with RSV+ samples at each time point to account for day to day variations in analysis. However, the data from all naïve adults were pooled and represented graphically as 0 DPI. The frequency of infant AMs (B) and their expression of $CD11b^+$ (D), $CD80^+$ (F), $MHCII^+$ (H), and $SR\text{-}A^+$ (J) were compared between naïve and RSV+ infants using 2-way ANOVA with Bonferroni post-test. Naïve, infant samples (2-3 infant BALs pooled per sample) were analyzed at each time point to account for developmental changes. Data points represent individual mice (naïve adults) or the mean of $n \geq 3\text{-}4$ samples (infants) per group ± SD; * ρ-value < 0.05. Data are representative of 2 independent experiments.

As the previous data regarding AM activation demonstrated, CD11b expression immediately proceeded or coincided with a number of additional markers of activation. To further investigate age-based differences and the relationship between CD11b expression and associated AM activation, AMs expressing $CD11b^+$ were compared directly to $CD11b^-$ AMs with respect to their expression of activation markers in RSV-infected adults and infants. At 3 DPI, the adult AM population was evenly split between $CD11b^+$ and $CD11b^-$ expression and although the $CD11b^+$ expression decreases by 7 DPI, approximately 18% of AMs still express $CD11b^+$ (**Figure 3.4A**) at that time point. In contrast, RSV-infected infants maintained a significantly higher proportion of $CD11b^-$ AMs throughout the time course analyzed and any increases in $CD11b^+$ expression at 3 DPI are lost by 7 DPI (**Figure 3.4B**). Interestingly, the $CD80^+$ expression on adult AMs coincides entirely with $CD11b^+$ expression (**Figure 3.4C**). While $MHCII^+$ (**Figure 3.4E**) and $SR\text{-}A^+$ (**Figure 3.4G**) expression was significantly higher on $CD11b^+$ AMs, $CD11b^-$ AMs also increased

expression of these markers in RSV-infected adults. In RSV-infected infants, the increases in expression of $CD80^+$ (**Figure 3.4D**), $MHCII^+$ (**Figure 3.4F**), and $SR\text{-}A^+$ (**Figure 3.4H**) coincided with $CD11b^+$ expression, with no increases in the activation markers noted for $CD11b^-$ AMs. It is important to note however that $CD11b^+$ expression on infant AMs decreased from nearly 35% at 3 DPI to 2% at 7 DPI, so the contribution of activation markers on the larger immune response from such a small population at time points later than 3 DPI is questionable. Taken together, these data suggest that activation of the innate immune system as well as the recruitment of additional inflammatory immune cells is reduced during the infant RSV immune responses compared to adults, which may have ramifications on the downstream activation of the adaptive immune response and subsequent viral clearance.

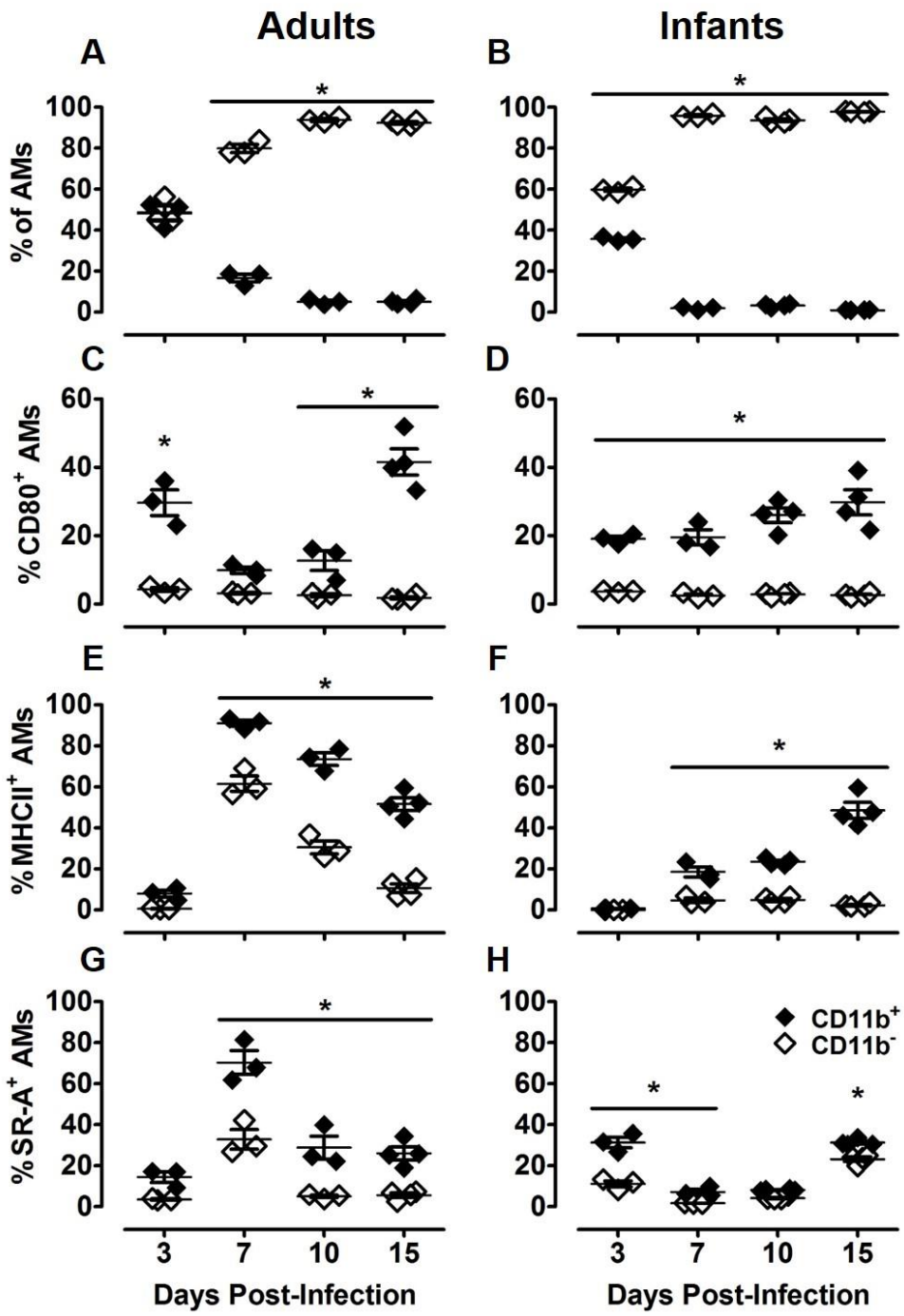

Figure 3.4. CD11b expression on AMs correlates with enhanced activation.

Figure 3.4 (continued) Adult (6-8 weeks) and infant (PND 4-5) Balb/c mice were infected with RSV L19. BAL was collected at 3, 7, 10, and 15 DPI and processed for flow cytometry. AMs were gated according to their expression of $CD11b^+$ (A and B) the frequency of activation markers, $CD80^+$ (C and D), $MHCII^+$ (E and F), and $SR\text{-}A^+$ (G and H) were compared to $CD11b^-$ AMs in RSV-infected adults and infants, respectively. Comparisons between $CD11b^+$ and $CD11b^-$ were made using 2-way ANOVA with Bonferroni post-test; bar across time points indicates a significant difference between $CD11b^-$ and $CD11b^+$ at each time point under the bar. Data points represent individual samples (2-3 infant BALs pooled per sample) and the lines represent the mean of $n \geq 3\text{-}4$ samples per group ± SD; * ρ-value < 0.05. Data are representative of 2 independent experiments.

3.2.1.3 Age-dependent differential gene expression in AMs using RNA sequencing

As the sentinels of the airway, AMs, along with airway epithelial cells, are the first cells to detect pathogens and initiate an immune response. Using phenotypic data, the previous figures demonstrated infant AMs had reduced activation following RSV challenge compared to adults. To determine how age-dependent transcriptional differences may influence AMs' responses following RSV challenge, AMs were isolated using FACS and their transcriptional data analyzed using RNA sequencing. The principle component analysis revealed that AM populations were highly clustered according to age and RSV status (**Figure 3.5**). There was significant separation between AMs from naïve and RSV infected adult mice suggesting large differences in genetic expression following RSV infection in adults. Adult and infant AMs were clearly segregated indicating substantial age-based genetic expression differences. Importantly, there was relatively little separation between AMs isolated from naïve and RSV infected infants, suggesting reduced differential gene expression in infant AMs following RSV infection compared to adults.

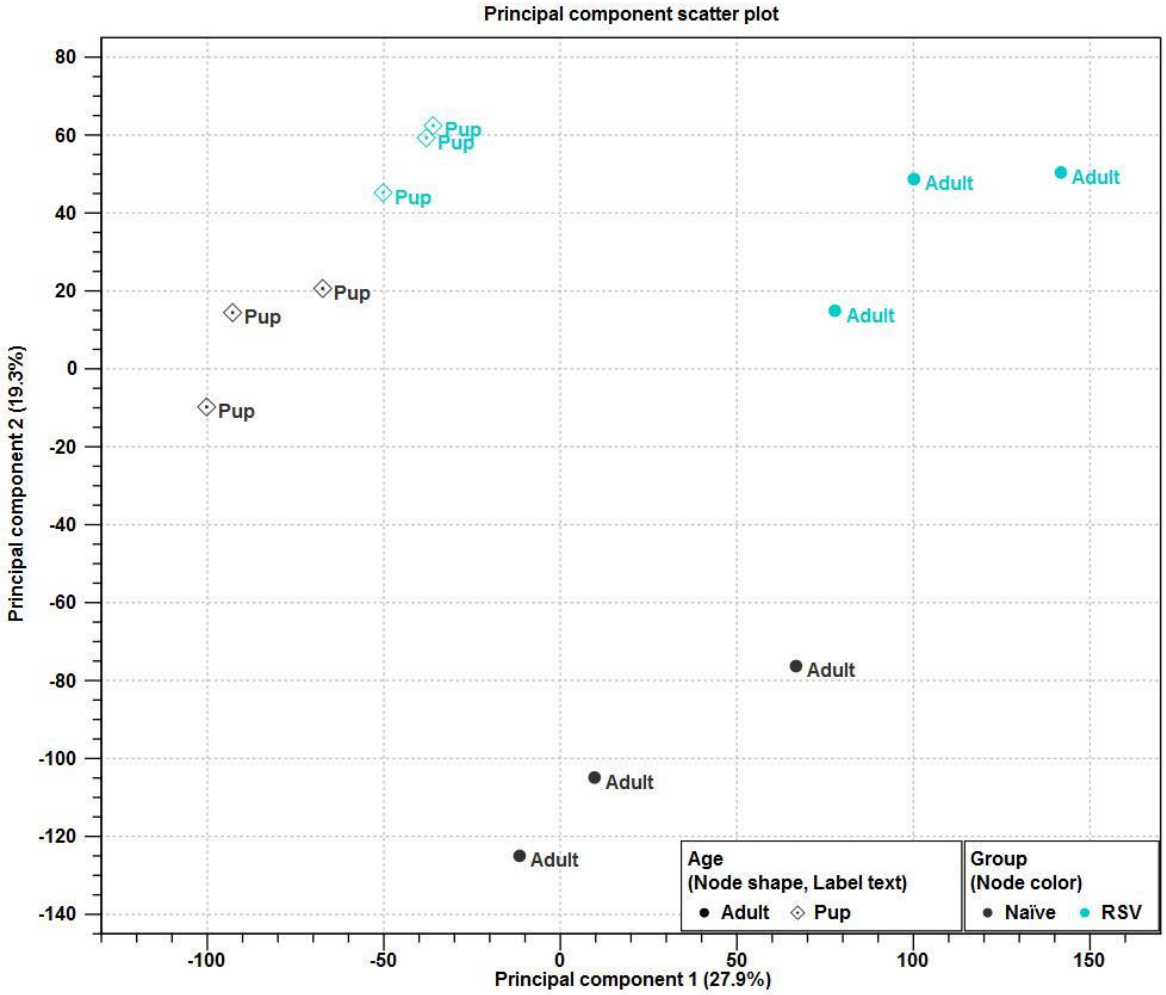

Figure 3.5. Principle component analysis of AMs

Adult (8-10 week old) and infant (4-6 PND) Balb/c mice were infected with RSV L19. AMs from pooled samples (3-4 adults and 6-7 infants/sample) were collected on post-infection days corresponding to peak CD11b expression on AMs (3 and 4 dpi for adults and infants, respectively) and stained for FACS. Isolated RNA was sent to National Jewish Health for RNA sequencing. RNA seq data was analyzed using CLC Genomics.

Transcripts per million (TPM) were modeled as a function of age, infection status, and using an age/infection status interaction term. Three comparisons were performed to find

differentially expressed genes (DEGs) between groups: adult naïve vs. adult RSV, infant naïve vs. infant RSV, and naïve vs. RSV while controlling for age (interaction term). A visualization of the number of significant genes for each of the three comparisons and their relationship to each other can be seen in **Figure 3.6** (FDR-adjusted p-value ≤ 0.05 and fold change ≥ 1.5). There were over four times as many DEGs between adult naïve and RSV samples as the infants (1376 compared to 326). Only 16.6% of the significant DEGs in AMs from naïve compared to RSV infected adults were also altered in infant AMs in response to RSV (**Figure 3.6**, 229 compared to 1376).

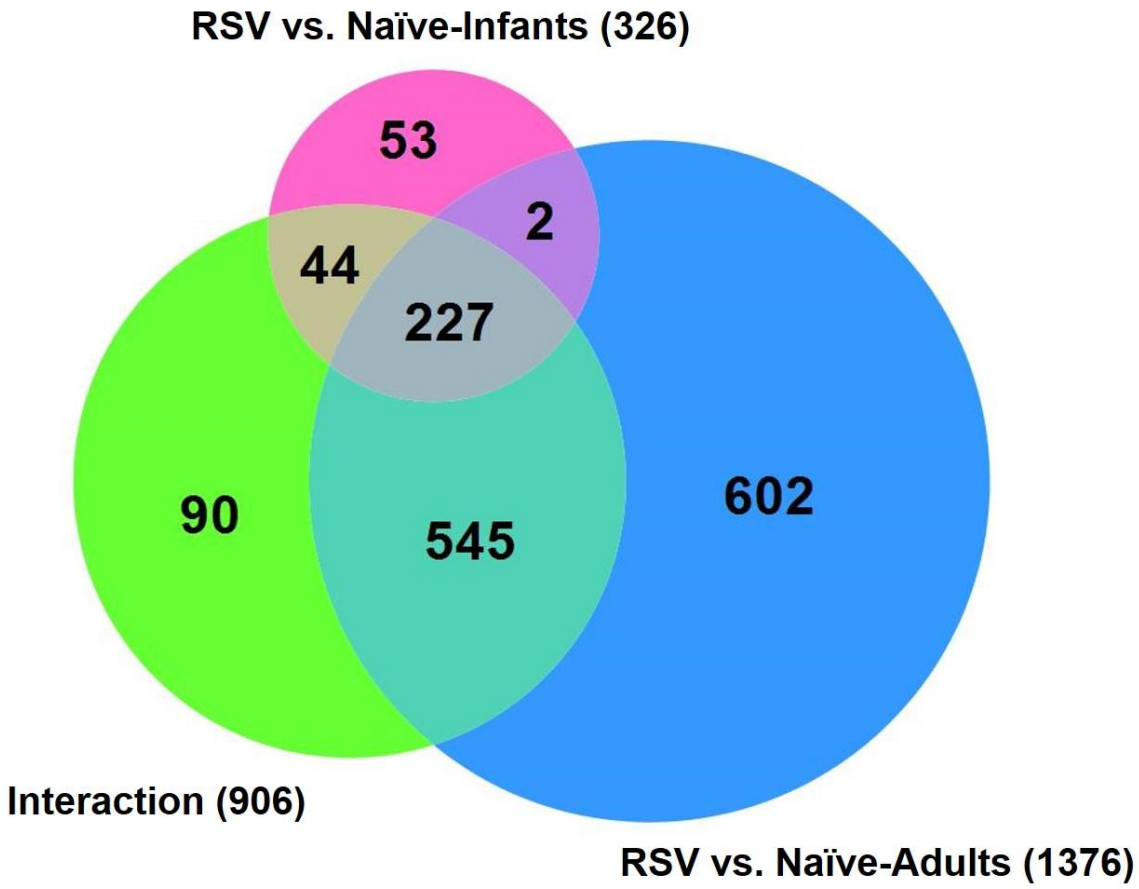

Figure 3.6. Venn diagram of DEGs in AMs in response to RSV.

Adult (8-10 week old) and infant (4-6 PND) Balb/c mice were infected with RSV L19. AMs from pooled samples (3-4 adults and 6-7 infants/sample) were collected on post-infection days corresponding to peak CD11b expression on AMs (3 and 4 dpi for adults and infants, respectively) and stained for FACS. Isolated RNA was sent to National Jewish Health for RNA sequencing. RNA seq data was analyzed using CLC Genomics and the Venn diagram represents overlapping expression resulting from three comparisons of isolated macrophages: RSV infected and naïve infants, RSV infected and naïve adults, and naïve versus RSV while controlling for age (interaction).

Using CLC Genomics software, a volcano plot of DEGs resulting from the comparison of naïve to RSV while controlling for age (interaction term) was created to identify genes that are highly significant and have $\geq \log_2$ fold changes in their expression following RSV infection. Highlighted in red on the volcano plot are three examples of genes that underwent significant differential expression in adult AMs following RSV exposure but remained largely unchanged in infants (**Figure 3.7**). Reports in the literature have demonstrated the importance of Spon1 in macrophage TLR4 activation, cytokine production, and migration (112, 113). Plac8 has been recognized to play a role in innate bacterial killing (114) and in $CD4^+$ Th1 T cell-driven clearance of *Chlamydia* from the genital tract (115). Finally, Runx3 has been shown to regulate macrophage differentiation (116) and negatively regulate the expression of the scavenger receptor, CD36 (117). The control of CD36 expression is particularly interesting because it is significantly higher in naïve infants compared to adults (data not shown). Collectively, the RNA seq. data from isolated AMs demonstrates that there are age-based transcriptional differences that contribute to the reduced innate immune response observed in infant compared to adult RSV-infected mice. These differences may also have important consequences for T cell recruitment and activation, which will be discussed next.

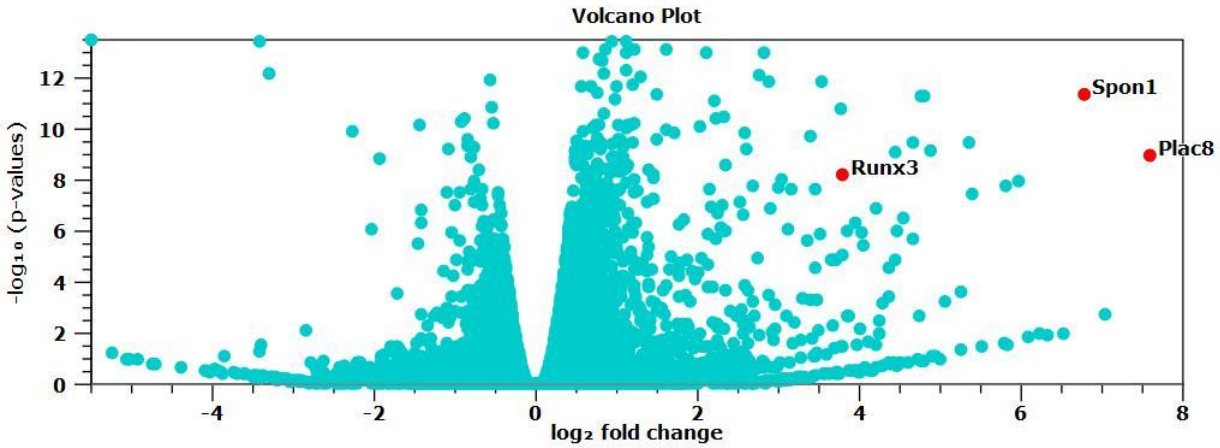

Figure 3.7. Naive vs. RSV-infected DEGs in AMs.

Adult (8-10 week old) and infant (4-6 PND) Balb/c mice were infected with RSV L19. AMs from pooled samples (3-4 adults and 6-7 infants/sample) were collected on post-infection days corresponding to peak CD11b expression on AMs (3 and 4 dpi for adults and infants, respectively) and stained for FACS. Isolated RNA was sent to National Jewish Health for RNA sequencing. RNA seq data was analyzed using CLC Genomics and the volcano plot shows DEGs for macrophages comparing naïve versus RSV while controlling for age (interaction). Red highlighted genes are genes of interest that may be explored in future studies.

3.2.2 Adult versus infant T cell responses

3.2.2.1 Pulmonary T-cell recruitment peaks 10 days after RSV infection in adult and infant mice

To determine peak pulmonary T-cell recruitment following RSV infection, we analyzed total $CD4^+$ and $CD8^+$ T cells recovered from the lungs of infant and adult Balb/c mice at multiple time points following RSV infection. Total $CD4^+$ and $CD8^+$ T-cells peaked at 10 DPI in RSV+ adults (**Figure 3.8A & B**) and infants (**Figure 3.8C & D**), indicating that infants and adults have similar

pulmonary T cell recruitment kinetics following RSV infection. Subsequent experiments characterized age-dependent, phenotypic T cell responses at this 10 DPI time point, which represented peak T-cell responses for both age groups.

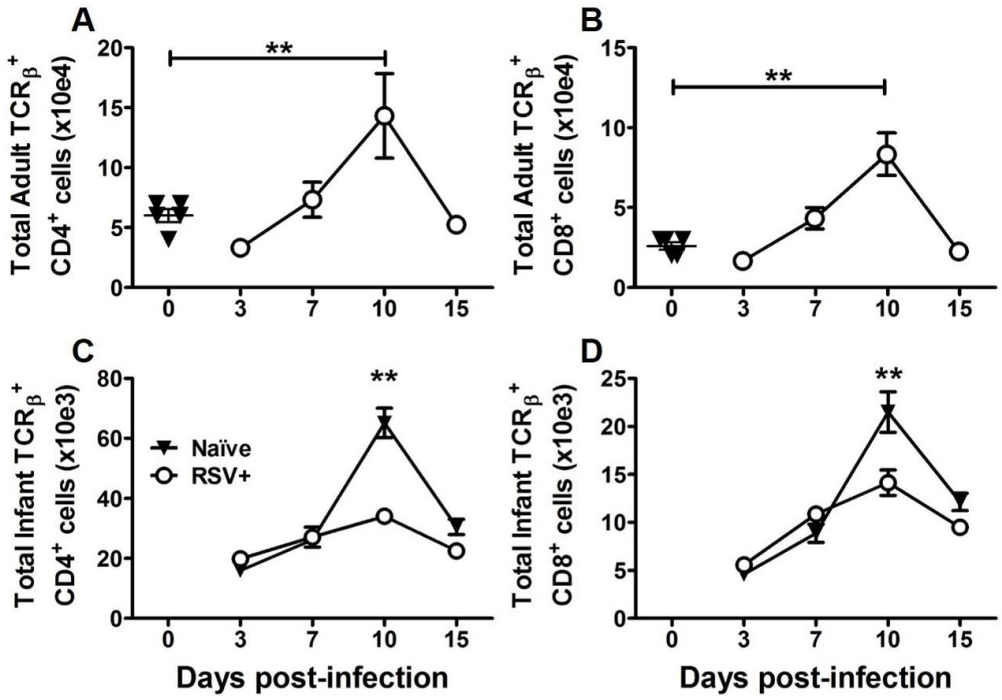

Figure 3.8. Pulmonary T-cell recruitment peaks 10 days after RSV infection in adult and infant mice.

Figure 3.8 (continued) Adult (6-8 weeks) and infant (PND 4-5) Balb/c mice were infected with RSV L19. Right lungs were collected at 3, 7, 10, and 15 DPI and processed for flow cytometry. Lymphocytes were gated from FSC vs. SSC, then $CD4^+$ and $CD8^+$ T-cells were determined from $TCR\beta^+$ cells in the lymphocyte gate. Total T cells were compared between naïve and RSV^+ adult mice (A & B) using ANOVA with a Bonferroni post-test. Infant T cell totals (C & D) were compared using 2-way ANOVA with a Bonferroni post-test. Naïve adult lungs ($n \geq 1$) were processed simultaneously with RSV+ samples at each time point to account for day to day variations in analysis. However, the data from all naïve adults were pooled and represented graphically as 0 DPI. Naïve, infant samples were analyzed at each time point to account for developmental changes over the course of the study. Data points represent individual mice (naïve adults) and lines, the mean of $n \geq 3$-4 samples per group ± SD; ** ρ-value < 0.01. Data in A-B & C-D are representative of 2 independent experiments. ***Originally published in***: Eichinger KM, Kosanovich JL, Empey KM. Localization of the T-cell response to RSV infection is altered in infant mice. *Pediatric pulmonology* 2018;53(2):145-153.

3.2.2.2 T-cell accumulation in the airway is reduced in RSV-infected infant mice

To better understand the role of age in T cell localization during RSV infection, flow cytometry was used to determine the frequency of $CD4^+$ and $CD8^+$ T-cells in the lung tissue and BAL of infant and adult mice. At 10 DPI, the frequencies of $CD4^+$ and $CD8^+$ T-cells were significantly higher in adult compared to infant BAL (**Figure 3.9A, B, E and F**). However, both adults and infants had significantly higher proportions of $CD4^+$ T-cells in the upper right lung (URL) compared to BAL (**Figure 3.9A-E**). Importantly, higher frequencies of adult $CD8^+$ T-cells were present in the BAL when compared to the URL (**Figure 3.9A, C, and F**), whereas $CD8^+$ T cells were greater in the URL compared to BAL in RSV-infected infant mice (**Figure 3.9B, D, and F**). Although the proportions of $CD8^+$ T cells in adult BAL were significantly higher than that of infants (**Figure 3.9F**), the ratio of $CD8^+$ to $CD4^+$ T-cells was greater in the infant BAL compared to URL. These data indicate that $CD4^+$ and $CD8^+$ T cells accumulate in the adult airway, but

aggregation of $CD8^+$ T cells is more prominent than $CD4^+$ T cells in the BAL. Moreover, frequencies of infant T cells in BAL were significantly diminished compared to adults, which may contribute to delayed RSV clearance among infants.

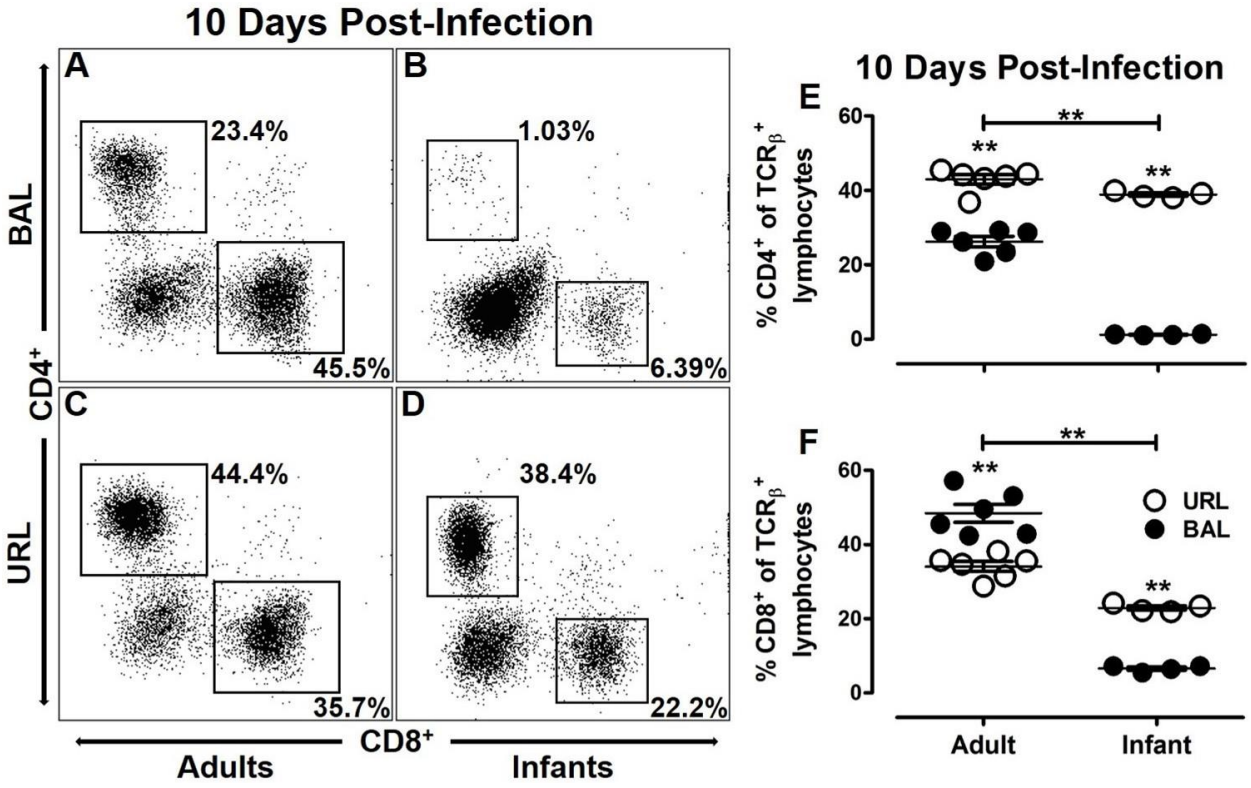

Figure 3.9. Infant T cell accumulation in the BAL is reduced compared to adults.

Adult (6-8 weeks) and infant (PND 4-5) Balb/c mice were infected with RSV L19. BAL and URL were collected at 10 DPI and processed for flow cytometry. The lymphocytes were gated according to typical FSC vs. SSC characteristics. $CD4^+$ and $CD8^+$ T cells were determined from $TCR_\beta{}^+$ cells in the lymphocyte gate. The dot plots represent adult and infant BAL (A & B) and URL (C & D), respectively. The frequencies of $CD4^+$ (E) and $CD8^+$ (F) T cells were compared between URL and BAL by 2-way ANOVA with a Bonferroni post-test. The frequencies of $CD4^+$ (E) and $CD8^+$ (F) T-cells in the BAL (black circles) were compared between age groups using 2-tailed unpaired *t* test. Points represent individual mice (adults) or individual samples from ≥ 2 pooled infants, lines represent the mean of $n \geq 4$ samples per group ± SD; ** ρ-value < 0.01. Data in E & F are representative of 2 independent experiments. ***Originally published in***: Eichinger KM, Kosanovich JL, Empey KM. Localization of the T-cell response to RSV infection is altered in infant mice. *Pediatric pulmonology* 2018;53(2):145-153.

3.2.2.3 T cells within the BAL display an activated phenotype compared to the URL

To determine the effect of age and location on T cell activation, $CD44^{HI}$ expression was compared on $CD4^+$ and $CD8^+$ T cells in the BAL and URL (**Figure 3.10**). Adults and infants had significantly higher $CD44^{HI}$ expression with an increased median fluorescence intensity (MFI) on $CD4^+$ T cells in the BAL when compared to the URL (**Figure 3.10A and B**). Age-based comparisons of $CD44^{HI}$ expression on $CD4^+$ T cells in the BAL demonstrated that adults had significantly higher proportions of $CD4^+$ $CD44^{HI}$ T cells and higher CD44 MFI than infants (**Figure 3.10A and B**). Similarly, frequency of $CD8^+$ $CD44^{HI}$ T cells and the MFI of CD44 on $CD8^+$ T cells was higher in adult compared to infant BAL (**Figure 3.10C and D**). As with the $CD4^+$ T cells, the BAL consistently contained a higher percentage of $CD8^+$ $CD44^{HI}$ T cells in both adults and infants when compared to the URL (**Figure 3.10C**). Age-dependent comparisons revealed a higher MFI of CD44 on $CD8^+$ T cells in adult BAL compared to URL. Infants showed a similar trend, but was not statistically significant. These results suggest that following RSV infection, T cells isolated from the alveolar space (BAL) are more highly activated compared to those isolated from lung tissue (URL).

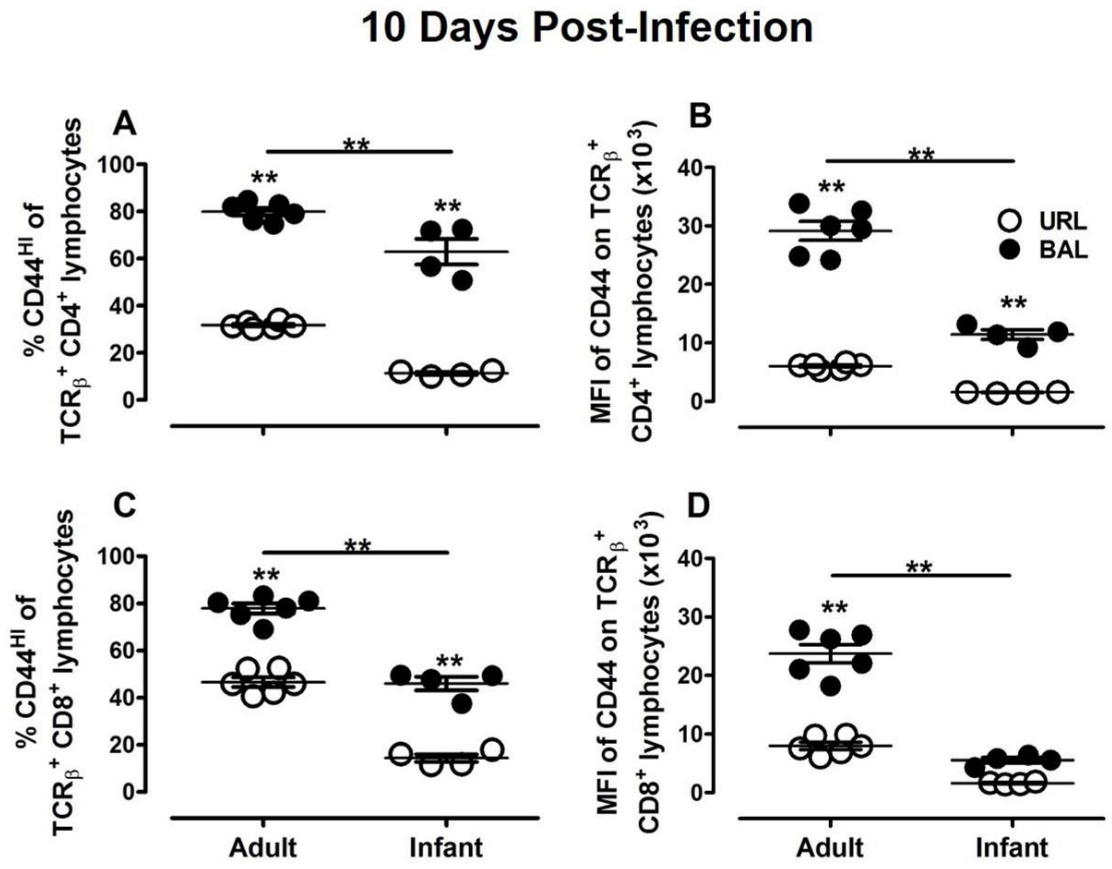

Figure 3.10. T cells isolated from the BAL express an activated phenotype compared to the URL.

Adult (6-8 weeks) and infant (PND 4-5) Balb/c mice were infected with RSV L19. BAL and URL were collected at 10 DPI and processed for flow cytometry. The lymphocytes were gated according to typical FSC vs. SSC characteristics. % $CD44^{HI}$ and MFI were determined from TCR_{β}^{+} $CD4^{+}$ or $CD8^{+}$ T cells in the lymphocyte gate. The $CD4^{+}$ T cell frequencies and MFI of $CD44^{HI}$ $CD4^{+}$ (A and B, respectively) and $CD8^{+}$ T cell frequencies and MFI of $CD44^{HI}$ $CD8^{+}$ T cells (C and D, respectively) were compared between the BAL and URL using 2-way ANOVA with a Bonferroni post-test. $CD4^{+}$ T cell frequencies and MFI of $CD44^{HI}$ $CD4^{+}$ (A and B, respectively) and $CD8^{+}$ T cell frequencies and MFI of $CD44^{HI}$ $CD8^{+}$ T cells (C and D, respectively) from the BAL (black circles) were compared between age groups using 2-tailed unpaired t test. Points represent individual mice (adults) or individual samples from ≥ 2 pooled infants, lines represent the mean of n ≥ 4 samples per group ± SD; ** ρ-value < 0.01. Data in A-D are representative of 2 independent experiments. All $CD44^{HI}$ cells were also $CD62L^{-}$. ***Originally published in***: Eichinger KM, Kosanovich JL, Empey KM. Localization of the T-cell response to RSV infection is altered in infant mice. *Pediatric pulmonology* 2018;53(2):145-153.

3.2.2.4 Localization of Tbet$^+$ CD4$^+$ T cells within the alveolar space is diminished in infant mice

To elucidate the phenotype of activated CD4$^+$ T cells responding to RSV infection at the peak of T cell recruitment (10 DPI), intracellular transcription factor staining of CD4$^+$ CD44^{HI} T cells in the BAL and URL of RSV-infected adults and infants was performed. The ratio of CD4$^+$ CD44^{HI} Tbet$^+$:GATA3$^+$ T cells (using total cell counts), was near zero in adult URL samples but rose significantly in the BAL (**Figure 3.11A**). The frequency of CD4$^+$ GATA3$^+$ T cells remained stable in both URL and BAL (**Figure 3.11B**), indicating that increases in adult CD4$^+$ Tbet$^+$ T cells drove the increased Tbet$^+$:GATA3$^+$ ratio in the BAL (**Figure 3.11A & B**). Strikingly, infants had elevated Tbet$^+$:GATA3$^+$ ratios in their URL and BAL that were comparable to adult ratios in the BAL (**Figure 3.11A**). Analysis of individual Tbet$^+$ and GATA$^+$ cells demonstrated that the majority of Tbet$^+$ cells were migrating to the BAL whereas in the infants, more than half of Tbet$^+$ T cells remained in the URL (**Figure 3.11B**), suggesting an incomplete localization of Tbet$^+$ T cells to the URL of infants. GATA3$^+$ T-cell frequency was higher than that of Tbet$^+$ T cells regardless of age or sample type (**Figure 3.11B**). These data suggest that infants do not localize CD4$^+$ CD44^{HI} Tbet$^+$ T cells to the BAL as efficiently as adults following RSV infection.

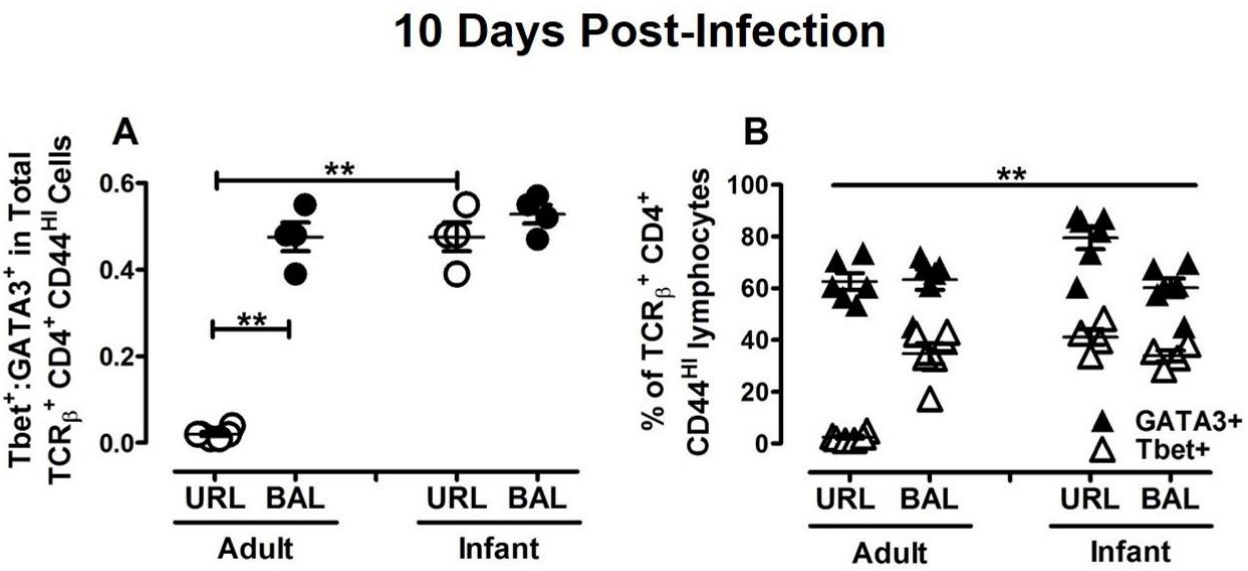

Figure 3.11. Localization of Tbet+ CD4+ T cells in the alveolar space is more efficient in RSV-infected adult compared to infant mice.

Adult (6-8 weeks) and infant (PND 4-5) Balb/c mice were infected with RSV L19. BAL and URL were collected at 10 DPI and processed for flow cytometry. Lymphocytes were gated according to typical FSC vs. SSC characteristics. A ratio of TCR_{β}^{+} $CD4^{+}$ $CD44^{HI}$ $Tbet^{+}$ cells to TCR_{β}^{+} $CD4^{+}$ $CD44^{HI}$ $GATA3^{+}$ cells was calculated from total cell counts of the URL and BAL (A). A 2-way ANOVA was used to compare the $Tbet^{+}$:$GATA3^{+}$ $CD4^{+}$ T cell ratios between sample type and age groups with a Bonferroni post-test (A). The frequency of $CD4^{+}$ $CD44^{HI}$ $GATA3^{+}$ and $Tbet^{+}$ T cells were compared in URL and BAL for adults and infants, respectively (B). The frequencies of $CD4^{+}$ $CD44^{HI}$ $GATA3^{+}$ and $Tbet^{+}$ T cells were compared in URL and BAL using 2-way ANOVA with a Bonferroni post-test (B). Points represent individual mice (adults) or individual samples from ≥ 2 pooled infants, lines represent the mean of $n \geq 4$ samples per group ± SD; ** $\rho < 0.01$. Data in A & B are representative of 2 independent experiments. All $CD44^{HI}$ cells were also $CD62L^{-}$. ***Originally published in***: Eichinger KM, Kosanovich JL, Empey KM. Localization of the T-cell response to RSV infection is altered in infant mice. *Pediatric pulmonology* 2018;53(2):145-153.

3.2.2.5 Delayed RSV clearance in infant BALB/c mice

We previously demonstrated that RSV-infected infant mice have reduced activation and recruitment of innate immune cells and decreased localization of T cells to the site of infection

compared to RSV-infected adults. To examine how these age-based differences in immune responses alter the kinetics of viral clearance, viral titers were quantified from left lung lobes at multiple time points following RSV infection in infants and adults (**Figure 3.12**). Viral titers peaked at 4 DPI in adults and became undetectable after 7 DPI. Infants had lower peak lung titers but virus was detectable as late as 10 DPI indicating more persistent viral growth compared to adults.

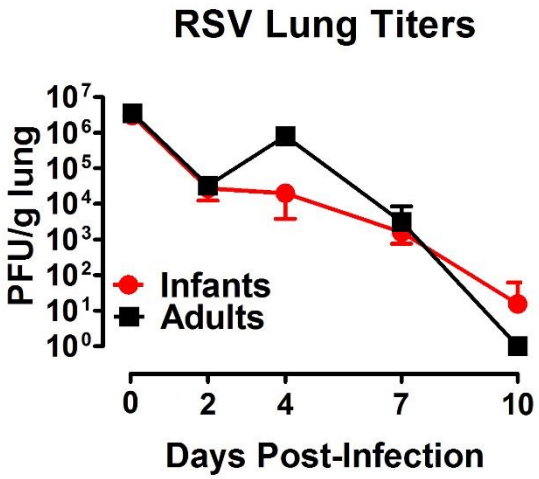

Figure 3.12. Delayed RSV clearance in infant mice.

Adult (8-9 weeks old) and infant (PND 2-4) BALB/c mice were infected with RSV L19. Serial viral titers were determined from the left lung lobe by standard H&E plaque assay. Data provided by KM Empey and JG Orend and published in its original form in: *Empey KM Orend JG, Stokes Peebles R, Egana L, Norris KA, Oury TD, Kolls JK. 2012. Stimulation of immature lung macrophages with intranasal interferon gamma in a novel neonatal mouse model of respiratory syncytial virus infection. PLoS One.*

3.2.2.6 The immunoregulatory role of extracellular adenosine

Our RNA seq data from isolated AMs demonstrated a lack of DGE in infants following RSV infection compared to adults. This lack of transcriptional upregulation in infants included markers of activation and inflammation, such as CD40, CD80, CD86, and TNF-α (data not shown), that aid in cellular recruitment and activation of T cells, which are required for RSV clearance (61). We hypothesized that an immunoregulatory molecule may be present in the extracellular space of the airway, thereby inhibiting AMs response to RSV. One such molecule that has not been investigated in the context of infant RSV infection is the purine nucleoside, adenosine. To investigate adenosine's role in dampening the infant immune response to RSV, extracellular concentrations of adenosine were quantified from BAL and the in-vivo immune response to RSV was evaluated in infant mice who received local delivery of a pan-adenosine receptor antagonist to the lung.

Our lab confirmed that extracellular adenosine concentrations were significantly higher in naïve infant compared to adult BAL (**Figure 3.13**) and may contribute to the age-dependent differential immune responses discussed previously.

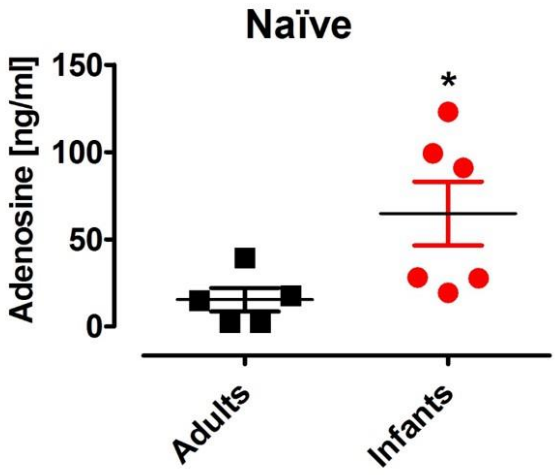

Figure 3.13. Extracellular adenosine elevated in infant airway.

Naïve adult (8-10 weeks old) and infant (PND 7-8) Balb/c mice were mock-infected. After 3 days, BAL was collected and extracellular adenosine was measured using LC-MS/MS. Adenosine concentrations were compared between adults and infants using a Student's t-test; *$\rho < 0.05$. Points represent individual mice, lines represent the mean of $n \geq 5$ samples per group ± SD.

In order to determine how elevated extracellular adenosine levels may affect the infant RSV immune response, DPSPX, a pan-adenosine receptor antagonist was administered i.n to PND 3 infants. A DPSPX concentration of 1 μM was administered and represents a 10 fold higher concentration than that used in in-vitro studies and confirmed to block adenosine signaling (118). DPSPX is negatively charged therefore, we felt confident that it would produce a local effect in the lungs and systemic exposure would remain negligible. Dosing of DPSPX began one day prior to infection to ensure that adenosine receptor blockade was in place at the time of infection and continued daily to completely inhibit adenosine signaling throughout RSV infection. Lastly, i.n. IFNγ was administered on 1, 3, and 5 DPI and served as a positive control. Previous work in our lab demonstrated i.n. IFNγ's capacity to stimulate the infant RSV immune response (1, 119).

Neither IFNγ nor DPSPX treatments inhibited the infant's ability to gain weight when compared to vehicle alone (**Figure 3.14A**). However, only IFNγ treatment significantly reduced virus in the lungs at 5 DPI (**Figure 3.14B**) but virus was undetectable by 10 DPI in all groups, indicating DPSPX treatment did not have a detrimental effect on viral clearance (data not shown).

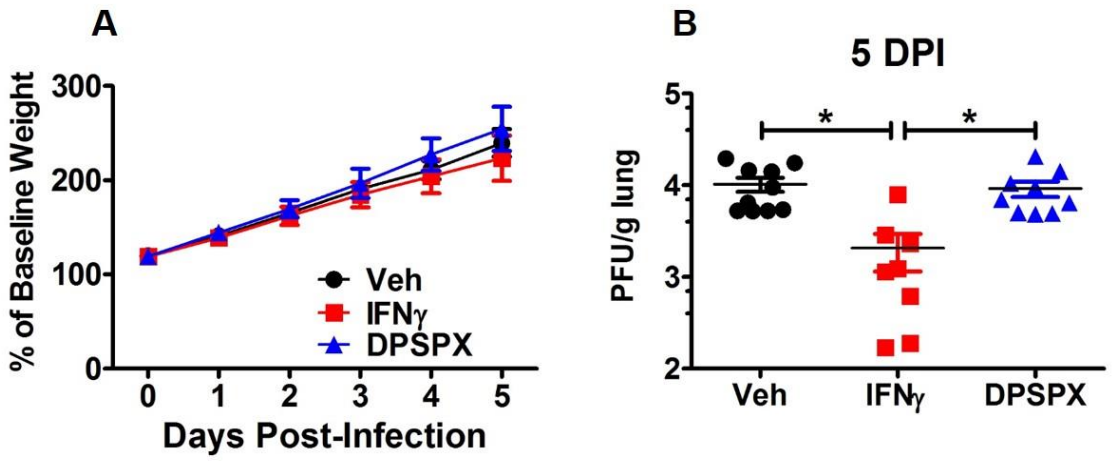

Figure 3.14. DPSPX does not inhibit weight gain or improve viral clearance.

Infant (PND 4) Balb/c mice were infected with RSV L19 and treated with IFNγ on 1, 3, and 5 dpi or DPSPX daily starting at -1 dpi. Mice (litters ≥ 3) were weighed daily beginning at -1 dpi and average weights were compared between groups using 2-way repeated measures ANOVA (A). RSV lung titers were quantified from left lungs collected at 5 dpi using H&E plaque assay (B) and comparisons were made using ANOVA with Tukey's post-test; *$\rho < 0.05$. Points represent individual samples, lines represent the mean of $n \geq 8$ samples per group ± SD.

We hypothesized that AMs, as a primary sentinel of the airway, would be the cell predominately affected by elevated extracellular adenosine concentrations. Adenosine is known to be immunosuppressive in macrophages, which respond to adenosine via 4 transmembrane

adenosine receptors (120). As such, we expected that in the presence of DPSPX, AMs would be stimulated by RSV and exhibit signs of activation.

AMs constituted significantly more SSC^{HI} cells of the BAL in DPSPX-treated infants compared to vehicle at 5 DPI and IFNγ at both time points, which may indicate a lesser degree of cellular recruitment to the BAL in this group (**Figure 3.15A**). Surprisingly, DPSPX treatment had no effect on $CD11b^+$ upregulation at 5 DPI and may have acted to further reduce $CD11b^+$ expression when compared to vehicle at 10 DPI. IFNγ treatment significantly increased $CD11b^+$ expression compared to vehicle and DPSPX at 5 and 10 DPI (**Figure 3.15B**). Blocking adenosine signaling had no effect on $CD73^+$ expression, the ecto-5'-nucleotidase enzyme that converts adenosine monophosphate (AMP) to adenosine, which would be expected to decrease initially with activation then increase to dampen the immune response (121), as was observed with IFNγ (although not statistically significant) (**Figure 3.15C**).

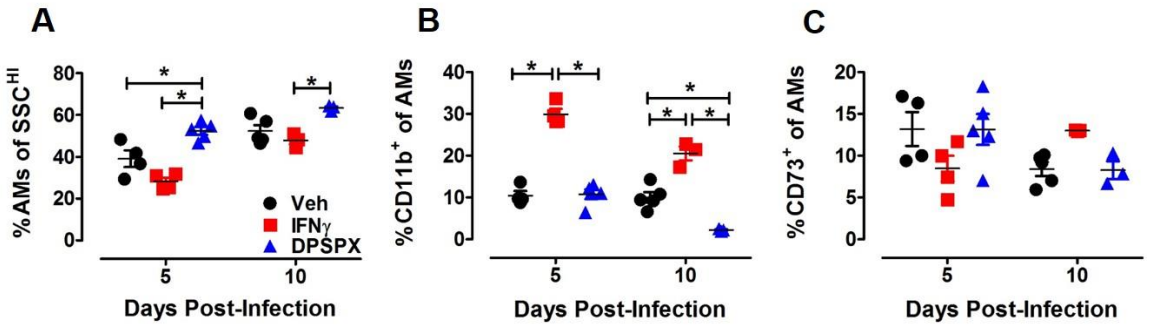

Figure 3.15. DPSPX treatment has no effect on AM activation.

Figure 3.15 (continued) Infant (PND 4) Balb/c mice were infected with RSV L19 and treated with IFNγ on 1, 3, and 5 dpi or DPSPX daily starting at -1 dpi. BAL was collected at 5 and 10 dpi and analyzed for the frequency of AMs and their expression of $CD11b^+$ (B) and $CD73^+$ (C). Comparisons were made between groups using 2-way ANOVA with a Bonferroni multiple comparisons test; $*\rho < 0.05$. Points represent individual samples from ≥ 2 pooled infants, lines represent the mean of $n \geq 3$ samples per group ± SD.

Interestingly, the frequency of DCs in SSC^{HI} cells of the BAL decreased significantly in DPSPX-treated infants compared to IFNγ- and vehicle-treated infants at 5 DPI (**Figure 3.16A**), which may suggest a prior trafficking event to the lymph node for T cell activation. This loss of DCs from the BAL correlated with increased total $CD4^+$ T cells, activated ($CD44^{HI}$ $CD25^+$) $CD4^+$ T cells, and activated Th1-poised ($CD44^{HI}$ $Tbet^+$) $CD4^+$ T cells in the MSLN of DPSPX-treated infants at 5 DPI compared to vehicle and IFNγ-treated animals (**Figure 3.16 B, D, F**). Similar trends were observed for $CD8^+$ T cells but only Th1-poised ($CD44^{HI}$ $Tbet^+$) $CD8^+$ T cells were significantly higher in DPSPX-treated infants (**Figure 3.16 C, E, and G**). This data suggests that DCs may be affected either directly or indirectly by a blockade of adenosine signaling within the airway and subsequently prime for a Th1-poised T cell response.

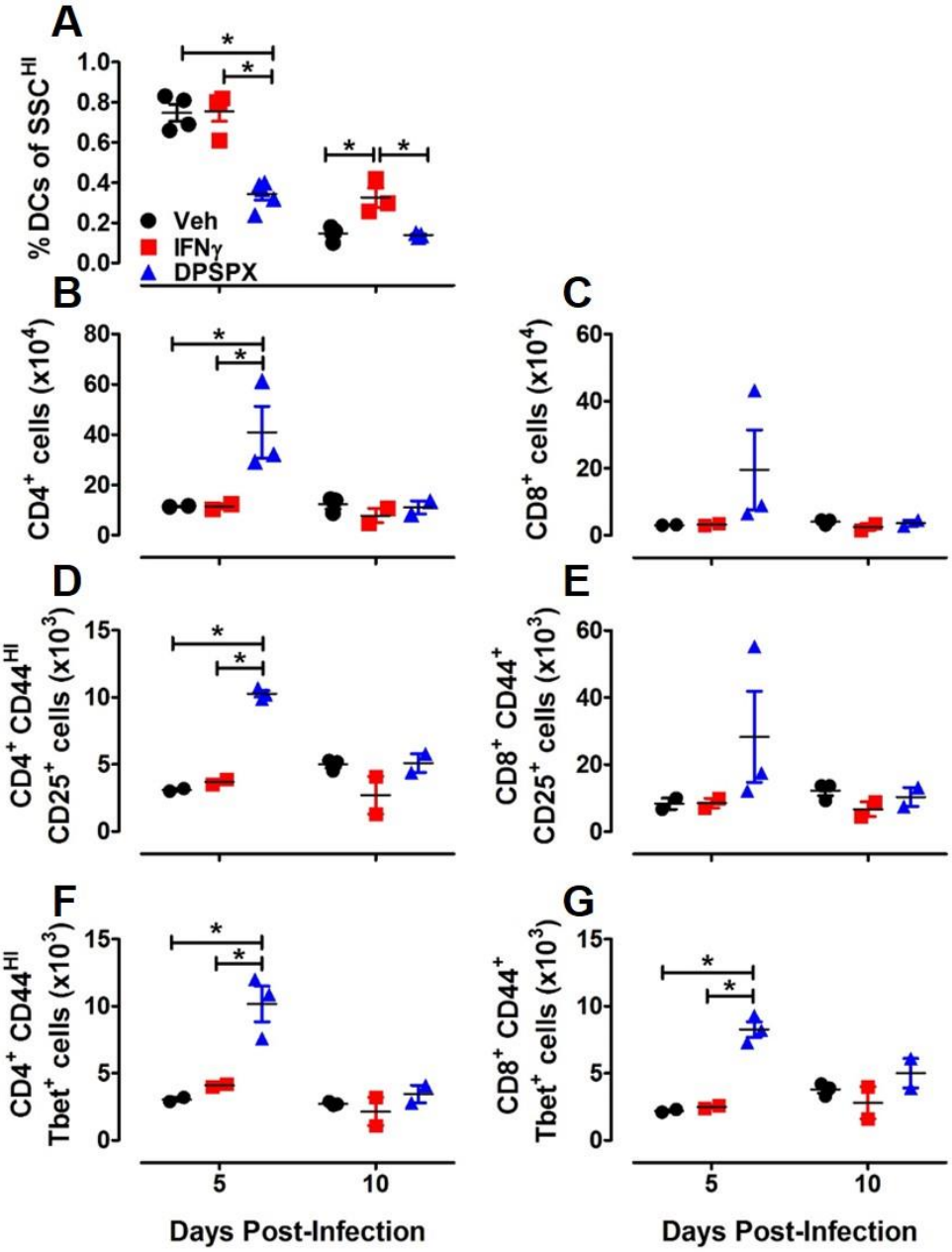

Figure 3.16. DPSPX treatment reduces DCs in the BAL and increases T cell activation in the MSLN.

Figure 3.16 (continued) Infant (PND 4) Balb/c mice were infected with RSV L19 and treated with IFNγ on 1, 3, and 5 dpi or DPSPX daily starting at -1 dpi. BAL was collected at 5 and 10 dpi and analyzed for the frequency of DCs (A; Sig F^- $CD11c^+$ $MHCII^{HI}$). In the MSLN, total $CD4^+$ (B) and $CD8^+$ (C) T cells were quantified from the MSLN and analyzed for expression of the activation markers, $CD44^{HI/+}$ $CD25^+$ (D and E, respectively). The expression of the transcription factor Tbet was analyzed on $CD44^{HI}$ $CD4^+$ (F) and $CD44^+$ $CD8^+$ (G) T cells. Comparisons were made between groups using 2-way ANOVA with a Bonferroni multiple comparisons test; $*\rho < 0.05$. Points represent individual samples from ≥ 2 pooled infants, lines represent the mean of $n \geq 2$-5 samples per group ± SD.

3.3 DISCUSSION

LRTIs represent the largest disease burden worldwide and disproportionately affect infants and children, which is why the scarcity of infant-specific research investigating mechanisms of pathogenicity and immunity in this cohort is concerning. We utilized our neonatal murine model of RSV to demonstrate phenotypic and transcriptional age-based differences in activation of the innate immune response, specifically AMs. Reduced innate activation was associated with distinct differences in the accumulation and phenotypic profiles of T cells within the pulmonary architecture. Moreover, we demonstrated increased concentrations of extracellular adenosine, a previously unidentified immunoregulatory molecule, in infant BAL and by blocking its effects gained insight into its influence on infant RSV immunity.

A number of prior studies have documented the importance of phagocytic mononuclear cells in the early control of respiratory viruses, including RSV (122-125). Neonates are immunologically Th2 biased and highly susceptible to microbial infections, largely due to the immunosuppressive nature of their immune responses, which are thought to prevent destructive

reactions to commensal gut microorganisms (126). In the lung, neonatal mononuclear stimulation through TLR triggering is known to elicit Th2/Th17 cytokine responses, which are thought to protect lung development but may also compromise innate responses that can suppress viral replication (47, 48, 50, 51, 92, 93, 127-132). As the most abundant phagocytic mononuclear cell in the alveolar sacs, AMs play a central role in coordinating immunity through cytokine production, recruitment of lymphocytes, antimicrobial activity, phagocytosis/efferocytosis, and tissue repair (133-137). Our study showed that infant AMs have reduced expression of activation markers, like $CD11b^{+}$, $CD80^{+}$ $MHCII^{+}$, and $SR\text{-}A^{+}$, compared to RSV-infected adults. Additionally, we correlated $CD11b^{+}$ expression on AMs with increased expression of the other markers of activation compared to $CD11b^{-}$ AMs, re-enforcing CD11b's place as a marker of acute inflammation. Reduced $CD11b^{+}$ expression on infant AMs with reductions in the other activation markers, suggests infant AMs suppress a pro-inflammatory AM phenotype. In correlation with our results, increased expression of $CD11b^{+}$ has been shown to occur on resident AMs during periods of acute inflammation in response to LPS or viral challenge (107). CD11b is a leukocyte integrin that binds to intercellular adhesion molecule, iC3b (cleaved product of complement 3b), and fibrinogen (138). Transient expression on AMs is likely involved in cell adhesion and phagocytosis but it is still not completely clear if inflammation associated with CD11b expression is mediated directly through the receptor or indirectly through AMs displaying the receptor (108).

Age-based alterations in phenotypic signals of enhanced AM activation led us to investigate differences in transcriptional regulation between naïve and RSV-infected adult and infant AMs, to better understand the underlying mechanisms limiting infant AM activation. RNA sequencing of AMs demonstrated a profound deficit in differential gene expression in infants compared to adults in response to RSV infection. Although the analysis of our RNA seq data is

not yet complete and we hope to gain a better understanding of the potential consequences of reduced differential gene expression in infants through pathway analysis, results from clinical studies have also identified genetic differences that influence RSV disease severity. Polymorphisms in cytokine genes have been found to modify illness severity and frequency of complications in infants with severe RSV (139), including IFNγ polymorphisms associated with increased severity of illness, duration of stay in the intensive care unit, and frequency of otitis media. IFNγ was originally described as macrophage-activating factor and orchestrates antimicrobial/antitumor mechanisms, and antigen processing and presentation pathways in macrophages (140). We have previously demonstrated an absence of IFNγ in the BAL of RSV-infected infant mice (1) and a lack of IFNγ may be contributing to reduced activation and minimal differential gene expression in infant AMs and will be further explored in upcoming chapters.

The phenotypic and transcriptional data demonstrating reduced AM activation in RSV-infected infants are likely indicative of functional deficits as well, and at least partially responsible for the reduced recruitment of DCs and monocytes. Clinical studies have demonstrated functional deficits in IL-6 (141) and TNFα (132) production or diminished HLA-DR expression (142) from/on monocytes isolated from pre-term infants. Moreover, neonatal plasmacytoid DCs exposed to viruses are significantly impaired in their release of type 1 interferons compared to adults (143), which, when combined with functional defects in monocyte activation, compromises an infant's ability to suppress viral replication. In addition to compromised innate anti-viral activity, reduced recruitment of DCs and monocytes can significantly impair the engagement of an adaptive immune response as DCs and monocytes have substantial roles in antigen presentation (144-146).

Infants have a dramatically reduced T-cell response compared to adults. Although infants had lower T-cell frequencies in lung tissue compared to adults, the differences were most striking

in the BAL, where average $CD4^+$ and $CD8^+$ T cell frequencies were reduced by 95% and 86% (**Figure 3.9**), respectively. Previous reports have demonstrated reduced and delayed infant T-cell responses when compared to adults in models of influenza, methicillin-resistant *Staphylococcus aureus* pneumonia, and *Pneumocystis carinii* pneumonia (102, 147, 148). A similar observation was made when infant and adult lung tissues were compared following primary RSV infection whereby the frequencies of infant $CD44^{HI}$ $CD62L^{LO}$ $CD4^+$ and $CD8^+$ T cells were significantly lower than that of adults (149). Consistent with work published by Tregoning et al., the current study demonstrated reduced $CD8^+$ T-cell frequencies in infant lung tissue. More importantly, data presented here showed the most dramatic age-dependent differences in the T-cell response following RSV infection occurred in the BAL, similar to findings published by Lines et al., in a neonatal murine model of influenza (102). In the infant influenza model, delayed viral clearance was associated with poor T cell accumulation in the BAL despite a vigorous T cell response in the interstitium (102). Moreover, the reduced T cell frequency in infant compared to adult airways is consistent with our previous findings demonstrating prolonged viral detection in RSV-infected infants compared to adults (1). In addition to quantitative T cell defects, these data suggest environmental or cellular differences are also important in regulating the activation phenotypes of T cells in the infant alveolar space.

A second critical finding generated from these studies was the higher proportion of activated T cells in the BAL compared to lung tissue (**Figure 3.10**). Specifically, a greater proportion of T cells isolated from the alveolar space of both adults and infants were effector/memory T cells ($CD4^+$/$CD8^+$ $CD44^{HI}$ $CD62L^-$) compared to T cells from lung homogenate. These findings are consistent with previous studies demonstrating that RSV infects the superficial cells of the upper and lower airways. In-vitro studies of RSV infection in primary

human cartilaginous airway epithelium, as well as histologic studies in RSV-infected patients, have consistently demonstrated the virus' tropism for ciliated epithelium while sparing goblet cells and underlying basal epithelial cells (36, 98, 150, 151). Moreover, Lukens et al. found larger proportions of activated and RSV-specific $CD8^+$ T cells in the airways of adult mice compared to lung tissue (152). Contrary to reports highlighting the functional inactivation of RSV-specific $CD8^+$ T cells in the lung parenchyma (152, 153), they also showed that RSV-specific $CD8^+$ T cells isolated from the BAL remained functionally active through 21 DPI (152). This was in sharp contrast to RSV-specific $CD8^+$ T cells isolated from lung homogenate whose production of IFN-γ dramatically decreased by ~43% between 8 and 21 DPI (152). Collectively, these results suggest that localization of T cells within the airway is important when considering their activation and functional status in response to RSV infection.

The importance of $CD8^+$ T cells in the clearance of RSV is widely appreciated (61, 94, 95, 154) but what may be less recognized is the location of these cells within the pulmonary architecture in RSV-infected infants versus adults. In our study, adult $CD8^+$ T cells were found in high frequencies in the air space where these cells made up a larger proportion of the lymphocytes (mean 48%) than in lung homogenate (mean 34%). Infants displayed a starkly different distribution, with higher frequencies of $CD8^+$ T cells in lung homogenate (mean 22.9%) compared to BAL (mean 6.6%). The accumulation of $CD8^+$ T cells in the adult airway suggests that high frequencies of $CD8^+$ T cells within the alveolar space is an important factor in effective RSV clearance, yet a similar $CD8^+$ T cell response is remarkably absent in infants.

Another important age-dependent distinction was the location of $CD4^+$ $Tbet^+$ T cells within the lung architecture. $CD4^+$ $CD44^{HI}$ $Tbet^+$ T cell responses accumulated in the airways of adult animals but were split between the lungs and airways of infants (**Figure 3.11**). The frequency of

effector memory $CD4^+$ T cells was higher in the BAL of RSV-infected infants than the lung tissue, yet infants still had significantly lower percentages than adults. Phenotypic analysis of $CD4^+$ effector memory cells revealed that adults had a higher $Tbet^+$ expression compared to infants. Although $GATA3^+$ $CD4^+$ T cells were found with high frequency throughout sample types and across age-groups, $Tbet^+$ $CD4^+$ T cells were virtually undetectable in adult lung homogenate and instead were found predominately in the BAL. In infants, $CD4^+$ $Tbet^+$ T cells were distributed throughout the lung tissue and airway with equal frequency, suggesting that while adults mount a pointed $CD4^+$ $Tbet^+$ T cell response at the site of RSV infection, the infant $CD4^+$ $Tbet^+$ T cell response was less focused, possibly leading to more immune-mediated pathology.

One criticism of the infant murine model of RSV has been the fact that RSV does not replicate as readily in infant mice as it does in adults. Clinically, RSV symptoms track with viral titers (78) and although mice do not develop clinical symptoms of RSV, reduced viral replication in infant mice could compromise the recruitment of T cells to the airspace. Nevertheless, quantitative and qualitative defects in infant T cell responses have been demonstrated in other viral illnesses like influenza (102). Additionally, we demonstrated that $CD8^+$ T cells in RSV-infected adults preferentially accumulate within the lumen of the airway, which did not occur in infants despite the continued presence of RSV in the infant airway at 10 DPI (Figure 3.12). Therefore, lower RSV titers in infants is unlikely to be the primary cause of the differences in T cell responses demonstrated in RSV-infected infants and adults.

Adenosine is an endogenous purine nucleoside with immunoregulatory properties that appears in extracellular spaces during metabolically stressful conditions, such as inflammation, ischemia, and cellular damage (106, 155-157). In the extracellular space, adenosine binds to adenosine receptors (A_1, A_{2A}, A_{2B}, and A_3) expressed on macrophages and monocytes and

modulates the inflammatory responses induced through TLR stimulation (106, 120). In this way, extracellular adenosine provides macrophages with a gauge of the intensity of stressful stimuli and allows them to modify their responses to limit immunopathology (106, 120).

Published reports have shown that infant plasma contains elevated concentrations of extracellular adenosine that divert normal Th1 TLR agonist responses to Th2/Th17-type cytokine responses (92, 93, 158). In the plasma, increased extracellular adenosine concentrations are mediated by the higher adenosine generating capacity of soluble enzymes, soluble 5'-nucleotidase and alkaline phosphatase, in neonatal blood (159). However, in this report we demonstrated that extracellular adenosine concentrations are elevated in the airways of infant mice compared to adults under homeostatic conditions. We hypothesized that elevated extracellular adenosine concentrations in the airways of infant mice may compromise the AM response to RSV infection but pan-adenosine receptor blockade with DPSPX would enhance AM activation. Contrary to our original hypothesis, DPSPX treatment did not lead to robust inflammation, as animals continued to gain weight normally. Nor did treatment hasten viral clearance as DPSPX and vehicle treated animals had similar viral titers. Only IFNγ treatment reduced viral titers, as we have previously demonstrated (1). Surprisingly, adenosine receptor blockade during RSV infection did not appear to enhance AM activation. The frequency of AMs in the BAL increased in animals treated with DPSPX, which may be reflective of a reduced inflammatory cell recruitment compared to the other groups. Additionally, adenosine receptor blockade did not result in signals of AM activation, as measured by increased expression of $CD11b^{+}$ and $CD73^{+}$. Even in the absence of adenosine signaling, this lack of activation may be due in part to inefficient TLR4 triggering (92) in infant AMs by RSV F protein (3). As expected, IFNγ treatment increased AM CD11b expression across both time points. Prolonged expression of the activation marker $CD11b^{+}$ on AMs in response to

IFNγ treatment is indicative of the adenosine de-sensitizing effect IFNγ has on macrophages, whereby IFNγ STAT1 signaling prevents adenosine receptor induction and extends the macrophage's inflammatory effects (120). Enhanced AM $CD73^{+}$ expression in IFNγ treated animals at 10 DPI likely represents an attempt by AMs to increase extracellular adenosine through CD73 activity, thereby dampening inflammation via adenosine receptor signaling and preventing immunopathology.

Interestingly, DPSPX treatment appeared to play a role in DC activation and the subsequent priming of $CD4^{+}$ and $CD8^{+}$ T cells in the lymph node. Animals treated with DPSPX had more activated ($CD44^{HI}$ $CD25^{+}$) $CD4^{+}$ and $CD8^{+}$ T cells in their lymph nodes and more activated T cells poised to produce IFNγ through the expression of the transcription factor Tbet. It is possible that adenosine receptor blockade directly or indirectly affected dendritic cells, leading to their enhanced activation and migration to the lymph node. However, a limitation of this study may be the time points analyzed. AM activation in the presence of DPSPX may have peaked very early in infection and was steadily declining at 5 dpi. Our study is also limited by small sample sizes and a small array of markers to analyze AM activation. Nevertheless, these results give insight into adenosine as a previously unrecognized immunoregulatory molecule, present in higher concentrations in the airways of infants, that modulates the innate infant RSV immune response.

Using our neonatal mouse model of RSV, we have demonstrated through phenotypic and differential gene expression data that infant AMs have reduced activation in response to RSV infection compared to adults. Decreased stimulation of the innate immune response may be partially influenced by the presence of elevated levels of extracellular adenosine in infant airway. An inefficient innate immune response has serious consequences on the induction of effective adaptive immunity, including infant T cell priming and recruitment to alveolar spaces. These

studies provide important information regarding the multi-level regulation of infant immunity and lend support to the hypothesis that simply blocking the effects of extracellular regulatory molecules in the milieu of the airway may not be enough to stimulate infant innate immunity. A combinatorial approach whereby the effects of immunoregulatory molecule(s) are blocked and direct stimulation is applied may be required to elicit effective infant RSV immunity.

4.0 IFN-GAMMA IMMUNOMODULATION

This chapter is adapted from the following published manuscripts:

Katherine M. Eichinger, Erin Resetar, Jacob Orend, Kacey Anderson, Kerry M. Empey

Age predicts cytokine kinetics and innate immune cell activation following intranasal delivery of IFNgamma and GM-CSF in a mouse model of RSV infection. *Cytokine*, 2017. 97: 25-37. (© Elsevier Ltd.),

Katherine M. Eichinger, Loreto Egaña, Jacob G. Orend, Erin Resetar, Kacey B. Anderson, Ravi Patel, Kerry M. Empey

Alveolar macrophages support interferon gamma-mediated viral clearance in RSV-infected neonatal mice. *Respiratory Research*, 2015. 16: 122. (© Eichinger, et al.),

and

Katherine M. Eichinger, Jessica L. Kosanovich, and Kerry M. Empey

Localization of the T-cell response to RSV infection is altered in infant mice. *Pediatric Pulmonology*, 2018. 53 (2): 145-153. (© Wiley Periodicals, Inc.).

4.1 INTRODUCTION

Conventional immunization strategies that depend on antigen specificity and conditioning of the adaptive immune response continue to be a primary focus of ongoing research, yet there remains no licensed vaccine for RSV or many other viral pathogens associated with childhood bronchiolitis (160). Infants, unlike older children and adults, have a limited capacity to sustain an efficient

memory response to vaccination due to limited prior antigen exposure and a suppressive lung environment that favors production of Th2-polarizing cytokines (59, 161, 162). Therefore, non-clonal stimulation of innate immunity is a viable strategy to prevent or treat viral-mediated infant bronchiolitis.

Stimulation of the innate host immune response with immune potentiators is gaining attention for their prospective application in populations with limited immune responses to antigenic stimuli or against pathogens for which vaccines do not exist. The macrophage-activating cytokine, IFNγ, is a commercially available immune potentiator used to prevent infections in patients with chronic granulomatous disease (163, 164). Despite the reported anti-viral activity, systemic toxicity with immune potentiating cytokines discourages their use in vulnerable patient populations, including young children. In adults, however, inhaled delivery of IFNγ largely bypasses systemic exposure and was shown to be well tolerated in clinical studies among healthy adults and adults with lung disease (165-167). A recent study further showed that local cytokine delivery to the lungs of influenza-infected mice improved disease outcomes to a greater degree when cytokine was retained in the airway using quantum dots (168). Yet, pulmonary absorption of immune potentiating cytokines from the infant lung remains unknown and limits the utility of this therapeutic strategy in young children.

AMs constitute 90-95% of the leukocytes in the alveoli at baseline, help to maintain homeostasis, and serve as the first line of defense against inhaled pathogens (168). They clear invading organisms through phagocytosis and microbicidal enzymes while regulating inflammatory responses through secretion of pro- and anti-inflammatory cytokines (107, 109, 133). Pulmonary DCs further contribute to the anti-viral cytokine milieu in the lung during viral infections and are essential for antigen presentation and initiation of adaptive immunity (144, 169,

170). However, efficient anti-viral cytokine production and engagement of the adaptive immune response depends largely on AM and DC maturation, suggesting that the Th2-dominant infant lung environment limits maturation and activation of innate immune cells and their anti-viral activity (171-173). Harker and colleagues showed enhanced innate immune cell activation and viral clearance following infection with recombinant RSV expressing IFNγ (174). Thus, local exposure to pro-inflammatory cytokines in the lung is critical for proper innate cell maturation and disease resolution. We demonstrated (**Chapter 3**) substantial age-based genomic differences in AMs isolated from naïve as well as, RSV-infected mice, which provides detailed information regarding defects in infant AM maturation in response to RSV. Additionally, our lab showed that i.n. IFNγ administration during infant RSV infection increases markers of antigen presentation and co-stimulation on AMs (1) but the specific role these stimulated cells have on the resolution of RSV is unknown.

Activation of the innate immune system is a critical link in the development of an effective adaptive immune response (144, 170). It is well appreciated that T cells are essential for RSV clearance (61, 95, 97) but Th2-biased T cell responses lead to pathology and airway hyperreactivity (175). Numerous studies have demonstrated infants' Th2 biased responses to RSV, however those with higher Th1 responses are associated with improved disease outcomes (176-178), expedited viral RSV clearance, and reduced Th2-driven pathogenesis (95, 179). Neonatal mice have demonstrated the ability to mount effective Th1 responses given the appropriate co-stimulation, such as IL-12 and/or IFNγ (180, 181). However, the ability of IFNγ to alter the T-cell phenotype of RSV-infected infants has not been investigated.

To gain a better understanding of how local administration of IFNγ affects infant RSV infection, we determined age-based IFNγ kinetic parameters, calculating and testing an IFNγ dose

capable of reaching adult-like exposure. We also examined the role of IFNγ-stimulated AMs in-vivo and showed that IFNγ's viral reducing potential is shared by AECs and AMs. Additionally, our study offers new insight into how local administration of IFNγ alters infant T cell phenotypes and $CD8^+$ T cell RSV specificity. We hypothesize that IFNγ will act locally in the lung, activating innate immune cells, which will increase recruitment of T cells to the airspace.

4.2 RESULTS

4.2.1 IFNγ elimination rates are reduced in infants compared to adults following intranasal delivery

Cytokines are broken down by proteolysis into individual amino acids or are otherwise distributed out of the central compartment from which they are produced and secreted. To determine if these elimination processes are age-dependent in the local lung environment, a single, weight-based dose of IFNγ was delivered i.n. to adult and infant Balb/c mice. A total of 16ng/g of body weight was delivered providing 1.52ng and 1.07ng of IFNγ per mg of lung in infants and adults, respectively (**Table 4.1**). IFNγ concentrations were then determined at nine separate time points from digested lung tissue and blood ranging from time zero through 48-hours post-dose.

Table 4.1. Age-based pulmonary IFNγ dosing

	IFNγ dose/body wt.	Avg. body wt.	Total avg. IFNγ dose	Avg. lung wt.	IFNγ delivered/lung wt.
Infants (PND4)	16ng/g	5.83g	93ng/10µl	61mg	1.52ng/mg
Adults (8-10wks)	16ng/g	21g	320ng/100µl	298mg	1.07ng/mg

IFNγ (interferon gamma)

A non-compartmental pharmacokinetic analysis was performed to elucidate age-dependent differences for key pharmacokinetic parameters (**Table 4.2**). Adult mice demonstrated a rapid increase in IFNγ concentrations in the lung, peaking one hour after intranasal delivery (**Figure 4.1A; Table 4.2**). The majority of IFNγ was cleared from the lungs by 12 hours post-administration, which is further reflected by a mean residence time (MRT) of only 20 hours. Terminal elimination from adult lungs was calculated from 12 to 48 hours post-dose and was used to generate the elimination half-life ($t_{½}$) of 14 hours, suggesting that IFNγ would be cleared from the lungs within 56-70 hours after delivery (4-5 half-lives) (**Figure 4.1C**, solid line). The terminal elimination half-life was 16 hours in infant mice as demonstrated by the reduced slope (**Figure 4.1C**, dashed line). Consistent with lung, terminal elimination of IFNγ from the blood was also more rapid in adult compared to infant mice (**Figure 4.1D**). Moreover, the average IFNγ area under the concentration time curve (AUC) in the blood of adult animals was markedly reduced compared to the lung (**Figure 4.1A**), suggesting that the majority of IFNγ is metabolized directly in the lung and/or not absorbed systemically. A closer look at the first 4 hours after intranasal delivery revealed a 2-hour delay in peak blood concentrations from that achieved in the lung (**Figure 4.1A**, inset), indicating that pulmonary absorption does not occur immediately. Many age-

dependent differences in IFNγ kinetics were noted between infants and adults. Specifically, AUCs and peak concentrations achieved in infant lungs were dramatically lower than that achieved in adults **(Figure 4.1B; Table 4.2),** despite identical weight-based dosing. This discrepancy may reflect reduced efficiency in cytokine delivery to the narrow infant airways or higher lung to body weight ratios in infants compared to adults. Unlike adults, infants demonstrated bi-modal IFNγ peak concentrations (C_{pk}) in the lung 1 and 8-hrs after delivery **(Figure 4.1B)**, possibly due to stimulation of endogenous IFNγ-secreting immune cells. Twelve and 48 hours were used to calculate the elimination $t_{½}$ of 16 hours, indicating ~64-80 hours would be required to clear IFNγ from infant lungs. Consistent with their longer $t_{½}$, infants compared to adults had a more gradual terminal elimination slope reflective of a reduced rate of IFNγ clearance from infant compared to adult lungs **(Figure 4.1C; Table 4.2)** Interestingly, IFNγ C_{pk} in the blood of infants was delayed by 6 hours compared to the 2-hour delay in adults, indicating that pulmonary absorption occurs more slowly in infants. Unlike cytokine clearance in the lung, only 31% of total IFNγ measured in the blood was cleared by 4 hours in infant mice, which is further reflected in the extended MRT of 102 hours compared to a MRT of 3.73 hours in adults. Together, these data describe important age-dependent differences in IFNγ kinetics following intranasal delivery, including reduced AUC, C_{pk}, and pulmonary clearance in infants compared to adults.

Table 4.2. Pharmacokinetic parameters following intranasal IFNγ

	IFNγ	AUC (ng*hr/ml)	Cl (ml/hr)	Cpk (ng/ml)	Time of Pk Conc (hrs)	MRT (hrs)	% cleared in 1, 4, 12hrs
Lung	Infants	79.19	0.55	10.07	1	14.62	51%, 81%, 99%
	Adults	285.95	1.12	29.05	1	20	43%, 82%, 98%
Blood	Infants	1.61	26.86	0.13	6	102	5%, 31%, 93%
	Adults	14.82	21.60	1.2	2	3.73	9%, 78%, 99%

IFNγ (interferon gamma); AUC (area under the curve); Cpk (peak concentration); MRT (mean residence time)

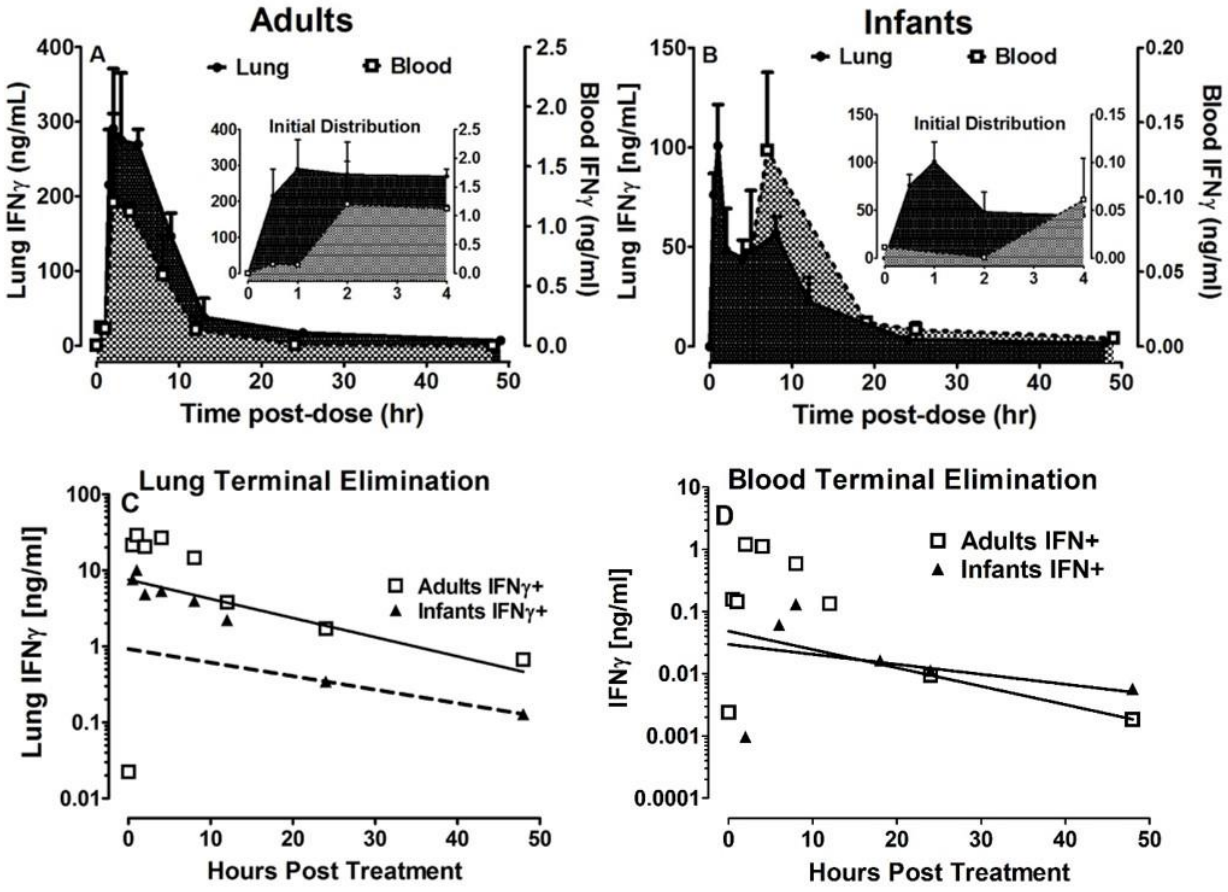

Figure 4.1. The pharmacokinetic profile of i.n. IFNγ depends largely on age at the time of administration.

Figure 4.1 (continued) Adult and infant Balb/c mice were treated with a single i.n. dose of IFNγ (16ng/gm). IFNγ concentrations were subsequently measured in homogenized lung tissue and serum at the indicated times. (A) Adult and (B) infant IFNγ concentrations in the lung (y-axis) and blood (z-axis) were reported on discriminate scales to accommodate differential concentration ranges; insets provide more detailed depiction of the kinetic changes during the early time points (0-4 hours). Data was transformed on a log scale to identify the terminal elimination phase of IFNγ in adult and infant (C) lungs and (D) blood. Each time point represents the mean of $n = 3$ samples per group ± SD. ***Originally published in***: Eichinger KM, Resetar E, Orend J, Anderson K, Empey KM. Age predicts cytokine kinetics and innate immune cell activation following intranasal delivery of IFNgamma and GM-CSF in a mouse model of RSV infection. *Cytokine* 2017;97:25-37.

4.2.2 Intranasal IFNγ increases innate recruitment and activation in RSV-infected infant mice

We previously demonstrated in Chapter 3 that infant mice had reduced recruitment of monocytes and DCs (**Figure 3.2 A, B and C, D**, respectively) in response to RSV infection when compared to adults. Additionally, the activation of infant AMs (**Figure 3.3**) was also reduced compared to adults following RSV infection. To determine if local IFNγ administration could increase inflammatory innate cell recruitment and activation of AMs, i.n. IFNγ was administered to infant mice on days 1, 3, and 5 post-RSV infection and immunophenotyping of cells isolated from the airway performed using flow cytometry. The frequency of monocytes (monos; Sig F^- $CD11c^+$ $CD11b^+$) in the BAL of IFNγ treated infants increased significantly by 3 DPI and remained elevated through 10 DPI compared to naïve and RSV+ infants (**Figure 4.2A**). The proportion of DCs (Sig F^- $CD11c^+$ MHCII ^{HI}) in the BAL also rose significantly in IFNγ-treated infants when compared to naïve (**Figure 4.2B**).

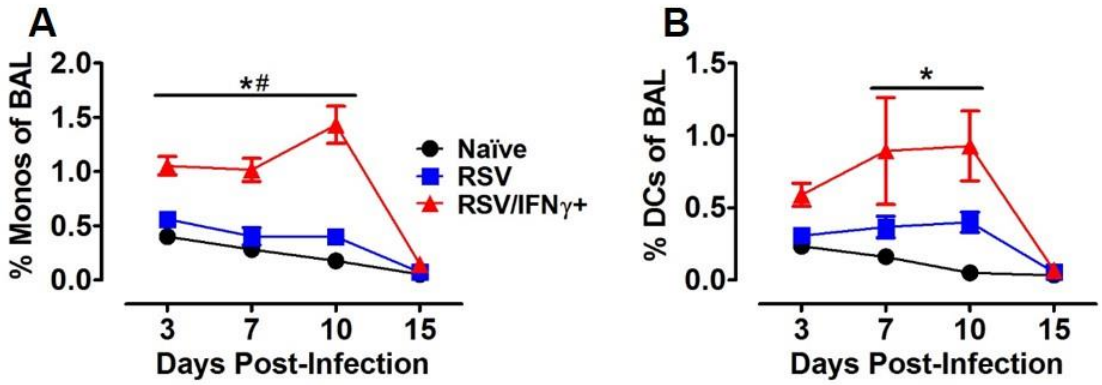

Figure 4.2. IFNγ treatment increases innate recruitment in RSV-infected infants.

Infant (PND 4-5) Balb/c mice were infected with i.n. RSV L19. Intranasal IFNγ (16ng/g) or vehicle was administered on 1, 3, and 5DPI. BAL was collected at 3, 7, 10, and 15 DPI and processed for flow cytometry. Frequencies of monocytes (monos) and DCs were calculated. The percentage of monos (A) and DCs (C) comprising the BAL were compared between naïve, RSV+, and RSV/IFNγ+ mice using 2-way ANOVA with Bonferroni post-test. Data points represent the mean of $n \geq 3$-4 samples (2-3 infant BALs pooled per sample) per group ± SD; * and # ρ-value < 0.05. * signifies a statistical difference between naïve and RSV/IFNγ+ and # between RSV and RSV/IFNγ+.

Unsurprisingly, IFNγ, a known macrophage-activating cytokine, led to increased expression of surface markers indicating activation on AMs in the BAL of IFNγ-treated infants. The proportion of AMs in the BAL of IFNγ-treated infants was significantly reduced at 7 and 10 DPI (**Figure 4.3A**) compared to naïve and RSV+ infants. This likely occurred due to increased infiltration of innate inflammatory cells into the BAL, such as previously mentioned monocytes and DCs. Expression of the activation markers $CD11b^+$ and $CD80^+$ were significantly increased in IFNγ-treated infants as early as 3 DPI and remained elevated through 10 DPI (**Figure 4.3B, C**). Upregulation of $MHCII^+$ was slightly delayed compared to $CD11b^+$ and $CD80^+$ with increased expression as a result of IFNγ treatment occurring at 7 and 10 DPI before dropping to near baseline

levels by 15 DPI (**Figure 4.3D**). IFNγ augmented the expression of SR-A when compared to RSV+ but followed a similar expression pattern as RSV+ infants with increases seen early and late in RSV infection at 3 and 15 DPI, respectively (**Figure 4.3E**).

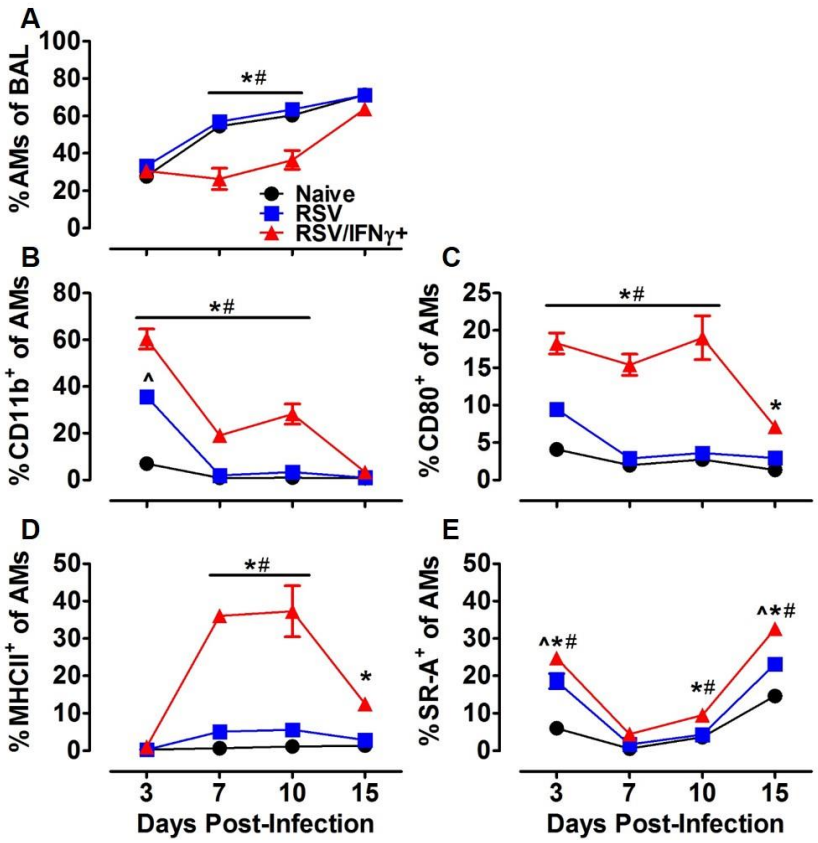

Figure 4.3. AM activation in RSV-infected infants increases with IFNγ treatment.

Figure 4.3 (continued) Infant (PND 4-5) Balb/c mice were infected with RSV L19. Intranasal IFNγ (16ng/g) or vehicle was administered on 1, 3, and 5 DPI. BAL was collected at 3, 7, 10, and 15 DPI and processed for flow cytometry. Frequencies of AMs and their expression of surface activation markers were calculated and compared between naïve, RSV+, and RSV/IFNγ+ mice using 2-way ANOVA with Bonferroni post-test. Data points represent the mean of n ≥ 3-4 samples (2-3 infant BALs pooled per sample) per group ± SD; * , ^ and # ρ-value < 0.05. * signifies a statistical difference between naïve and RSV/IFNγ+, # between RSV and RSV/IFNγ+, and ^ between naïve and RSV+.

Although repeated treatment with intranasal IFNγ at a dose of 16ng/g resulted in increased recruitment of innate cells and activation of AMs in infant mice, we know from our pharmacokinetic analysis that IFNγ exposure was lower in infants than adults after a single, i.n. IFNγ dose. In fact, average, adult AUCs were 3.6 times greater than AUCs in infant mice (**Table 4.2**). This was associated with significant increases in the expression of MHCII on adult compared to infant $CD11c^{+}$ $CD11b^{-}$ cells through 48 hours **(Figure 4.4)**.

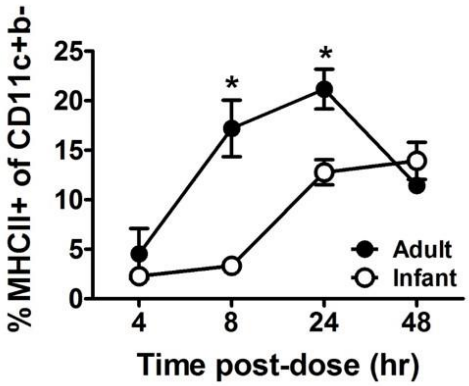

Figure 4.4. Age-dependent IFNγ pharmacokinetics affect innate activation.

Figure 4.4 (continued) A single, i.n. IFNγ dose (16ng/g) was administered to naive infant (PND 4-5) and adult (8-10wks) Balb/c mice. Whole right lung was harvested at the indicated times post-dose and processed for flow cytometry. $MHCII^+$ expression on myeloid cells ($CD11c^+$ $CD11b^-$) was compared between infants and adults using 2-way ANOVA with Bonferroni post-test. Data points represent the mean of $n = 3$ samples per group ± SD; * ρ-value < 0.05. ***Originally published in***: Eichinger KM, Egaña L, Orend JG, Resetar E, Anderson KB, Patel R, Empey KM. Alveolar macrophages support interferon gamma-mediated viral clearance in RSV-infected neonatal mice. *Respiratory research* 2015;16:122.

To optimize infant IFNγ AUCs and subsequent innate cell activation, a non-compartmental pharmacokinetic approach, as described in our methods, estimated a new 60ng/g dose of i.n. IFNγ would be required to achieve adult-level AUCs (280ng*hr/ml) in the infant mice. Thus, we predicted that 60ng/g of i.n. IFNγ would generate faster and greater expression of MHCII on $CD11c^+$ $CD11b^-$ cells with enhancement of RSV clearance.

To test the effect of IFNγ dose response on myeloid cell activation and viral clearance, RSV-infected infant mice receiving PBS (vehicle) only were compared to those treated with 16 or 60ng/g of IFNγ. Significant differences in IFNγ BAL concentrations occurred as soon as 4 DPI and dissipated over time reflecting the end of IFNγ dosing at 5 DPI (**Figure 4.5A**). Despite its potential for toxicity, neither the 16ng/g nor the 60ng/g IFNγ groups demonstrated significant impairment in weight gain compared to PBS-treated controls over the course of the study (**Figure 4.5B**), suggesting minimal pulmonary absorption. These findings are consistent with published data generated in our lab showing negligible IFNγ levels in the serum of infant (PND 4) Balb/c mice following a single i.n. dose of IFNγ (182).

To determine the effect of IFNγ dose on myeloid cell ($CD11c^+$ $CD11b^-$) activation in RSV-infected infant lungs, the expression of MHCII was examined. At each time point tested, the 60ng/g dose increased myeloid cell activation significantly more than infants treated with 16ng/g or PBS alone (**Figure 4.5C**). $CD11c^+$ $CD11b^-$ cells from mice receiving 16ng/g also significantly increased MHCII expression on 7 and 10 DPI compared to PBS-treated mice (**Figure 4.5C**) but not at 4 DPI, suggesting a stronger activation signal may be required for initial activation of infant $CD11c^+$ $CD11b^-$ cells.

To determine the functional effect of optimizing i.n. IFNγ dosing, RSV clearance was quantified by viral plaque assay. By 4 DPI, RSV clearance was greatest in the 60ng/g group followed by the 16ng/g of IFNγ compared to PBS; however, only the group receiving 60ng/g demonstrated enhanced RSV clearance at 7 DPI (**Figure 4.5D**). By 10 DPI, 80% (4/5) of animals in both IFNγ groups had undetectable viral loads while only 50% (2/4) of infants in the PBS group had similarly undetectable virus.

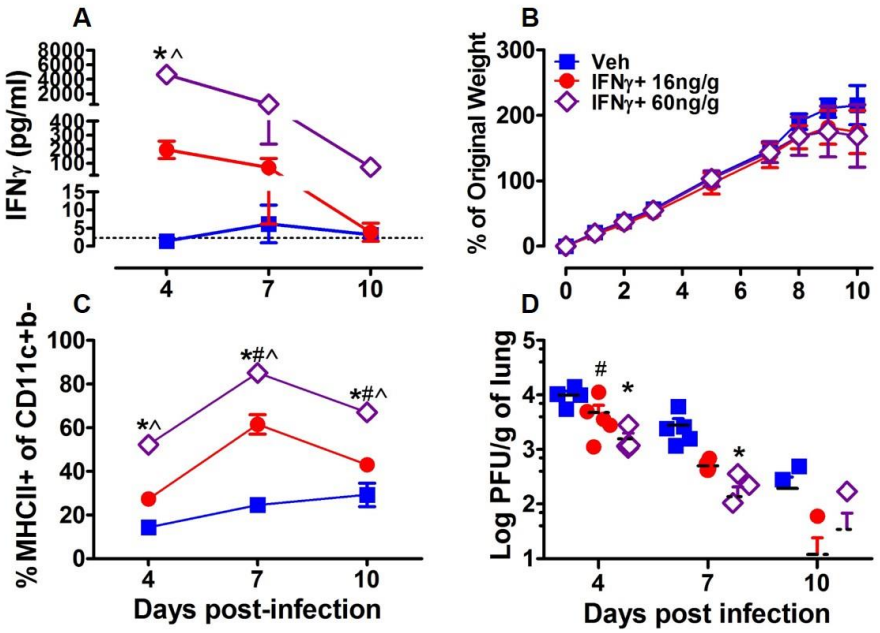

Figure 4.5. Infants demonstrate dose dependent myeloid activation and viral clearance.

Infant (PND 5-7) Balb/c mice were infected with RSV L19 and treated with i.n. IFNγ (16 or 60ng/g) or Veh. (PBS) on 1, 3, and 5 dpi. Luminex was used to quantify IFNγ in BAL (A) and % of original weight was calculated from baseline litter weights (B). Lungs were collected for flow cytometry to analyze the % of $CD11c^+$ $CD11b^-$ cells expressing $MHCII^+$ (C) and viral titers using H&E plaque assay (D). # and * represent significant differences between infants treated with 16 and 60ng/g compared to PBS treated infants, respectively. ^ indicates significant differences between infants treated with 16 vs. 60ng/g of IFNγ using a 2-way ANOVA with Bonferroni post-test; $p<0.05$. Data points represent the mean of $n \geq$ 2-5 samples per group ± SD. ***Originally published in***: Eichinger KM, Egaña L, Orend JG, Resetar E, Anderson KB, Patel R, Empey KM. Alveolar macrophages support interferon gamma-mediated viral clearance in RSV-infected neonatal mice. *Respiratory research* 2015;16:122.

4.2.3 Intranasal IFNγ treatment reduces pulmonary mucus and detection of apoptotic cells in the lungs of RSV-infected infant mice

To determine the pathological consequences of achieving higher, adult-like IFNγ AUCs in the infant airway during RSV infection, mucus production was determined in RSV-infected mice treated with 16 or 60ng/g of IFNγ or PBS alone; IFNγR1KO (Balb/c background) mice were included as an additional control group to assess mucus production in the absence of IFNγ signaling (**Figure 4.6A-E**). Airway mucin scores were determined as previously described (1). Mucus production was evident (bright pink staining; arrows) in representative RSV-infected infant lung sections (**Figure 4.6A & B**). Conversely, mucus production was absent in uninfected infant mice (**Figure 4.6C**), those treated with 16ng/g of IFNγ (**Figure 4.6D**) and mucus was markedly reduced in infants that received 60ng/g of IFNγ (**Figure 4.6E**).

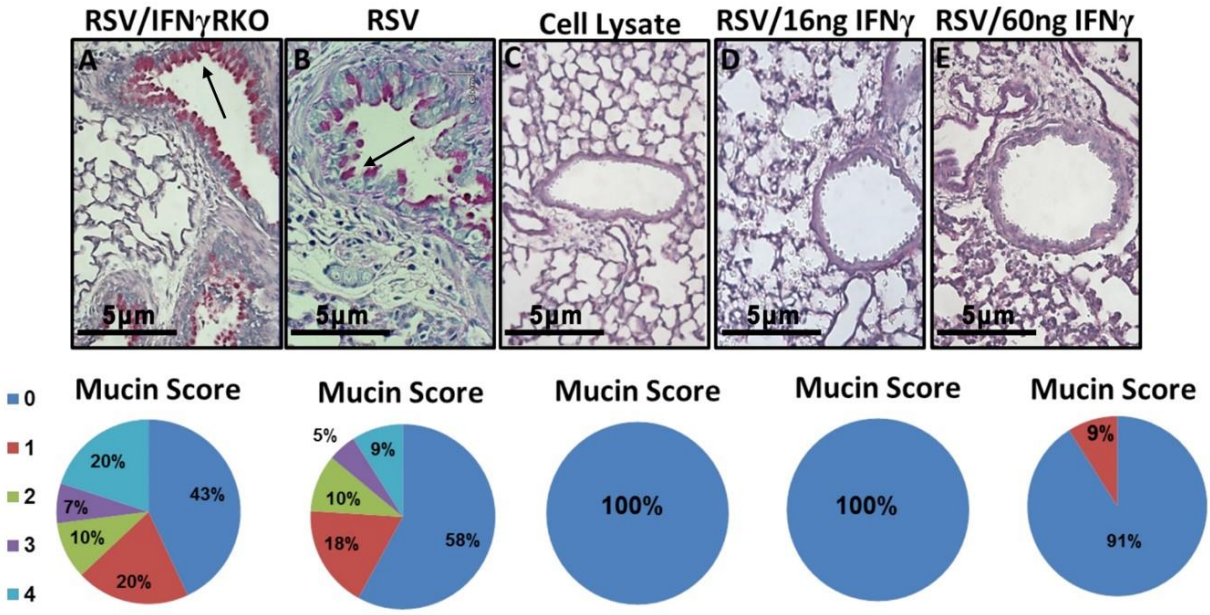

Figure 4.6. Local IFNγ reduces airway mucus production.

WT and IFNγ receptor knock out (IFNγRKO) infants (PND 5-7) were infected with RSV L19 or cell lysate, then treated with i.n. IFNγ (16 ng/g or 60 ng/g) or PBS on 1, 3, and 5 DPI. The lungs (n = 5 samples per group) were harvested at 8 DPI and sections compared by extent of PAS staining, indicated by bright pink staining (arrows). Airways were scored 0 to 4 for PAS positivity according to previously published methods (1). Representative examples of airway mucin production from RSV/IFNγRKO (A), RSV (B), Cell lysate (C), RSV/16ng/g IFNγ (D), and RSV/60ng/g IFNγ (E). Pie charts are provided to numerically represent a percentage of the total airways ranked according to mucin scores. ***Originally published in***: Eichinger KM, Egaña L, Orend JG, Resetar E, Anderson KB, Patel R, Empey KM. Alveolar macrophages support interferon gamma-mediated viral clearance in RSV-infected neonatal mice. *Respiratory research* 2015;16:122.

To determine the effect of i.n. IFNγ on RSV-mediated apoptosis in the infant lung, TUNEL staining was performed at 8 DPI on lung sections from infant mice that were A) mock-infected;

B) RSV-infected; C) RSV-infected and treated with 16ng/g of i.n. IFNγ; or D) RSV-infected and treated with 60ng/g of i.n. IFNγ (**Figure 4.7**). Figure 4.7 shows representative lung section from each mouse per group. RSV-infected (**Figure 4.7B**) lungs had significant increases in TUNEL staining compared to uninfected lungs (**Figure 4.7A**). Interestingly, both 16ng/g (**Figure 4.7C**) and 60ng/g (**Figure 4.7D**) IFNγ-treated groups had reduced TUNEL staining compared to RSV-infected lungs at 8 DPI, which is graphically represented in **Figure 4.7E**.

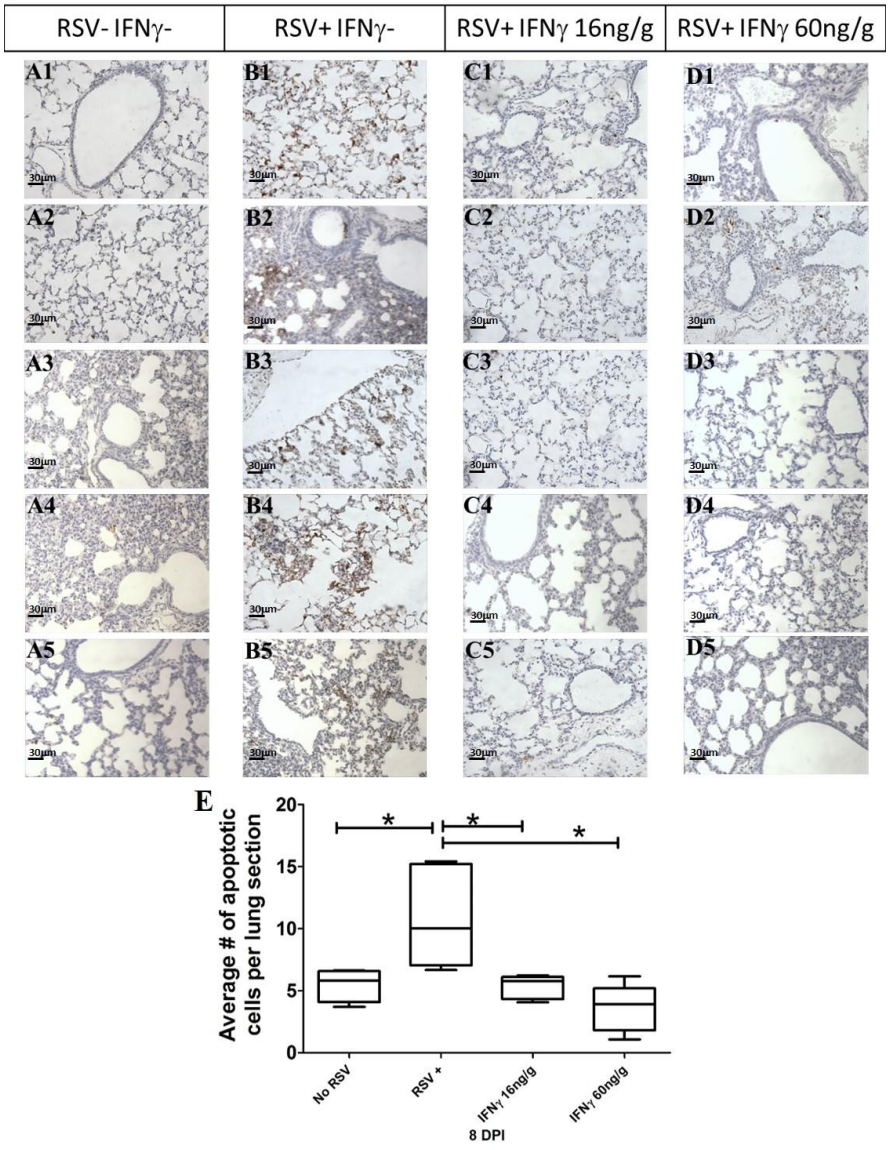

Figure 4.7. Intranasal IFNγ reduces apoptosis in infant lungs at 8DPI.

Figure 4.7 (continued) Infant Balb/c mice (PND 5-7) were infected with RSV L19 and treated with i.n. IFNγ (16 or 60ng/g) or PBS on 1, 3, and 5 dpi. At 8 dpi right lungs were harvested, fixed with formalin and TUNEL stained. Represents a single lung section from each animal in RSV-/IFNγ- (A1-A5), RSV+/IFNγ- (B1-B5), RSV+ IFNγ 16ng/g (C1-C5), and RSV+ IFNγ 60ng/g (D1-D5). Images were captured at 40X magnification and the average number of apoptotic cells per lung section were quantified and graphed (E); *n* = 5 samples per group. * indicates a significant difference compared to RSV+ using ANOVA with a Tukey post-test; $p<0.05$. ***Originally published in***: Eichinger KM, Egaña L, Orend JG, Resetar E, Anderson KB, Patel R, Empey KM. Alveolar macrophages support interferon gamma-mediated viral clearance in RSV-infected neonatal mice. *Respiratory research* 2015;16:122.

4.2.4 The loss of AMs impairs RSV clearance in infant mice

AMs are the predominate phagocytic cell in the airway, responsible for clearing debris, pathogens, and apoptotic cells from the air space, thereby working to return the airway to homeostasis yet, they are ideally poised to initiate a strong inflammatory response if required (110). Through the use of locally delivered CLip, we sought to understand the role of AMs in infant RSV infection by eliminating them from the airspace. Based on previously performed pilot studies in our lab, daily dosing of i.n. CLip was shown to effectively reduce the $CD11c^+$ $CD11b^-$ population, commonly referred to as AMs in the literature, in RSV-infected neonatal mice. CLip treatment began -1 DPI in PND 2; dosing continued daily with either CLip or PBS; pups then received i.n. IFNγ (16ng/g) or PBS on days 1, 3, and 5 DPI. Regardless of i.n. IFNγ treatment, numbers of $CD11c^+$ $CD11b^-$ cells in both the BAL and lung digest were significantly reduced with CLip at 4 and 8 DPI (**Figure 4.8**). The $CD11c^+$ $CD11b^-$ cell population was reduced by 84% and 91% at 4 and 8 DPI, respectively **(Figure 4.8A & B).** Moreover, total $CD11c^+$ $CD11b^-$ cells harvested from the lung

digest (LD) were significantly reduced by 57% and 55% at 4 and 8 DPI, respectively, following CLip treatment (**Figure 4.8C & D**).

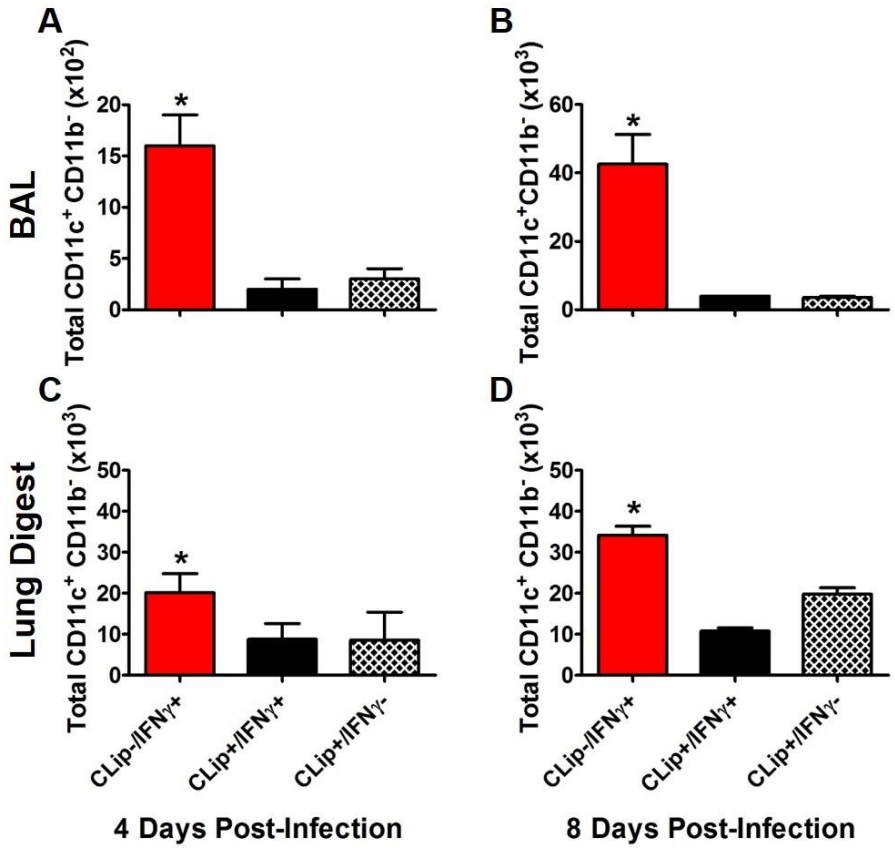

Figure 4.8. Depletion of pulmonary infant CD11c$^+$ CD11b$^-$ cells using CLip.

Infant Balb/c mice (PND 2) were treated with i.n. CLip and/or IFNγ. BAL (A and B) and digested right lung lobes (C and D) were harvested at 4 (A and C) and 8 (B and D) DPI. Total CD11c$^+$ CD11b$^-$ cells were determined via flow cytometry. * Indicates a significant difference between groups using ANOVA. $p < 0.05$. Data points represent the mean of $n \geq$ 2-5 samples per group ± SD. ***Originally published in***: Eichinger KM, Egaña L, Orend JG, Resetar E, Anderson KB, Patel R, Empey KM. Alveolar macrophages support interferon gamma-mediated viral clearance in RSV-infected neonatal mice. *Respiratory research* 2015;16:122.

The functional effects of AM depletion and i.n. IFNγ treatment were tested following RSV infection via viral plaque assay. At 4 DPI, CLip (-)/ IFNγ (+) animals had the lowest viral titers, which were significantly lower than CLip (-)/ IFNγ (-) and CLip (+)/ IFNγ (-) treated animals **(Figure 4.9A).** The CLip (-)/ IFNγ (+) group had lower viral titers than the CLip (+)/ IFNγ (+) group but the difference was not significant. The CLip (+)/ IFN (+) group had significantly lower viral titers than CLip (+)/ IFNγ (-) treated animals. These results suggest that IFNγ treatment played a larger role in reducing viral burdens than AM depletion. To evaluate the contribution of each treatment independently, we analyzed viral titers by 2-way ANOVA. This analysis confirmed our hypothesis that IFNγ treatment was primarily responsible for the differences in viral titers. In fact, IFNγ treatment accounted for 45% of the variability; however macrophage depletion also significantly contributed to differences in viral titers, accounting for 10% of the variability. Bonferroni post-hoc analysis revealed that the significant effect of macrophage depletion (CLip treatment) was primarily a result of the differences in viral titers of CLip (+) vs. CLip (-) animals that were not treated with IFNγ.

At 8 DPI, CLip (+)/IFNγ (-) animals had the highest viral burden which was significantly higher than both CLip (-)/ IFNγ (-) and CLip (-)/IFNγ (+) animals **(Figure 4.9B).** However, viral titers of CLip (+)/IFNγ (-) animals were not significantly higher than CLip (+)/IFNγ (+) animals demonstrating that the effects of IFNγ on reducing RSV in the lungs was lost by 8 DPI in the absence of AMs. In fact, treatment with IFNγ accounted for only 5% of the variability observed. The presence or absence of AMs played a critical role in RSV clearance, accounting for 43% of the variability. Regardless of IFNγ treatment, infants whose AM populations were eliminated with CLip had RSV viral titers that were nearly a log fold higher than CLip (-) neonates at 8 DPI.

The potential for biological toxicity resulting from either CLip or IFNγ treatment was analyzed by calculating the neonates' ability to gain weight over time. CLip treatment but not IFNγ significantly impaired the ability of neonates to gain weight (**Figure 4.9C**). Irrespective of IFNγ treatment, the daily percent gain in weight began to slow in CLip (+) neonates when compared to CLip (-) neonates beginning at 4 DPI and continued until the final time point. At 7 DPI, both CLip (+) groups demonstrated significantly impaired weight gain when compared to CLip (-)/IFNγ (-) neonates. These data suggest that AM depletion, either directly and/or indirectly, plays an important role in viral clearance late in RSV infection while the presence of IFNγ in the airway is important in reducing the viral burden early in RSV.

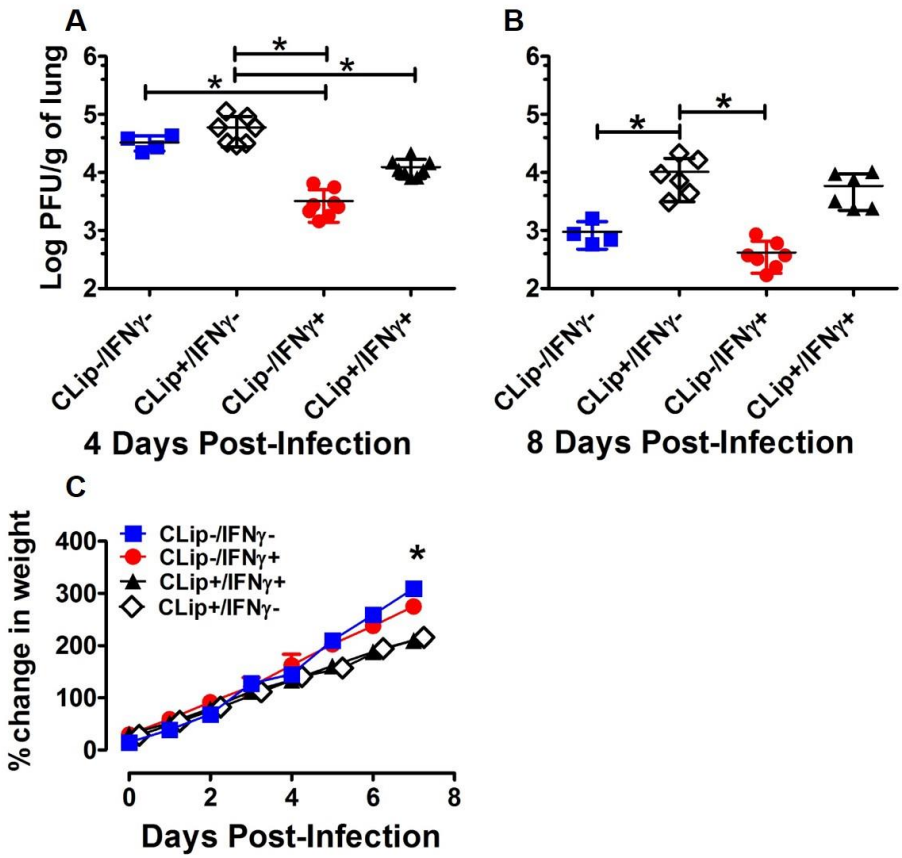

Figure 4.9. AM depletion reduces RSV clearance and impairs weight gain.

Infant Balb/c mice (PND 2) were treated with i.n. CLip and/or IFNγ. Left lungs were collected on 4 (A) and 8 (B) DPI for RSV quantification using plaque assay. Litters were weighed daily and the percent change in weight (C) was calculated from their baseline weight prior to i.n. treatments. Data points represent the means of $n \geq 4$-8 samples per group ± SD. (A and B); * indicates $\rho < 0.05$ using ANOVA with a Tukey post-test. (C); *indicates a statistical difference between control (CLip-/IFNγ-) and CLip treatment groups (CLip+/IFNγ+ and CLip+/IFNγ-) using repeated measures ANOVA with a Bonferroni post-test ($\rho < 0.05$). ***Originally published in***: Eichinger KM, Egaña L, Orend JG, Resetar E, Anderson KB, Patel R, Empey KM. Alveolar macrophages support interferon gamma-mediated viral clearance in RSV-infected neonatal mice. *Respiratory research* 2015;16:122.

4.2.5 IFNγ treatment of human airway epithelial cells decreases RSV replication

To determine IFNγ's ability to reduce the RSV burden directly in AECs, we used an in-vitro assay using the A549 human alveolar basal epithelial cell line, in which A549 cells were pre-treated for 1 hour with IFNγ and infected with RSV for 24-48 hours. RSV was quantified from lysed A549 cells (intracellular) as well as the extracellular media surrounding the cells in order to quantify budded RSV (extracellular). RSV quantified from within A549 cells (intracellular) continued to replicate in untreated A549 cells, increasing by a log-fold in 24 hours (**Figure 4.10A**). RSV within cells pre-treated with IFNγ did not effectively replicate between 24 and 48 hours as evidenced by the unchanged RSV burden quantified from within A549 cells (**Figure 4.10A**). Similar to the intracellular data, significantly more budded (extracellular) RSV was quantified from untreated A549 cells between 24 and 48 hours (**Figure 4.10B**). Pre-treatment of A549 cells with IFNγ resulted in significantly less extracellular RSV than untreated cells at 48 hours and remained relatively unchanged from the viral burden quantified from IFNγ treated cells at the 24 hour time point (**Figure 4.10B**). This data suggests that IFNγ can effectively inhibit viral replication in airway epithelial cells.

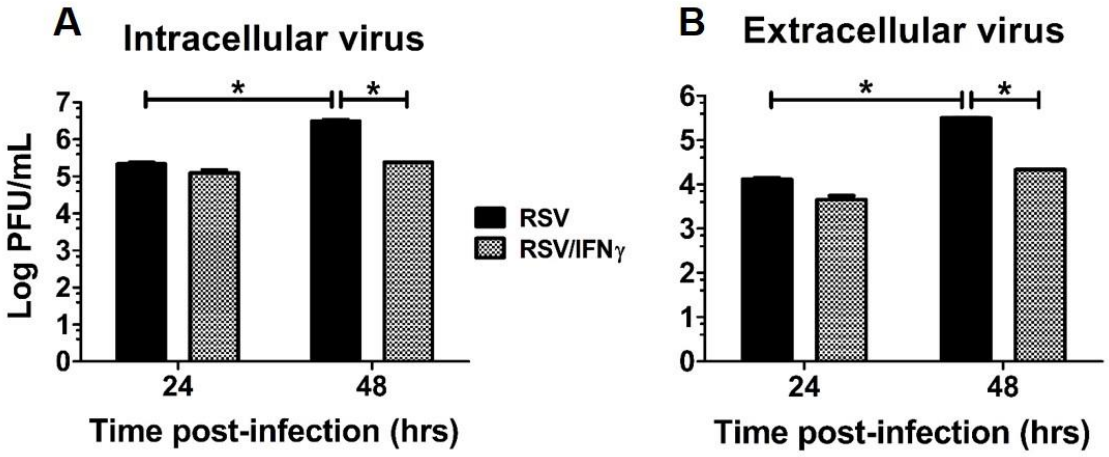

Figure 4.10. IFNγ pre-treatment of A549 cells prevents RSV replication.

A549 cells pre-treated for 1 hour with IFNγ (100ng/mL) then infected with RSV L19 (Multiplicity of infection = 2). At 24 and 48 hours, intracellular (A) and budded (B, extracellular) virus was harvested and used to infect HEp2 cells. After 5 days, a standard H&E plaque assay was performed to quantify virus. * Indicates a significant difference between groups/ time points using 2-way ANOVA; Data points represent the mean of $n \geq 2$ samples per group ± SD; $p < 0.05$.

4.2.6 Human monocyte differentiation

By eliminating AMs through the use of CLip, our data has demonstrated the importance of infant murine macrophages in the clearance of RSV. We have also shown the stimulatory potential of IFNγ on AMs, including the increased expression of SR-A, which is known to participate in the clearance of apoptotic debris (183). We sought to investigate the clinical relevance of our findings in the infant murine RSV model to human samples. An Exempt IRB was written and approved (PRO14120128) for the acquisition of human infant monocytes from cord blood samples. Our objective was to differentiate infant monocytes into macrophages and test the ability of IFNγ treatment to increase efferocytosis of apoptotic debris.

Before obtaining infant cord blood samples, we began to optimize the differentiation of human monocytes into macrophages using human blood samples obtained from healthy adult volunteers. We first attempted to isolate human monocytes by taking advantage of their adherent nature. Following isolation of mononuclear cells from heparinized whole blood samples using centrifugation with Lymphoprep™, mononuclear cells (MNCs) were plated into 6-well plates at a density of 3×10^6 cells /well and incubated for 90 minutes. Our first check on the purity of our samples involved harvesting and visualizing the non-adherent cells in the supernatant as well as, the plated cells adhered to the culture dish. Microscopic evaluation showed contaminating lymphocytes in the plated cells (**Figure 4.11A**) and that a significant proportion of non-adherent cells in the supernatant were monocytes (**Figure 4.11B**).

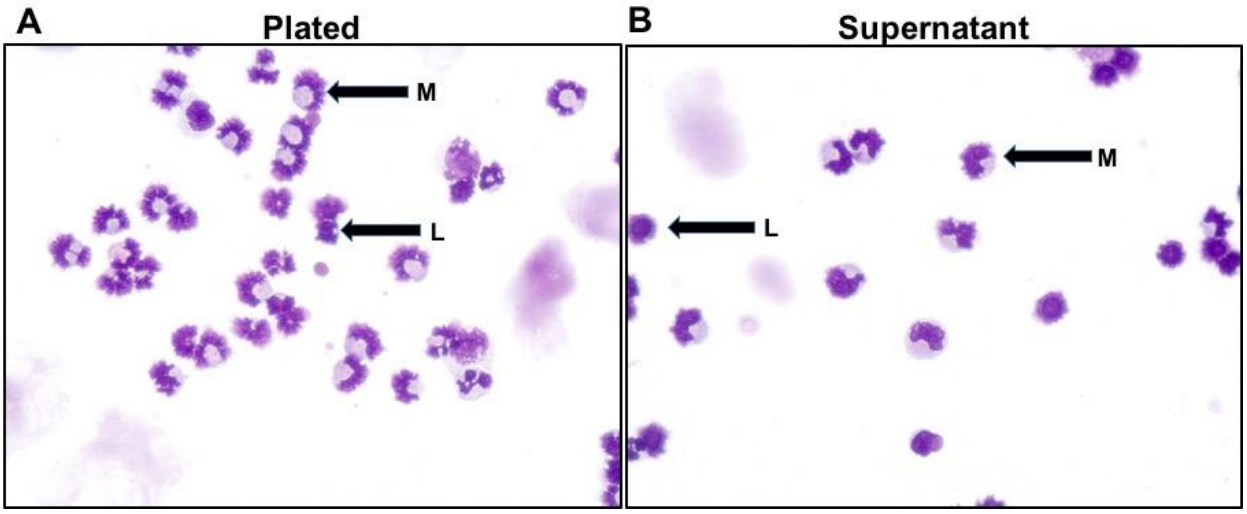

Figure 4.11. Inefficient monocyte isolation following plating method.

MNCs were isolated from heparinized whole blood by using Lymphoprep in SepMate50 tubes. Following MNC isolation, 3 x10^6 cells were added to a 6-well plate and allowed to adhere for 90 minutes. After incubation, supernatant containing non-adherent cells was collected and spun onto glass slides. Plated cells were harvested using TrypLE and spun onto glass slides. Microscopic analysis occurred following differential cell staining at 40X.

Monocyte isolation following plating was also analyzed by phenotypic characterization via flow cytometry (**Figure 4.12A & B**). All adherent cells recovered after a 90 minute incubation are displayed according to their forward (FSC) and side scatter (SSC) characteristics (**Figure 4.12A**). Cell populations were identified using a panel of surface and intracellular markers and overlaid onto the FSC vs. SSC plots. Cells were identified as follows: monocytes (SSC^{HI} $CD14^+$ $CD16^-$), probable NK cells (SSC^{lo} $CD14^-$ $CD16^+$ HLA-DR^- $CD36^-$ $CD68^-$ $CD11b^+$), and probable lymphocytes (SSC^{lo} $CD14^-$ $CD16^+$ HLA-$DR^{+/-}$ $CD36^-$ $CD68^-$ $CD11b^-$). The proportions of these cell types in the population of cells recovered from the surface of the plate are listed (**Figure 4.12B**). Monocytes and lymphocytes were recovered from the plate in similar percentages (~40%),

while NK cells represented a smaller percentage (6.5%). In the supernatant, NK cells and lymphocytes constituted the majority of cells recovered (75%) but a significant monocyte population (13%) was detected. The results demonstrated non-specific and inefficient monocyte isolation using the plating method in 6 well plates.

In order to increase monocyte recovery using the plating method, we hypothesized that increasing the surface area would allow more monocytes to adhere to the plate surface while contaminating cells like lymphocytes would remain in the supernatant. Increasing surface area only slightly improved monocyte recovery with 49% of adherent cells identified as monocytes ($CD14^+$ $CD16^-$, **Figure 4.12C**). The process remained highly inefficient as the majority of adherent cells were not monocytes and 17% of cells identified in the supernatant were monocytes (**Figure 4.12C**). To maximize monocyte recovery, our next step was to test an immunomagnetic negative selection cell isolation kit. This kit utilizes a combination of magnetic bead linked antibodies targeting surface receptors of T cells, B cells, NK cells, neutrophils, etc. The sample is then run through a powerful magnet which binds magnetically labeled cells and allows unlabeled, enriched monocytes to be poured from the magnet for subsequent studies. Our use of the monocyte enrichment kit, following MNC isolation with Lymphoprep, resulted in a very pure (94%) $CD14^+$ $CD16^-$ cell population (**Figure 4.12C**). The enriched $CD14^+$ cells were seeded in a 24-well plate at a density 3.5 times higher than the recommended density for HeLa cells to create a "monocyte lawn", which increases adherence and is in contrast to our previous hypothesis that more space would enhance monocyte adherence. The media was supplemented with GM-CSF (25ng/mL) to induce macrophage differentiation and after 7 days of culturing with GM-CSF, 89% of monocytes had differentiated to macrophages ($CD14^+$ $CD16^+$, **Figure 4.12C**). Under the microscope, differentiated macrophages appeared flattened with pseudopods extending outward, which differs

from monocyte's rounded appearance (personal observation). These results demonstrate the superiority of immunomagnetic cell isolation compared to plating for the enrichment and isolation of human monocytes and the successful differentiation of the enriched monocytes to macrophages using GM-CSF. Effective monocyte enrichment and differentiation will be crucial as our lab moves forward in working with infant cord blood samples to discern the effect of IFNγ treatment on infant macrophages.

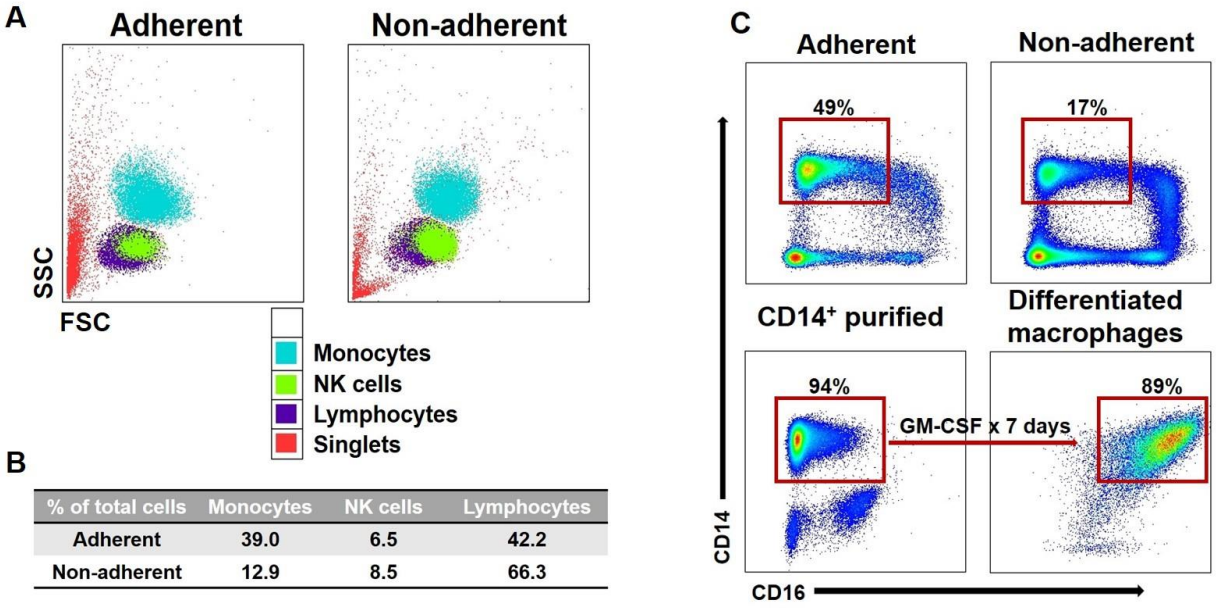

% of total cells	Monocytes	NK cells	Lymphocytes
Adherent	39.0	6.5	42.2
Non-adherent	12.9	8.5	66.3

Figure 4.12. Optimization of human monocyte enrichment and differentiation.

Figure 4.12 (continued) MNCs were using Lymphoprep in SepMate50 tubes. Following MNC isolation, 3 x10^6 cells were added to a 6-well plate (A & B) or 17 x 10^6 cells were added to a 150mm petri-dish (C, top panels) and allowed to adhere for 90 minutes. After incubation, supernatant containing non-adherent cells was collected while plated cells were harvested using TrypLE. Alternatively, MNCs underwent immunomagnetic cell isolation according to manufacturer instructions to obtain enriched monocytes (C, bottom left panel, $CD14^+$ purified). Enriched monocytes were cultured with GM-CSF (25ng/mL) x 7 days to obtain differentiated macrophages (C, bottom right panel). Samples from each scenario were collected and processed for flow cytometry.

4.2.7 The effect of IFNγ treatment on T cell immunity in RSV-infected infant mice

Data presented in this report have demonstrated the importance of IFNγ and AMs in the resolution of primary, infant RSV infection, but the importance of T lymphocytes in clearing RSV has been well established (61, 94-97). Activation of APCs, like macrophages and dendritic cells, largely determines the T-helper cell phenotype priming of naïve T cells (133, 144, 170, 184). However, the ability of local pulmonary delivery of IFNγ to alter the T cell phenotype of RSV-infected infant mice has not been previously investigated.

4.2.7.1 IFNγ reduces CD4$^+$ CD44^{HI} Tbet$^+$:GATA3$^+$ T-cell ratios compared to RSV infection alone

To determine how T cell phenotype changes in infants following the local delivery of a Th1-type cytokine, i.n. IFNγ was administered to RSV-infected infant mice. Intracellular Tbet$^+$ and GATA3$^+$ expression in CD4$^+$ CD44^{HI} T-cells in the URL and BAL was subsequently analyzed. Although frequencies of CD4$^+$ and CD4$^+$ CD44^{HI} T cells were unaltered following i.n. IFNγ (**Figure 4.13**), Tbet$^+$:GATA3$^+$ CD44^{HI} CD4$^+$ T cell ratios were significantly reduced in the URL and BAL compared to untreated controls (**Figure 4.14A**). Importantly, reduced CD4$^+$ CD44^{HI} Tbet$^+$:GATA3$^+$ T cell ratios in the BAL were driven by reductions in CD4$^+$ CD44^{HI} Tbet$^+$ T cell frequency rather than increases in CD4$^+$ CD44^{HI} GATA3$^+$ T cells (**Figure 4.14B**). These data suggest that local IFNγ delivery to the infant airway during early RSV infection reduced the frequency of CD4$^+$ Tbet$^+$ T-cells without altering CD4$^+$ GATA3$^+$ frequencies at 10 DPI.

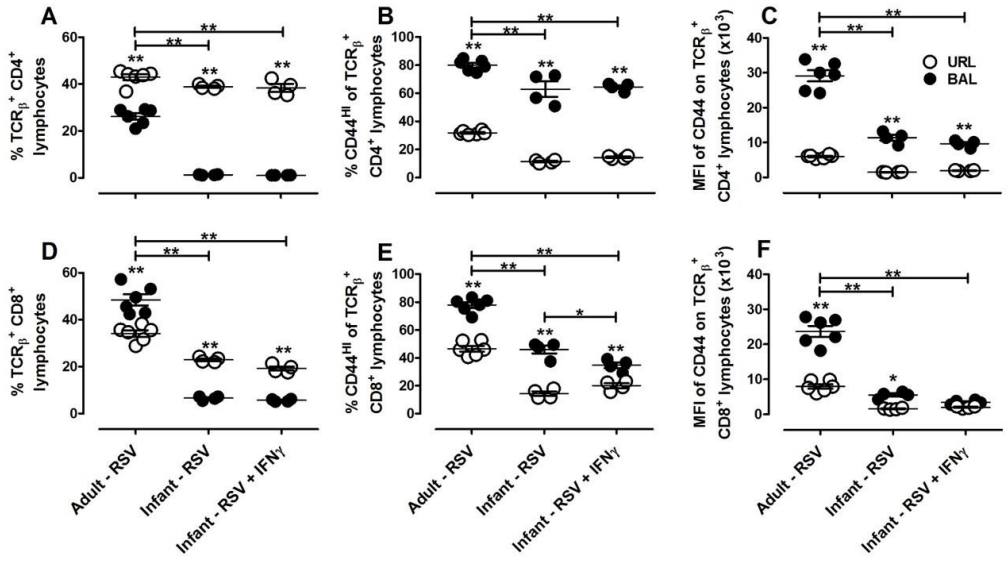

Figure 4.13. Following i.n. IFNγ, T cell frequencies remain similar to RSV infected infants while both groups have reduced frequencies when compared to RSV-infected adults.

Figure 4.13 (continued) Adult (6-8 weeks) and infant (PND 4-5) Balb/c mice were infected with RSV L19. Infants received i.n. IFNγ (16ng/g) or vehicle on days 1, 3, and 5 DPI. BAL and URL were collected at 10 DPI and processed for flow cytometry. The lymphocytes were gated according to typical FSC vs. SSC characteristics. % $CD44^{HI}$ and MFI was determined from TCR_{β}^{+} $CD4^{+}$ or $CD8^{+}$ T cells in the lymphocyte gate. The $CD4^{+}$ T cell frequencies and MFI of $CD44^{HI}$ CD4+ (A, B, and C, respectively) and $CD8^{+}$ T cell frequencies and MFI of $CD44^{HI}$ CD8+ T cells (D, E, and F, respectively) were compared between the BAL and URL using 2-way ANOVA with a Bonferroni post-test. Additionally, the $CD4^{+}$ T cell frequencies and MFI of $CD44^{HI}$ $CD4^{+}$ (A, B, and C, respectively) and $CD8^{+}$ T cell frequencies and MFI of $CD44^{HI}$ $CD8^{+}$ T cells (D, E, and F, respectively) were compared between age and treatment groups for BAL using ANOVA with a Bonferroni post-test. Points represent individual mice (adults) or individual samples from ≥ 2 pooled infants, lines represent the mean of $n \geq 4$ samples per group ± SD; * ρ-value < 0.05, ** ρ-value < 0.01. Data in A - F are representative of 2 independent experiments. All $CD44^{HI}$ cells were also $CD62L^{-}$**.** ***Originally published in***: Eichinger KM, Kosanovich JL, Empey KM. Localization of the T-cell response to RSV infection is altered in infant mice. *Pediatric pulmonology* 2018;53(2):145-153.

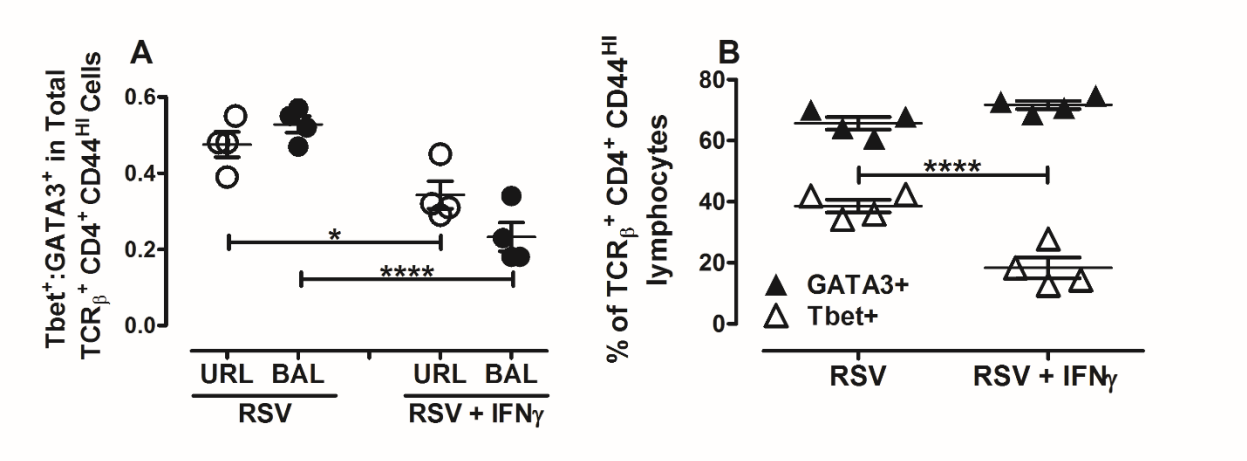

Figure 4.14. Intranasal IFNγ reduces $Tbet^{+}$:$GATA3^{+}$ $CD4^{+}$ T-cell ratios at 10 DPI compared to RSV infection alone.

Figure 4.14 (continued) Infant (PND 4-5) Balb/c mice were infected with RSV L19 and administered i.n. IFNγ (16ng/g) or vehicle on 1, 3, and 5 DPI. BAL and URL were collected at 10 DPI and processed for flow cytometry. Lymphocytes were gated according to typical FSC vs. SSC characteristics. Ratios of TCR_{β}^{+} $CD4^{+}$ $CD44^{HI}$ $Tbet^{+}$ cells to TCR_{β}^{+} $CD4^{+}$ $CD44^{HI}$ $GATA3^{+}$ cells were calculated from total cell counts of the URL and BAL (A). The frequency of $CD4^{+}$ $CD44^{HI}$ $GATA3^{+}$ and $Tbet^{+}$ T-cells were compared in BAL for RSV and RSV + IFNγ infants (B). A 2-way ANOVA was used to compare the $Tbet^{+}$:$GATA3^{+}$ $CD4^{+}$ T-cell ratios between URL, BAL, and treatment groups with a Bonferroni post-test (A). The frequencies of $CD4^{+}$ $CD44^{HI}$ $GATA3^{+}$ and $Tbet^{+}$ T cells in the BAL were compared between RSV and RSV + IFNγ infants using 2-way ANOVA with a Bonferroni post-test (B). Points represent individual samples of ≥ 2 pooled infants, lines represent the mean of $n = 4$ samples per group ± SD; * $\rho < 0.05$, ** $\rho < 0.01$. Data is representative of a single experiment. All $CD44^{HI}$ cells were also $CD62L^{-}$. ***Originally published in***: Eichinger KM, Kosanovich JL, Empey KM. Localization of the T-cell response to RSV infection is altered in infant mice. *Pediatric pulmonology* 2018;53(2):145-153.

4.2.7.2 Local IFNγ increases RSV F-protein specific $CD8^{+}$ T-cells in infant murine BAL

We next sought to determine if IFNγ altered the $CD8^{+}$ T cell response in the RSV-infected infant airway. Following i.n. delivery of IFNγ, total $CD8^{+}$ T cells were reduced in the infant airway compared to untreated controls (**Figure 4.15A**). The overall reduction in the $CD8^{+}$ T cells was accompanied by significant reductions in $CD8^{+}$ $CD44^{HI}$ T cells (data not shown) and reductions in $CD8^{+}$ $CD44^{HI}$ T cells expressing the transcription factor Tbet (**Figure 4.15B**). These data were surprising given our previous findings, which showed that i.n. IFNγ expedited viral clearance compared to age-matched controls (1). To resolve these seemingly incongruous results, we utilized an RSV $F_{85\text{-}93}$-protein specific pentamer to determine the effect of i.n. IFNγ on $CD8^{+}$ T cell specificity. Intriguingly, local IFNγ administration significantly increased the frequency of RSV $F_{85\text{-}93}$ protein-specific $CD8^{+}$ T cells in the BAL of RSV-infected infant mice compared to untreated

controls (**Figure 4.15C**). Together, these results suggest that IFNγ contracts the $CD8^+$ T cell population and increases $CD8^+$ T cell RSV F_{85-93} protein specificity in the BAL of RSV-infected infant mice.

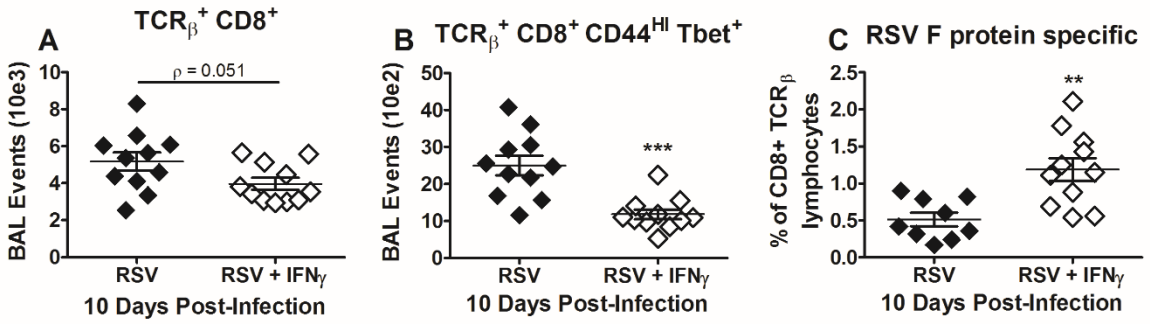

Figure 4.15. IFN-γ priming of RSV-infected infant mice improves RSV F_{85-93} -protein specific CD8+ T cell accumulation within the BAL compared to RSV alone, despite overall reductions in CD8+ T-cells.

Infant (PND 4-5) Balb/c mice were infected with RSV L19 and administered i.n. IFNγ (16ng/g) or vehicle on 1, 3 and 5 DPI. BAL was collected at 10 DPI and processed for flow cytometry. The lymphocytes were gated according to typical FSC vs. SSC characteristics. Total $CD8^+$ T-cells (A), total $CD8^+$ $CD44^{HI}$ $Tbet^+$ T-cells (B), and the percentage of $CD19^-$ RSV F_{85-93} protein-specific $CD8^+$ T-cells (C) were compared between groups using an unpaired, 2-tailed *t* test. For the quantification of RSV F_{85-93} protein-specific $CD8^+$ T-cells, we first subtracted the percentage of background obtained from an LPS negative control BAL sample stained with RSV F_{85-93} protein-specific pentamer. Points represent individual samples of ≥ 2 pooled infants, lines represent the mean of $n \geq 9$ samples per group ± SD; ** ρ-value < 0.01. Data in A - C are representative of 2 independent experiments. All $CD44^{HI}$ cells were also $CD62L^-$. ***Originally published in***: Eichinger KM, Kosanovich JL, Empey KM. Localization of the T-cell response to RSV infection is altered in infant mice. *Pediatric pulmonology* 2018;53(2):145-153.

4.3 DISCUSSION

In this study, the cytokine kinetics and immune stimulating effects of IFNγ were examined in adult and infant Balb/c mice following i.n. administration. Long-term protection against RSV by vaccination is a global health priority, yet concerns over vaccine-enhanced RSV disease and limited infant host immunity continue to pose a significant challenge. Moreover, repeated infections with RSV throughout life suggests that induction of sterilizing immunity may not be feasible and vaccinations that induce sufficient immunity to protect against serious RSV infection may be a more realistic goal. Stimulating the innate immune response to prevent or treat pulmonary infections is of growing interest in the areas of antimicrobial resistance, impaired host immunity, and for viral infections lacking an effective vaccine (185-187). Many of these strategies target pattern recognition receptors to activate transcription factors such as NF-kB and interferon regulatory transcription factor (IRF3), resulting in the expression of inflammatory cytokines and other facets of cellular activation (188). Vaccine strategies combine non-infectious antigen with immune potentiating adjuvants in an effort to condition the adaptive immune response in preparation for subsequent exposure to infectious organisms. However, infants often do not reap the same protective benefits from vaccination as older children and adults due to inefficient or suppressive innate and adaptive host immunity (189, 190). A growing number of studies have reported safe and effective antiviral activity with vaccine-mediated enhancement of pro-inflammatory cytokines (191-194), yet less is known about direct immune stimulation.

In the present investigation, analysis of cytokine delivery was focused on pulmonary innate immune cell exposure and activation following intranasal delivery of IFNγ in infant versus adult murine lungs. Following identical weight-based dosing, infant compared to adult mice had markedly reduced AUCs and Cpks, indicating reduced cytokine concentrations were achieved in

infant compared to adult murine lungs. It is reasonable to consider that the narrow infant airways compared to adults' limited delivery of this 50kDa protein in an age-dependent manner. However, examination of lung and body weights over time indicated that the rate of postnatal infant lung growth exceeded that of body weight through 10 days of age, suggesting that pulmonary doses of weight-based drugs were underestimated when scaling from adult doses. These findings are consistent with previous studies demonstrating that pulmonary deposition of aerosolized drugs depend primarily on differences in ventilation per gram of body weight and may account, in part, for lower AUCs and Cpks in infant compared to adult mice treated with IFNγ or GM-CSF (195). Moreover, reduced cytokine clearance (apparent) rates, which are calculated based on dose and AUC, were also lower in infant compared to adult murine lungs and blood, suggesting that bioavailability rather than increased proteolytic activity was responsible for the reduced infant concentrations. Together, these data showed reduced AUCs and clearance rates in infant compared to adult mice treated with a single intranasal dose of IFNγ.

Discrete weight-based doses of IFNγ were used based on previous studies in infant and adult mice designed to optimize immune activation (1, 119, 148). Indeed, IFNγ treatment on days 1, 3, and 5 DPI resulted in increased recruitment of monocytes and DCs to the BAL during infant RSV infection. This recruitment is likely the result of activation and the release of chemokines by airway epithelial cells and AMs. Activation of AMs followed IFNγ treatment of RSV-infected infants as demonstrated by increased expression of CD11b, CD80, MHCII, and SR-A. However, following a single, weight-based dose of IFNγ, adult animals had an IFNγ AUC that was 3.6 times larger than that of infants, which resulted in expedited and enhanced MHCII expression on $CD11c^{+}$ $CD11b^{-}$ cells in adults compared to infants. The large age-based differences in IFNγ exposure was

not a result of differential IFNγ metabolism but was most likely an artifact of the neonate's larger lung to body size ratio or the potential loss of some of the dose due to ingestion.

Taking this into consideration, a non-compartmental model analysis was used to determine a new neonatal dose of IFNγ that would achieve more adult-level AUCs. We predicted the new neonatal IFNγ dose of 60ng/g would not only expedite viral clearance, but would also modulate associated risk factors linked to skewed Th2 pathology, such as mucus production. The data presented here showed the capacity of IFNγ to induced AM activation and RSV clearance in a clear, dose-dependent manner without provoking weight loss. To determine the extent to which AMs contributed to RSV clearance, we then depleted neonatal AMs using CLip, which further demonstrated that AMs significantly contribute to viral clearance in the neonatal lung.

Low levels of IFNγ in the BAL are consistently associated with greater disease severity in neonates (196), yet it is unclear what IFNγ's protective role is. Consistent with this finding is data published by Cohn et al. demonstrating that mucus production is inhibited by IFNγ in an adult mouse model (197) and our previously published data showing greater mucus production in RSV-infected neonatal mice in which there is minimal IFNγ production compared to RSV-infected adult mice (1). Consistent with previous findings, these data show reductions in goblet cell hyperplasia (as indicated by PAS staining) in RSV+ neonatal lungs treated with inhaled IFNγ (16ng/g and 60ng/g) when compared to untreated RSV+ pups. Mounting evidence continues to support the role of IFNγ as a regulator of mucus production (198-201).

RSV non-structural proteins, NS1 and NS2, have been shown to impair early cellular apoptosis. It is speculated that this is advantageous to the virus; allowing RSV to spread from one cell to another throughout the airway (14). Other data support the idea that RSV sensitizes cells to tumor necrosis factor-related apoptosis-inducing ligand (TRAIL)-mediated apoptosis by

upregulating the expression of death-receptors 4 and 5 (202). The sensitization is tempered however by early increases in Mcl-2, a member of the anti-apoptotic Bcl-2 family, which acts to delay the effects of TRAIL-mediated signaling and delays apoptosis in infected epithelial cells (202). We reasoned, then, that IFNγ, a well-established and appreciated inducer of cellular apoptosis (203) may be associated with less severe RSV disease clinically due to its facilitation of apoptosis thereby limiting the spread of the virus. To test the hypothesis that IFNγ interferes with RSV-mediated impairment of apoptosis, we examined the effect of i.n. IFNγ on apoptosis in RSV infected neonatal mice. Surprisingly, RT-PCR data showed that i.n. IFNγ elicited no change in caspase 3 or 8 expression by 4 or 7 DPI in RSV infected neonates treated with 60ng/g of IFNγ compared to PBS-treated controls (data not shown), despite enhanced viral clearance. However, significant reductions in TUNEL-positive cells in groups receiving i.n. IFNγ suggest possible enhanced clearance of apoptotic cells rather than IFNγ-mediated apoptosis.

We postulated that IFNγ may be augmenting mechanisms of viral resistance in airway epithelial cells that dramatically reduce the viral burden at the onset of infection. IFNγ treatment was independently associated with significantly lower viral titers at our earliest time point, 4 DPI, suggesting that IFNγ treatment reduced the initial viral burden. High levels of IFNγ exposure prior to RSV infection have been shown to dramatically inhibit RSV replication in adult Balb/c mice (204). Additionally, exposure of a human airway epithelial cell line (A549) to IFNγ for 48 hours prior to RSV infection reduced 2-day post-infection viral titers when compared to IL-4 treated or control cells. This reduction was associated with the upregulation of antiviral proteins, such as IFIT1 and Mx1 (205). Similarly, we demonstrated that A549 pretreatment with IFNγ (100ng/mL) for one hour prior to RSV infection significantly inhibited RSV replication within the cell (intracellular) and reduced budded virus (extracellular).

This is the first study to our knowledge, using a neonatal animal model, to examine the role of AMs in the clearance of RSV through the i.n. administration of CLip. We demonstrated that AMs play a significant role in RSV clearance and that delayed viral clearance is associated with reduced weight gain in a neonatal murine model of RSV. Although AM-mediated regulation of weight gain requires further investigation, impaired weight gain in CLip versus PBS-treated pups highlights the importance of AMs during neonatal RSV infection. Mice do not develop clinical symptoms of RSV but a failure to appropriately gain weight suggests that the animals experienced detrimental effects from a lack of effective viral clearance. Clinical data from human neonates < 2 years of age found that faster RSV viral clearance was associated with shorter hospitalizations (206). In a model of influenza, ablation of AMs resulted in significant increases in pulmonary viral load, severe airway inflammation, weight loss, and death in an otherwise sublethal influenza infection (207). Collectively, this suggests that AMs play a critical role in the clearance of respiratory infections like RSV and are essential in returning the host to homeostasis.

Data presented previously (**Chapter 3**) demonstrated the striking differences in $CD4^+$ and $CD8^+$ T cell frequencies in the BAL between RSV-infected adults and infants, in line with results published by Lines et al., in a neonatal murine model of influenza (102). In the infant influenza model, delayed viral clearance was associated with poor T-cell accumulation in the BAL despite a vigorous T-cell response in the interstitium (102). The small proportions of T-cells found in the BAL of RSV-infected infants may indicate a lack of effective recruitment. However, delivery (i.n.) of either IFNγ, CXCL9, or CCL2 did not increase T cells in the BAL in an infant model of influenza (102). Although these agents were administered late in infection (7, 8, and 9 DPI), our studies also showed that i.n. IFNγ early in RSV infection (1, 3, and 5 DPI) did not increase the frequencies of T cells recovered from the alveolar space at 10 DPI. Local delivery of IFNγ to the

infant airway unexpectedly lowered the frequency of $CD4^+$ $Tbet^+$ T cells compared to untreated controls, while the frequencies of $CD4^+$ $GATA3^+$ T cells remained stable. Surprisingly, $CD8^+$ T cell populations were also reduced in IFNγ-treated infants yet, the RSV F protein-specific $CD8^+$ T cell response increased compared to untreated controls.

Initially, we suspected the decrease in $CD4^+$ $Tbet^+$ T cells may be reflective of a rebound effect given the strong inflammatory pressure of IFNγ, but analysis of an earlier seven-day time point showed similar reductions in $Tbet^+$ $CD4^+$ T -cells with no differences in overall $CD4^+$ T cell numbers or $GATA3^+$ expression (data not shown). Given that $CD4^+$ $Tbet^+$ frequencies decreased but $GATA3^+$ $CD4^+$ frequencies remained unchanged, further studies will be required to understand what phenotype these $CD4^+$ T cells became, including investigating frequencies of Th17 $CD4^+$ T cells.

Finally, IFNγ-treated infants demonstrated a reduction in the BAL effector memory $CD8^+$ T cell pool compared to untreated controls but increased RSV F-protein-specific $CD8^+$ T cells, suggesting that IFNγ may regulate $CD8^+$ T cell contraction while enriching the pool of RSV-specific effector memory $CD8^+$ T cells by 10 DPI. The current findings are consistent with previously published reports showing that IFNγ is associated with $CD8^+$ effector/memory contraction and enhanced specificity (208-210). Moreover, Sercan and colleagues demonstrated the importance of IFNγ receptor signaling in $CD11b^+$ macrophage-like cells in the control of $CD8^+$ effector proliferation (208, 209). This is consistent with our previous reports and data presented here, showing the upregulation of $CD11b^+$ on AMs in the BAL of infant mice primed with i.n. IFNγ (1) and provides indirect evidence that IFNγ may contribute to the observed decrease in $CD8^+$ effector/memory cells. Furthermore, IFNγ signaling blocked the formation of memory precursor $CD8^+$ T cells that respond to weak TCR agonists and instead promoted the accrual of

high-affinity memory $CD8^+$ T cells (210). Although the F protein is highly antigenic, it does not contain the primary, immunodominant epitope, thus future studies will determine the effect of i.n. IFNγ on effector/memory $CD8^+$ T cell development targeting the immunodominant M2 protein.

Clinical studies correlate higher IFNγ responses during infant RSV infection with improved clinical symptoms but the mechanisms underlying this response remain poorly understood. In this report, we demonstrate that local administration of IFNγ to RSV-infected infant mice stimulates innate immune cell activation, reduces viral titers, and increases RSV $F_{85\text{-}93}$ $CD8^+$ T cell specificity. Our data suggests that careful consideration be given to IFNγ dosing in infants due to altered IFNγ pharmacokinetics and reduced exposure, but that with adequate dosing increased AM activation can be achieved. A complete pharmacokinetic profile of an inhaled IFNγ dose response study in infants has not been conducted, so it is difficult to predict the upper-end of the therapeutic threshold of inhaled IFNγ. However, the study presented in this chapter as well as clinical data (167) demonstrated low systemic absorption with an intranasal/inhaled dose. This suggests that the dose of locally administered IFNγ could be increased significantly to achieve appropriate levels of activation within the lung and remain below the therapeutic levels of IFNγ in the blood following administration for systemic conditions such as chronic granulomatous disease (164). Additionally, IFNγ had profound ameliorating effects on primary RSV-related pathology resulting in reduced mucus production and apoptotic cellular debris, which may be a result of increased AM activation. Results from these studies have implications for the therapeutic potential of acute, immunomodulation administered directly to the lungs of RSV-infected infants.

5.0 SECONDARY RSV IMMUNE RESPONSES

5.1 INTRODUCTION

RSV infections show distinct seasonality in temperate regions with onset beginning in fall, peaking between mid-December and early February, and dropping off dramatically in late spring. In tropical regions, outbreak patterns are less predictable, having multiple peaks throughout the year or remaining fairly constant (34). In the United States, primary attack rates in infants during RSV outbreaks ranged from 64-98% (33, 211, 212). Virtually all children less than 24 months of age have experienced at least one RSV infection (211) and 50-75% have been infected twice (211, 212). While an amelioration of symptoms following secondary RSV infection has been demonstrated (211), another study showed no symptom improvement during secondary infection and a third infection was necessary to appreciably reduce illness severity (212). Recovering from the acute effects of primary RSV infection is not the only hurdle for infants. Inefficient immunity developed in response to primary infant exposure has profound effects on disease patterns later in life (66, 213, 214) and leaves individuals vulnerable to re-infection throughout life.

Analysis of cytokine signatures measured from the nasal lavages of RSV-infected infants with symptoms of an upper respiratory tract infection (mild RSV) compared to acute bronchiolitis (a severe form of RSV) demonstrated that infants afflicted with acute bronchiolitis had higher IL-4/IFNγ ratios (178). This clinical finding prompted researchers to investigate modes of cytokine delivery during primary RSV infection to understand how various cytokines alter primary, as well as secondary RSV immune responses. Recombinant RSV virus expressing IL-4 did not affect viral titers in primary infant RSV infection and significantly enhanced Th2 immune responses upon

wild-type RSV re-challenge (174). IFNγ delivered via pulmonary instillation or through recombinant RSV technology attenuated RSV during primary infant RSV infection (174) and protected animals from histopathology and airway hyperresponsiveness upon secondary challenge (174, 215). However, in adult mice, IFNγ-expressing RSV virus resulted in enhanced disease following secondary wild-type RSV challenge (216), highlighting the importance of an age appropriate RSV animal model.

Given the importance of the adaptive immune response in preventing or attenuating secondary RSV infections, it is of no surprise that most research has focused on fine-tuning RSV adaptive immunity. However, the innate immune response not only plays an important role in initiating primary RSV responses but also in orchestrating secondary RSV immunity. Mice exposed to RSV as neonates and then re-challenged as adults showed increased levels of innate inflammatory cytokines and AM depletion attenuated weight loss and reduced recruitment of NK and T cells (217). These results hint at a recently recognized phenomenon known as "trained immunity". Immunological dogma states that only members of adaptive immunity can mount pathogen-specific memory following antigen receptor gene rearrangements, but studies have shown that a number of innate immune cells can develop increased responsiveness to secondary stimuli. Trained immunity or innate immune memory occurs following germline-encoded recognition and/or effector molecule exposure (pathogen-associated molecular patterns (PAMPs), danger-associated molecular patterns (DAMPs), cytokines, etc.) resulting in epigenetic rewiring and sustained alterations in translational programs (218).

In this study, our aim was to characterize changes in innate and adaptive immunity in secondary RSV immune responses as a result of IFNγ treatment during primary infant RSV infection to determine the long-term beneficial effects of this treatment. We demonstrate

incomplete protection from RSV re-challenge and similar T cell phenotype signatures between animals treated with IFNγ or vehicle during primary RSV. IFNγ treatment sustained improvements in $CD8^+$ RSV F_{85-93} specificity and reduced central airway resistance. Using an adoptive transfer model, we also show signals of AM trained immunity as a result of IFNγ treatment during primary, infant RSV. These findings demonstrate the broad, far-reaching effects of local IFNγ administration during primary infant RSV and have important implications for future vaccine/therapeutic development.

5.2 RESULTS

5.2.1 Infant mice infected with RSV are partially protected from secondary RSV

Our data demonstrates that primary RSV infection in adult Balb/c mice elicits complete, sterilizing immunity for up to 11 weeks against secondary RSV challenge (**Figure 5.1A**). Chapter 4 outlined how local administration of IFNγ during infant, primary RSV infection effected changes in innate and adaptive RSV immune responses. To determine how IFNγ during primary, infant RSV infection affects protection against secondary RSV exposure, infants were infected with RSV and i.n. IFNγ or vehicle was administered. Then, the animals were allowed to recover for 6 weeks and were re-challenged with RSV. Secondary RSV groups were compared to age-matched naïve and primary RSV controls. Unlike the complete sterilizing immunity seen in adults receiving secondary RSV exposure (**Figure 5.1A**), infant mice infected with RSV and then re-challenged as adults developed only partially protective RSV immunity (**Figure 5.1B**). Both secondary exposure groups demonstrated a log-fold reduction in detectable virus at 2 DPI and effectively inhibited

viral replication between 2 and 4 DPI compared to primary RSV controls (**Figure 5.1B**). Infants who received IFNγ during primary RSV infection (RSV+IFNγ/RSV) had a small but non-significant reduction in detectable virus in the lungs at 4 DPI compared to infants who received only PBS during primary infection (RSV/RSV) (**Figure 5.1B**).

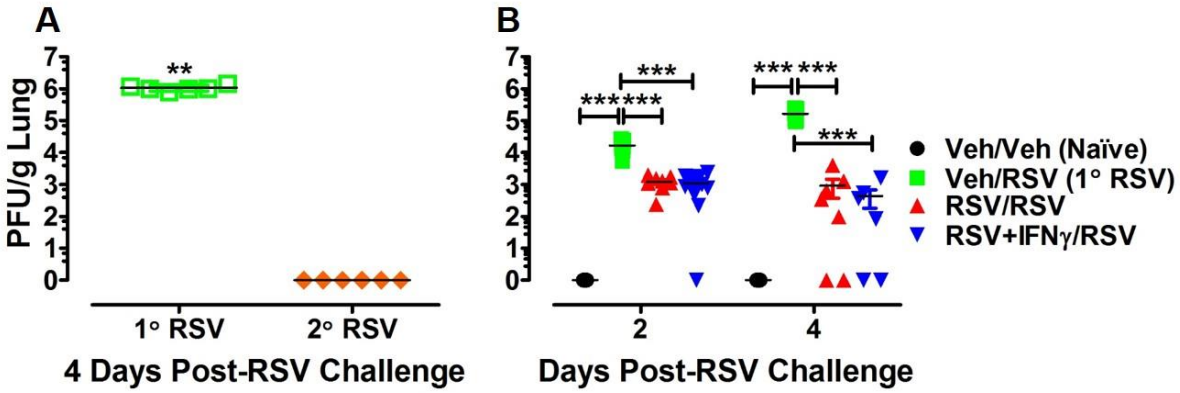

Figure 5.1 RSV infection during infancy is partially protective in secondary RSV exposure.

Adult (4 week old) Balb/c mice (A) were infected with RSV L19 or vehicle and the animals were then rested for 11 weeks. Then, they were challenged (1° RSV) or re-challenged (2° RSV) with RSV and left lung collected for viral titers at 4 days post-RSV challenge. Infant mice (B; PND 4-5) were infected with RSV or vehicle and treated with IFNγ (16ng/g) or vehicle on 1, 3, and 5 DPI. After 6 weeks, the mice were re-challenged with RSV and left lungs collected for viral titers at 2 and 4 days post-RSV challenge. * represent significant differences between experimental groups using Mann-Whitney (A) or 2-way ANOVA with Bonferroni post-test (B); **$\rho = 0.0028$, ***$\rho < 0.001$. Data points represent individual mice, the line represents the mean of $n \geq 4$-11 samples per group ± SD.

5.2.2 IFNγ treatment during primary, infant RSV increases AM and DC activation upon secondary RSV exposure

Macrophages represent a larger proportion of SSC^{HI} cells in the BAL of 1° RSV mice (**Figure 5.2A**) but macrophages (Sig F^{+} $CD11c^{HI}$ +/- CD11b) from RSV-experienced animals had higher expression of the co-stimulatory and antigen presentation receptors, $CD86^{+}$ and $MHCII^{+}$, respectively, with RSV+IFNγ/RSV mice having the highest expression (**Figure 5.2B & C**). RSV+IFNγ/RSV animals also had increased frequencies of Siglec F^{-} macrophages (Sig F^{-} $CD11c^{HI}$ +/- CD11b) (**Figure 5.2D**), which are associated with an inflammatory phenotype (219), with enhanced $CD86^{+}$ and $MHCII^{+}$ expression (**Figure 5.2E & F**).

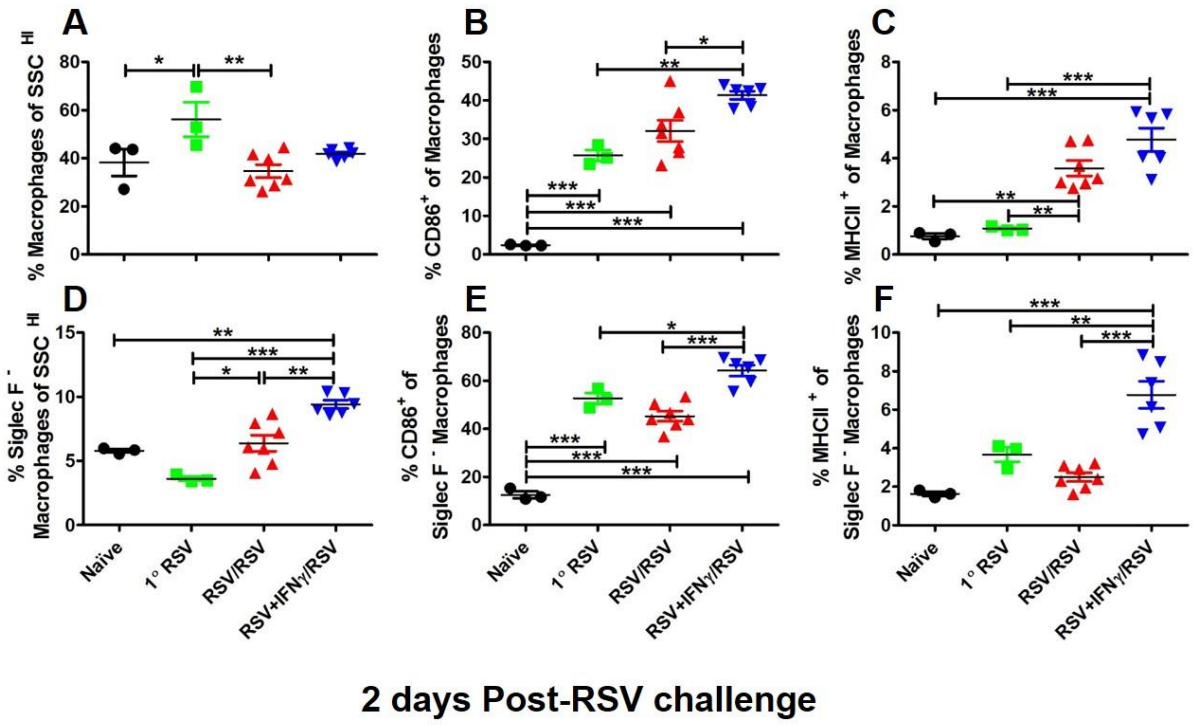

Figure 5.2 IFNγ treatment during primary, infant RSV increases AM activation upon secondary exposure.

Figure 5.2 (continued) Infant mice (PND 4-5) were infected with RSV or vehicle and treated with IFNγ (16ng/g) or vehicle on 1, 3, and 5 dpi. After 6 weeks, the mice were re-challenged with RSV and BAL collected and processed for flow cytometry at 2 days post-RSV challenge. The percentage of cells identified as macrophages (A; Sig F^+ $CD11c^{HI}$ +/- CD11b) were analyzed for expression of $CD86^+$ (B) and $MHCII^+$ (C). Percentages of Sig F- macrophages (D; Sig F^+ $CD11c^{HI}$ +/- CD11b) expressing $CD86^+$ (E) and $MHCII^+$ (F) were also analyzed. * represent significant differences between experimental groups using ANOVA with Tukey's post-test; *$\rho < 0.05$, ** $\rho < 0.01$, or ***$\rho < 0.001$. Data points represent individual mice, the line represents the mean of $n \geq 3$-7 samples per group ± SD.

Given the signals of enhanced antigen presentation and activation on macrophages, we hypothesized that RSV+IFNγ/RSV DCs would similarly display an activated phenotype in the MSLN. The frequency of DCs ($CD11c^+$ $MHCII^{HI}$) was highest in 1° RSV animals, which may be due to higher RSV lung titers and a lack of RSV immune memory (**Figure 5.3A**). Studies of pulmonary DC subtypes have demonstrated the superiority of $CD103^+$ over $CD11b^+$ DCs in eliciting effective cytotoxic $CD8^+$ T cell responses generated from apoptotic cell-associated antigen (220), similar to RSV-infected apoptotic cells that are extruded into the airway. Therefore, we analyzed DC phenotype in the MSLN to determine how the DC phenotype may influence T cell responses upon secondary exposure. There were no significant differences in the frequencies of $CD11b^+$ DCs between groups (**Figure 5.3B**). $CD103^+$ DCs made up a larger proportion of DCs in the lymph node across groups and 1° RSV mice had the highest frequency of $CD103^+$ DCs (**Figure 5.3C**). Interestingly, RSV+IFNγ/RSV mice had higher $CD86^+$ expression on $CD11b^+$ and $CD103^+$ DCs compared to RSV/RSV (**Figure 5.3D**). Lower co-stimulatory expression on $CD103^+$ DCs in RSV/RSV mice was accompanied by increased expression of $CD73^+$ (**Figure 5.3E**). This ecto-5'-nucleotidase converts extracellular adenosine monophosphate to adenosine, which may reduce the inflammatory signaling (106) of $CD103^+$ DCs in RSV/RSV animals. Collectively, these

data suggest that IFNγ treatment during primary, infant RSV elicits a memory response that enhances AM and DC activation upon secondary challenge.

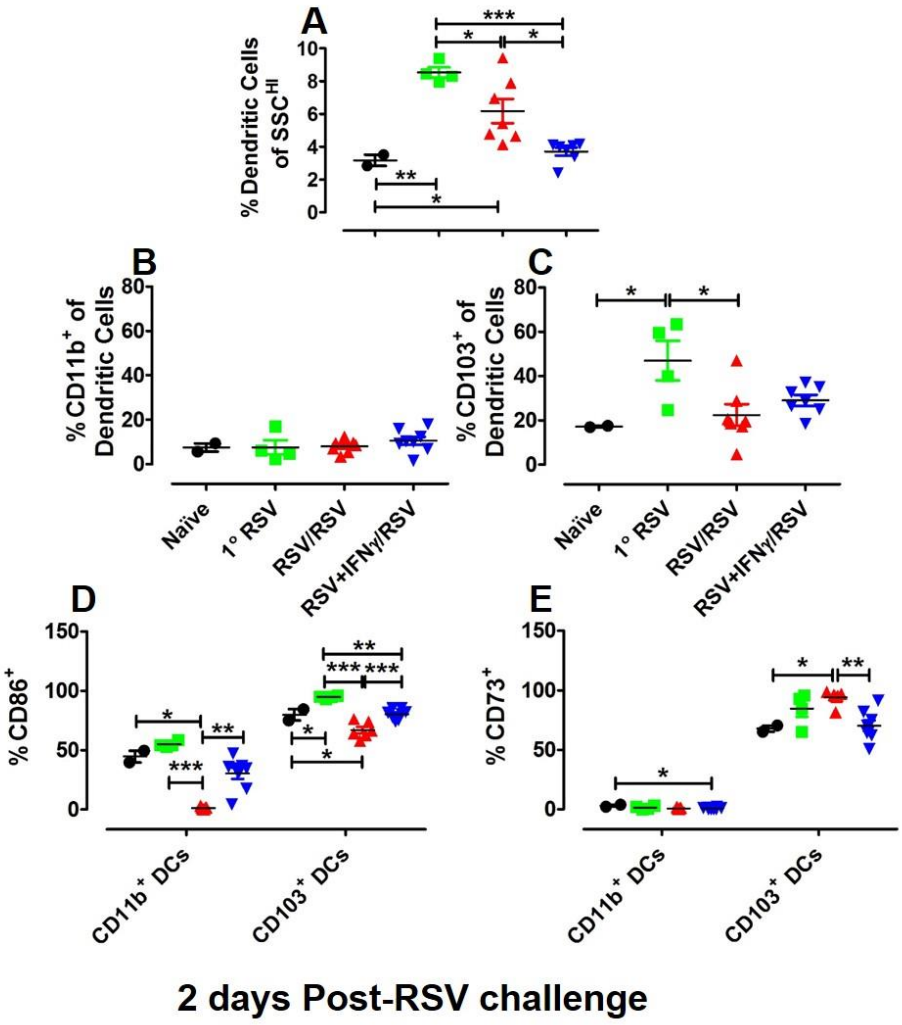

Figure 5.3 IFNγ treatment during primary, infant RSV enhances activation of DCs in MSLN.

Infant mice (PND 4-5) were infected with RSV or vehicle and treated with IFNγ (16ng/g) or vehicle on 1, 3, and 5 dpi. After 6 weeks, the mice were re-challenged with RSV and MSLN collected and processed for flow cytometry at 2 days post-RSV challenge. The percentage of cells identified as DCs (A; $CD11c^+$ $MHCII^{HI}$) were analyzed for expression of $CD11b^+$ (B) and $CD103^+$ (C). $CD86^+$ (D) and $CD73^+$ (E) expression were than analyzed on $CD11b^+$ and $CD103^+$ DCs and graphed side by side but were not compared across $CD11b^+$ and $CD103^+$ DC groups. * represent significant differences between experimental groups using ANOVA with Tukey's post-test; *$\rho < 0.05$, ** $\rho < 0.01$, or ***$\rho < 0.001$. Data points represent individual mice, the line represents the mean of $n \geq$ 2-8 samples per group ± SD.

5.2.3 Infants treated with IFNγ during primary RSV infection have greater RSV specificity upon re-challenge

DCs in the lymph nodes of RSV+IFNγ/RSV mice demonstrated increased $CD86^{+}$ and decreased $CD73^{+}$, suggesting enhanced activation that may result in improved T cell responses. To determine the effects of differential DC activation on T cell memory, BAL was collected and memory T cell phenotypes analyzed via flow cytometry. As expected, re-exposure groups had more $CD4^{+}$ and $CD8^{+}$ effector memory (**Figure 5.4 A and C**, respectively; TCR_{β}^{+} $CD4/8^{+}$ $KLRG^{lo}$ $CD127^{HI}$ $CD44^{HI}$ $CD62L^{-}$) as well as, short-lived effector memory $CD4^{+}$ and $CD8^{+}$ T cells (**Figure 5.4 B and D**, respectively; TCR_{β}^{+} $CD4/8^{+}$ $KLRG^{HI}$ $CD127^{lo}$ $CD44^{HI}$) compared to 1° RSV and naïve mice. However, there were no differences between RSV/RSV and RSV+IFNγ/RSV in the number of memory $CD4^{+}$ or $CD8^{+}$ T cells recovered from the BAL.

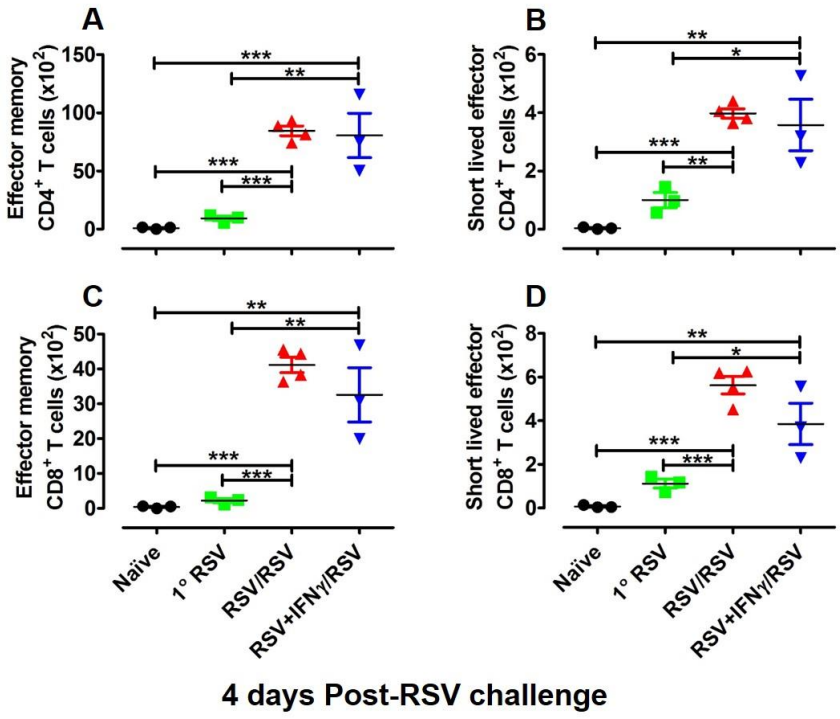

Figure 5.4 Primary, infant RSV infection elicits memory T cells found in the BAL during secondary exposure.

Infant mice (PND 4-5) were infected with RSV or vehicle and treated with IFNγ (16ng/g) or vehicle on 1, 3, and 5 dpi. After 6 weeks, the mice were re-challenged with RSV and BAL collected and processed for flow cytometry at 4 days post-RSV challenge. The numbers of $CD4^+$ (A) and $CD8^+$ (C) effector memory cells (TCR_β^+ $CD4/8^+$ $KLRG^{lo}$ $CD127^{HI}$ $CD44^{HI}$ $CD62L^-$), as well as, $CD4^+$ (B) and $CD8^+$ (D) short-lived effector memory cells (TCR_β^+ $CD4/8^+$ $KLRG^{HI}$ $CD127^{lo}$ $CD44^{HI}$) were compared across experimental groups. * represent significant differences between experimental groups using ANOVA with Tukey's post-test; *$\rho < 0.05$, ** $\rho < 0.01$, or ***$\rho < 0.001$. Data points represent individual mice, the line represents the mean of $n \geq 3$-4 samples per group ± SD.

Although both re-exposure groups had similar numbers of memory T cells in the BAL, we hypothesized that IFNγ treatment during primary, infant RSV infection would lead to improved RSV $F_{85\text{-}93}$-protein specificity in $CD8^+$ T cells during secondary RSV exposure, as was seen in RSV+IFNγ infants during primary RSV infection (Chapter 4). A similar number of $CD8^+$ T cells

(TCR_{β}^{+} $CD8^{+}$) were recovered from the BALs of secondary exposure groups at 4 days post-RSV challenge but both groups had more $CD8^{+}$ T cells than 1º RSV or naïve animals (**Figure 5.5A**). RSV/RSV and RSV+IFNγ/RSV animals had more activated ($CD44^{HI}$) $CD8^{+}$ T cells expressing Tbet, the transcription factor required for IFNγ production, than control groups (**Figure 5.5B**). Importantly, the higher numbers of RSV $F_{85\text{-}93}$ $CD8^{+}$ T cells ($CD19^{-}$ TCR_{β}^{+} $CD8^{+}$ $F_{85\text{-}93}{}^{+}$) demonstrated in IFNγ-treated infants during primary infection were similarly elevated in RSV+ IFNγ/RSV mice following RSV re-challenge (**Figure 5.5C**).

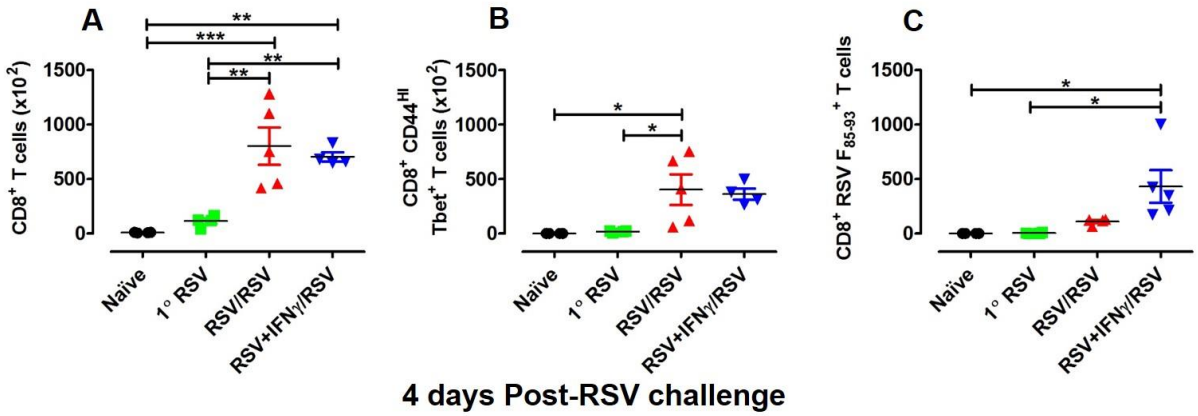

Figure 5.5 Increased RSV $F_{85\text{-}93}$-specific $CD8^+$ T cells from the BAL of RSV+IFNγ/RSV mice.

Infant mice (PND 4-5) were infected with RSV or vehicle and treated with IFNγ (16ng/g) or vehicle on 1, 3, and 5 dpi. After 6 weeks, the mice were re-challenged with RSV and BAL collected and processed for flow cytometry at 4 days post-RSV challenge. The numbers of $CD8^+$ (A; $TCR_\beta{}^+$ $CD8^+$), activated Tbet+ CD8+ cells (B; $TCR_\beta{}^+$ $CD8^+$ $CD44^{HI}$ $Tbet^+$), and RSV F-specific $CD8^+$ T cells (C; $CD19^-$ $TCR_\beta{}^+$ $CD8^+$ RSV $F_{85\text{-}93}{}^+$) were compared across experimental groups. * represent significant differences between experimental groups using ANOVA with Tukey's post-test; *$\rho < 0.05$ or ** $\rho < 0.01$. Data points represent individual mice, the line represents the mean of $n \geq 4$-5 samples per group ± SD.

We next sought to determine what type of T-helper memory response was elicited by secondary RSV challenge by quantifying Th1 (IL-2 and IFNγ) and Th2 (IL-4, IL-5, and IL-13) cytokines from the BAL. IL-2 concentrations increased more quickly in the BAL of RSV/RSV and RSV+IFNγ/RSV mice compared to control groups but 1° RSV had comparable levels by 4 days post-RSV challenge (**Figure 5.6A**). The primary Th1 cytokine, IFNγ, was elevated in both re-exposure groups at both time points analyzed (**Figure 5.6B**). RSV/RSV and RSV+IFNγ/RSV groups had elevated concentrations of IL-4 (**Figure 5.6C**) and IL-13 (**Figure 5.6E**) by 4 days post-

challenge compared to 1° RSV controls but IL-5 (**Figure 5.6D**) was elevated in re-exposure groups at both time points. Together these results suggest that although primary, infant RSV stimulates memory T cell development, it is only partially protective against secondary challenge. Administration of IFNγ during primary, infant RSV increased $CD8^+$ RSV F_{85-93} specificity following secondary RSV exposure but did not alter the T helper cytokine signature in the BAL.

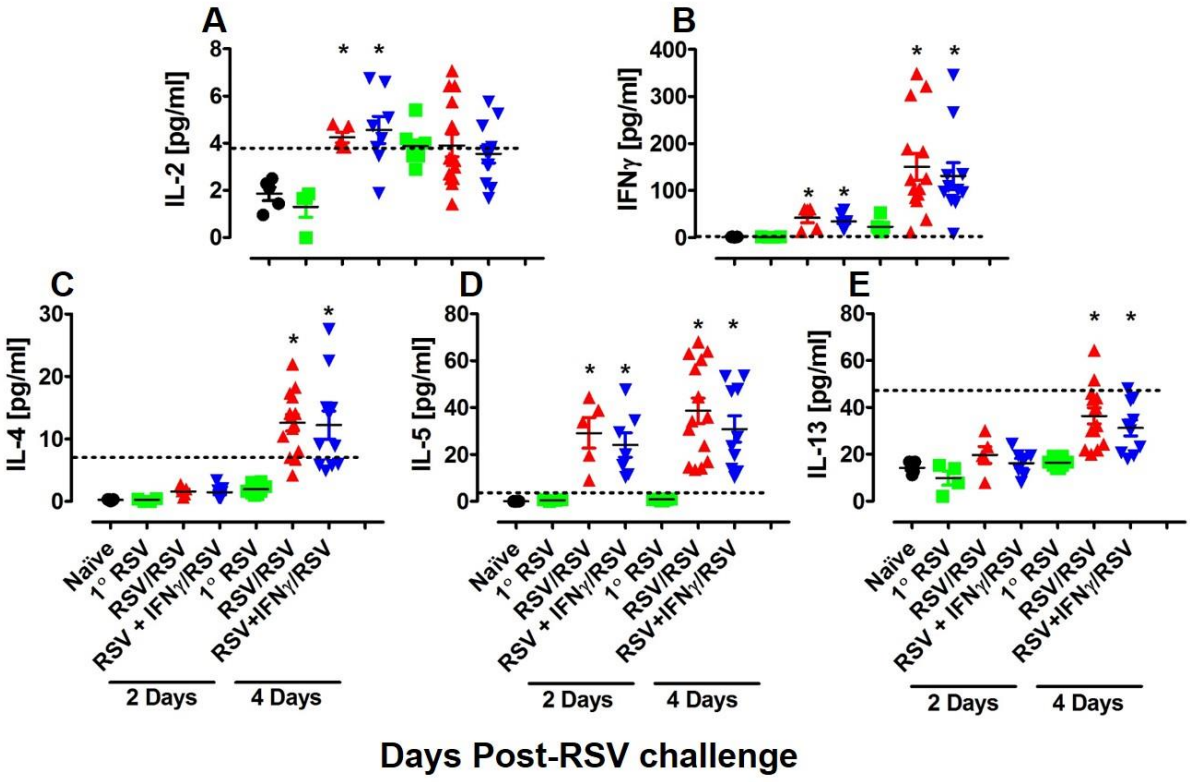

Figure 5.6 IFNγ treatment during primary, infant RSV does not alter T helper cytokine profile.

Figure 5.6 (continued) Infant mice (PND 4-5) were infected with RSV or vehicle and treated with IFNγ (16ng/g) or vehicle on 1, 3, and 5 dpi. After 6 weeks, the mice were re-challenged with RSV and BAL collected for cytokine analysis using Luminex at 2 and 4 days post-RSV challenge. Concentrations of IL-2 (A), IFNγ (B), IL-4 (C), IL-5 (D), and IL-13 (E) were compared across experimental groups at each time point. * represent significant differences between RSV-exposure groups using ANOVA with Tukey's post-test; *$\rho < 0.05$ vs. 1° RSV. Data points represent individual mice, the line represents the mean of $n \geq 4$-14 samples per group ± SD. Dotted line represents the limit of detection.

5.2.4 Following secondary RSV exposure, network complexity and airway resistance decreased with IFNγ treatment during primary, infant RSV infection

Given that the T helper cytokine response was similar between re-exposure groups at both 2 and 4 days post-RSV exposure, we employed a dynamic network analysis to help elucidate what relationships existed between cytokines and how those relationships may influence RSV immune responses. The schematics of dynamic network analyses show all cytokines (circles) for which concentration data from first-wash was provided. If the cytokine participated in the network analysis, it appears red; white if the cytokine was not involved. The black arrows show positive feed-forward responses between cytokines and the red arrows show an inhibitory relationship between cytokines. Overall, we observed that network complexity increased with secondary RSV exposure and that more cytokine networks were engaged between days 2 and 4 post-secondary exposure in these groups (**Figure 5.7**). Interestingly, IFNγ treatment during primary, infant RSV infection reduced the complexity of cytokine networks upon secondary exposure and eliminated the inhibitory feedback (red arrows) demonstrated by the RSV/RSV group at 2 days post-RSV challenge (**Figure 5.7**).

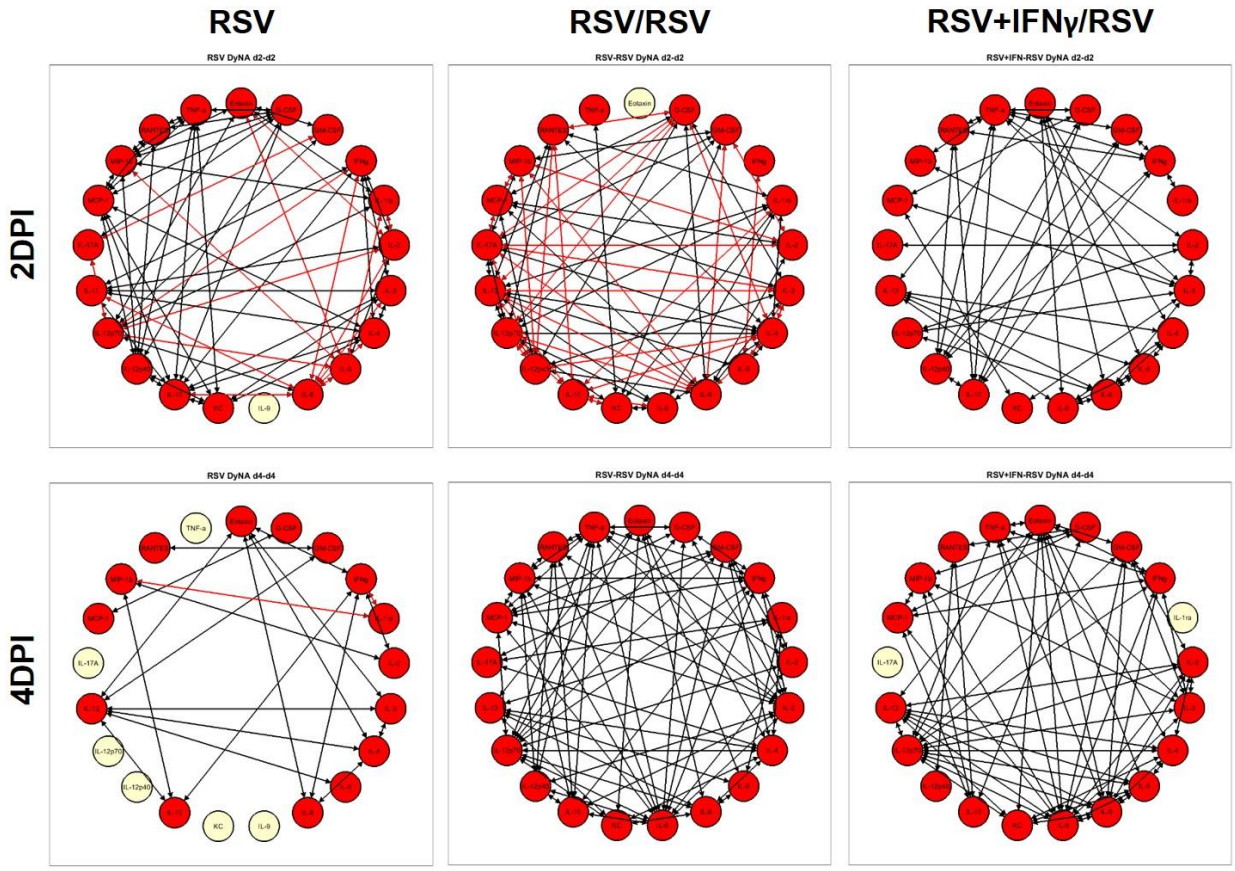

Figure 5.7 IFNγ treatment during primary, infant RSV reduces cytokine network complexity following secondary exposure.

Infant mice (PND 4-5) were infected with RSV or vehicle and treated with IFNγ (16ng/g) or vehicle on 1, 3, and 5 dpi. After 6 weeks, the mice were re-challenged with RSV and BAL collected for cytokine analysis using Luminex at 2 and 4 days post-RSV challenge. Collaborators, Drs. Yoram Vodovotz and Ruben Zamora, used cytokine concentrations to develop dynamic network analyses using a stringency limit of 0.7. Red circles indicate cytokines actively involved in the immune response while white circle represent cytokines that are not playing a role in the network. Black lines demonstrate a stimulatory relationship and red lines indicate an inhibitory relationship between cytokines. Neither black nor red arrows suggest directionality. Based off of cytokine values from $n \geq 4$-11 samples per group ± SD.

Our observation of a loss of inhibitory cytokine feedback at 2 days post-RSV exposure in RSV+IFNγ/RSV compared to RSV/RSV animals led us to hypothesize that innate inflammatory cell recruitment would be increased in the RSV+IFNγ/RSV group. To determine if innate

inflammatory cell recruitment was increased in RSV+IFNγ/RSV animals, BAL was collected and cell identification and quantification was performed via flow cytometry and chemokine quantification by Luminex. Monocytes (**Figure 5.8A**; Sig F^- $F4/80^+$ $CD206^-$ $CD11c^+$ $CD11b^+$) and neutrophils (**Figure 5.8C**; Sig F^- $Ly6G^+$ $CD11b^{HI}$ $CD11c^-$) were elevated in both re-exposure groups compared to the controls. DCs (**Figure 5.8B**; Sig F^- $CD11c^+$ $MHCII^{HI}$) were also elevated in RSV/RSV and RSV+IFNγ/RSV groups compared to naïve controls. Although the total number of eosinophils was small, RSV+IFNγ/RSV animals had more of this inflammatory cell type (**Figure 5.8D**; Sig F^+ $F4/80^+$ $CD206^-$ $CD200R^-$ $CD11c^-$ $CD11b^+$) than controls. Neutrophil (KC; keratinocyte chemokine) and eosinophil (eotaxin) chemokine concentrations correlated with the cellular composition of the BAL. KC was elevated at 2 and 4 days post-RSV challenge for both re-exposure groups (**Figure 5.8E**). It should be noted that KC was elevated in the 1° RSV group at 2 days post-RSV challenge but neutrophils were not identified in BAL samples via flow cytometry (**Figure 5.8C**). This is likely a kinetic effect observed in 1° RSV, in which neutrophil recruitment to the BAL peaks around 2 days post-infection (data not shown) when KC concentrations are high. This is supported by the fact that KC values returned to baseline by 4 days post-RSV challenge in 1° RSV animals. A difference in kinetics may also explain increased eosinophils in the BAL of RSV+IFNγ/RSV animals at 4 days post-RSV challenge. Eotaxin began to rise in RSV+IFNγ/RSV animals at 2 days post-RSV challenge but both secondary exposure groups had similar concentrations by 4 days post-RSV challenge (**Figure 5.8F**), which suggests that eosinophils may increase in the BAL of RSV/RSV animals at later time points.

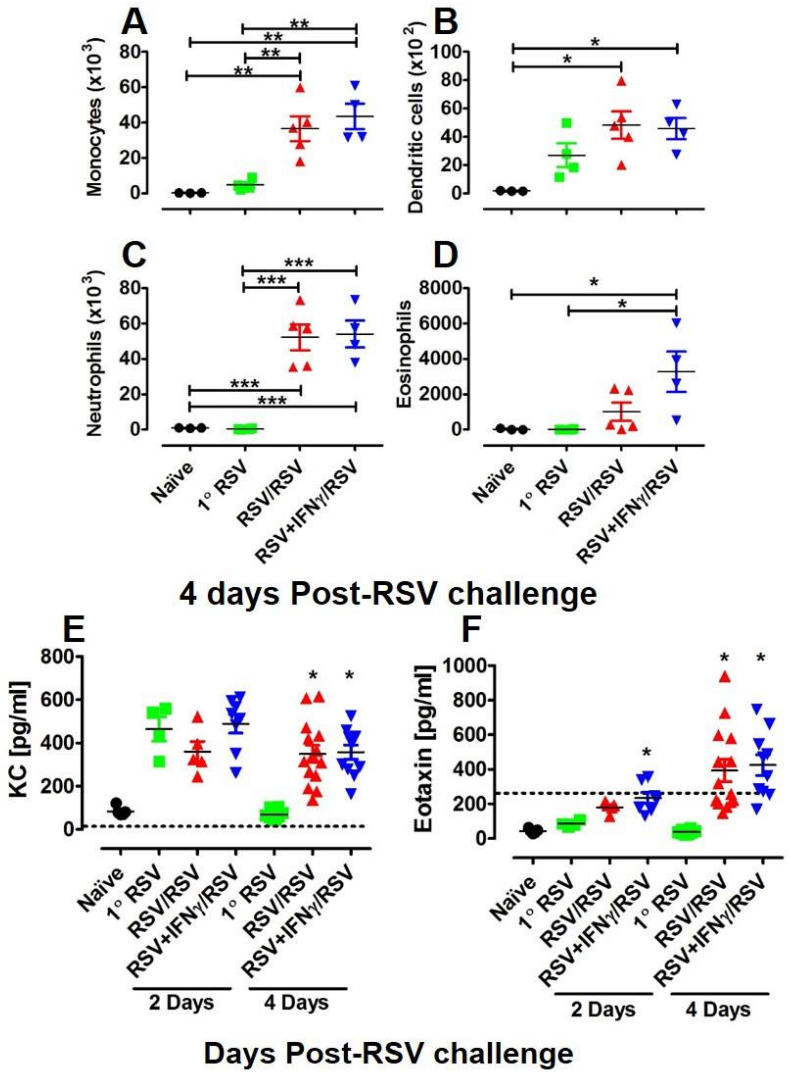

Figure 5.8 IFNγ treatment during primary, infant RSV does not alter secondary innate inflammatory cell recruitment.

Infant mice (PND 4-5) were infected with RSV or vehicle and treated with IFNγ (16ng/g) or vehicle on 1, 3, and 5 dpi. After 6 weeks, the mice were re-challenged with RSV and BAL collected and processed for flow cytometry and chemokine analysis. The total number of monocytes (A; Sig F^- $F4/80^+$ MR^- $CD11c^+$ $CD11b^+$), dendritic cells (B; Sig F^- $CD11c^+$ $MHCII^+$), neutrophils (C; Sig F^- $Ly6G^+$ $CD11b^{HI}$ $CD11c^-$), and eosinophils (D; Sig F^+ $F4/80^+$ $CD206^-$ $CD200R^-$ $CD11c^-$ $CD11b^+$) were compared across experimental groups at 4 days post-RSV challenge using ANOVA with Tukey's post-test; *$\rho < 0.05$, ** $\rho < 0.01$, or ***$\rho < 0.001$. KC (E) and eotaxin (F) concentrations were compared between groups at 2 and 4 day time points. * represent significant differences between RSV-exposure groups using ANOVA with Tukey's post-test; *$\rho < 0.05$ vs. 1° RSV. Dotted line represents the limit of detection. Data points represent individual mice, the line represents the mean of $n \geq 3$-14 samples per group ± SD.

Due to the differences in cytokine network complexity between RSV/RSV and RSV+IFNγ/RSV groups observed previously, we sought to determine the physiological effects of IFNγ treatment during primary infant RSV infection on secondary RSV responses. To understand how IFNγ treatment may have altered airway hyperresponsiveness, we collected measures of airway mechanics at baseline and during methacholine-induced bronchoconstriction. Static compliance, a measure of the lung's ability to stretch and expand, was reduced across all RSV-infected groups (**Figure 5.9A**). Hysteresis, which can be thought of as collective atelectasis, was reduced in the RSV+IFNγ/RSV group compared to 1° RSV controls (**Figure 5.9B**). Importantly, IFNγ treatment of infants infected with RSV decreased central resistance to the level of control groups, while resistance in RSV/RSV animals remained elevated at the highest dose of methacholine tested (**Figure 5.9C**). Furthermore, the cytokines IL-3 and IL-9 were elevated in the BALs of RSV/RSV animals (**Figure 5.9 D & E**, respectively) and have been associated with the development of allergic asthma in both humans (221) and murine models of asthma (222-224).

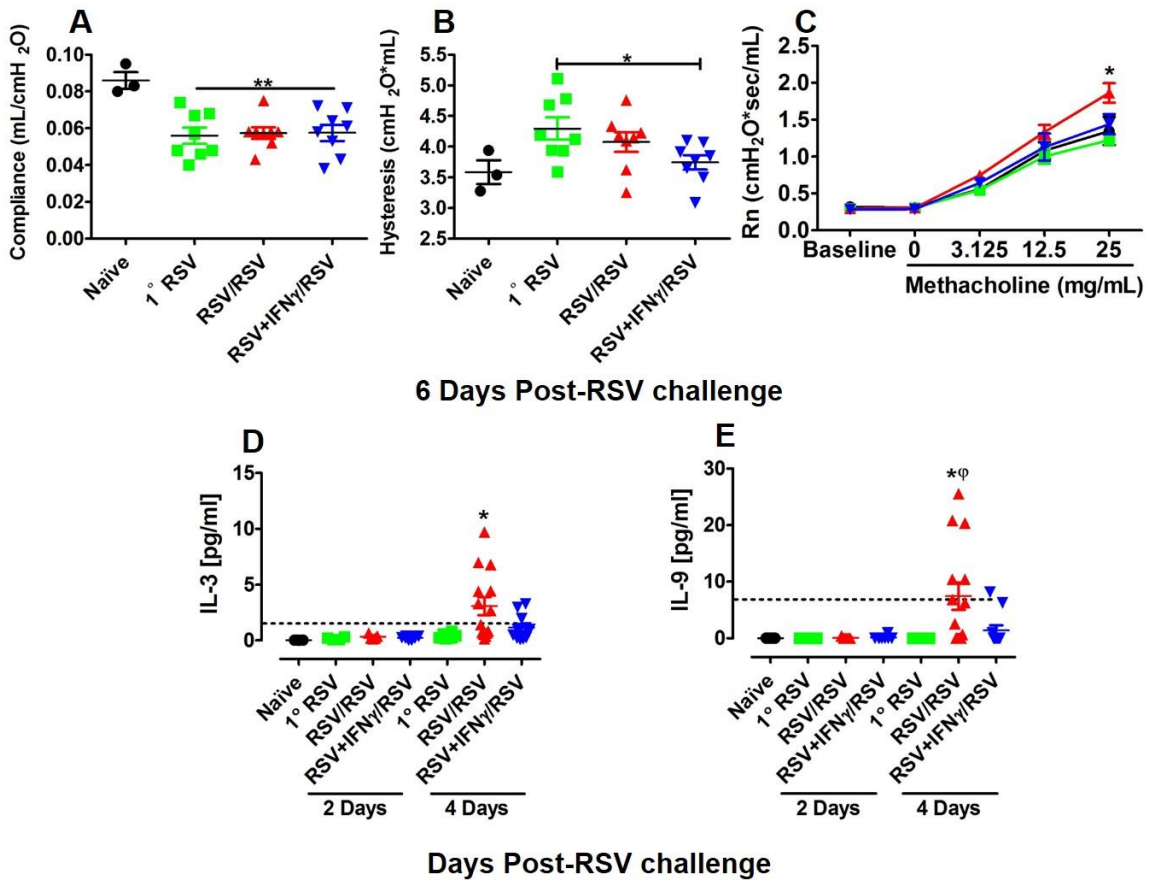

Figure 5.9 IFNγ treatment during primary, infant RSV reduces AHR upon secondary challenge.

Infant mice (PND 4-5) were infected with RSV or vehicle and treated with IFNγ (16ng/g) or vehicle on 1, 3, and 5 dpi. After 6 weeks, the mice were re-challenged with RSV and BAL collected for cytokine analysis at 2 and 4 days post-RSV challenge. At 6 days post-challenge, animals from each group were tested for AHR using FlexiVent. Baseline compliance (A) and hysteresis (B) were compared across groups using ANOVA with Tukey's (A) or Bonferroni (B) post-test; uncapped line (A) indicates difference between naïve and all RSV-exposed groups, *$\rho < 0.05$ or ** $\rho < 0.01$. Airway resistance (C, Rn) measures were compared using 2-way ANOVA with Bonferroni post-test; *$\rho < 0.05$ for RSV/RSV vs. 1° RSV. IL-3 (D) and IL-9 (E) concentrations were compared between groups; * represent significant differences between RSV-exposure groups using ANOVA with Tukey's post-test; *$\rho < 0.05$ vs. 1° RSV, $^{\varphi}$ $\rho < 0.05$ vs. RSV+IFNγ/RSV. Dotted line represents the limit of detection. Data points represent individual mice, the line represents the mean of $n \geq 3$-14 samples per group ± SD.

Under more stringent analytical conditions, the dynamic network analysis supported the finding that IL-3 and IL-9 may be contributing to elevated airway resistance in RSV/RSV animals (**Figure 5.10**). This positive feedforward interaction between IL-3 and IL-9 in the RSV/RSV group will require further studies investigating what cells are the primary producers of these cytokines and how IFNγ treatment during primary, infant RSV infection alters this response. Together these results suggest that IFNγ treatment of RSV-infected infants alters their RSV immune response by reducing both the complexity and inhibitory feedback of the cytokine network and protects against the development of AHR following secondary exposure.

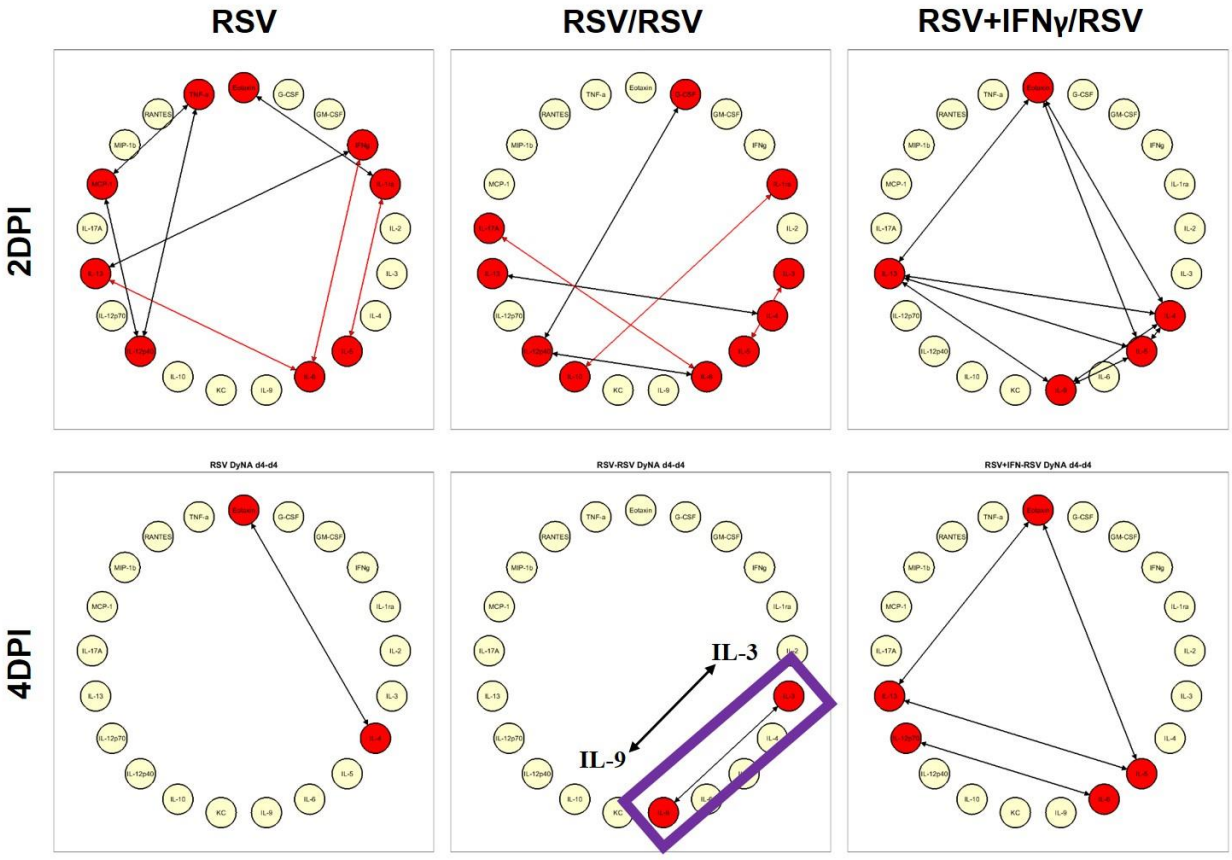

Figure 5.10 Elevated IL-3 and IL-9 associated with increased AHR in RSV/RSV animals.

Figure 5.10 (continued) Infant mice (PND 4-5) were infected with RSV or vehicle and treated with IFNγ (16ng/g) or vehicle on 1, 3, and 5 dpi. After 6 weeks, the mice were re-challenged with RSV and BAL collected for cytokine analysis using Luminex at 2 and 4 days post-RSV challenge. Using a higher stringency level of 0.95, collaborators, Drs. Yoram Vodovotz and Ruben Zamora, used cytokine concentrations to develop dynamic network analyses. Purple rectangle highlights the stimulatory relationship between IL-3 and IL-9 in RSV/RSV animals. Based off of cytokine values from $n \geq$ 4-14 samples per group ± SD.

5.2.5 AMs stimulated with IFNγ during primary, infant RSV display signals of innate immune memory

Our results from 2 days post-RSV challenge (**Figures 5.2**) suggested AMs, which are long-lived airway resident cells (110), may have been directly impacted by IFNγ treatment during primary, infant RSV. To determine if the activation threshold of infant AMs may have been lowered by IFNγ treatment during primary RSV infection, innate inflammatory cytokines/chemokines typically produced by AMs were measured from the BAL at early time points following RSV re-exposure. The inflammatory cytokines IL-6 (**Figure 5.11A**) and IL-12p70 (**Figure 5.11C**) were elevated in RSV+IFNγ/RSV mice 2 days after RSV re-exposure. Similarly, concentrations of RANTES/CCL5 (chemokine ligand-5; **Figure 5.11B**) and MCP-1/CCL2 (chemokine ligand-2; **Figure 5.11D**), which recruit various leukocytes to sites of inflammation, were increased in RSV+IFNγ/RSV animals earlier than other groups.

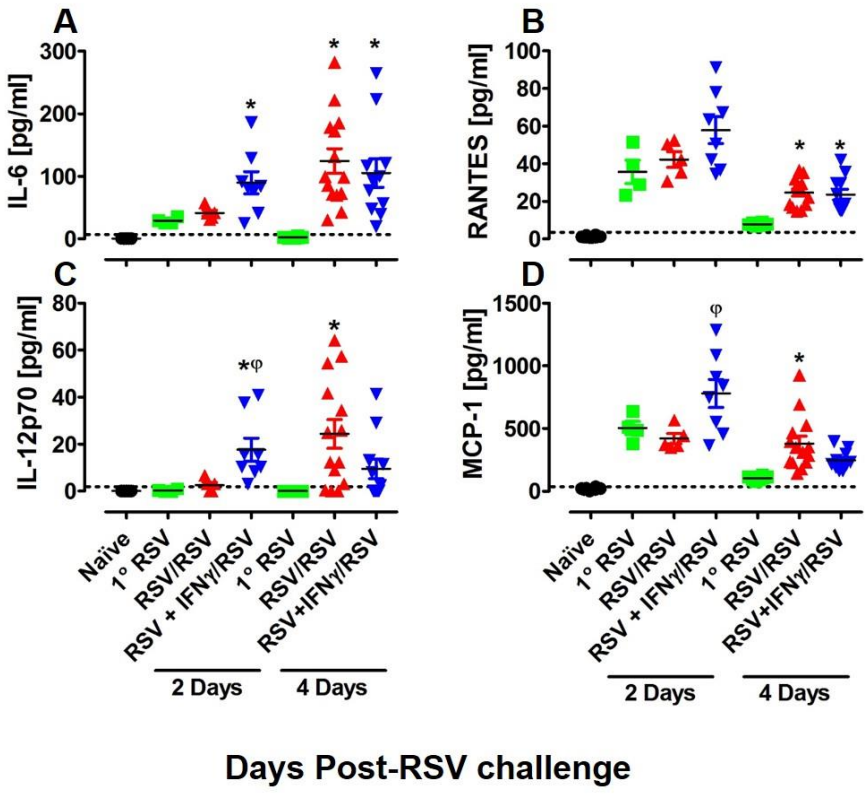

Figure 5.11 Inflammatory cytokine/chemokine production hastened in RSV+IFNγ/RSV mice.

Infant mice (PND 4-5) were infected with RSV or vehicle and treated with IFNγ (16ng/g) or vehicle on 1, 3, and 5 dpi. After 6 weeks, the mice were re-challenged with RSV and BAL collected for cytokine/chemokine analysis using Luminex at 2 and 4 days post-RSV challenge. Concentrations of IL-6 (A), RANTES/CCL5 (B), IL-12p70 (C), and MCP-1/CCL2 (D) were compared across experimental groups at each time point. * represent significant differences between RSV-exposed groups (naïve graphed for reference) using ANOVA with Tukey's post-test; *$\rho < 0.05$ vs. 1° RSV, $^{\varphi}$ $\rho < 0.05$ vs. RSV+IFNγ/RSV. Data points represent individual mice, the line represents the mean of $n \geq 4$-14 samples per group ± SD. Dotted line represents the limit of detection.

Next, AMs were identified from the BAL using the gating strategy outline in Chapter 3 (**Figure 3.1**). All RSV-infected groups had a reduction in AMs (**Figure 5.12A**; Sig F^+ $F4/80^+$ $CD206^+$ $CD200R^+$ $CD11c^{HI}$) compared to naïve controls. CD11b expression was not significantly

increased in secondary exposure groups but was increased in 1° RSV controls (**Figure 5.12B**), as was seen previously in Chapter 3. Fewer AMs expressed $CD73^+$ in secondary exposure groups compared to controls (**Figure 5.12C**) suggesting less inhibition of inflammatory signaling. While the expression of $CD86^+$ on AMs did not differ significantly between groups (**Figure 5.12D**), secondary exposure groups had greater numbers of $MHCII^+$ AMs (**Figure 5.12E**).

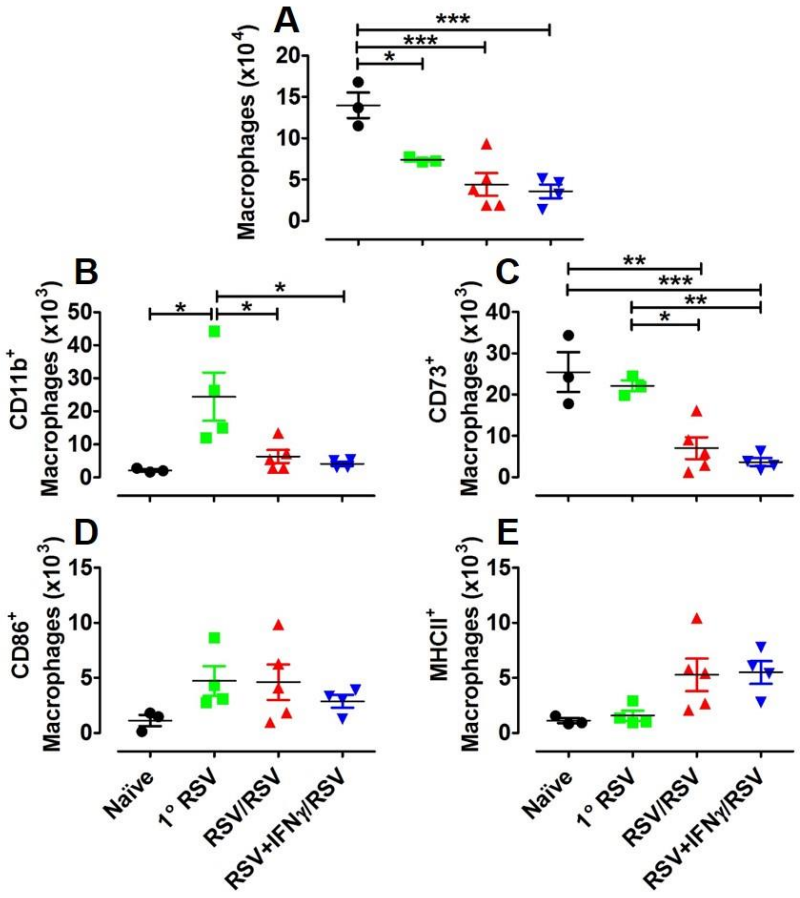

Figure 5.12 AMs from secondary exposure groups display activated phenotype.

Figure 5.12 (continued) Infant mice (PND 4-5) were infected with RSV or vehicle and treated with IFNγ (16ng/g) or vehicle on 1, 3, and 5 dpi. After 6 weeks, the mice were re-challenged with RSV and BAL collected and processed for flow cytometry at 4 days post-RSV challenge. The number of cells identified as AMs (A; Sig F^+ $F4/80^+$ $CD206^+$ $CD200R^+$ $CD11c^{HI}$) were analyzed for expression of $CD11b^+$ (B), $CD73^+$ (C), $CD86^+$ (D) and $MHCII^+$ (E). * represent significant differences between experimental groups using ANOVA with Tukey's post-test; *$\rho < 0.05$, ** $\rho < 0.01$, or ***$\rho < 0.001$. Data points represent individual mice, the line represents the mean of $n \geq 3$-5 samples per group ± SD.

It was noted at 2 days post-RSV challenge that a higher proportion of cells in the BALs of secondary exposure groups were Siglec F^- AMs, especially in RSV+IFNγ/RSV animals (**Figure 5.2D**). We hypothesized that conventional AMs, which are defined by Siglec F expression, downregulate Siglec F in response to RSV detection, becoming more inflammatory and that this response is exaggerated in a memory RSV immune response. Indeed, a larger population of Sig F^- AMs (Sig F^- $F4/80^+$ $CD206^+$ $CD200R^+$ $CD11c^{HI}$) were identified in the BALs of secondary exposure animals (**Figure 5.13A**). These Sig F^- AMs demonstrated an activated phenotype including increased expression of $CD11b^+$ (**Figure 5.13B**) and $CD73^+$ (**Figure 5.13C**), whose production of adenosine may be required to temper the inflammatory response. Additionally, Sig F^- AMs in secondary exposure groups were found to have greater co-stimulatory/antigen-presentation capabilities, characterized by enhanced expression of $CD86^+$ (**Figure 5.13D**) and $MHCII^+$ (**Figure 5.13E**).

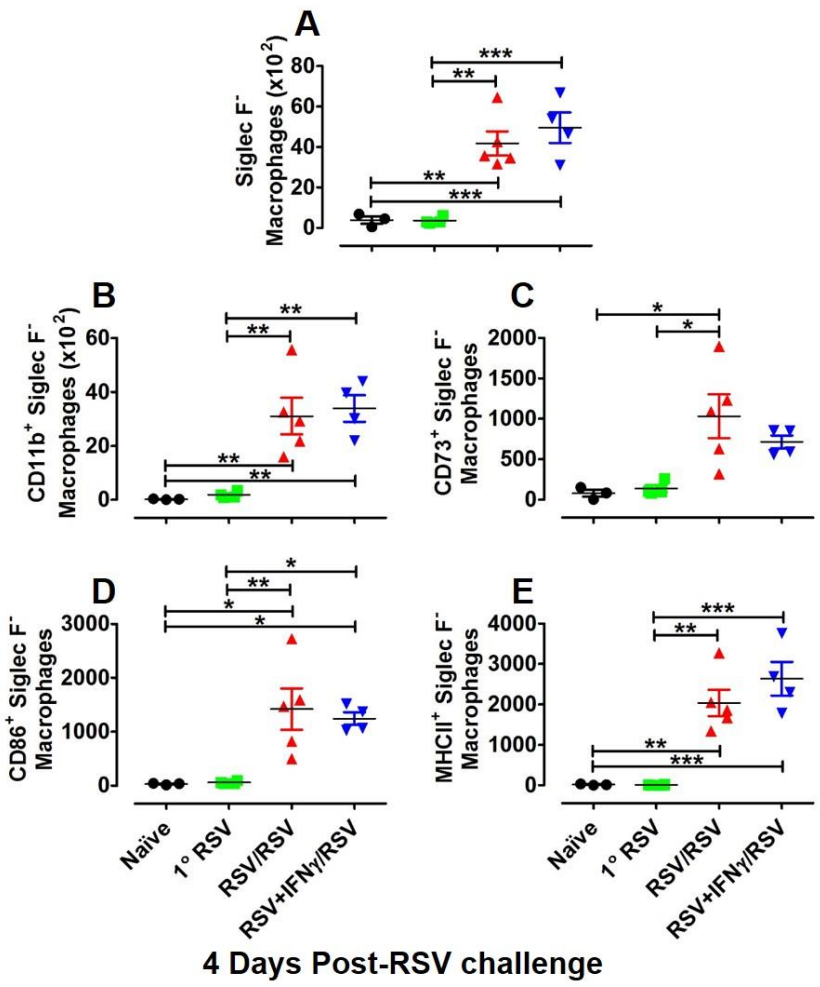

Figure 5.13 Secondary RSV exposure increases Siglec F⁻ AM population.

Infant mice (PND 4-5) were infected with RSV or vehicle and treated with IFNγ (16ng/g) or vehicle on 1, 3, and 5 dpi. After 6 weeks, the mice were re-challenged with RSV and BAL collected and processed for flow cytometry at 4 days post-RSV challenge. The number of cells identified as Sig F^- macrophages (A; Sig F^- $F4/80^+$ $CD206^+$ $CD200R^+$ $CD11c^{HI}$) were analyzed for expression of $CD11b^+$ (B), $CD73^+$ (C), $CD86^+$ (D) and $MHCII^+$ (E). * represent significant differences between experimental groups using ANOVA with Tukey's post-test; *$\rho < 0.05$, ** $\rho < 0.01$, or ***$\rho < 0.001$. Data points represent individual mice, the line represents the mean of $n \geq 3$-5 samples per group ± SD.

In the secondary RSV challenge model, we could not discount the possibility that enhanced AM activation may have occurred as a result of an adaptive, memory immune response, including RSV-specific antibodies, memory B cells, and lung-resident, memory T cells, becoming activated and producing cytokines, etc. with the re-introduction of RSV. To determine whether AMs can develop innate memory in response to RSV and eliminate the influence of an adaptive, memory immune response, we performed an adoptive transfer of AMs from mice exposed to RSV during infancy (+/- IFNγ treatment) into naïve adults who were then challenged with RSV. Briefly, infant Balb/c mice were infected with RSV or vehicle and treated with i.n. IFNγ or vehicle on days 1, 3 and 5 post-infection. The mice were allowed to recover for 6 weeks then were sacrificed and their AMs were harvested. Each experimental group's AMs were pooled and stained with CFSE so that they could be tracked in recipient animals. Then, CFSE-stained AMs were transferred into RSV-naïve recipient mice. One day after the $CFSE^+$ AM transfer, recipient mice were challenged with RSV and samples were collected at 4 DPI.

AMs were identified in BAL samples harvested from recipient mice using the gating strategy outlined in **Figure 5.14**. Cells were first divided according to CFSE staining then, AMs were defined as Sig F^+ $F4/80^+$ $CD206^+$ $CD11c^+$ or Sig F^- $F4/80^+$ $CD206^+$ $CD11c^+$ for Sig F^- AMs.

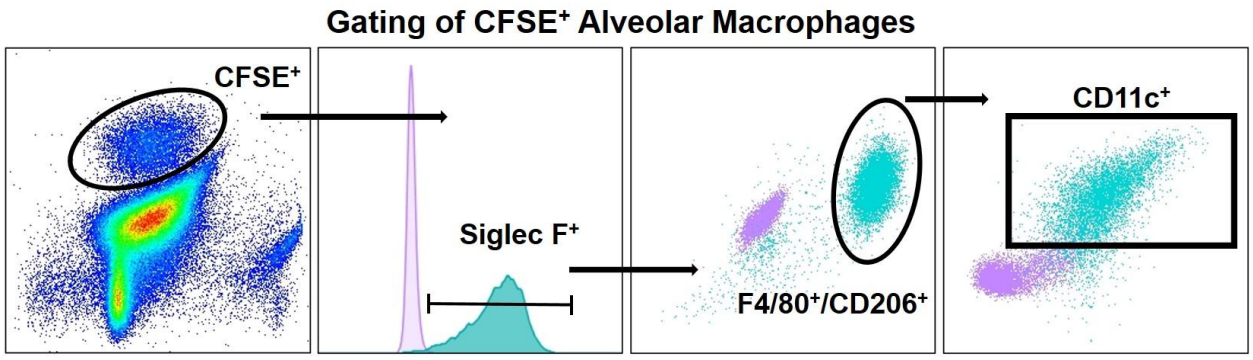

Figure 5.14 Gating of CFSE$^+$ AMs.

Infant mice (PND 4-5) were infected with RSV or vehicle and treated with IFNγ (16ng/g) or vehicle on 1, 3, and 5 dpi. After 6 weeks, the mice were culled, BAL collected, and AMs isolated and stained with CFSE. CFSE$^+$ macrophages were adoptively transferred (i.n. 5 x 10^5 cells/100mcl) into naïve recipients. One day after transfer, recipient mice were challenged with RSV or vehicle. BAL was collected at 4 days post-RSV challenge and analyzed via flow cytometry. Cells were first separated according to their CFSE status then identified as AMs (Sig F$^+$ F4/80$^+$ CD206$^+$ CD11c$^+$) or Sig F$^-$ AMs (Sig F$^-$ F4/80$^+$ CD206$^+$ CD11c$^+$).

The overwhelming majority of BAL cells in recipient mice were CFSE$^-$ but approximately 6% of BAL cells were CFSE$^+$ and this percentage was similar across groups (**Figure 5.15A**). Nearly 100% of CFSE+ cells were identified as AMs (**Figure 5.15B**) however, a small percentage of CFSE$^+$ cells were Sig F$^-$ AMs (**Figure 5.15C**). Interestingly, a higher percentage of AMs downregulated Sig F$^-$, in response to RSV infection if they were exposed IFNγ during infancy. When MHCII$^+$ expression was examined as a marker of activation, we found that a higher percentage of CFSE$^+$ AMs and Sig F$^-$ AMs expressed MHCII compared to their CFSE$^-$ counterparts (**Figure 5.15D & E**). Furthermore, MHCII$^+$ MFI on CFSE$^+$ AMs and Sig F$^-$ AMs in RSV+IFNγ/RSV animals was significantly higher than the same CFSE$^-$ populations (**Figure 5.15F**

& G). Of note, the average MHCII$^+$ MFI on RSV+IFNγ/RSV CFSE$^+$ Sig F$^-$ AMs was approximately 5x higher than MHCII$^+$ MFI on CFSE$^+$ AMs from the same population.

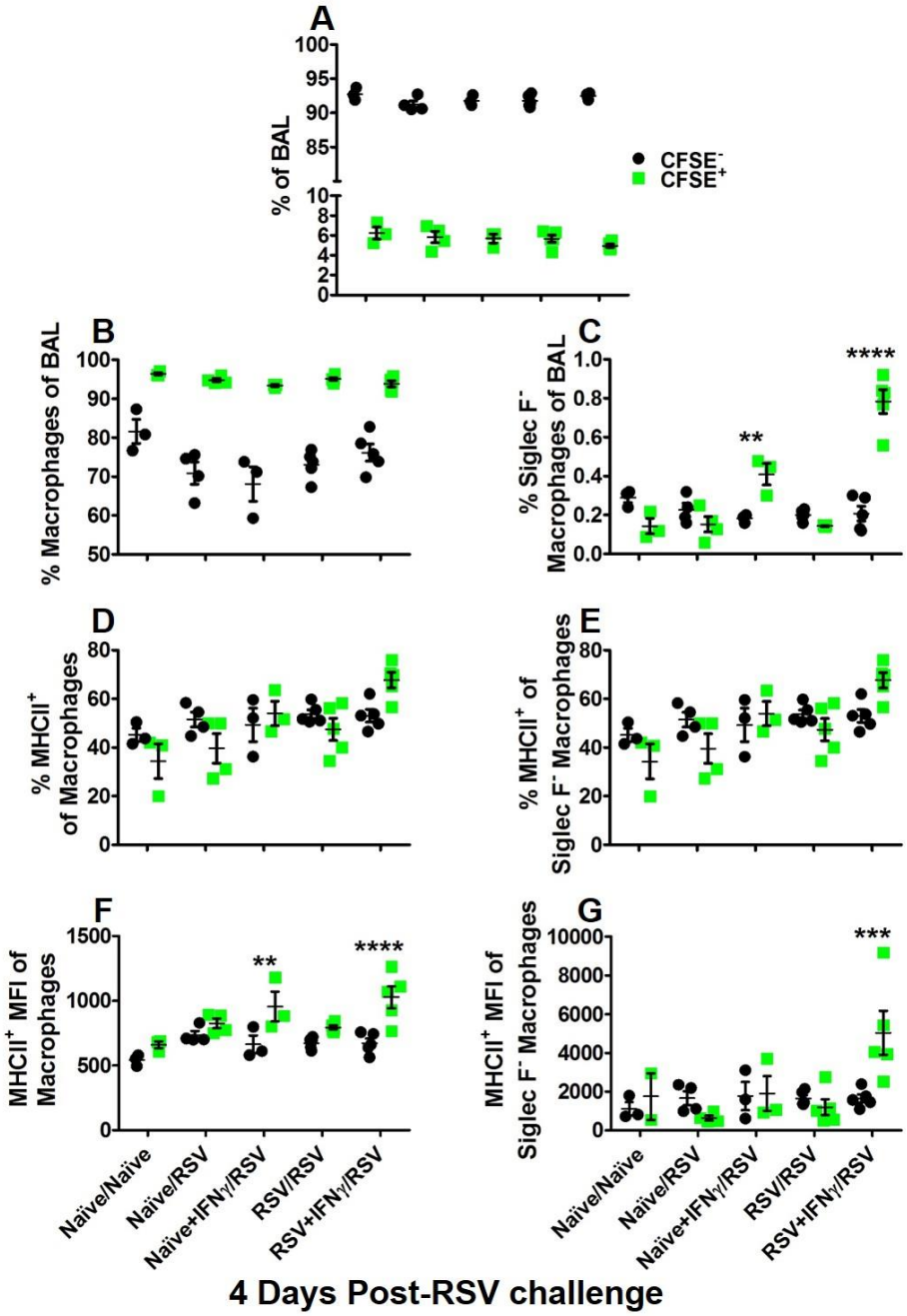

Figure 5.15 CFSE$^+$ RSV+IFNγ/RSV macrophages express more MHCII$^+$ than CFSE$^-$ macrophages.

Figure 5.15 (continued) Infant mice (PND 4-5) were infected with RSV or vehicle and treated with IFNγ (16ng/g) or vehicle on 1, 3, and 5 dpi. After 6 weeks, the mice were culled, BAL collected, and AMs isolated and stained with CFSE. $CFSE^+$ macrophages were adoptively transferred into naïve recipients. One day after transfer, recipient mice were challenged with RSV or vehicle. BAL was collected at 4 days post-RSV challenge and analyzed via flow cytometry. The proportion of BAL cells that were $CFSE^+$ (A), AMs (B), Sig F^- AMs (C) were compared to their $CFSE^-$ counterparts. Expression of $MHCII^+$ was analyzed on AMs (D) and Sig F^- AMs (E), as well as, the MFI of $MHCII^+$ AMs (F) and Sig F^- AMs (G) were compared between $CFSE^+$ and $CFSE^-$ cells. * represent significant differences between experimental groups using 2-way ANOVA with Bonferroni post-test; *$\rho < 0.05$, ** $\rho < 0.01$, or ***$\rho < 0.001$. Data points represent individual mice, the line represents the mean of $n \geq 3$-5 samples per group ± SD.

Next, the total number of $CFSE^+$ events in the BAL were analyzed to verify that animals within each group had a similar number of surviving, transferred $CFSE^+$ cells. Although the number of surviving, transferred macrophages varied within and between groups, with the IFNγ control group (Naïve+IFNγ/RSV) having the smallest number, no significant differences were detected (**Figure 5.16A**). Most $CFSE^+$ cells were identified as AMs (**Figure 5.16B**) and there was a small but non-significant trend toward a higher number of $CFSE^+$ AMs expressing $MHCII^+$ in the groups re-exposed to RSV (**Figure 5.16D**). Importantly, the number of $CFSE^+$ Sig F^- AMs was significantly higher in the RSV+IFNγ/RSV group (**Figure 5.16C**) and this group had the highest number of $CFSE^+$ Sig F^- AM expressing $MHCII^+$ (**Figure 5.16E**). These data suggest that in the absence of adaptive memory, AMs exposed to IFNγ during primary, infant RSV display "trained memory", lowering their threshold of activation upon RSV re-exposure.

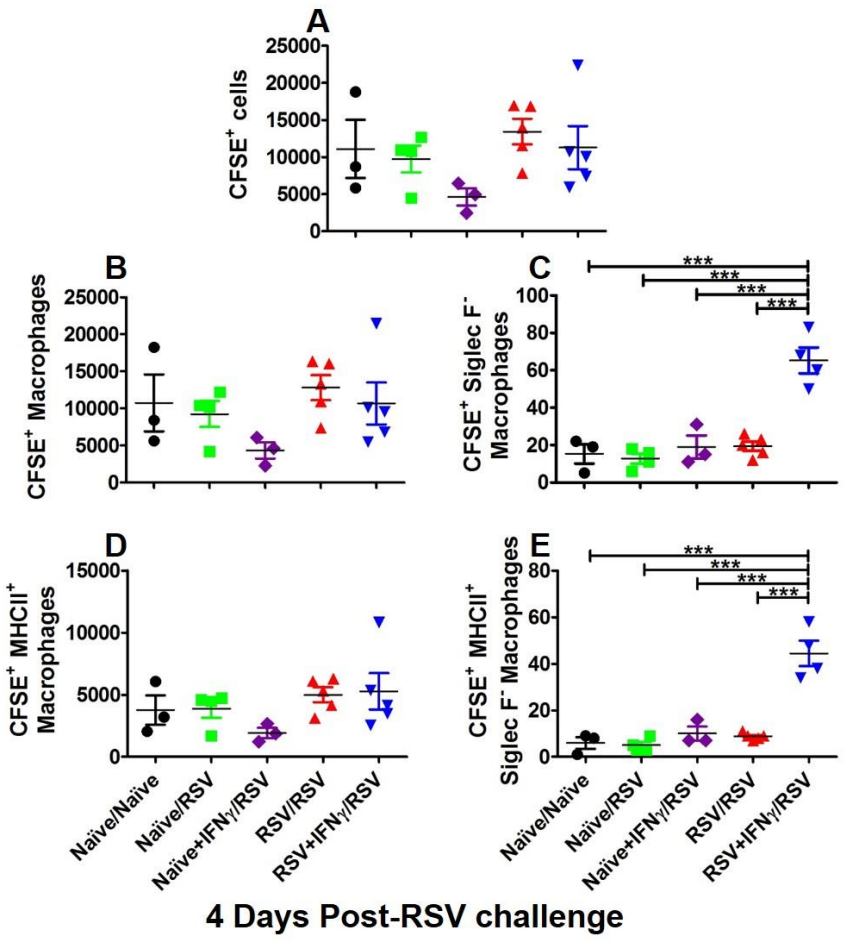

Figure 5.16 RSV+IFNγ/RSV Sig F$^-$ AMs differentially activated upon RSV re-exposure.

Infant mice (PND 4-5) were infected with RSV or vehicle and treated with IFNγ (16ng/g) or vehicle on 1, 3, and 5 dpi. After 6 weeks, the mice were culled, BAL collected, and AMs isolated and stained with CFSE. CFSE$^+$ AMs were adoptively transferred (i.n. 5 x 10^5 cells/100mcl) into naïve recipients. One day after transfer, recipient mice were challenged with RSV or vehicle. BAL was collected at 4 days post-RSV challenge and analyzed via flow cytometry. The number of CFSE$^+$ BAL cells (A), CFSE$^+$ AMs (B), CFSE$^+$ Sig F$^-$ AMs (C) were compared between experimental groups. Expression of MHCII$^+$ was analyzed on CFSE$^+$ AMs (D) and CFSE$^+$ Sig F$^-$ AMs (E). * represent significant differences between experimental groups using 2-way ANOVA with Bonferroni post-test; ***$\rho < 0.001$. Data points represent individual mice, the line represents the mean of $n \geq$ 3-5 samples per group ± SD.

To determine if the phenotypic signals of "memory" in RSV+IFNγ/RSV AMs resulted in improved functional outcomes, viral titers were analyzed at 4 days post-RSV challenge (**Figure 5.17A & B**). No significant differences in lung viral titers were detected although, RSV+IFNγ/RSV animals had slightly lower average titers when compared to other RSV+ groups when viewed on log-scale (**Figure 5.17A**) and linear scale (**Figure 5.17B**) where the variability can be seen more easily.

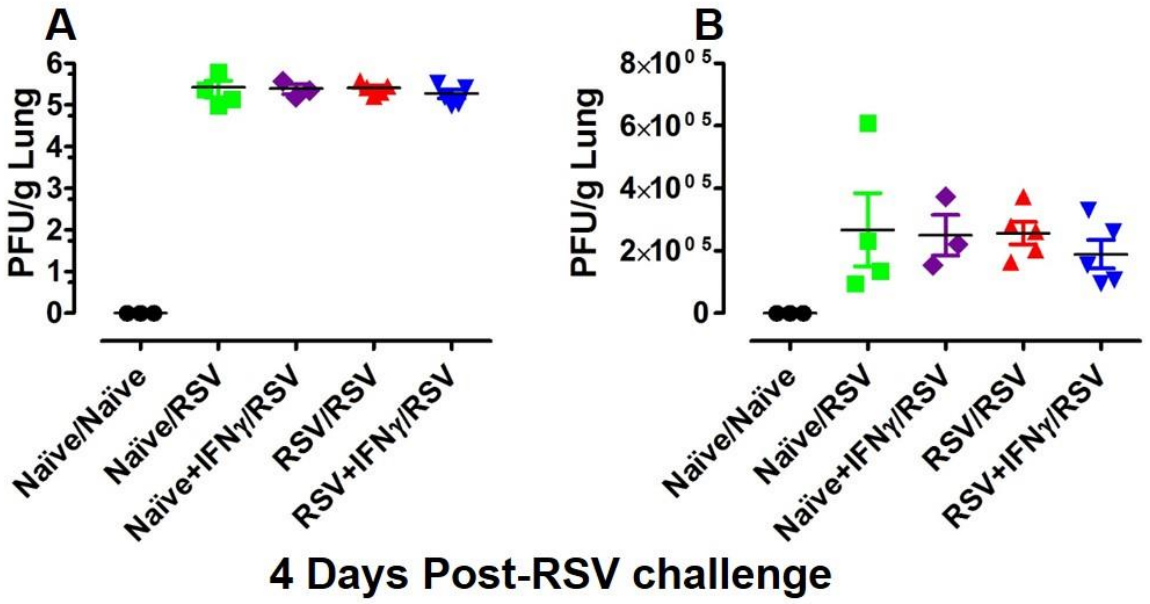

Figure 5.17 Viral titers unaltered by adoptive transfer of AMs.

Figure 5.17 (continued) Infant mice (PND 4-5) were infected with RSV or vehicle and treated with IFNγ (16ng/g) or vehicle on 1, 3, and 5 dpi. After 6 weeks, the mice were culled, BAL collected, and AMs isolated and stained with CFSE. $CFSE^+$ AMs were adoptively transferred into naïve recipients. One day after transfer, recipient mice were challenged with RSV or vehicle. Left lungs were collected at 4 days post-RSV challenge and viral titers quantified using H&E plaque assay. Calculated viral titers viewed on a log-scale (A) or linear scale (B) and compared using ANOVA with Tukey's post-test. Data points represent individual mice, the line represents the mean of $n \geq$ 3-5 samples per group ± SD.

5.2.6 IFNγ signaling necessary to control eosinophil recruitment and AM activation

Our data has shown that intrapulmonary IFNγ treatment during primary infant RSV infection activates AMs, increasing their co-stimulatory and antigen presentation capabilities through the increased expression of $CD80^+$/$CD86^+$ and $MHCII^+$ during both primary and secondary RSV exposures. However, to confirm that IFNγ signaling is necessary to elicit these effects, we reproduced our RSV model in IFNγR1KO mice. However, the IFNγR1KO mice were bred on a C57BL/6 background and our infant RSV model was developed using Balb/c mice. Therefore, before we began testing in IFNγR1KO mice, we validated the effects of local, IFNγ treatment in a C57BL/6 infant RSV model.

Briefly, C57BL/6 infants were infected with RSV at PND 4-5 and then treated with IFNγ (16ng/gm) on 1, 3, and 5 days post-infection. At 3 DPI, BAL was collected and analyzed for AM activation and left lungs were collected for viral quantification. The frequency of AMs (Sig F^+ $F4/80^+$ $CD206^+$ $CD200R^+$ $CD11c^{HI}$) in the BAL was similar across all groups (**Figure 5.18A**). Like in Balb/c infants, AMs in C57BL/6 infants were very responsive to IFNγ demonstrated by

significant increases in CD86^{+} (**Figure 5.18B**) and MCHII^{+} (**Figure 5.18C**). Additionally, we confirmed that IFNγ treatment in C57BL/6 infants reduced RSV titers in the lung (**Figure 5.18D**).

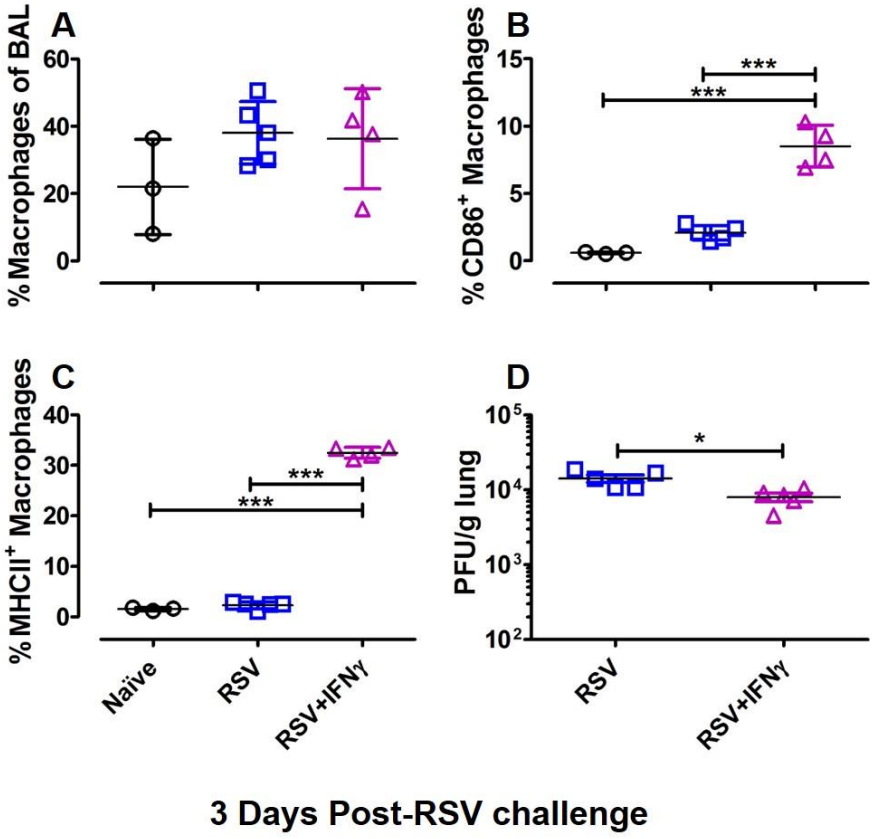

Figure 5.18 Infant RSV model validated in C57BL/6 infant mice.

Infant (PND 4-5) C57BL6 mice were infected with i.n. RSV L19 ($5x10^5$ pfu/g). Intranasal IFNγ (16ng/g) or vehicle was administered on 1 DPI. BAL was collected at 3 DPI and processed for flow cytometry and left lungs collected for RSV quantification using H&E plaque assays. Frequencies of AMs (A; Sig F^{+} F4/80^{+} CD206^{+} CD200R^{+} CD11c^{HI}) and their expression of CD86^{+} (B) and MHCII^{+} (C) were compared between groups using ANOVA with Tukey's post-test. Viral titers (D) of RSV and RSV+IFNγ were compared using an unpaired t-test.). * represent significant differences between experimental groups; * $\rho < 0.05$ or ***$\rho < 0.001$. Data points represent individual mice, the line represents the mean of $n \geq$ 3-5 samples per group ± SD.

To determine how IFNγ signaling during primary RSV infection influences secondary immune responses, WT and IFNγR1KO mice were infected with RSV and i.n. IFNγ or vehicle was administered, then the animals were allowed to recover for 6 weeks and were re-challenged with RSV. At 4 days post-RSV challenge, BAL was collected and analyzed via flow cytometry. A number of reports have shown a correlation between elevated levels of IFNγ in the lungs during primary infection and a reduction in the recruitment of eosinophils during secondary exposure (174, 215, 216). Eosinophils in the BAL of IFNγR1KO animals receiving secondary RSV exposure were significantly elevated (**Figure 5.19A**), whereas the populations in WT secondary exposure animals were not different compared to naïve. AM populations (Sig F^+ $F4/80^+$ $CD206^+$) were similar across both IFNγR1KO and WT animals (**Figure 5.19B**). As expected, expression of $CD86^+$ (**Figure 5.19C**) and $MHCII^+$ (**Figure 5.19D**) increased on AMs in WT secondary exposure groups but a similar increase was not observed in these IFNγR1KO groups. These data demonstrate the importance of IFNγ signaling in controlling eosinophil recruitment to the BAL following RSV re-exposure and its critical role in activating AMs.

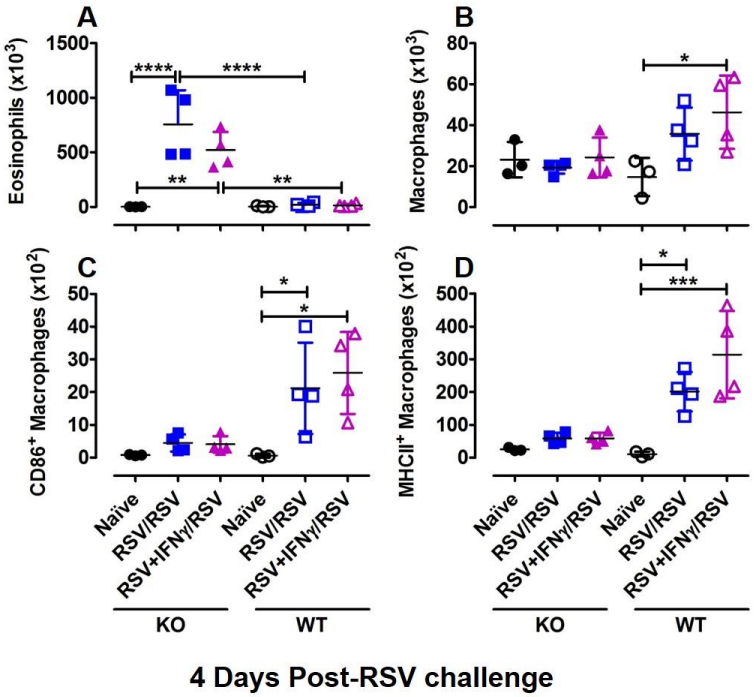

Figure 5.19 IFNγ signaling critical in controlling eosinophil recruitment and AM activation.

Adult (6-8 week old) KO and wild-type (WT) C57BL6 mice were infected with RSV or vehicle and treated with IFNγ (16ng/g) or vehicle on 1, 3, and 5 dpi. After 6 weeks, the mice were re-challenged with RSV and BAL collected and processed for flow cytometry at 4 days post-RSV challenge. The number of eosinophils (A; Sig F^+ $F4/80^+$ $CD206^-$ $CD11c^-$ $CD11b^+$) and macrophages (B; Sig F^+ $F4/80^+$ $CD206^+$) were compared between groups. Macrophages expressing $CD86^+$ (C) and $MHCII^+$ (D) were graphed for each group. * represent significant differences between experimental groups using ANOVA with Bonferroni's post-test; *$\rho < 0.05$, ** $\rho < 0.01$, *** $\rho < 0.001$, or ****$\rho < 0.0001$. Data points represent individual mice, the line represents the mean of $n \geq 3$-4 samples per group ± SD.

5.3 DISCUSSION

Severe RSV disease predominately affects infants (28, 34) but the virus continues to infect individuals throughout their lives (33, 225) and the immune response mounted during primary exposure has a profound influence on responses to subsequent infections (66, 149, 213, 214). Manipulation of the infant RSV immune response using archetypal Th2 (IL-4) or Th1 (IFNγ) cytokines have demonstrated the ability to alter secondary immune responses but only IFNγ has shown improvements in reducing eosinophilia and airway hyperresponsiveness (174, 215). Given IFNγ's successes in animal models and its association with less severe RSV disease clinically (178), we used our infant mouse model to investigate the effect of IFNγ during primary RSV infection on secondary challenge.

Our results demonstrated that RSV immunity elicited following infant RSV infection provided incomplete protection from secondary challenge. IFNγ treatment during infant, primary RSV infection sustained improved $CD8^+$ RSV $F_{85\text{-}93}$ specificity but did not appear to dramatically alter the T helper cytokine profile in the airway. Interestingly, IFNγ treatment reduced inhibitory feedback within the dynamic cytokine network and simplified the cumulative cytokine response, while also significantly reducing airway resistance. Moreover, this study demonstrated the importance of IFNγ signaling in the activation of AMs and that IFNγ treatment during infant primary RSV infection produces long-term changes in AMs, increasing their activation upon secondary exposure even in the absence of adaptive immunity. Our study provides insight into the long-term immunomodulatory effects of IFNγ stimulation during primary infant RSV infection and demonstrates preliminary evidence for a role in the induction of trained immunity. These results will be important in informing future age-specific vaccine and therapeutic approaches.

The importance of adaptive immunity in protection from RSV infection is well documented, with neutralizing antibody (4) and T cells (61, 94, 226) representing central correlates of protection. Although neutralizing antibody titers were not measured in our study, increased concentrations of IFNγ during primary, infant RSV infection have been shown to attenuate antibody responses (174, 227). However, viral titers were similar in both secondary exposure groups with RSV+IFNγ/RSV animals having slightly lower viral titers by 4 days post-challenge, which makes a significant decrease in neutralizing antibody development as a result of IFNγ treatment unlikely. The improvement in RSV $F_{85\text{-}93}$ $CD8^+$ T cell specificity observed following IFNγ treatment during primary infection (**Chapter 4**) was maintained in secondary RSV challenge. We previously demonstrated negligible IFNγ production by infants in response to primary RSV (1). IFNγ signaling has been shown to be important in regulating $CD8^+$ T cell memory development (208, 209) and restricts the formation of memory $CD8^+$ T cells responding to weak T cell receptor signaling, which promotes the accumulation of high-affinity T cells (210). The absence of IFNγ in primary infant RSV suggests that infants may develop low-affinity $CD8^+$ memory T cells that compromises their ability to clear secondary RSV infections. Surprisingly, IFNγ treatment during primary infant RSV did not appear to alter T helper phenotypes based on cytokine signals measured from BAL. These results are supported by data from Harker et al. that showed no alterations in Th phenotypes resulting from primary neonatal infection with a recombinant RSV virus expressing IFNγ (174). The same recombinant RSV virus used in an adult secondary RSV infection model demonstrated reduced viral titers but enhanced disease upon secondary RSV exposure, highlighting the importance of utilizing age-appropriate animal models in the evaluation of potential therapies or investigating mechanisms of RSV immunity.

IFNγ treatment during primary infant RSV infection reduced the production of IL-3 and IL-9 during secondary RSV challenge. Both cytokines have been associated with enhanced AHR (222-224) and may have been factors in the elevated resistance seen in the airways of RSV/RSV mice. Previous work in our lab has shown that IFNγ treatment of macrophages induces transcription of inducible nitric oxide synthase (iNOS) (1), which is responsible for the creation of nitric oxide. The presence of nitric oxide or via direct induction by IFNγ, stimulates the expression of cyclooxygenase-2 (COX-2) (228), leading to increased conversion of arachidonic acid to prostaglandins. Prostaglandins work to control the development of Th9 T cells (223, 229), which may be responsible for the reduction in IL-9 levels in RSV+IFNγ/RSV animals. Preliminary evidence from our lab has demonstrated that RSV-infected infants treated with IFNγ had higher concentrations of the prostaglandin, PGD2, in the BAL compared to RSV-infected infants treated with vehicle (data not shown). This finding lends support to the role of IFNγ-induced expression of COX-2 and subsequent production of prostaglandins that may suppress Th9 development. However, more studies are required to identify the source of IL-9 in RSV/RSV animals and understand the mechanism behind IFNγ's ability to limit its production and improve airway mechanics.

Previous studies of secondary RSV infections have primarily focused on manipulating factors during primary RSV infection with a goal of improving one or more aspects of adaptive immunity to prevent secondary infection. One area that has been largely overlooked is how immunomodulation during primary infection alters innate immunity in the absence of adaptive responses. This effect has been termed "trained immunity or innate immune memory" (218) and has been demonstrated in organisms lacking adaptive immunity (230), as well as, in mammalian studies demonstrating cross-protection when challenged with different pathogens (231). One study

by Yamaguchi and colleagues showed that when the TLR9 agonist, CpG, was administered to mice four weeks after primary infant RSV infection the animals had higher concentrations of IFNγ, lower IL-5, and reduced eosinophil accumulation in the BAL when they were re-challenged with RSV four weeks after CpG treatment (232). This suggests that, in the absence of antigen, stimulation of TLR9 on innate immune cells alters secondary RSV responses.

In our study, AMs previously exposed to RSV (a TLR3/4/7/8 agonist) and IFNγ during infancy underwent enhanced activation following adoptive transfer into naïve animals that were subsequently challenged with RSV. These results are suggestive of AM trained immunity and may indicate an epigenetic reprogramming resulting in a pro-inflammatory phenotype elicited by re-stimulation. The induction of an inflammatory AM phenotype relies on a metabolic switch from oxidative phosphorylation under homeostatic conditions, to glycolysis following activation via PAMPs, such as TLRs (120). The metabolic intermediates of glycolysis (ex. acetyl-coenzyme A) have been shown to be essential for epigenetic changes, such as histone acetylation, resulting in trained immunity (218, 233). One mechanism by which IFNγ sustains AM pro-inflammatory responses induced by TLR stimulation is through the prevention of adenosine receptor upregulation (A2bR), thereby reducing adenosine's negative-feedback signaling (234), prolonging glycolytic metabolism, and promoting the accumulation of metabolic intermediates required for trained immunity (218, 233).

In summary, immunomodulation of a primary, infant RSV infection via local IFNγ treatment can have a broad range of effects on secondary RSV immune responses; improving memory $CD8^+$ T cell responses, reducing AHR, and eliciting innate immune memory. These studies provide important information regarding potential benefits of immunomodulation during severe RSV or possibly as a prophylactic measure. Nearly 50% of children hospitalized with severe

RSV disease go on to develop asthma later in childhood (40, 42). Based on results showing an amelioration of AHR through IFNγ treatment demonstrated by us and others (215), IFNγ treatment may be a beneficial therapeutic approach during severe RSV. Moreover, the demonstration of trained immunity in IFNγ treated AMs from RSV-infected infants poses interesting questions regarding its potential utility in modulating vaccine immunogenicity.

6.0 RSV PRE-FUSION F PROTEIN PAIRED WITH A DELTA INULIN-DERIVED ADJUVANT PROTECTS VACCINATED DAMS AND THEIR OFFSPRING AGAINST RSV INFECTION AND ALTERS PRIMARY INFANT IMMUNE RESPONSE TO VIRAL CHALLENGE

6.1 INTRODUCTION

The only commercially available option for prevention of RSV infection is prophylaxis with the monoclonal antibody palivizumab (Synagis®) (235). Palavizumab is costly, requires multiple doses throughout the RSV season, and is only indicated for use in high-risk infants (236). Yet, the majority of infants hospitalized with severe RSV are otherwise healthy (30), emphasizing the critical need for a better means of RSV protection. The development of an effective RSV vaccine has been hampered by neonatal immune immaturity (75), the risk of vaccine-enhanced disease (VED) in infants (73, 76), and the short time frame between birth and first RSV exposure. While maternally-derived antibodies may protect infants from infection as their own immune systems develop, infants often develop severe RSV disease in the first months of life, suggesting that maternal-to-infant anti-RSV antibody transfer is often inadequate and likely varies from one individual to another based on their RSV exposure history. Thus, immunizing mothers during pregnancy is a promising approach to ensure the passive transfer of sufficiently high levels of RSV neutralizing antibodies from mothers to their offspring.

The RSV fusion (RSV F) glycoprotein, which mediates viral entry into host cells, is the primary target of neutralizing antibodies in human sera (237). RSV F rapidly rearranges from a pre-fusion to a post-fusion conformation, with the former inducing more potent neutralizing

antibodies. VED was observed with a formalin-inactivated alum-adjuvanted RSV (FI-RSV) immunization in vaccine trials of the 1960's that resulted in the death of two young children. Analyses of lung sections from these children along with additional preclinical studies suggest that the FI-RSV-associated VED was due to a combination of poorly neutralizing antibodies and excess Th2 priming of the infants' immune systems to RSV (22, 238-240). Stabilized forms of pre-fusion RSV F protein such as, DS-Cav1, are believed to be more representative of live RSV (22) and induce high neutralizing antibody titers, particularly when combined with an appropriate adjuvant (27). As such, stabilized pre-fusion RSV F protein vaccine candidates have advanced to clinical trials to determine their safety and efficacy in adults and RSV-seropositive toddlers (241).

Subunit vaccines are generally poor immunogens, requiring adjuvants for adequate immunogenicity. Aluminum salts are the most widely used vaccine adjuvants because their Th2 immune bias makes them highly effective at increasing antibody titers (242-244). However, investigations into the causes of VED in FI-RSV-vaccinated children have consistently demonstrated the contribution of Th2-mediated pathology (63, 175, 245, 246). Thus, an ideal RSV vaccine adjuvant would be one that elicits a strong antibody response without imparting Th2-bias. Advax adjuvant is derived from delta inulin, a plant-based polysaccharide, which in its microcrystalline form, enhances vaccine immunogenicity and protection against a wide range of pathogens, including Japanese encephalitis virus (247, 248), hepatitis B virus (249), HIV (250), SARS coronavirus (251, 252), West Nile virus (253), *Listeria monocytogenes* (254), *Bacillus anthracis* (255), and influenza (256). Advax adjuvant has been further shown to overcome immune insufficiencies associated with young age (257) and pregnancy (258). The addition of a TLR9 agonist (CpG oligonucleotide) to Advax (Advax–SM) enhanced vaccine protection and ameliorated eosinophilic lung pathology in a murine model of SARS coronavirus infection (251).

We therefore hypothesized that Advax-SM may be an ideal adjuvant for a pre-fusion RSV F protein vaccine, to enhance the humoral and cellular response while mitigating potential Th2-associated lung pathology (250, 251, 253-256, 259-261). Additionally, this study sought to determine the safety and efficacy of anti-RSV maternal antibodies as a form of immunomodulation on the primary RSV immune response of offspring. T cell and neutralizing antibody responses, viral lung titers, and histopathology were assessed in immunized and challenged dams and their offspring at pre- and post-wean time-points.

6.2 RESULTS

6.2.1 Protective immunity in the lungs of DS-Cav1 + Advax-SM immunized dams following RSV challenge

To determine the efficacy of immunization with DS-Cav1 formulated with or without Advax-SM, 7-8-week-old female Balb/c mice were i.m. vaccinated with DS-Cav1 + Advax-SM (DS-Cav1 + Advax-SM dams), unadjuvanted DS-Cav1 (DS-Cav1 dams), or PBS vehicle control (PBS dams). Immunized females were then bred and boosted with their respective vaccine formulation, as boosting during pregnancy has been shown to provide superior protection to infants in clinical studies of pertussis (262-264). After weaning of their pups, immunized dams were challenged with RSV according to the experimental timeline (**Figure 6.1A**). Pre-challenge plaque reducing neutralizing titers ($1/PRNT_{50}$) indicated that the addition of Advax-SM to DS-Cav1 enhanced the RSV neutralizing antibody response by an average of 4-fold over unadjuvanted vaccine (**Figure 6.1B**). DS-Cav1, but not DS-Cav1 + Advax-SM or PBS dams, lost weight transiently at 2 DPI

(**Figure 6.1C**). At 4 DPI, the time of peak RSV replication, DS-Cav1 + Advax-SM and DS-Cav1 dams had significantly reduced viral titers compared to PBS dams (**Figure 6.1D**). When challenged 57 days after initial vaccination, only DS-Cav1 + Advax-SM completely protected dams with 100% (n=12/12) of animals in this group showing no detectable virus in their lungs. Within each vaccination group, viral titers (right y-axis) were negatively correlated with neutralizing antibody titers (left y-axis); $1/PRNT_{50}$ values $\geq$ 40 were associated with complete protection from RSV (**Figure 6.1E**). PBS dams had no detectable neutralizing antibody and had high viral titers, whereas all DS-Cav1 + Advax-SM dams had $1/PRNT_{50}$ values $\geq$ 40 and sterilizing immunity. Unadjuvanted DS-Cav1 dams with $1/PRNT_{50}$ values $\geq$ 40 similarly had sterile lungs, whereas those with undetectable neutralizing antibody had detectable virus in their lungs (**Figure 6.1D-E**). These results demonstrate that immunization of dams with DS-Cav1 + Advax-SM augments neutralizing antibody responses and provides greater anti-viral protection compared to DS-Cav1 alone.

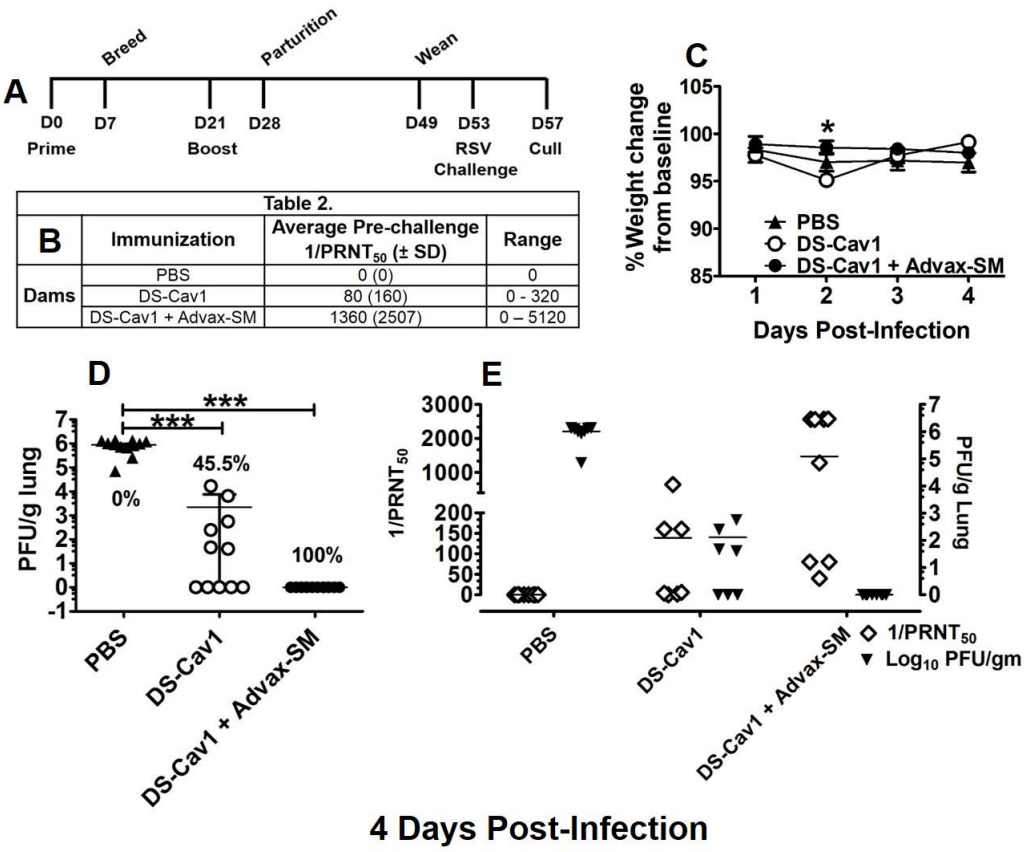

Table 2.			
B	Immunization	Average Pre-challenge $1/PRNT_{50}$ (± SD)	Range
Dams	PBS	0 (0)	0
	DS-Cav1	80 (160)	0 - 320
	DS-Cav1 + Advax-SM	1360 (2507)	0 – 5120

Figure 6.1 Protective immunity in the lungs of DS-Cav1 + Advax-SM immunized dams following RSV challenge.

Figure 6.1 (continued) Female, Balb/c mice (7-8 week old) were immunized at the time of co-housing (Day 0; D0) and again 2 weeks after breeding, in the second week of gestation (D21) as outlined (A). Vaccine formulations were as follows: PBS – vehicle control, DS-Cav1 alone, DS-Cav1 + Advax-SM. Dams gave birth (D28) and nursed their offspring for 21 days until weaning (D49). Four days after their pups were weaned, dams were subjected to an intranasal (i.n.) challenge with RSV L19 (D53). Pre-challenge serum was collected immediately prior to RSV challenge for $1/PRNT_{50}$ levels (B). Weights were recorded daily and comparisons between immunization groups were made using repeated measures ANOVA with a Bonferroni post-test where * indicates $\rho < 0.05$ between DS-Cav1 and DS-Cav1 + Advax-SM (C). At 4 DPI, dams were culled and tissues collected for analysis (D57). Left lungs were harvested and processed for viral quantification using H&E plaque assays (D). Viral titers were performed in triplicate and individual symbols within each group represent the mean titer for each animal, lines represent the mean of $n \geq 11$ animals per group ± SD. Viral titers were compared between groups using ANOVA with a Tukey post-test; *** $\rho < 0.001$. Lungs with no detectable virus were considered sterile and percentages of sterile lungs were calculated for each vaccine formulation; percentages are shown in panel D. In panel E, $1/PRNT_{50}$ titers at 4 DPI are shown on the y-axis and are represented by open symbols and compared to viral lung titers (z-axis) represented by closed symbols. Results are representative of 2 independent experiments.

6.2.2 DS-Cav1 + Advax-SM immunization of dams reduces lung inflammation and mucus production

To evaluate the risk of VED in immunized dams, histologic analysis was performed on lungs of immunized dams 4 days after RSV challenge to assess inflammation (**Figure 6.2A-C**) and mucus production (**Figure 6.2D-F**). H&E-stained lung sections showed enhanced peri-bronchial and peri-vascular inflammation in DS-Cav1 compared to PBS- or DS-Cav1 + Advax-SM dams (**Figure 6.2A-C**). Additionally, DS-Cav1 dams had increased mucin production as evidenced by increases in PAS staining of cells lining the airway (**Figure 6.2E**). Limited mucin production was detected in lung sections of PBS- and DS-Cav1 + Advax-SM-immunized dams (**Figure 6.2D or 2F,**

respectively). Quantification of mucin production (1, 119) confirmed that DS-Cav1 dams produced more mucus than DS-Cav1 + Advax-SM or PBS dams following RSV challenge (**Figure 6.2G-I**).

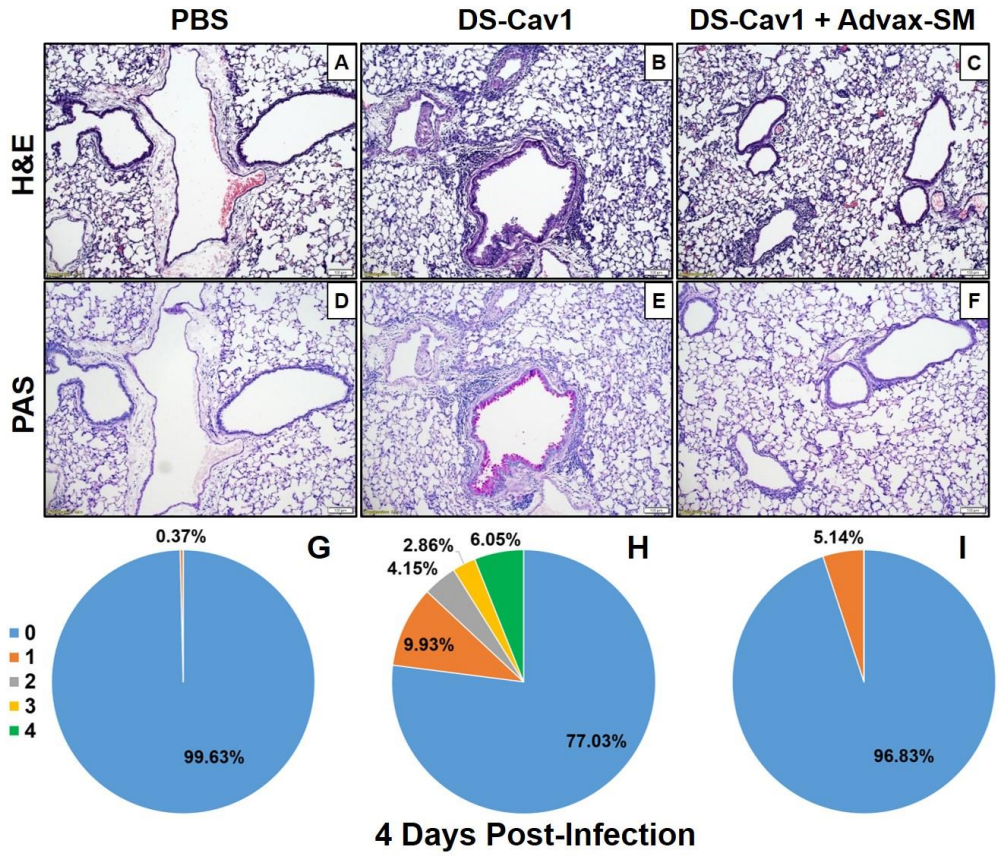

Figure 6.2 DS-Cav1 + Advax-SM immunization of dams reduces lung inflammation and mucus production.

Female, Balb/c mice (7-8 week old) were immunized, bred, and challenged with RSV L19 in accordance with Figure 6.1. At 4 DPI, right lungs (*n* = 3/group) were harvested and stained with H&E (A-C) and PAS (D-F) and imaged at 10X magnification; bar indicates 100um. Lung sections stained with PAS were scored 0 to 4 for PAS positivity for PBS (G), DS-Cav1 (H), and DS-Cav1 + Advax-SM (I), with 0 having no PAS and 4 being 76-100% PAS+, according to the methods.

6.2.3 Formulation of DS-Cav1 with Advax-SM ameliorates increased Th2-type cytokine production exhibited by DS-Cav1 dams following RSV challenge

Following RSV challenge of immunized mice, Th2 biased immune responses have consistently been implicated in airway hyperresponsiveness (AHR) and VED immunopathology, characterized by inflammation, mucus production, and pulmonary eosinophilia (175, 245, 246). Consistent with histology demonstrating peri-vascular and -bronchial inflammation and enhanced mucus production in DS-Cav1 dams, these animals had significantly elevated concentrations of the Th2 cytokines, IL-4 and IL-13, quantified from first-wash BAL samples (**Figure 6.3A and B**). Concentrations of the Th1 cytokine, IFNγ, were significantly higher in DS-Cav1 + Advax-SM dams while PBS and DS-Cav1 dams had similarly low levels (**Figure 6.3C**). IL-4 and IL-13 concentrations were reduced in DS-Cav1 + Advax-SM dams and these animals had minimal inflammation on H&E staining with only a small increase in PAS-staining over PBS dams (**Figure 6.2D-F**).

In models of allergic asthma, signaling through the common β subunit by the Th2 cytokines IL-3, IL-5, and GM-CSF was found to be critical for the expansion and accumulation of eosinophils in the lungs of sensitized mice (222). At 4 DPI, PBS and DS-Cav1 + Advax-SM dams had low levels of these Th2 cytokines whereas concentrations were significantly elevated in DS-Cav1 dams (**Figure 6.3D-F**).

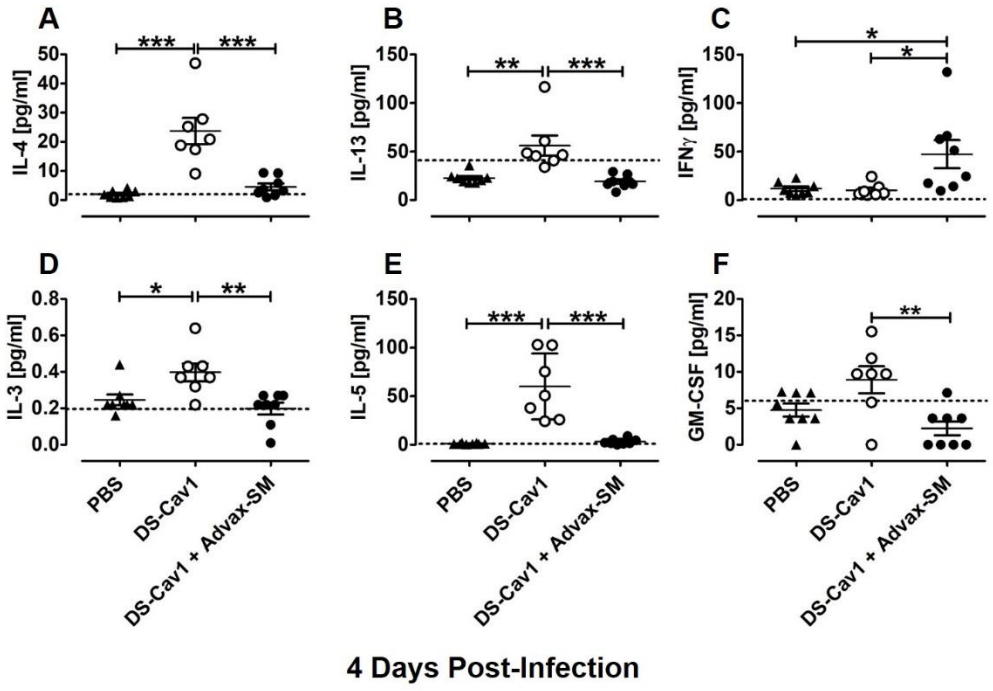

Figure 6.3 Formulation of DS-Cav1 with Advax-SM ameliorates increased Th2-type cytokine production exhibited by DS-Cav1 dams following RSV challenge.

At 4 DPI, first wash samples were collected from immunized dams and analyzed for cytokines using Luminex, dotted lines indicate the assay's limit of detection for individual cytokines. Cytokine concentrations were compared between groups using ANOVA with a Tukey post-test. Symbols represent individual mice in their respective immunization groups and lines represent the mean of $n \geq 7$ animals per group ± SD; *$\rho < 0.05$, **$\rho < 0.01$, ***$\rho < 0.001$.

6.2.4 Contrasting innate immune responses in the airways of immunized dams following RSV challenge

Pulmonary eosinophilia is an important indicator of VED as it has been a feature in FI-RSV immunized hosts following RSV exposure (73, 265, 266). As expected, elevated concentrations of IL-3, IL-5, and GM-CSF in the first wash of DS-Cav1 dams (**Figure 6.3D-F**) were associated with alveolar (**Figure 6.4A**) and interstitial eosinophilia (**Figure 6.4E**; Siglec F^+ $F4/80^+$ $CD206^-$ $CD11c^{lo/-}$ $CD11b^+$), which were absent in PBS and DS-Cav1 + Advax-SM dams. In the lung tissue of DS-Cav1 dams, eosinophils were producing IL-5 (**Figure 6.4F**) and TNFα (**Figure 6.4G**), which may be propagating further eosinophil recruitment and enhancing inflammation, respectively.

FI-RSV-immunized children who developed VED following natural RSV exposure also had high numbers of infiltrating neutrophils and mononuclear cells in their airways (76, 267, 268). Monocyte (Siglec F^- $F4/80^+$ $CD206^-$ $CD11c^+$ $CD11b^+$) numbers in the BAL were greater in DS-Cav1 + Advax-SM compared to PBS dams, though a similar increase in DS-Cav1 dams was noted (**Figure 6.4B**). Similarly, significant increases in neutrophils (Siglec F^- $CD11b^{HI}$ $Ly6G^+$ $CD11c^{lo}$) were seen in the BALs of DS-Cav1 and DS-Cav1 + Advax-SM dams (**Figure 6.4C**).

Siglec F^- (Sig F^-) macrophages (Siglec F^- $F4/80^+$ $CD206^+$ $CD11c^+$ $CD11b^+$), which are associated with an inflammatory lung environment (219), were significantly increased in the BAL and lungs of DS-Cav1 dams (**Figure 6.4D & H**). Sig F- macrophages in the lungs of DS-Cav1 dams were producing IL-5 (**Figure 6.4I**) and TNFα (**Figure 6.4J**), both of which were absent in PBS and DS-Cav1 + Advax-SM dams.

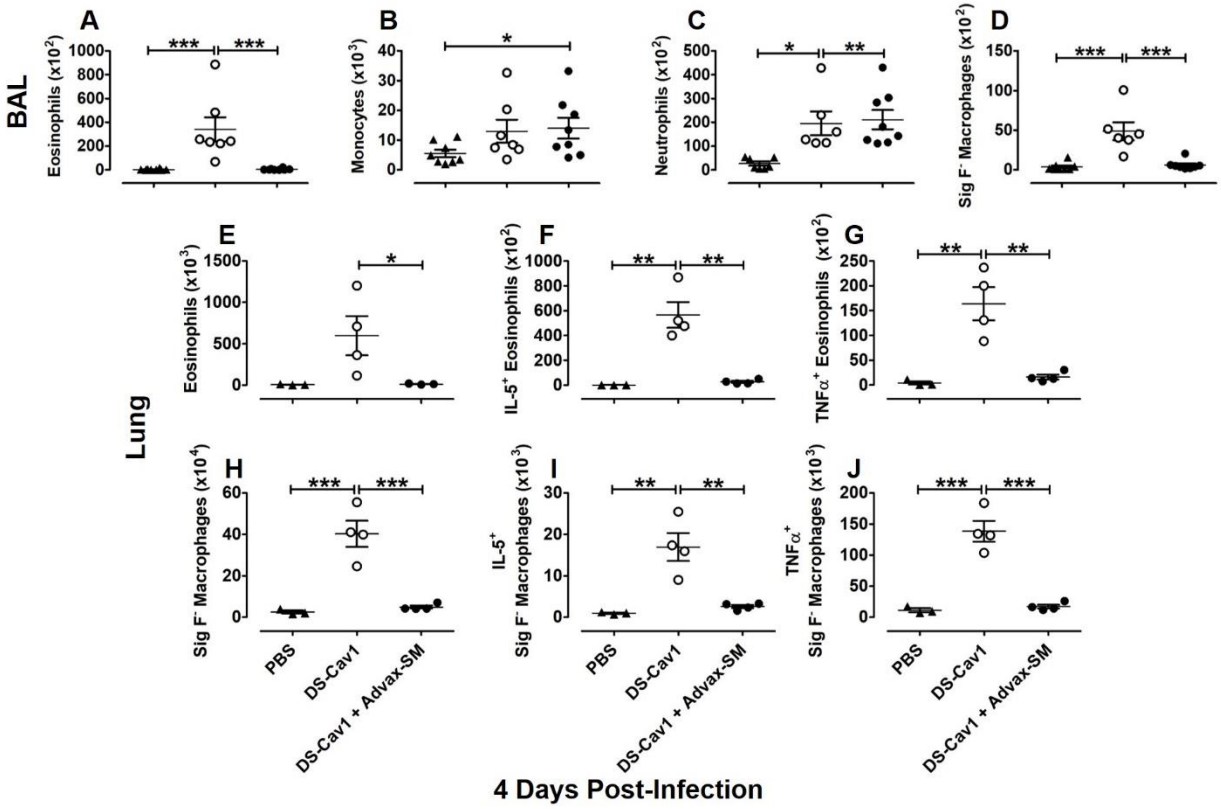

Figure 6.4 Disparate innate immune responses in the airways of immunized dams following RSV challenge.

Total cells quantified in the BAL at 4 DPI (A-D) or digested lung tissue (E-J) are shown for eosinophils (A, E) making IL-5 (F) or TNFα (G), monocytes (B), neutrophils (C), Siglec F$^-$ macrophages (D), and Siglec F$^-$ macrophages (H) making IL-5 (I) or TNFα (J). Populations of cells within the BAL and digested lung tissue, surface marker expression, and intracellular cytokines were compared between immunization groups using ANOVA with a Tukey post-test. Symbols represent individual mice in their respective immunization groups and lines represent the mean of n = 3-8 animals per group ± SD; *$\rho < 0.05$, **$\rho < 0.01$, ***$\rho < 0.001$.

6.2.5 Immunization with DS-Cav1 + Advax-SM increases Th1 responses to RSV infection

Previously published reports have highlighted the importance of T cells in RSV clearance, as well as their role in promoting or preventing VED (61, 65, 175). Cytokine and innate cellular data reported above suggested that Advax-SM adjuvant ameliorates the Th2 bias observed in dams immunized with DS-Cav1 alone. To further investigate the T-helper bias elicited by maternal DS-Cav1 immunization in the presence or absence of Advax-SM, RSV-specific IgG subtypes were assessed.

Anti-RSV IgG1 titers were increased in both DS-Cav1 + Advax-SM- and DS-Cav1 dams (**Figure 6.5A**). However, IgG2a titers were significantly elevated only in DS-Cav1 + Advax-SM dams (**Figure 6.5B**). The mean IgG1/IgG2a ratio, which if > 1 is reflective of a greater Th2 bias and if < 1 a greater Th1 bias, was 7.6 in DS-Cav1 dams, whereas the ratio was 0.53 in DS-Cav1 + Advax-SM dams (**Figure 6.5C**).

To further assess the T helper response, T cells from the BAL were phenotyped, quantified, and intracellular cytokines measured. At 4 DPI, the number of activated ($CD44^+$ $CD25^+$) $CD4^+$ T cells producing IL-4 was elevated in the BAL of DS-Cav1 dams (**Figure 6.5D**), while the number of IFNγ-producing, activated $CD4^+$ T cells was not different between immunization groups (**Figure 6.5E**). There was a non-significant trend toward reduced numbers of activated $CD8^+$ T cells producing IFNγ in the BAL of DS-Cav1 dams (**Figure 6.5F**). In order to measure Th1 (IFNγ) vs. Th2 (IL-4) cytokine production from the general T cell population, we compared the numbers of TCR_β^+ cells producing IFNγ to those producing IL-4. The $IFN\gamma^+$/$IL\text{-}4^+$ ratio was significantly higher in TCR_β^+ cells from DS-Cav1 + Advax-SM dams compared to DS-Cav1 dams (**Figure 6.5G**), signifying a collective reduction in IL-4 and a greater IFNγ response from T cells in DS-Cav1 + Advax-SM dams.

Using an MHC I pentamer specific for RSV F_{85-93}, we next asked whether RSV F-specific $CD8^+$ T cell responses were increased in dams immunized with DS-Cav1 + Advax-SM compared to the other immunization groups. Strikingly, F_{85-93} specific Ki-67^+ $Tbet^+$ $CD44^{HI}$ $CD8^+$ T cells were significantly higher in DS-Cav1 + Advax-SM dams compared to PBS or DS-Cav1 dams (**Figure 6.5H**). DS-Cav1 + Advax-SM dams also had increased numbers of *non*-F_{85-93} specific $CD8^+$ T cells expressing markers of proliferation (Ki-67^+), activation ($CD44^{HI}$), and $Tbet^+$, the transcription factor that drives IFNγ production, compared to PBS- and DS-Cav1 dams (**Figure 6.5I**). Together, these results indicate that DS-Cav1 + Advax-SM induced a Th1-biased response with a low IgG1/IgG2a RSV-specific antibody response, increased RSV F_{85-93}-specific $CD8^+$ T cells, and an elevated T cell IFNγ to IL-4 ratio compared to dams immunized with DS-Cav1 alone.

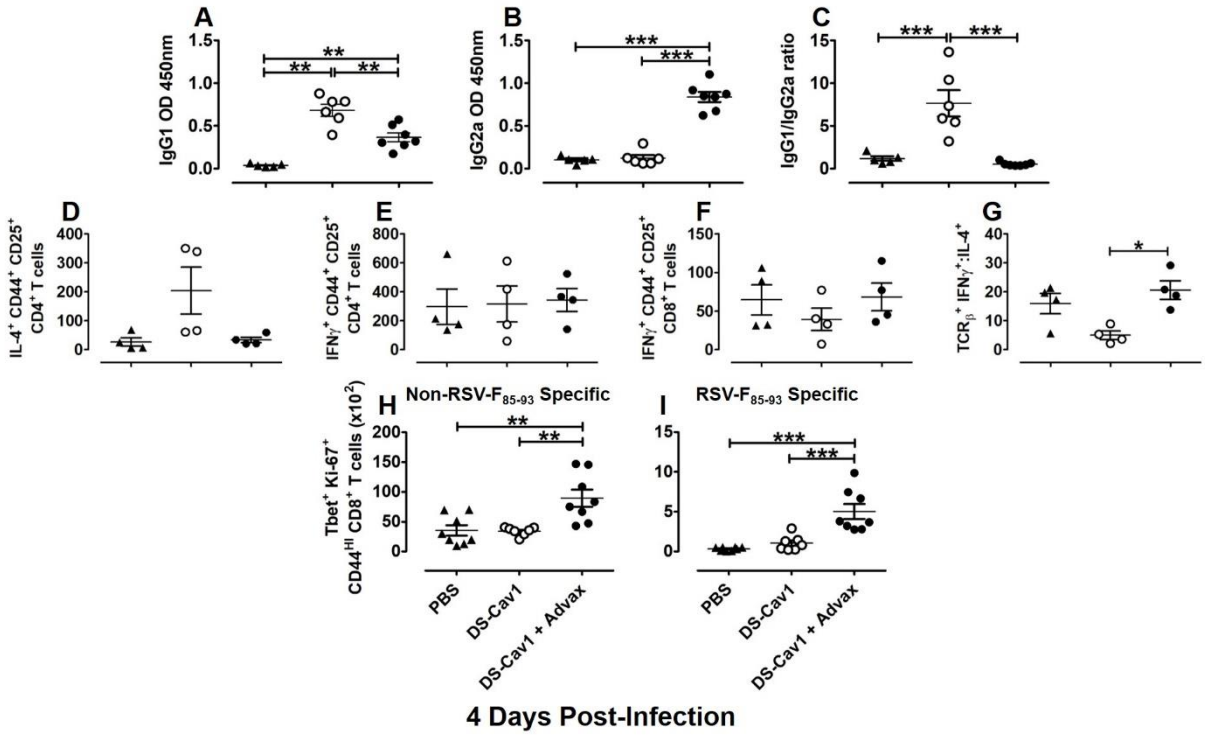

Figure 6.5 Immunization with DS-Cav1 + Advax-SM increases Th1 responses to RSV infection.

Figure 6.5 (continued) RSV-specific IgG isotype titers were measured from the serum of immunized dams at 4 DPI, according to the methods. IgG1 (A), IgG2a (B), and the IgG1 to IgG2a ratio (C) were compared between immunization groups using ANOVA with Tukey post-test. At 4 DPI, activated ($CD44^+$ $CD25^+$) $CD4^+$ T cells producing IL-4^+ (D) and $IFN\gamma^+$ (E), as well as, activated $CD8^+$ producing $IFN\gamma^+$ (F) were analyzed from the BAL. A ratio of IFNγ vs. IL-4 producing TCR_{β}^+ cells was created from BAL cells. Additionally, an MHC I pentamer specific for RSV $F_{85\text{-}93}$ was used to identify RSV $F_{85\text{-}93}$ specific, activated ($CD44^{HI}$), proliferating (Ki-67^+) $Tbet^+$ $CD8^+$ T cells (H) and non-RSV $F_{85\text{-}93}$ specific, activated, proliferating $Tbet^+$ $CD8^+$ T cells (I) from the BAL at 4 dpi. Lymphocyte populations were compared using ANOVA with Tukey post-test. Symbols represent individual mice in their respective immunization groups and lines represent the mean of $n \geq 4$ animals per group ± SD; *$\rho < 0.05$, **$\rho < 0.01$, ***$\rho < 0.001$. Data represents 2 independent experiments.

6.2.6 Infants and weanlings of DS-Cav1 + Advax-SM dams are protected from RSV

The primary objective of maternal vaccination is to protect offspring through the passive transfer of neutralizing antibody. In humans, transplacental transfer of maternal antibody to the fetus occurs during pregnancy and through breast milk postnatally. In mice the predominant source of maternal antibody is breast milk. To assess the capacity of maternal immunization to prevent RSV infection in their offspring, nursing infant mice (PND 5-6) born to immunized mothers were challenged with RSV. At 4 DPI, infants born to DS-Cav1 + Advax-SM dams (DS-Cav1 + Advax-SM infants) exhibited significantly greater RSV protection (sterilizing immunity in 11/15; 73%) compared to infants born to DS-Cav1 dams (DS-Cav1 infants) (sterilizing immunity in 1/9; 11.1%) (**Figure 6.6A**). Correlating with RSV protection, 58% (n = 7/12) of DS-Cav1 + Advax-SM infants had $1/PRNT_{50} \geq 40$ compared to only 38% (n = 3/8) of DS-Cav1 infants (**Figure 6.6C**).

To determine if RSV protection was maintained in offspring after nursing ceased, offspring (PND 35) that were weaned at 21 days of age were challenged with RSV. Weanlings born to dams immunized with DS-Cav1 + Advax-SM (DS-Cav1 + Advax-SM weanlings) had higher levels of sterilizing immunity (57%, n = 8/14) at 4 DPI compared to weanlings of DS-Cav1 dams (DS-Cav1 weanlings) (0%, n = 0/7) (**Figure 6.6B**). Similarly, a higher proportion of DS-Cav1 + Advax-SM weanlings had $1/PRNT_{50} \geq 40$ (38%, n = 3/8) compared to DS-Cav1 weanlings (0%, n = 0/7) (**Figure 6.6D**). In offspring born to both DS-Cav1 immunized groups, nursing infants had higher neutralizing antibody titers compared to weanlings born to mothers in the same immunization groups, reflecting the expected decay of neutralizing antibody levels post-wean (**Figure 6.6C-D**). As expected, offspring of PBS dams (PBS infants/ PBS weanlings) had high viral lung titers and no measurable neutralizing antibody at 4 DPI. Taken together these results demonstrate that maternal DS-Cav1 + Advax-SM immunization provides RSV protection immediately after birth that persists up to 2 weeks after cessation of the passive transfer of antibodies through breast milk.

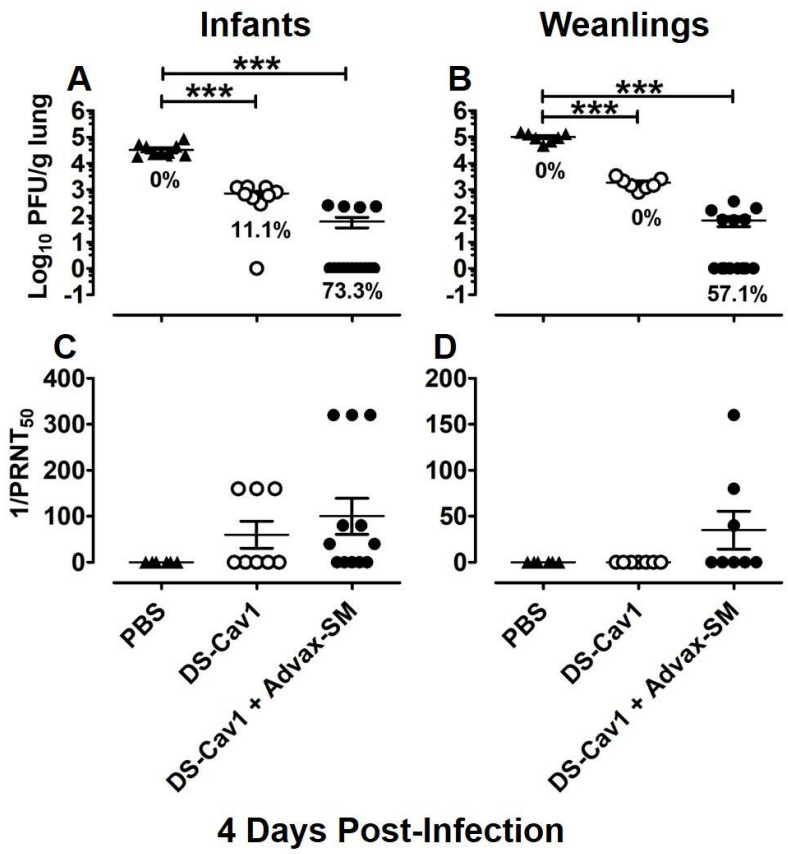

Figure 6.6 Infants and weanlings of DS-Cav1 + Advax-SM dams are protected from RSV.

Infants (PND 5-6) and weanlings (PND 35) born to immunized dams (PBS infants/weanlings, DS-Cav1 infants/weanlings, DS-Cav1 + Advax-SM infants/weanlings) were challenged with RSV and left lungs harvested and processed for viral quantification using H&E plaque assays (A and B). Lungs with no detectable virus were considered sterile and percentages of sterile lungs were calculated for each offspring group; percentages are shown in panels A and B. Serum was collected from offspring at 4 DPI and $1/PRNT_{50}$ titers measured. Viral titers and RSV neutralization assays were performed in triplicate and individual symbols within each group represent the mean titers for each animal, lines represent the mean of $n \geq 7$ animals per group ± SD. Viral titers and neutralizing antibody levels were compared between groups using ANOVA with a Tukey post-test; *** $\rho < 0.001$.

6.2.7 Innate cellular responses of offspring are influenced by maternal immunization

During viral infections, protection of RSV-naïve infants is largely dependent on the presence of maternal antibodies and innate immunity (269). To determine if maternal immunization influenced innate cellular responses in their offspring, flow cytometry was used to characterize innate immunity in the BAL of infants and weanlings of immunized dams. At 4 DPI, no differences in the frequency of NK cells within the SSC^{lo} gate were detected between groups of infants (**Figure 6.7A**) or weanlings (**Figure 6.7G**). $CD11b^{+}$ $CD27^{-}$ expression on NK cells, denoting increased cytolytic activity (270), was similar across infant and weanling groups, although overall expression was higher in weanlings suggesting an age-dependent maturation of the immune response (**Figure 6.7C and I**). FcγRIII ($CD16^{+}$) expression on cytolytic NK cells decreased in DS-Cav1 + Advax-SM infants and weanlings (**Figure 6.7E, K,** respectively), as well as DS-Cav1 weanlings, which may indicate shedding of the receptor post-antibody dependent cell-mediated cytotoxicity (ADCC) to limit inflammation (271-273).

Alveolar macrophages (AMs) are the most abundant leukocyte in the airways, acting as sentinels, and expressing both activating and inhibitory Fcγ receptors (269, 274), which may be differentially affected by passively-acquired IgG subtypes. Following RSV exposure, maternal antibody IgG subtypes complexed with RSV may bind to Fcγ receptors on macrophages leading to differences in activation. The frequency of AMs (Sig F^{+} $F4/80^{+}$ $CD206^{+}$ $CD11c^{HI}$) within the SSC^{HI} population was greater in DS-Cav1 infants as compared to PBS infants (**Figure 6.7B**); a non-significant trend toward a higher AM frequency was also observed in DS-Cav1 + Advax-SM infants**.** An increase in the frequency of activated AMs ($MHCII^{+}$) was observed in DS-Cav1 + Advax-SM weanlings (**Figure 6.7J**) but not infants (**Figure 6.7D**). Lastly, DS-Cav1 + Advax-SM

infants showed a reduced frequency of AMs expressing SR-A (**Figure 6.7F**), which may suggest a reduced need for scavenging and phagocytosis of cellular debris.

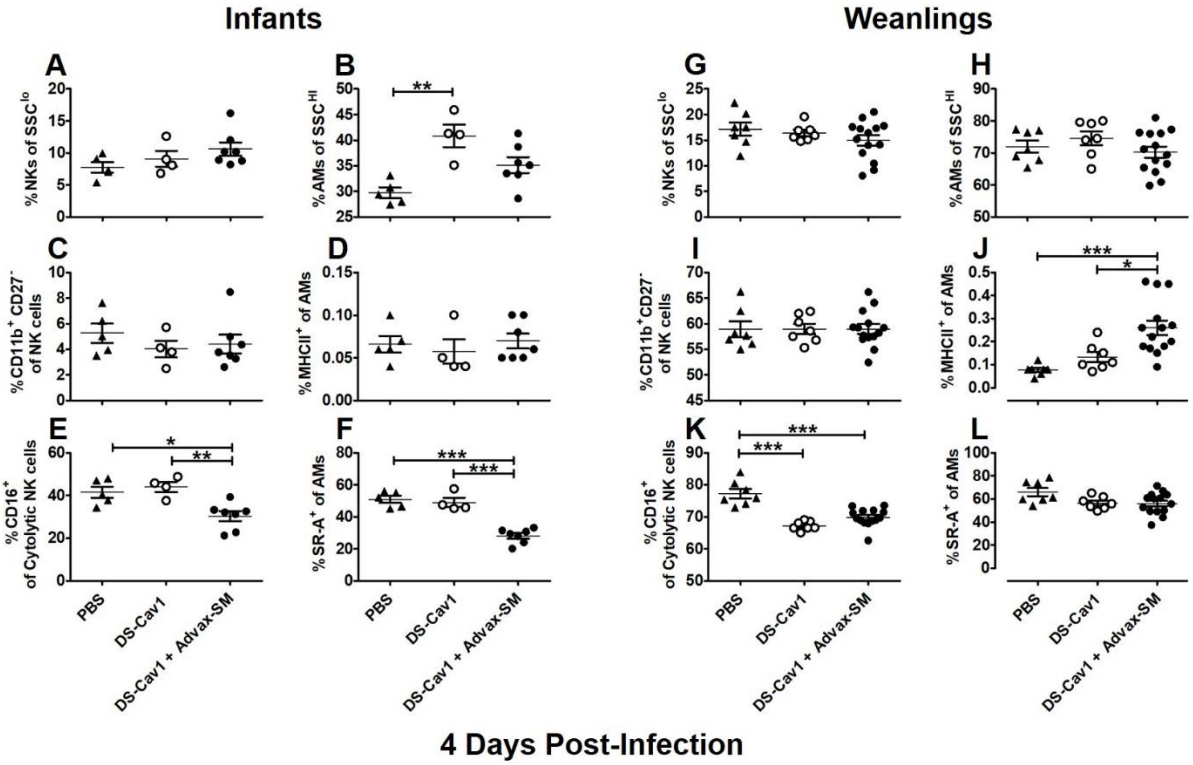

Figure 6.7 Innate cellular responses of offspring are influenced by maternal immunization.

Infants (PND 5-6) and weanlings (PND 35) born to immunized dams were challenged with RSV and BAL cells harvested. The percentages of NK cells ($CD3^-$ or $TCR\beta^-/DX5^+$) of SSC^{lo} cells and AMs (Sig F^+ $F4/80^+$ $CD206^+$ $CD11c^{HI}$) of SSC^{HI} cells were compared between infant (A and B, respectively) and weanling (G and H, respectively) groups. The percentages of NK cells expressing $CD11b^+$ $CD27^-$ and the percentages of activated ($MHCII^+$) AMs were compared between infant (C and D, respectively) and weanling (I and J, respectively) groups. Lastly, $CD16^+$ expression on cytolytic NK cells and expression of $SR\text{-}A^+$ on AMs were compared between infant (E and F, respectively) and weanling (K and L, respectively) groups. Individual symbols within each group represent individual samples (2-3 pooled infant BALs) or individual animals (weanlings), lines represent the mean of ≥ 4 samples per group ± SD. Comparisons between passive-immunization groups were made using ANOVA with a Tukey post-test; *$\rho < 0.05$, **$\rho < 0.01$, ***$\rho < 0.001$.

Despite a small reduction in the number of monocytes and neutrophils in the BAL of DS-Cav1 + Advax-SM infants compared to DS-Cav1 or PBS infants, no significant differences were observed between groups (**Figure 6.8A and B**). Similarly, no differences in monocytes were observed in the BAL of weanlings born to dams from any of the immunization groups (**Figure 6.8D**). A slight increase in neutrophils was detected in the BAL of DS-Cav1 + Advax-SM weanlings compared to PBS weanlings (**Figure 6.8E**). A small population of eosinophils was identified in the BAL of infants, but no significant differences were observed between groups (**Figure 6.8C**). No eosinophils were detected in the BALs of weanling groups (**Figure 6.8F**).

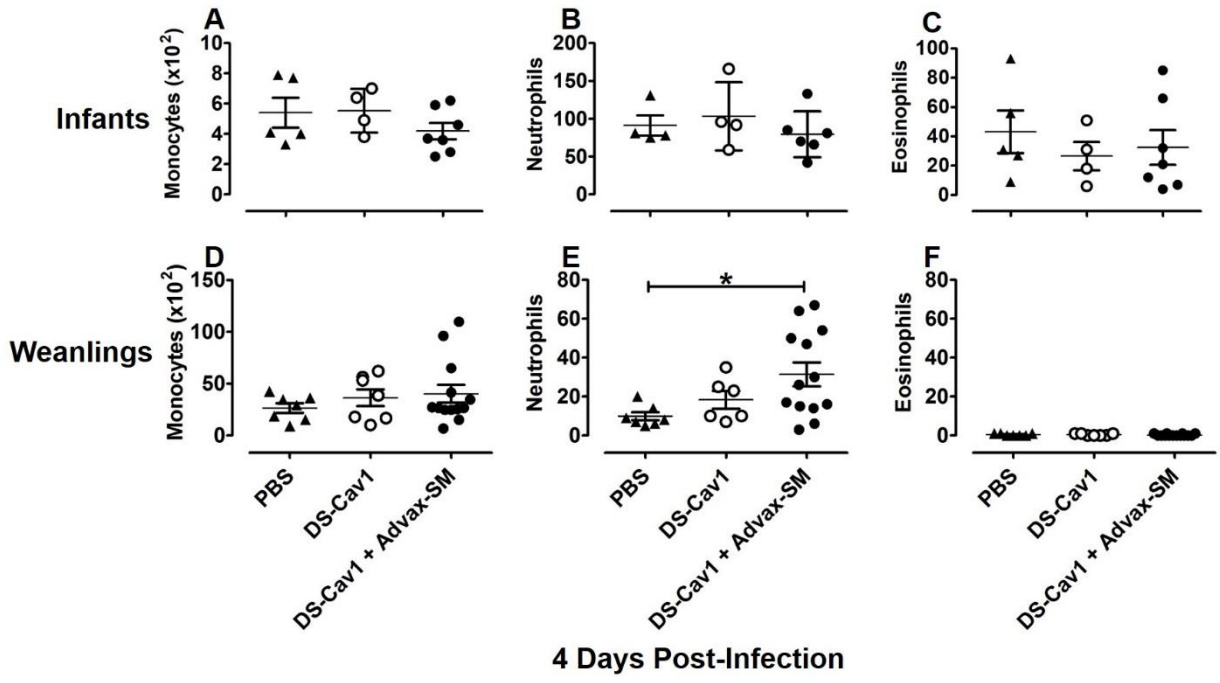

Figure 6.8 Similar innate, inflammatory cell populations in offspring.

Figure 6.8 (continued) Infants (PND 5-6) and weanlings (PND 35) born to immunized dams were challenged with RSV and BAL cells harvested. Monocytes (Sig F^- $F4/80^+$ $CD206^-$ $CD11c^+$ $CD11b^+$) in infant (A) and weanling (D) groups, as well as, neutrophils (Sig F^- $CD11b^{HI}$ $Ly6G^+$ $CD11c^{-/lo}$) in infant (B) and weanling (E) groups were analyzed. Eosinophils (Sig F^+ $F4/80^+$ $CD206^-$ $CD11c^-$ $CD11b^+$) from infant and weanling BALs were also identified (C and F, respectively). Individual symbols within each group represent individual samples (2-3 pooled infant BALs) or individual animals (weanlings), lines represent the mean of ≥ 4 samples per group ± SD. Comparisons between passive-immunization groups were made using ANOVA with a Tukey post-test; *$\rho < 0.05$.

6.2.8 DCs and T cells of weanlings are influenced by maternal vaccination

DCs express Fcγ receptors which can acquire and initiate cross-presentation of antigen from immune complexes resulting in the induction of antigen-specific $CD4^+$ and $CD8^+$ T cell responses (275, 276). Here, we examined the pre-challenge RSV-specific IgG subtype ratios in weanlings of immunized dams to determine if maternal antibodies may influence DC activation and T cell responses following RSV challenge. RSV-specific antibody subtype levels measured in weanling sera prior to challenge were largely reflective of subtype levels in dams from their respective immunization groups (**Figure 6.5A-C**). DS-Cav1 weanlings had significantly higher anti-RSV IgG1 titers than DS-Cav1 + Advax-SM weanlings (**Figure 6.9A**) but low titers of IgG2a (**Figure 6.9B**), resulting in a mean IgG1/IgG2a ratio > 14 (**Figure 6.9C**). Conversely, DS-Cav1 + Advax-SM weanlings had extremely low IgG1 titers and high IgG2a levels producing a mean IgG1/IgG2a ratio approaching zero (**Figure 6.9C**).

Given that IgG2a antibodies generally have higher binding affinities than IgG1 to activating Fcγ receptors (274), we hypothesized that DCs from DS-Cav1 + Advax-SM weanlings

would exhibit greater activation following RSV challenge leading to an enhanced T cell response. The total number of DCs in the BAL of weanlings at 4 DPI did not differ significantly between groups (**Figure 6.9D**). Expression of the co-stimulatory marker, CD86, on DCs was highest in DS-Cav1 + Advax-SM weanlings, although both passively-immunized groups had greater expression than PBS weanlings who had no maternally-acquired anti-RSV IgG (**Figure 6.9E**). A similar pattern of enhanced expression was observed when the mean fluorescence intensity (MFI) of CD86 was analyzed, demonstrating the highest CD86 MFI on the DCs of DS-Cav1 + Advax-SM weanlings (**Figure 6.9F**). At 8 DPI, PBS weanlings had a non-significant trend toward more total $CD8^+$ lymphocytes in the BAL than either DS-Cav1 groups (**Figure 6.9G**). Total activated ($CD44^+$ $CD25^+$) $CD8^+$ T cells producing IFNγ was not significantly different between groups, but this cell population was slightly increased in DS-Cav1 and DS-Cav1 + Advax-SM weanling groups (**Figure 6.9H**). Notably, the IFNγ MFI was highest for $CD8^+$ T cells from the DS-Cav1 + Advax-SM weanlings and was significantly higher in DS-Cav1 and DS-Cav1 + Advax-SM weanling groups compared to PBS (**Figure 6.9I**). Together, these data indicate that anti-RSV antibodies in weanlings (predominately IgG2a) resulting from maternal vaccination with DS-Cav1 + Advax-SM provided greater RSV neutralization following RSV challenge, more rapid DC maturation in the BAL, and greater IFNγ production by $CD8^+$ lymphocytes.

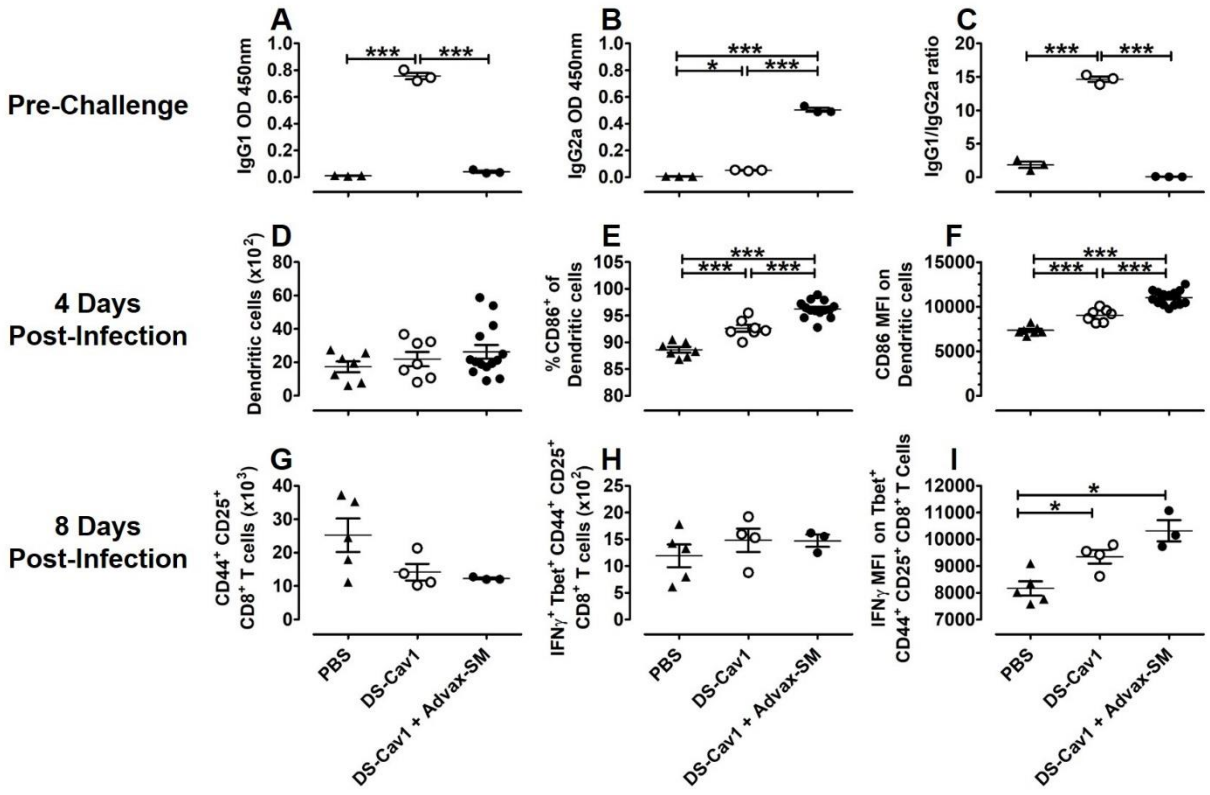

Figure 6.9 DCs and T cells of weanlings are influenced by maternal vaccination.

Pre-challenge serum was collected from weanlings (PND 37) born to immunized dams then the animals were challenged with RSV. IgG1 (A), IgG2a (B), and the IgG1 to IgG2a ratios (C) were measured from weanling pre-challenge serum and compared between passive-immunization groups using ANOVA with Tukey post-test. DCs (Sig F^- $CD11c^+$ $MHCII^{HI}$) (D), the percentages of DCs expressing $CD86^+$ (E), and the MFIs of CD86 on DCs (F) were compared between groups. BAL samples were collected from weanling groups and analyzed for activated ($CD44^+$ $CD25^+$) $CD8^+$ T cells (G), $IFN\gamma^+$ activated $Tbet^+$ $CD8^+$ T cells (H), and the IFNγ MFI of activated $Tbet^+$ $CD8^+$ T cells (I). Individual symbols within each group represent individual mice, lines represent the mean of ≥ 3 samples per group ± SD. Comparisons between groups were made using ANOVA with a Tukey post-test; *$\rho < 0.05$, ***$\rho < 0.001$. Data represents 2 independent experiments.

6.2.9 Lung pathology in weanling mice is influenced by maternal vaccination

Based on the lymphocyte changes observed in weanlings born to immunized dams, we next asked if there were differences in lung pathology in these offspring following viral challenge. At 8 DPI, lung sections from each weanling group showed mild perivascular and peribronchial lymphocytic inflammation with no major differences in inflammation observed between groups (**Figure 6.10A-C**). However, quantification of PAS staining demonstrated a greater amount of mucus within the airways of DS-Cav1 and DS-Cav1 + Advax-SM weanlings, as compared to PBS weanlings (**Figure 6.10D-I**). Mucus was reduced in all groups by 12 DPI, though the differences between groups remained consistent (S2). These results suggest that the presence of RSV-specific maternal antibodies alters the response to primary RSV otherwise mounted by the weanlings of non-immunized mothers.

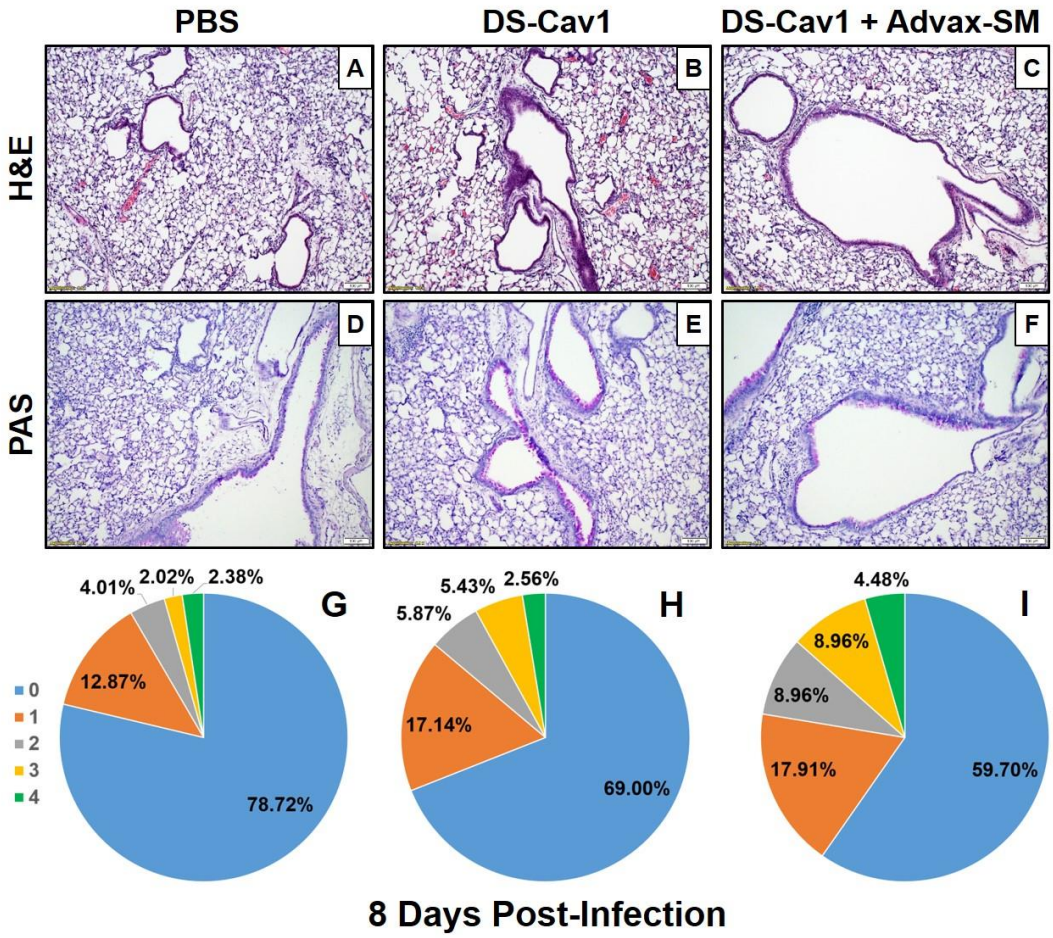

Figure 6.10 Lung pathology in weanling mice is influenced by maternal vaccination.

Weanlings (PND 37) born to immunized dams were challenged with RSV and right lung harvested for histology at 8 DPI. Lungs were stained with H&E (A-C) and PAS (D-F) and imaged at 10X magnification; bar indicates 100um. Lung sections stained with PAS were scored 0 to 4 for PAS positivity for PBS (G), DS-Cav1 (H), and DS-Cav1 + Advax-SM (I) weanlings, with 0 having no PAS and 4 being 76-100% PAS+, according to the methods.

6.3 DISCUSSION

Neutralizing anti-RSV antibodies have long been known to protect against RSV infection, yet natural infection fails to elicit long-lasting, protective neutralizing antibody (277-280), which is cited as the cause of RSV reinfection throughout life (281). The isolation of antigenic sites on pre-fusion RSV F protein, capable of eliciting robust and potent RSV neutralization, has renewed hope for RSV vaccines for disease prevention, including through maternal immunization (27, 282-284). However, it remains critically important to understand the immune factors that may protect or pose a risk to mothers and their children when assessing newly proposed RSV vaccines. The goal of this work was to elucidate the safety, efficacy, and infant immune response to maternal immunization with a pre-fusion RSV F candidate in combination with a non-Th2-polarizing adjuvant.

The results showed that dams immunized with DS-Cav1 + Advax-SM had high pre-challenge neutralizing antibody, comprised of both IgG1 and IgG2a, which translated into sterilizing immunity in 100% of dam lungs at 4 DPI. By contrast, dams immunized with DS-Cav1-alone showed lower levels of neutralizing antibody that was of the IgG1 subclass and only partial viral protection with more than half of the dams having detectable virus at 4 DPI. This is consistent with previously published data showing that DS-Cav1 alone provided only partial protection in adult cotton rats and mice (243, 285), but that when combined with an adjuvant, was capable of eliciting sterilizing immunity against RSV challenge (243).

In a previous RSV vaccination study, mice that were immunized intramuscularly with live RSV + Advax-2 adjuvant, a formulation similar to Advax-SM comprising delta inulin plus CpG, or alum adjuvant, showed increases in neutralizing antibody levels and viral protection compared to unadjuvanted live RSV immunization (286). In contrast to our findings, the authors saw

moderate bronchial and minor alveolar or interstitial inflammation after RSV challenge in protected, immunized mice with and without an adjuvant, although there was a trend toward lower lung inflammation scores in mice immunized with live RSV formulated with Advax-1 (delta inulin). Unfortunately, the presence of lung eosinophilia or evidence of Th2 bias was not reported in that study. Unpublished data generated in our lab suggests that use of a live RSV virus as antigen likely caused Th2 priming and the subsequent airway inflammation observed in the above studies. By contrast, our data shows that the Th2-biased immunity and VED induced by RSV in animals immunized with DS-Cav1 alone can be ameliorated by a non-Th2 polarizing adjuvant such as Advax-SM. Our results with Advax-SM adjuvant in RSV are consistent with that from SARS coronavirus vaccines, where Advax-SM adjuvant similarly prevented lung eosinophilic immunopathology otherwise seen in mice immunized with inactivated virus or recombinant spike protein alone or with alum adjuvant (251). This further highlights the importance of understanding the discrete immune responses elicited by different adjuvants, antigens, and the combinations thereof (243, 285).

Notably, despite having lower lung RSV titers than PBS control animals, DS-Cav1 dams exhibited features suggestive of VED with increased airway inflammation and mucus production. This pulmonary pathology was associated with markedly increased Th2 cytokines in the BAL and inflammatory eosinophils and macrophages expressing IL-5 and TNFα in the lung. DS-Cav1 dams also had an increased number of IL-4^+ CD4 T cells, a trend toward lower IFNγ^+ CD8 T cells, and IgG1 RSV-specific antibodies, consistent with a strong Th2 bias following RSV challenge. Importantly, these features of Th2 polarization and associated VED were not seen in dams immunized with DS-Cav1 formulated with Advax-SM.

Eosinophils have remained a focus of investigation into the cause of VED since they were noted in autopsy samples from the FI-RSV vaccinated children who died as a result of VED after RSV infection (73). The exact contribution of eosinophils to the excess inflammation and general pathology of VED remains uncertain since neutrophils and monocytes comprised a larger proportion of the cellular infiltrate in these post-mortem specimens (73, 76, 268). In our study, both DS-Cav1 and DS-Cav1 + Advax-SM dams had higher frequencies of neutrophils and monocytes in the BAL compared to PBS controls, whereas only dams immunized with DS-Cav1 alone demonstrated increased lung pathology post-RSV challenge. These data suggest that the frequency of eosinophils and Sig F^- inflammatory macrophages producing IL-5 and TNFα in the lung and BAL, rather than the presence of neutrophils or monocytes, correlated most closely with VED.

Siglec F^- macrophages are a less well characterized cell type that can be identified in the alveolar space and promote inflammation during infections (219). Interestingly, much like eosinophils, these cells were significantly elevated in the BAL of DS-Cav1 dams (Fig. 4D) and both eosinophils and Sig F^- macrophages producing IL-5 and TNFα were significantly elevated in the lung tissue of DS-Cav1 dams (Fig. F, G and I, J, respectively). These inflammatory macrophages and eosinophils are likely promoting pulmonary pathology in DS-Cav1 dams and may have contributed to the elevated IL-5 concentrations detected in the BAL (Fig. 3E).

IL-5 is an important factor in the recruitment and activation of eosinophils during acute inflammation and is associated with airway remodeling processes, such as fibrotic changes and enhanced collagen deposition in the lungs of asthmatics (287-290). In clinical trials, neutralization of IL-5 or blockade of the IL-5 receptor-α with the use of the monoclonal antibodies, mepolizumab and benralizumab, respectively, have proven effective in reducing blood and airway eosinophilia

but this reduction has not always improved functional measures of lung physiology in asthmatics (290, 291). It has been posited that the closely related cytokines, IL-3 and GM-CSF may be able to overcome IL-5 neutralization by mepolizumab, possibly limiting its ability to improve asthma symptoms (291).

In addition to IL-5, IL-3 and GM-CSF, Th2 cytokines that share a common β chain (βc) with IL-5 drive eosinophil differentiation in the bone marrow and are central to eosinophil survival, migration, and activation (288, 292, 293). In the $\beta c^{-/-}$ model of acute asthma, knockdown of the common beta receptor subunit for IL-3, IL-5, and GM-CSF significantly reduced airway eosinophilia, AHR, and recruitment of activated T cells to the lungs after allergen challenge, highlighting the close interplay between AHR, eosinophilia, and Th2 immunity (222). In our study, RSV-challenged DS-Cav1 dams had elevated levels of IL-3, IL-5, and GM-CSF in the BAL, in conjunction with airway and pulmonary eosinophilia. These factors, together with elevated concentrations of IL-13 and IL-4, increased IL-4^+ CD4 T cells, and increased mucus in DS-Cav1 dams following RSV challenge, are suggestive of an AHR-promoting phenotype and are consistent with a Th2-polarized immune response.

Multiple models of RSV vaccination have investigated the importance of $CD4^+$ T cells in the development of VED (175, 245, 246). Consistent with the results of our studies, a study by Knudson et al. demonstrated the critical role of Th2 $CD4^+$ T cells in mediating VED, including weight loss, mucus hypersecretion, and AHR in FI-RSV-immunized mice (175). Similarly, $CD4^+$ T cells and their production of IL-4 and IL-13 were shown to be important drivers of VED in a model of immunization with vaccinia virus expressing RSV G glycoprotein. In fact, IL-13, a potent Th2 cytokine, was shown to be sufficient to induce mucus hypersecretion and AHR in naïve

mice (294), while also promoting the recruitment of eosinophils to the lung parenchyma and airway in VED (63).

$CD8^+$ T cells are important in the clearance of RSV during primary infection (61) and have also been shown to play a role in preventing VED in models of RSV vaccination (64, 65, 179). A study by Stevens et al. suggested that memory $CD8^+$ T cells reduce pulmonary eosinophilia without modulating the $CD4^+$ T cell response (295), while others have suggested that $CD8^+$ T cells are important modulators of $CD4^+$ T cells and eosinophil recruitment (64, 179). Ultimately, the number of RSV-specific $CD8^+$ T cells (64) producing IFNγ (179) is important in controlling Th2-driven pathology. Our results showed that DS-Cav1 + Advax-SM immunization increased the number of $CD8^+$ T cell in the BAL with a higher ratio of $IFN\gamma^+$/IL-4^+ $TCR_\beta{}^+$ lymphocytes. Dams immunized with DS-Cav1 + Advax-SM also had increased RSV $F_{85\text{-}93}$-specific $CD8^+$ T cells expressing Tbet, the transcription factor that drives IFNγ production in $CD8^+$ T cells. Given that our antigen was RSV pre-F, increases at 4 DPI in non-RSV $F_{85\text{-}93}$- $CD8^+$ T cells expressing Tbet were likely representative of F-specific $CD8^+$ T cells targeting alternate F epitopes.

Despite enhanced RSV viral clearance, memory $CD8^+$ T cells directed toward single RSV epitopes have been shown to induce severe pathology upon RSV exposure. Morbidity and immunopathology in this model were attributed to rapid production of IFNγ by these memory $CD8^+$ T cells, which were primed in the absence of RSV-specific $CD4^+$ T cells and antibodies (62). While the potential for pathogenic memory $CD8^+$ T cell responses should be considered when evaluating RSV vaccine candidates, our results suggest that enhanced RSV-specific $CD8^+$ T cell responses do not cause excess pathology when accompanied by high titers of RSV-specific neutralizing antibody and increased proliferating $CD4^+$ T cells (S3), both of which provide regulatory signals that likely temper memory CD8+ T cell responses. Therefore, we hypothesize

that maternal DS-Cav1 + Advax-SM immunization primes for enhanced $CD8^+$ T cell RSV F-specificity and IFNγ production that in combination with a reduced Th2 bias, will help control the virus and prevent mucus production and mitigate the recruitment of inflammatory eosinophils and macrophages following RSV challenge.

The precise mechanism of VED remains unknown, however, FI-RSV studies suggest that poorly neutralizing antibody contributes to immune complex deposition in the small airways leading to exacerbated inflammation with RSV infection (240). To date, there have been no reports of VED in RSV seropositive individuals, suggesting that previous RSV exposure may mitigate the risk (296). In a maternal immunization model, the transfer of maternally-derived antibody establishes a seropositive-like environment in offspring. However, there is no guarantee that enhanced responses to RSV will be fully prevented in passively immunized infants or that a heavily Th2-biased response in the mother will not adversely affect the infant response upon RSV exposure. In fact, it remains unknown why some, otherwise healthy, infants develop a more severe form of RSV disease at an age when maternally-derived antibody should provide protection (90, 297, 298).

Our findings indicate that a majority of offspring from DS-Cav1 + Advax-SM dams were completely protected from RSV, both immediately after birth, as well as 2 weeks after offspring were weaned and the transfer of maternal antibodies via breast milk had ceased. However, the frequency of DS-Cav1 + Advax-SM infants and weanlings with neutralizing antibody levels ≥ 40 was lower than the frequency of infants and weanlings with undetectable virus in their lungs. This discrepancy may indicate a lack of sensitivity in our neutralizing antibody assay or may suggest a role for non-neutralizing antibodies in controlling infection through processes such as ADCC. In support of this theory, the expression of FcγRIII ($CD16^+$) on cytolytic NK cells was significantly

reduced in DS-Cav1 + Advax-SM infants and weanlings and DS-Cav1 weanlings. Loss of FcγRIII on NK cells has been shown to occur following ADCC as a result of membrane-type 6 matrix metalloproteinase (MMP6) (272) and/or metalloproteinase-17 (ADAM-17) (271, 273) activity, inducing receptor shedding to minimize inflammation. Only DS-Cav1 dams had reduced FcγRIII expression on cytolytic NK cells (Fig. S4), which may suggest an increased need for ADCC due to ineffective RSV neutralization and a reduced $CD8^+$ T cell response. Greater concentrations of IgG2a produced by DS-Cav1 + Advax-SM dams and transferred to their offspring may bind more efficiently to FcγRIII on NK cells in infants eliciting ADCC. Reduced FcγRIII expression on NK cells in DS-Cav1 and DS-Cav1 + Advax-SM weanling groups may reflect the more robust innate immune responses mounted by older compared to infant mice (50, 299). These hypotheses regarding changes in NK cell phenotype due to the influence of maternal antibody require further investigation.

This study raises interesting questions regarding the role of IgG subtypes in the protection mediated by maternal immunization. The pre-challenge serum of DS-Cav1 + Advax-SM weanlings was dominated by IgG2a antibodies and this correlated with higher neutralization titers, sterilizing immunity, and enhanced DC maturation. Studies investigating the link between pathogen-pattern recognition receptors, like Toll-like receptors (TLRs), and pathogen clearance through IgG immune complex (IgGIC) formation, along with engagement of Fc receptors have shown the critical role TLR4 plays in the activation of phagocytic cells via its interaction with IgGIC bound to FcγRIII (300). RSV F protein is a known TLR4 agonist (3) therefore, the improved RSV neutralization by IgG2a following RSV challenge of DS-Cav1 + Advax-SM weanlings may lead to immune complex formation that is detected by FcγRIII and TLR4 on dendritic cells resulting in their activation. It is possible that more effective innate antiviral responses in DS-Cav1

+ Advax weanlings resulted in an overall decrease in the number of CD8+ T cells in the BAL but an increase in their functionality, as evidenced by a higher IFNγ MFI.

Increased PAS staining at 8 DPI in the airways of both DS-Cav1 weanling groups may reflect enhanced T cell activity compared to PBS but requires further investigation, including AHR testing and memory T cell studies. Moving forward, it will be important to investigate passively-acquired IgG subtype ratios in the promotion or amelioration of lung pathology in response to RSV infection, considering both the activating and anti-inflammatory roles of IgG subtypes (19, 269, 301).

A limitation of this study is that human mothers would have been previously infected with RSV prior to maternal immunization, whereas in this study dams were RSV-naïve prior to immunization. Therefore, the VED we observed in DS-Cav1 dams challenged with RSV may not occur in sero-positive human mothers. Nevertheless, this study provides important insights into the mechanisms of VED associated with DS-Cav1 immunization. In particular, the data provide supporting evidence for the use of a non-Th2-polarizing adjuvant, such as Advax-SM, to improve the safety and efficacy of DS-Cav1 immunization, which is currently being tested alone or in combination with alum adjuvant in Phase I clinical trials (NCT03049488).

Taken together, these results demonstrate that maternal immunization with DS-Cav1 + Advax-SM warrants further investigation, as it was found to protect dams and offspring from primary RSV infection. Just as importantly, our studies provide novel insights regarding the influence maternally-transferred anti-pre-F antibodies may have on offspring's innate and adaptive immune responses to primary RSV exposure. Undoubtedly, the influence imparted during this initial infection will also affect the nature of subsequent RSV immune responses, constituting a form of immune imprinting. Functional studies will be important in the future to reveal the impact

of this on lung physiology and risk of long-term AHR. Future research in maternal immunization should aim to elucidate how the quantity, affinity/avidity, and IgG subtype ratios of maternally-derived antibodies impact acute and memory immune responses in offspring, as these factors will have important consequences on the efficacy and safety of maternal vaccination.

7.0 CONCLUSIONS AND FUTURE DIRECTIONS

7.1 CONCLUSIONS

In this dissertation, we have provided evidence of age-based differences in RSV immune responses but that immunomodulation during primary, infant RSV infection can have acute and long-term effects on RSV immunity. From the moment newborns take their first breaths, the neonatal lung is bombarded by aeroallergens and microorganisms and the neonatal immune system must balance its responsibility to protect against infection and promote the continued development of the respiratory system. RSV has taken advantage of this internal balancing act and established itself as the most significant viral cause of serious respiratory tract infections in the very young.

While it is thought that infants' Th2-biased immune responses may protect them from over-exuberant Th1 immunopathology, we have demonstrated that the administration of the archetypal Th1 cytokine, IFNγ, during primary, infant RSV infection reduced viral titers, stimulated the innate immune system, reduced mucus production, reduced the detection of apoptotic cells, and improved RSV-specific $CD8^+$ T cell responses. Moreover, we provided evidence of long-term benefits of IFNγ treatment through the reduction of airway resistance upon secondary RSV exposure and demonstrated preliminarily that IFNγ-treated AMs exhibit phenotypic signs of trained immunity. Also, detection of elevated levels of the immunoregulatory molecule, extracellular adenosine, in infant airways identified a previously unrecognized mechanism of immunosuppression specific to infants that may differentially affect cells of the immune system. RNA sequencing of infant and adult AMs showed four times less DEGs in infants in response to RSV infection, highlighting the

multi-level control of immune responses and the degree to which the infant immune response is blunted.

Finally, we demonstrated that effective RSV immunity can be passively-acquired in infants through maternal immunization. Maternal immunization with DS-Cav1 + Advax-SM elicited a balanced Th1/Th2 response in dams and IgG2a RSV-specific maternal antibodies were more effectively neutralizing in offspring. Importantly, the presence of maternal anti-RSV antibodies augmented innate and adaptive immune responses in offspring and increased mucus production upon RSV exposure. The last finding of enhanced active immunity upon RSV exposure is important given the Phase III status of Novavax's maternal RSV vaccine candidate and requires further investigation. It serves as a reminder that upon natural RSV exposure, the role of protective maternal antibodies does not end with pathogen neutralization; antibody-bound pathogens also serve as immunomodulatory agents in the development of memory immune responses.

7.2 FUTURE DIRECTIONS

Studying RSV in the context of an infant model of the disease has deepened my desire to continue studying age-specific differences in immunity and has also left many avenues open for further exploration, namely metabolic and epigenetic alterations in infant AMs and the induction of active immunity by maternal antibody-pathogen immune complexes. In the lung, AMs play critical roles in immune surveillance and the maintenance of homeostasis. As the most abundant leukocyte in the airways, they represent a critical link between innate and adaptive immunity. Our RNA sequencing data demonstrated far fewer DEGs in infants in response to RSV compared to adults, suggesting multifactorial inhibition, likely from internal and external forces. One such external

force may be elevated levels of extracellular adenosine in the airways, which may be acting as an important metabolic signal that maintains AMs in a metabolic state favoring oxidative phosphorylation and a homeostatic phenotype. There is evidence that increased production of adenosine is promoted in the blood in an age-specific manner (159). It would be interesting to investigate the mechanism behind elevated adenosine levels in the infant airspace as well as examine age-specific differences in AM cellular metabolism using the Seahorse Live-cell metabolic assay platform (Agilent; North Billerica, Massachusetts). Highlighting age-related differences in innate immune cell metabolism may lead to new avenues of therapeutic exploration for the treatment of pediatric respiratory tract infections.

The role of IFNγ treatment on the development of trained immunity in AMs is another intriguing area that requires further inquiry. A recent and elegant paper by Yao and colleagues demonstrated the critical link between direct contact with effector $CD8^+$ T cells and production of IFNγ in the priming of memory AMs in a model of adenovirus (302). Many of the findings and points of discussion suggested in this dissertation are corroborated by evidence presented by Yao, et al. including, high expression of MHCII on memory AMs, increased glycolytic metabolism, a defense ready gene signature, and heightened chemokine production (302). Future studies examining epigenetic, metabolic, and functional differences in AMs, trained during infant RSV infection in the presence of IFNγ, will give critical insight into how early-life viral infections affect cross protection against other respiratory viruses or bacterial infections.

Lastly, more studies are required to fully evaluate the influence of anti-RSV maternal antibodies on the development of active immunity in offspring exposed to RSV. Data presented in this dissertation showed enhanced innate activation in the presence of maternal antibody and there was evidence to suggest that IgG subtype may differentially affect those responses. Additionally,

the presence of maternal anti-RSV antibody resulted in increased mucus production compared to PBS controls. The physiological significance of the increased mucus that was observed requires further evaluation but should provoke some degree of caution given the current Phase III status of Novavax's maternal RSV vaccine. Some degree of mucus production is beneficial and helps trap and remove debris but the threshold beyond which mucus becomes pathogenic is not clearly defined. Therefore, studies are underway that will provide a more definitive link between changes in histology, including mucus production, and compromised airway mechanics measured by flexiVent technology.

Typically, the assumption for maternal vaccination approaches is that higher maternal antibody production will result in better protection for their offspring. While that may be true acutely in terms of inhibiting RSV infection, our data suggests that following RSV exposure, anti-RSV maternal antibodies that are likely bound to RSV elicit more robust RSV immunity in offspring. Future studies will investigate how the presence (quantity, quality, and dominant IgG subtype) of maternal anti-RSV antibodies affect RSV memory responses in offspring exposed to RSV. Interestingly, we have preliminary data that shows anti-RSV maternal antibodies have non-specific, stimulatory effects on innate immune cells in offspring. In our pilot study, offspring born to dams immunized with DS-Cav1 + Advax-SM were compared to offspring born to dams immunized with vehicle alone. Both groups were then challenged with i.n. ova and at 4 days post-challenge their innate immune responses were evaluated via flow cytometry. Type 2 innate lymphoid cells produced significantly more IL-9 in DS-Cav1 + Advax-SM offspring compared to PBS offspring, suggesting the presence of RSV-specific maternal antibody elicits a heightened response to a non-specific antigen. Together, this information suggests that thoughtful, detailed,

and perhaps, unconventional studies of maternal vaccination should be conducted to ensure the safety of this vaccination approach.

Moving forward I intend on pursuing the hypothesis that age-dependent differences in cellular metabolism, especially of alveolar macrophages, contribute to many of the signals and consequences of reduced activation in RSV-infected infants demonstrated in this thesis. Central to this is understanding how extracellular levels of adenosine become elevated in the infant airway and how extracellular adenosine affects alveolar macrophage cellular metabolism. Seahorse Live-cell analysis of infant alveolar macrophages will provide detailed information on these cells' metabolic conditions that set the stage for understanding how alveolar macrophages develop trained immunity. Through my research investigating the immunomodulatory potential of IFNγ and maternal antibodies, I have been convinced that in the presence of RSV these stimuli activate macrophages to produce innate memory. Understanding trained immunity is especially important in the context of maternal immunization/maternal antibody given the announcement of topline results from the Phase III clinical trial of ResVax, a maternal RSV immunization for the protection of infants by Novavax. Although the results of the trial did not meet the company's primary objective of prevention of medically significant RSV lower respiratory tract infection, the trial produced enough promising results that the company is moving forward in pursuing licensure. The caveat of this trial is that the primary and secondary endpoints were only measured through the infants' first 90 days of life. Additionally, the safety evaluation only occurred through the first 180 days of life, which is likely not long enough for a secondary RSV exposure to occur. My objective is to understand how the presence of maternal antibody at the time of initial RSV exposure influences secondary RSV immune responses as well as whether its presence elicits cross-

protection or induces pathology against other respiratory pathogens through innate immune memory.

BIBLIOGRAPHY

1. Empey KM OJ, Stokes Peebles R, Egana L, Norris KA, Oury TD, Kolls JK. Stimulation of immature lung macrophages with intranasal interferon gamma in a novel neonatal mouse model of respiratory syncytial virus infection. PLoS One. 2012;7(7).

2. Knipe David M. HPM, editor. Fields' Virology. 5 ed. Philadelphia: Wolters Kluwer Health/Lippincott Williams & Wilkins; 2007.

3. Collins PL, Graham BS. Viral and host factors in human respiratory syncytial virus pathogenesis. J Virol. 2008;82(5):2040-55.

4. Collins Peter L. CJE. Respiratory Syncytial Virus and Metapneumovirus. In: Knipe David M. HPM, editor. Fields' virology. 5 ed. Philadelphia: Wolters Kluwer Health/Lippincott Williams & Wilkins; 2007. p. 1601-36.

5. Dupuy LC, Dobson S, Bitko V, Barik S. Casein kinase 2-mediated phosphorylation of respiratory syncytial virus phosphoprotein P is essential for the transcription elongation activity of the viral polymerase; phosphorylation by casein kinase 1 occurs mainly at Ser(215) and is without effect. J Virol. 1999;73(10):8384-92.

6. Fearns R, Collins PL. Role of the M2-1 transcription antitermination protein of respiratory syncytial virus in sequential transcription. J Virol. 1999;73(7):5852-64.

7. Bossert B, Marozin S, Conzelmann KK. Nonstructural proteins NS1 and NS2 of bovine respiratory syncytial virus block activation of interferon regulatory factor 3. J Virol. 2003;77(16):8661-8.

8. Buchholz UJ, Ward JM, Lamirande EW, Heinze B, Krempl CD, Collins PL. Deletion of nonstructural proteins NS1 and NS2 from pneumonia virus of mice attenuates viral replication and reduces pulmonary cytokine expression and disease. J Virol. 2009;83(4):1969-80.

9. Elliott J, Lynch OT, Suessmuth Y, Qian P, Boyd CR, Burrows JF, et al. Respiratory syncytial virus NS1 protein degrades STAT2 by using the Elongin-Cullin E3 ligase. J Virol. 2007;81(7):3428-36.

10. Ling Z, Tran KC, Teng MN. Human respiratory syncytial virus nonstructural protein NS2 antagonizes the activation of beta interferon transcription by interacting with RIG-I. J Virol. 2009;83(8):3734-42.

11. Lo MS, Brazas RM, Holtzman MJ. Respiratory syncytial virus nonstructural proteins NS1 and NS2 mediate inhibition of Stat2 expression and alpha/beta interferon responsiveness. J Virol. 2005;79(14):9315-9.

12. Spann KM, Tran KC, Chi B, Rabin RL, Collins PL. Suppression of the induction of alpha, beta, and lambda interferons by the NS1 and NS2 proteins of human respiratory syncytial virus in human epithelial cells and macrophages [corrected]. J Virol. 2004;78(8):4363-9.

13. Spann KM, Tran KC, Collins PL. Effects of nonstructural proteins NS1 and NS2 of human respiratory syncytial virus on interferon regulatory factor 3, NF-kappaB, and proinflammatory cytokines. J Virol. 2005;79(9):5353-62.

14. Bitko V, Shulyayeva O, Mazumder B, Musiyenko A, Ramaswamy M, Look DC, et al. Nonstructural Proteins of Respiratory Syncytial Virus Suppress Premature Apoptosis by an NF-κB-Dependent, Interferon-Independent Mechanism and Facilitate Virus Growth. Journal of Virology. 2007;81(4):1786-95.

15. Munir S, Hillyer P, Le Nouën C, Buchholz UJ, Rabin RL, Collins PL, et al. Respiratory Syncytial Virus Interferon Antagonist NS1 Protein Suppresses and Skews the Human T Lymphocyte Response. PLoS Pathog. 2011;7(4):e1001336.

16. Munir S, Le Nouen C, Luongo C, Buchholz UJ, Collins PL, Bukreyev A. Nonstructural proteins 1 and 2 of respiratory syncytial virus suppress maturation of human dendritic cells. J Virol. 2008;82(17):8780-96.

17. Yang P, Zheng J, Wang S, Liu P, Xie M, Zhao D. Respiratory syncytial virus nonstructural proteins 1 and 2 are crucial pathogenic factors that modulate interferon signaling and Treg cell distribution in mice. Virology. 2015;485:223-32.

18. Teng MN, Whitehead SS, Collins PL. Contribution of the respiratory syncytial virus G glycoprotein and its secreted and membrane-bound forms to virus replication in vitro and in vivo. Virology. 2001;289(2):283-96.

19. Bukreyev A, Yang L, Collins PL. The Secreted G Protein of Human Respiratory Syncytial Virus Antagonizes Antibody-Mediated Restriction of Replication Involving Macrophages and Complement. Journal of Virology. 2012;86(19):10880-4.

20. Bukreyev A, Yang L, Fricke J, Cheng L, Ward JM, Murphy BR, et al. The secreted form of respiratory syncytial virus G glycoprotein helps the virus evade antibody-mediated restriction of replication by acting as an antigen decoy and through effects on Fc receptor-bearing leukocytes. J Virol. 2008;82(24):12191-204.

21. Tripp RA, Dakhama A, Jones LP, Barskey A, Gelfand EW, Anderson LJ. The G glycoprotein of respiratory syncytial virus depresses respiratory rates through the CX3C motif and substance P. J Virol. 2003;77(11):6580-4.

22. Killikelly AM, Kanekiyo M, Graham BS. Pre-fusion F is absent on the surface of formalin-inactivated respiratory syncytial virus. Sci Rep. 2016;6:34108.

23. Krarup A, Truan D, Furmanova-Hollenstein P, Bogaert L, Bouchier P, Bisschop IJ, et al. A highly stable prefusion RSV F vaccine derived from structural analysis of the fusion mechanism. Nat Commun. 2015;6:8143.

24. McLellan JS. Neutralizing epitopes on the respiratory syncytial virus fusion glycoprotein. Current opinion in virology. 2015;11:70-5.

25. McLellan JS, Yang Y, Graham BS, Kwong PD. Structure of respiratory syncytial virus fusion glycoprotein in the postfusion conformation reveals preservation of neutralizing epitopes. J Virol. 2011;85(15):7788-96.

26. Ngwuta JO, Chen M, Modjarrad K, Joyce MG, Kanekiyo M, Kumar A, et al. Prefusion F-specific antibodies determine the magnitude of RSV neutralizing activity in human sera. Sci Transl Med. 2015;7(309):309ra162.

27. McLellan JS, Chen M, Joyce MG, Sastry M, Stewart-Jones GBE, Yang Y, et al. Structure-Based Design of a Fusion Glycoprotein Vaccine for Respiratory Syncytial Virus. Science. 2013;342(6158):592.

28. Shi T, McAllister DA, O'Brien KL, Simoes EAF, Madhi SA, Gessner BD, et al. Global, regional, and national disease burden estimates of acute lower respiratory infections due to respiratory syncytial virus in young children in 2015: a systematic review and modelling study. The Lancet. 2017;390(10098):946-58.

29. Welliver RC. Review of epidemiology and clinical risk factors for severe respiratory syncytial virus (RSV) infection. The Journal of pediatrics. 2003;143(5 Suppl):S112-7.

30. Hall CB, Weinberg GA, Blumkin AK, Edwards KM, Staat MA, Schultz AF, et al. Respiratory Syncytial Virus–Associated Hospitalizations Among Children Less Than 24 Months of Age. Pediatrics. 2013;132(2):e341-e8.

31. Hall CB. Respiratory Syncytial Virus and Parainfluenza Virus. New England Journal of Medicine. 2001;344(25):1917-28.

32. Kapikian AZ, Bell JA, Mastrota FM, Johnson KM, Huebner RJ, Chanock RM. An outbreak of febrile illness and pneumonia associated with respiratory syncytial virus infection. Am J Hyg. 1961;74:234-48.

33. Hall CB, Geiman JM, Biggar R, Kotok DI, Hogan PM, Douglas GR, Jr. Respiratory syncytial virus infections within families. N Engl J Med. 1976;294(8):414-9.

34. Borchers AT, Chang C, Gershwin ME, Gershwin LJ. Respiratory Syncytial Virus—A Comprehensive Review. Clinical Reviews in Allergy & Immunology. 2013;45(3):331-79.

35. Scull MA, Gillim-Ross L, Santos C, Roberts KL, Bordonali E, Subbarao K, et al. Avian Influenza virus glycoproteins restrict virus replication and spread through human airway epithelium at temperatures of the proximal airways. PLoS Pathog. 2009;5(5):e1000424.

36. Zhang L, Peeples ME, Boucher RC, Collins PL, Pickles RJ. Respiratory Syncytial Virus Infection of Human Airway Epithelial Cells Is Polarized, Specific to Ciliated Cells, and without Obvious Cytopathology. Journal of Virology. 2002;76(11):5654-66.

37. Liesman RM, Buchholz UJ, Luongo CL, Yang L, Proia AD, DeVincenzo JP, et al. RSV-encoded NS2 promotes epithelial cell shedding and distal airway obstruction. J Clin Invest. 2014;124(5):2219-33.

38. Hall WJ, Hall CB, Speers DM. Respiratory syncytial virus infection in adults: clinical, virologic, and serial pulmonary function studies. Ann Intern Med. 1978;88(2):203-5.

39. Szabo SM, Levy AR, Gooch KL, Bradt P, Wijaya H, Mitchell I. Elevated risk of asthma after hospitalization for respiratory syncytial virus infection in infancy. Paediatr Respir Rev. 2013;13 Suppl 2:S9-15.

40. Zomer-Kooijker K, van der Ent CK, Ermers MJ, Uiterwaal CS, Rovers MM, Bont LJ. Increased risk of wheeze and decreased lung function after respiratory syncytial virus infection. PLoS One. 2014;9(1):e87162.

41. Krishnamoorthy N, Khare A, Oriss TB, Raundhal M, Morse C, Yarlagadda M, et al. Early infection with respiratory syncytial virus impairs regulatory T cell function and increases susceptibility to allergic asthma. Nature medicine. 2012;18:1525.

42. Turi KN, Shankar J, Anderson LJ, Rajan D, Gaston K, Gebretsadik T, et al. Infant Viral Respiratory Infection Nasal-Immune-Response Patterns and Their Association with Subsequent Childhood Recurrent Wheeze. Am J Respir Crit Care Med. 2018.

43. Blanken MO, Rovers MM, Molenaar JM, Winkler-Seinstra PL, Meijer A, Kimpen JL, et al. Respiratory syncytial virus and recurrent wheeze in healthy preterm infants. N Engl J Med. 2013;368(19):1791-9.

44. Scheltema NM, Nibbelke EE, Pouw J, Blanken MO, Rovers MM, Naaktgeboren CA, et al. Respiratory syncytial virus prevention and asthma in healthy preterm infants: a randomised controlled trial. Lancet Respir Med. 2018;6(4):257-64.

45. Miller EK, Lu X, Erdman DD, Poehling KA, Zhu Y, Griffin MR, et al. Rhinovirus-associated hospitalizations in young children. The Journal of infectious diseases. 2007;195(6):773-81.

46. Vitoratos N, Papadias C, Economou E, Makrakis E, Panoulis C, Creatsas G. Elevated Circulating IL-1beta; and TNF-Alpha, and Unaltered IL-6 in First-Trimester Pregnancies Complicated by Threatened Abortion With an Adverse Outcome. Mediators of Inflammation. 2006;2006.

47. Marodi L. Down-regulation of Th1 responses in human neonates. Clinical and experimental immunology. 2002;128(1):1-2.

48. Angelone DF, Wessels MR, Coughlin M, Suter EE, Valentini P, Kalish LA, et al. Innate Immunity of the Human Newborn Is Polarized Toward a High Ratio of IL-6/TNF-[alpha] Production In Vitro and In Vivo. Pediatric research. 2006;60(2):205-9.

49. Chelvarajan RL, Collins SM, Doubinskaia IE, Goes S, Van Willigen J, Flanagan D, et al. Defective macrophage function in neonates and its impact on unresponsiveness of neonates to polysaccharide antigens. J Leukoc Biol. 2004;75(6):982-94.

50. Levy O. Innate immunity of the newborn: basic mechanisms and clinical correlates. Nature reviews Immunology. 2007;7(5):379-90.

51. Sadeghi K, Berger A, Langgartner M, Prusa AR, Hayde M, Herkner K, et al. Immaturity of infection control in preterm and term newborns is associated with impaired toll-like receptor signaling. The Journal of infectious diseases. 2007;195(2):296-302.

52. Boukhvalova MS, Prince GA, Soroush L, Harrigan DC, Vogel SN, Blanco JC. The TLR4 agonist, monophosphoryl lipid A, attenuates the cytokine storm associated with respiratory syncytial virus vaccine-enhanced disease. Vaccine. 2006;24(23):5027-35.

53. Haeberle HA, Takizawa R, Casola A, Brasier AR, Dieterich HJ, Van Rooijen N, et al. Respiratory syncytial virus-induced activation of nuclear factor-kappaB in the lung involves alveolar macrophages and toll-like receptor 4-dependent pathways. The Journal of infectious diseases. 2002;186(9):1199-206.

54. Kurt-Jones EA, Popova L, Kwinn L, Haynes LM, Jones LP, Tripp RA, et al. Pattern recognition receptors TLR4 and CD14 mediate response to respiratory syncytial virus. Nat Immunol. 2000;1(5):398-401.

55. Liu P, Jamaluddin M, Li K, Garofalo RP, Casola A, Brasier AR. Retinoic acid-inducible gene I mediates early antiviral response and Toll-like receptor 3 expression in respiratory syncytial virus-infected airway epithelial cells. J Virol. 2007;81(3):1401-11.

56. Murawski MR, Bowen GN, Cerny AM, Anderson LJ, Haynes LM, Tripp RA, et al. Respiratory syncytial virus activates innate immunity through Toll-like receptor 2. J Virol. 2009;83(3):1492-500.

57. Krishnan S, Craven M, Welliver RC, Ahmad N, Halonen M. Differences in participation of innate and adaptive immunity to respiratory syncytial virus in adults and neonates. The Journal of infectious diseases. 2003;188(3):433-9.

58. Ruckwardt TJ, Malloy AM, Morabito KM, Graham BS. Quantitative and qualitative deficits in neonatal lung-migratory dendritic cells impact the generation of the CD8+ T cell response. PLoS Pathog. 2014;10(2):e1003934.

59. Rose S, Lichtenheld M, Foote MR, Adkins B. Murine neonatal CD4+ cells are poised for rapid Th2 effector-like function. J Immunol. 2007;178(5):2667-78.

60. Webster RB, Rodriguez Y, Klimecki WT, Vercelli D. The human IL-13 locus in neonatal CD4+ T cells is refractory to the acquisition of a repressive chromatin architecture. The Journal of biological chemistry. 2007;282(1):700-9.

61. Graham BS BL, Wright PF, Karzon DT. Role of T lymphocyte subsets in the pathogenesis of primary infection and rechallenge with respiratory syncytial virus in mice. J Clin Invest. 1991;88(3):1026-33.

62. Schmidt ME, Knudson CJ, Hartwig SM, Pewe LL, Meyerholz DK, Langlois RA, et al. Memory CD8 T cells mediate severe immunopathology following respiratory syncytial virus infection. PLoS Pathog. 2018;14(1):e1006810.

63. Castilow EM, Meyerholz DK, Varga SM. IL-13 Is Required for Eosinophil Entry into the Lung during Respiratory Syncytial Virus Vaccine-Enhanced Disease. The Journal of Immunology. 2008;180(4):2376.

64. Olson MR, Hartwig SM, Varga SM. The Number of Respiratory Syncytial Virus (RSV)-Specific Memory CD8 T Cells in the Lung Is Critical for Their Ability to Inhibit RSV Vaccine-Enhanced Pulmonary Eosinophilia. The Journal of Immunology. 2008;181(11):7958.

65. Olson MR, Varga SM. CD8 T Cells Inhibit Respiratory Syncytial Virus (RSV) Vaccine-Enhanced Disease. The Journal of Immunology. 2007;179(8):5415.

66. Culley FJ, Pollott J, Openshaw PJ. Age at first viral infection determines the pattern of T cell-mediated disease during reinfection in adulthood. The Journal of experimental medicine. 2002;196(10):1381-6.

67. Haines CJ, Giffon TD, Lu LS, Lu X, Tessier-Lavigne M, Ross DT, et al. Human CD4+ T cell recent thymic emigrants are identified by protein tyrosine kinase 7 and have reduced immune function. The Journal of experimental medicine. 2009;206(2):275-85.

68. Opiela SJ, Koru-Sengul T, Adkins B. Murine neonatal recent thymic emigrants are phenotypically and functionally distinct from adult recent thymic emigrants. Blood. 2009;113(22):5635-43.

69. Siegrist CA. Mechanisms by which maternal antibodies influence infant vaccine responses: review of hypotheses and definition of main determinants. Vaccine. 2003;21(24):3406-12.

70. Siegrist CA, Aspinall R. B-cell responses to vaccination at the extremes of age. Nature reviews Immunology. 2009;9(3):185-94.

71. Siegrist CA. Neonatal and early life vaccinology. Vaccine. 2001;19(25-26):3331-46.

72. Cardenas S, Auais A, Piedimonte G. Palivizumab in the prophylaxis of respiratory syncytial virus infection. Expert review of anti-infective therapy. 2005;3(5):719-26.

73. Kim HW, Canchola JG, Brandt CD, Pyles G, Chanock RM, Jensen K, et al. Respiratory syncytial virus disease in infants despite prior administration of antigenic inactivated vaccine. Am J Epidemiol. 1969;89(4):422-34.

74. PATH. RSV Vaccine and mAb Snapshot 2018 [updated December 10, 2018. Available from: https://www.path.org/resources/rsv-vaccine-and-mab-snapshot/.

75. PrabhuDas M, Adkins B, Gans H, King C, Levy O, Ramilo O, et al. Challenges in infant immunity: implications for responses to infection and vaccines. Nat Immunol. 2011;12(3):189-94.

76. Acosta PL, Caballero MT, Polack FP. Brief History and Characterization of Enhanced Respiratory Syncytial Virus Disease. Clin Vaccine Immunol. 2015;23(3):189-95.

77. Xing Y, Proesmans M. New therapies for acute RSV infections: where are we? European journal of pediatrics. 2019;178(2):131-8.

78. DeVincenzo JP, Wilkinson T, Vaishnaw A, Cehelsky J, Meyers R, Nochur S, et al. Viral Load Drives Disease in Humans Experimentally Infected with Respiratory Syncytial Virus. American Journal of Respiratory and Critical Care Medicine. 2010;182(10):1305-14.

79. Graham BS, Perkins MD, Wright PF, Karzon DT. Primary respiratory syncytial virus infection in mice. J Med Virol. 1988;26(2):153-62.

80. McDuffie E, Obert L, Chupka J, Sigler R. Detection of cytokine protein expression in mouse lung homogenates using suspension bead array. J Inflamm (Lond). 2006;3:15.

81. Bae SY, Jung YJ, Woo SY, Park MH, Seoh JY, Ryu KH. Distinct locomotive patterns of granulocytes, monocytes and lymphocytes in a stable concentration gradient of chemokines. Int J Lab Hematol. 2008;30(2):139-48.

82. Empey KM, Hollifield M, Garvy BA. Exogenous Heat-Killed Escherichia coli Improves Alveolar Macrophage Activity and Reduces Pneumocystis carinii Lung Burden in Infant Mice. Infection and immunity. 2007;75(7):3382-93.

83. Alcorn JF, Rinaldi LM, Jaffe EF, van Loon M, Bates JH, Janssen-Heininger YM, et al. Transforming growth factor-beta1 suppresses airway hyperresponsiveness in allergic airway disease. Am J Respir Crit Care Med. 2007;176(10):974-82.

84. Fuentes S, Crim RL, Beeler J, Teng MN, Golding H, Khurana S. Development of a simple, rapid, sensitive, high-throughput luciferase reporter based microneutralization test for measurement of virus neutralizing antibodies following Respiratory Syncytial Virus vaccination and infection. Vaccine. 2013;31(37):3987-94.

85. Quan F-S, Kim Y, Lee S, Yi H, Kang S-M, Bozja J, et al. Viruslike Particle Vaccine Induces Protection Against Respiratory Syncytial Virus Infection in Mice. The Journal of infectious diseases. 2011;204(7):987-95.

86. Mizgerd JP. Lung infection--a public health priority. PLoS Med. 2006;3(2):e76.

87. Organization WH. Global Health Estimates 2015: Deaths by Cause, Age, Sex, by Country and by Region, 2000-2015 Geneva, Switzerland2016 [

88. Nair H, Nokes DJ, Gessner BD, Dherani M, Madhi SA, Singleton RJ, et al. Global burden of acute lower respiratory infections due to respiratory syncytial virus in young children: a systematic review and meta-analysis. Lancet. 2010;375(9725):1545-55.

89. Wegzyn C, Toh LK, Notario G, Biguenet S, Unnebrink K, Park C, et al. Safety and Effectiveness of Palivizumab in Children at High Risk of Serious Disease Due to Respiratory Syncytial Virus Infection: A Systematic Review. Infect Dis Ther. 2014;3(2):133-58.

90. Hall CB, Weinberg GA, Iwane MK, Blumkin AK, Edwards KM, Staat MA, et al. The Burden of Respiratory Syncytial Virus Infection in Young Children. New England Journal of Medicine. 2009;360(6):588-98.

91. Levy O, Suter EE, Miller RL, Wessels MR. Unique efficacy of Toll-like receptor 8 agonists in activating human neonatal antigen-presenting cells. Blood. 2006;108(4):1284-90.

92. Levy O, Zarember KA, Roy RM, Cywes C, Godowski PJ, Wessels MR. Selective Impairment of TLR-Mediated Innate Immunity in Human Newborns: Neonatal Blood Plasma Reduces Monocyte TNF-α Induction by Bacterial Lipopeptides, Lipopolysaccharide, and Imiquimod, but Preserves the Response to R-848. The Journal of Immunology. 2004;173(7):4627-34.

93. Levy O, Coughlin M, Cronstein BN, Roy RM, Desai A, Wessels MR. The Adenosine System Selectively Inhibits TLR-Mediated TNF-α Production in the Human Newborn. The Journal of Immunology. 2006;177(3):1956-66.

94. Cannon MJ, Openshaw PJ, Askonas BA. Cytotoxic T cells clear virus but augment lung pathology in mice infected with respiratory syncytial virus. The Journal of experimental medicine. 1988;168(3):1163-8.

95. Lee S, Stokes KL, Currier MG, Sakamoto K, Lukacs NW, Celis E, et al. Vaccine-Elicited CD8(+) T Cells Protect against Respiratory Syncytial Virus Strain A2-Line19F-Induced Pathogenesis in BALB/c Mice. Journal of Virology. 2012;86(23):13016-24.

96. Ostler T, Ehl S. Pulmonary T cells induced by respiratory syncytial virus are functional and can make an important contribution to long-lived protective immunity. European journal of immunology. 2002;32(9):2562-9.

97. Hall CB, Powell KR, MacDonald NE, Gala CL, Menegus ME, Suffin SC, et al. Respiratory syncytial viral infection in children with compromised immune function. N Engl J Med. 1986;315(2):77-81.

98. Johnson JE, Gonzales RA, Olson SJ, Wright PF, Graham BS. The histopathology of fatal untreated human respiratory syncytial virus infection. Modern pathology : an official journal of the United States and Canadian Academy of Pathology, Inc. 2006;20(1):108-19.

99. Welliver TP, Garofalo RP, Hosakote Y, Hintz KH, Avendano L, Sanchez K, et al. Severe Human Lower Respiratory Tract Illness Caused by Respiratory Syncytial Virus and

Influenza Virus Is Characterized by the Absence of Pulmonary Cytotoxic Lymphocyte Responses. Journal of Infectious Diseases. 2007;195(8):1126-36.

100. Everard ML, Swarbrick A, Wrightham M, McIntyre J, Dunkley C, James PD, et al. Analysis of cells obtained by bronchial lavage of infants with respiratory syncytial virus infection. Arch Dis Child. 1994;71(5):428-32.

101. Heidema J, Lukens MV, van Maren WW, van Dijk ME, Otten HG, van Vught AJ, et al. CD8+ T cell responses in bronchoalveolar lavage fluid and peripheral blood mononuclear cells of infants with severe primary respiratory syncytial virus infections. J Immunol. 2007;179(12):8410-7.

102. Lines JL, Hoskins S, Hollifield M, Cauley LS, Garvy BA. The migration of T cells in response to influenza virus is altered in neonatal mice. J Immunol. 2010;185(5):2980-8.

103. Kraft JD, Horzempa J, Davis C, Jung JY, Pena MM, Robinson CM. Neonatal macrophages express elevated levels of interleukin-27 that oppose immune responses. Immunology. 2013;139(4):484-93.

104. Restori KH, Srinivasa BT, Ward BJ, Fixman ED. Neonatal Immunity, Respiratory Virus Infections, and the Development of Asthma. Frontiers in Immunology. 2018;9(1249).

105. Ruckwardt TJ, Morabito KM, Graham BS. Determinants of early life immune responses to RSV infection. Current opinion in virology. 2016;16:151-7.

106. Haskó G, Pacher P, Deitch EA, Vizi ES. Shaping of monocyte and macrophage function by adenosine receptors. Pharmacology & therapeutics. 2007;113(2):264-75.

107. Duan M, Li WC, Vlahos R, Maxwell MJ, Anderson GP, Hibbs ML. Distinct macrophage subpopulations characterize acute infection and chronic inflammatory lung disease. J Immunol. 2012;189(2):946-55.

108. Duan M, Steinfort DP, Smallwood D, Hew M, Chen W, Ernst M, et al. CD11b immunophenotyping identifies inflammatory profiles in the mouse and human lungs. Mucosal immunology. 2016;9(2):550-63.

109. Johnston LK, Rims CR, Gill SE, McGuire JK, Manicone AM. Pulmonary macrophage subpopulations in the induction and resolution of acute lung injury. Am J Respir Cell Mol Biol. 2012;47(4):417-26.

110. Hussell T, Bell TJ. Alveolar macrophages: plasticity in a tissue-specific context. Nature reviews Immunology. 2014;14(2):81-93.

111. Grigg J, Riedler J, Robertson CF, Boyle W, Uren S. Alveolar macrophage immaturity in infants and young children. The European respiratory journal. 1999;14(5):1198-205.

112. Chen T-A, Liao C-C, Cheng Y-C, Chen Y-P, Hsu Y-F, Liang C-M, et al. Stimulation of Proliferation and Migration of Mouse Macrophages by Type B CpG-ODNs Is F-Spondin and IL-1Ra Dependent. PLOS ONE. 2015;10(6):e0128926.

113. Lee G-L, Wu J-Y, Yeh C-C, Kuo C-C. TLR4 induces CREB-mediated IL-6 production via upregulation of F-spondin to promote vascular smooth muscle cell migration. Biochemical and biophysical research communications. 2016;473(4):1205-10.

114. Ledford JG, Kovarova M, Koller BH. Impaired Host Defense in Mice Lacking ONZIN. The Journal of Immunology. 2007;178(8):5132.

115. Johnson RM, Kerr MS, Slaven JE. Plac8-Dependent and Inducible NO Synthase-Dependent Mechanisms Clear Chlamydia muridarum Infections from the Genital Tract. The Journal of Immunology. 2012;188(4):1896-904.

116. Estecha A, Aguilera-Montilla N, Sánchez-Mateos P, Puig-Kröger A. RUNX3 Regulates Intercellular Adhesion Molecule 3 (ICAM-3) Expression during Macrophage Differentiation and Monocyte Extravasation. PLOS ONE. 2012;7(3):e33313.

117. Puig-Kröger A, Domínguez-Soto A, Martínez-Muñoz L, Serrano-Gómez D, Lopez-Bravo M, Sierra-Filardi E, et al. RUNX3 Negatively Regulates CD36 Expression in Myeloid Cell Lines. The Journal of Immunology. 2006;177(4):2107.

118. Newell EA, Exo JL, Verrier JD, Jackson TC, Gillespie DG, Janesko-Feldman K, et al. 2′,3′-cAMP, 3′-AMP, 2′-AMP and adenosine inhibit TNF-α and CXCL10 production from activated primary murine microglia via A2A receptors. Brain research. 2015;1594:27-35.

119. Eichinger KM, Egaña L, Orend JG, Resetar E, Anderson KB, Patel R, et al. Alveolar macrophages support interferon gamma-mediated viral clearance in RSV-infected neonatal mice. Respiratory research. 2015;16:122.

120. Hamidzadeh K, Mosser DM. Purinergic signaling to terminate TLR responses in macrophages. Frontiers in Immunology. 2016;7.

121. Zanin RF, Braganhol E, Bergamin LS, Campesato LFI, Filho AZ, Moreira JCF, et al. Differential Macrophage Activation Alters the Expression Profile of NTPDase and Ecto-5′-Nucleotidase. PLOS ONE. 2012;7(2):e31205.

122. Goritzka M, Makris S, Kausar F, Durant LR, Pereira C, Kumagai Y, et al. Alveolar macrophage-derived type I interferons orchestrate innate immunity to RSV through recruitment of antiviral monocytes. The Journal of experimental medicine. 2015;212(5):699-714.

123. Makris S, Bajorek M, Culley FJ, Goritzka M, Johansson C. Alveolar Macrophages Can Control Respiratory Syncytial Virus Infection in the Absence of Type I Interferons. J Innate Immun. 2016;8(5):452-63.

124. Ugonna K, Bingle CD, Plant K, Wilson K, Everard ML. Macrophages are required for dendritic cell uptake of respiratory syncytial virus from an infected epithelium. PLoS One. 2014;9(3):e91855.

125. Verhoeven D. Influence of Immunological Maturity on Respiratory Syncytial Virus-Induced Morbidity in Young Children. Viral Immunology. 2018;0(0):null.

126. Bordon Y. Neonatal immunity: Hush-a by baby. Nature reviews Immunology. 2014;14(1):4-5.

127. Belderbos ME, Levy O, Stalpers F, Kimpen JL, Meyaard L, Bont L. Neonatal plasma polarizes TLR4-mediated cytokine responses towards low IL-12p70 and high IL-10 production via distinct factors. PLoS One. 2012;7(3):e33419.

128. Bendelja K, Vojvoda V, Aberle N, Cepin-Bogovic J, Gagro A, Mlinaric-Galinovic G, et al. Decreased Toll-like receptor 8 expression and lower TNF-alpha synthesis in infants with acute RSV infection. Respiratory research. 2010;11:143.

129. Cuenca AG, Wynn JL, Moldawer LL, Levy O. Role of innate immunity in neonatal infection. American journal of perinatology. 2013;30(2):105-12.

130. Kollmann TR, Crabtree J, Rein-Weston A, Blimkie D, Thommai F, Wang XY, et al. Neonatal innate TLR-mediated responses are distinct from those of adults. J Immunol. 2009;183(11):7150-60.

131. Valero N, Mosquera J, Levy A, Anez G, Marcucci R, Alvarez-Mon M. Differential induction of cytokines by human neonatal, adult, and elderly monocyte/macrophages infected with dengue virus. Viral Immunol. 2014;27(4):151-9.

132. Weatherstone KB, Rich EA. Tumor necrosis factor/cachectin and interleukin-1 secretion by cord blood monocytes from premature and term neonates. Pediatric research. 1989;25(4):342-6.

133. Lambrecht BN. Alveolar Macrophage in the Driver's Seat. Immunity. 2006;24(4):366-8.

134. Mogensen SC. Role of macrophages in natural resistance to virus infections. Microbiol Rev. 1979;43(1):1-26.

135. Pribul PK, Harker J, Wang B, Wang H, Tregoning JS, Schwarze J, et al. Alveolar Macrophages Are a Major Determinant of Early Responses to Viral Lung Infection but Do Not Influence Subsequent Disease Development. Journal of Virology. 2008;82(9):4441-8.

136. Zasłona Z, Przybranowski S, Wilke C, van Rooijen N, Teitz-Tennenbaum S, Osterholzer JJ, et al. Resident Alveolar Macrophages Suppress, whereas Recruited Monocytes Promote, Allergic Lung Inflammation in Murine Models of Asthma. The Journal of Immunology. 2014;193(8):4245.

137. Martin CJ, Peters KN, Behar SM. Macrophages clean up: efferocytosis and microbial control. Current Opinion in Microbiology. 2014;17(0):17-23.

138. Anderson DC, Springer TA. Leukocyte adhesion deficiency: an inherited defect in the Mac-1, LFA-1, and p150,95 glycoproteins. Annu Rev Med. 1987;38:175-94.

139. Gentile DA, Doyle WJ, Zeevi A, Howe-Adams J, Kapadia S, Trecki J, et al. Cytokine gene polymorphisms moderate illness severity in infants with respiratory syncytial virus infection. Hum Immunol. 2003;64(3):338-44.

140. Schroder K, Hertzog PJ, Ravasi T, Hume DA. Interferon-gamma: an overview of signals, mechanisms and functions. J Leukoc Biol. 2004;75(2):163-89.

141. Iliodromiti Z, Anastasiadis A, Varras M, Pappa KI, Siristatidis C, Bakoulas V, et al. Monocyte function in the fetus and the preterm neonate: immaturity combined with functional impairment. Mediators Inflamm. 2013;2013:753752.

142. Schefold JC, Porz L, Uebe B, Poehlmann H, von Haehling S, Jung A, et al. Diminished HLA-DR expression on monocyte and dendritic cell subsets indicating impairment of cellular immunity in pre-term neonates: a prospective observational analysis. J Perinat Med. 2015;43(5):609-18.

143. Simon AK, Hollander GA, McMichael A. Evolution of the immune system in humans from infancy to old age. Proc Biol Sci. 2015;282(1821):20143085.

144. Banchereau J, Steinman RM. Dendritic cells and the control of immunity. Nature. 1998;392:245.

145. Jakubzick CV, Randolph GJ, Henson PM. Monocyte differentiation and antigen-presenting functions. Nature reviews Immunology. 2017;17(6):349-62.

146. Liu K, Nussenzweig MC. Origin and development of dendritic cells. Immunological reviews. 2010;234(1):45-54.

147. Fitzpatrick EA, You D, Shrestha B, Siefker D, Patel VS, Yadav N, et al. A Neonatal Murine Model of MRSA Pneumonia. PLoS One. 2017;12(1):e0169273.

148. Qureshi MH, Garvy BA. Neonatal T Cells in an Adult Lung Environment Are Competent to Resolve Pneumocystis carinii Pneumonia. The Journal of Immunology. 2001;166(9):5704-11.

149. Tregoning JS, Yamaguchi Y, Harker J, Wang B, Openshaw PJ. The role of T cells in the enhancement of respiratory syncytial virus infection severity during adult reinfection of neonatally sensitized mice. J Virol. 2008;82(8):4115-24.

150. Liesman RM, Buchholz UJ, Luongo CL, Yang L, Proia AD, DeVincenzo JP, et al. RSV-encoded NS2 promotes epithelial cell shedding and distal airway obstruction. The Journal of Clinical Investigation. 2014;124(5):2219-33.

151. Villenave R, Thavagnanam S, Sarlang S, Parker J, Douglas I, Skibinski G, et al. In vitro modeling of respiratory syncytial virus infection of pediatric bronchial epithelium, the primary target of infection in vivo. Proceedings of the National Academy of Sciences. 2012;109(13):5040-5.

152. Lukens MV, Claassen EA, de Graaff PM, van Dijk ME, Hoogerhout P, Toebes M, et al. Characterization of the CD8+ T cell responses directed against respiratory syncytial virus during primary and secondary infection in C57BL/6 mice. Virology. 2006;352(1):157-68.

153. Chang J, Braciale TJ. Respiratory syncytial virus infection suppresses lung CD8+ T-cell effector activity and peripheral CD8+ T-cell memory in the respiratory tract. Nature medicine. 2002;8(1):54-60.

154. Ostler T, Davidson W, Ehl S. Virus clearance and immunopathology by CD8(+) T cells during infection with respiratory syncytial virus are mediated by IFN-gamma. European journal of immunology. 2002;32(8):2117-23.

155. Burnstock G, Brouns I, Adriaensen D, Timmermans J-P. Purinergic Signaling in the Airways. Pharmacological Reviews. 2012;64(4):834-68.

156. Koeppen M, Di Virgilio F, Clambey ET, Eltzschig HK. Purinergic Regulation of Airway Inflammation. In: Picher M, Boucher CR, editors. Purinergic Regulation of Respiratory Diseases. Dordrecht: Springer Netherlands; 2011. p. 159-93.

157. Ohta A, Sitkovsky M. Extracellular adenosine-mediated modulation of regulatory T cells. Front Immunol. 2014;5:304.

158. Philbin VJ, Levy O. Immunostimulatory activity of Toll-like receptor 8 agonists towards human leucocytes: basic mechanisms and translational opportunities. Biochemical Society transactions. 2007;35(Pt 6):1485-91.

159. Pettengill M, Robson S, Tresenriter M, Millán JL, Usheva A, Bingham T, et al. Soluble Ecto-5′-nucleotidase (5′-NT), Alkaline Phosphatase, and Adenosine Deaminase (ADA1) Activities in Neonatal Blood Favor Elevated Extracellular Adenosine. Journal of Biological Chemistry. 2013;288(38):27315-26.

160. Hilleman MR. Vaccines in historic evolution and perspective: a narrative of vaccine discoveries. Vaccine. 2000;18(15):1436-47.

161. Mold JE, Michaelsson J, Burt TD, Muench MO, Beckerman KP, Busch MP, et al. Maternal alloantigens promote the development of tolerogenic fetal regulatory T cells in utero. Science. 2008;322(5907):1562-5.

162. Weitzel RP, Lesniewski ML, Haviernik P, Kadereit S, Leahy P, Greco NJ, et al. microRNA 184 regulates expression of NFAT1 in umbilical cord blood CD4+ T cells. Blood. 2009;113(26):6648-57.

163. Yamashita K, Miyoshi T, Arai Y, Mizugishi K, Takaori-Kondo A, Ueyama T. Enhanced generation of reactive oxygen species by interferon-gamma may have contributed to successful treatment of invasive pulmonary aspergillosis in a patient with chronic granulomatous disease. Int J Hematol. 2013;97(4):505-10.

164. ACTIMMUNE (Interferon gamma-1b). In: Horizon Pharma I, editor. 2018.

165. Koh WJ, Kwon OJ, Suh GY, Chung MP, Kim H, Lee NY, et al. Six-month therapy with aerosolized interferon-gamma for refractory multidrug-resistant pulmonary tuberculosis. J Korean Med Sci. 2004;19(2):167-71.

166. Raju B, Hoshino Y, Kuwabara K, Belitskaya I, Prabhakar S, Canova A, et al. Aerosolized gamma interferon (IFN-gamma) induces expression of the genes encoding the IFN-gamma-inducible 10-kilodalton protein but not inducible nitric oxide synthase in the lung during tuberculosis. Infection and immunity. 2004;72(3):1275-83.

167. Virgolini I, Kurtaran A, Leimer M, Smith-Jones P, Agis H, Angelberger P, et al. Inhalation scintigraphy with iodine-123-labeled interferon gamma-1b: pulmonary deposition and dose escalation study in healthy volunteers. J Nucl Med. 1997;38(9):1475-81.

168. Subramaniam R, Hillberry Z, Chen H, Feng Y, Fletcher K, Neuenschwander P, et al. Delivery of GM-CSF to Protect against Influenza Pneumonia. PLoS One. 2015;10(4):e0124593.

169. Hart DNJ. Dendritic Cells: Unique Leukocyte Populations Which Control the Primary Immune Response. Blood. 1997;90(9):3245.

170. Mellman I. Dendritic Cells: Master Regulators of the Immune Response. Cancer Immunology Research. 2013;1(3):145-9.

171. Davidson S, Kaiko G, Loh Z, Lalwani A, Zhang V, Spann K, et al. Plasmacytoid dendritic cells promote host defense against acute pneumovirus infection via the TLR7-MyD88-dependent signaling pathway. J Immunol. 2011;186(10):5938-48.

172. Naessens T, Schepens B, Smet M, Pollard C, Van Hoecke L, De Beuckelaer A, et al. GM-CSF treatment prevents respiratory syncytial virus-induced pulmonary exacerbation responses in postallergic mice by stimulating alveolar macrophage maturation. The Journal of allergy and clinical immunology. 2016;137(3):700-9 e9.

173. Zanini A, Spanevello A, Baraldo S, Majori M, Della Patrona S, Gumiero F, et al. Decreased maturation of dendritic cells in the central airways of COPD patients is associated with VEGF, TGF-beta and vascularity. Respiration. 2014;87(3):234-42.

174. Harker JA, Lee DC, Yamaguchi Y, Wang B, Bukreyev A, Collins PL, et al. Delivery of cytokines by recombinant virus in early life alters the immune response to adult lung infection. J Virol. 2010;84(10):5294-302.

175. Knudson CJ, Hartwig SM, Meyerholz DK, Varga SM. RSV Vaccine-Enhanced Disease Is Orchestrated by the Combined Actions of Distinct CD4 T Cell Subsets. PLOS Pathogens. 2015;11(3):e1004757.

176. Kristjansson S, Bjarnarson SP, Wennergren G, Palsdottir AH, Arnadottir T, Haraldsson A, et al. Respiratory syncytial virus and other respiratory viruses during the first 3 months of life promote a local TH2-like response. The Journal of allergy and clinical immunology. 2005;116(4):805-11.

177. Lee FE, Walsh EE, Falsey AR, Lumb ME, Okam NV, Liu N, et al. Human infant respiratory syncytial virus (RSV)-specific type 1 and 2 cytokine responses ex vivo during primary RSV infection. The Journal of infectious diseases. 2007;195(12):1779-88.

178. Legg JP, Hussain IR, Warner JA, Johnston SL, Warner JO. Type 1 and Type 2 Cytokine Imbalance in Acute Respiratory Syncytial Virus Bronchiolitis. American Journal of Respiratory and Critical Care Medicine. 2003;168(6):633-9.

179. Hussell T, Baldwin CJ, O'Garra A, Openshaw PJ. CD8+ T cells control Th2-driven pathology during pulmonary respiratory syncytial virus infection. European journal of immunology. 1997;27(12):3341-9.

180. Arulanandam BP, Mittler JN, Lee WT, O'Toole M, Metzger DW. Neonatal administration of IL-12 enhances the protective efficacy of antiviral vaccines. J Immunol. 2000;164(7):3698-704.

181. Pertmer TM, Oran AE, Madorin CA, Robinson HL. Th1 genetic adjuvants modulate immune responses in neonates. Vaccine. 2001;19(13-14):1764-71.

182. Eichinger KM, Resetar E, Orend J, Anderson K, Empey KM. Age predicts cytokine kinetics and innate immune cell activation following intranasal delivery of IFNgamma and GM-CSF in a mouse model of RSV infection. Cytokine. 2017;97:25-37.

183. Todt JC, Hu B, Curtis JL. The scavenger receptor SR-A I/II (CD204) signals via the receptor tyrosine kinase Mertk during apoptotic cell uptake by murine macrophages. J Leukoc Biol. 2008;84(2):510-8.

184. Malloy AMW, Ruckwardt TJ, Morabito KM, Lau-Kilby AW, Graham BS. Pulmonary Dendritic Cell Subsets Shape the Respiratory Syncytial Virus–Specific CD8⁺ T Cell Immunodominance Hierarchy in Neonates. The Journal of Immunology. 2017;198(1):394.

185. Lembo A, Pelletier M, Iyer R, Timko M, Dudda JC, West TE, et al. Administration of a synthetic TLR4 agonist protects mice from pneumonic tularemia. J Immunol. 2008;180(11):7574-81.

186. Luhrmann A, Tschernig T, Pabst R. Stimulation of bronchus-associated lymphoid tissue in rats by repeated inhalation of aerosolized lipopeptide MALP-2. Pathobiology. 2002;70(5):266-9.

187. Ulevitch RJ. Therapeutics targeting the innate immune system. Nature reviews Immunology. 2004;4(7):512-20.

188. Pashine A, Valiante NM, Ulmer JB. Targeting the innate immune response with improved vaccine adjuvants. Nature medicine. 2005;11(4 Suppl):S63-8.

189. Adkins B, Levy O, Betz AG. A new unexpected twist in newborn immunity. Nature medicine. 2014;20(1):22-3.

190. Levy O. Innate immunity of the newborn: basic mechanisms and clinical correlates. Nature reviews Immunology. 2007;7(5):379-90.

191. Gillis PA, Hernandez-Alvarado N, Gnanandarajah JS, Wussow F, Diamond DJ, Schleiss MR. Development of a novel, guinea pig-specific IFN-gamma ELISPOT assay and characterization of guinea pig cytomegalovirus GP83-specific cellular immune responses following immunization with a modified vaccinia virus Ankara (MVA)-vectored GP83 vaccine. Vaccine. 2014;32(31):3963-70.

192. Sawant PM, Verma PC, Subudhi PK, Chaturvedi U, Singh M, Kumar R, et al. Immunomodulation of bivalent Newcastle disease DNA vaccine induced immune response by co-delivery of chicken IFN-gamma and IL-4 genes. Vet Immunol Immunopathol. 2011;144(1-2):36-44.

193. Wang X, Zhang J, Liang J, Zhang Y, Teng X, Yuan X, et al. Protection against Mycobacterium tuberculosis infection offered by a new multistage subunit vaccine correlates with increased number of IFN-gamma+ IL-2+ CD4+ and IFN-gamma+ CD8+ T cells. PLoS One. 2015;10(3):e0122560.

194. Wang YP, Liu D, Guo LJ, Tang QH, Wei YW, Wu HL, et al. Enhanced protective immune response to PCV2 subunit vaccine by co-administration of recombinant porcine IFN-gamma in mice. Vaccine. 2013;31(5):833-8.

195. McMahon TA, Brain JD, Lemott S. Species differences in aerosol deposition. Inhaled Part. 1975;4 Pt 1:23-33.

196. Garcia C, Soriano-Fallas A, Lozano J, Leos N, Gomez AM, Ramilo O, et al. Decreased innate immune cytokine responses correlate with disease severity in children with respiratory syncytial virus and human rhinovirus bronchiolitis. The Pediatric infectious disease journal. 2012;31(1):86-9.

197. Cohn L, Homer RJ, Niu N, Bottomly K. T helper 1 cells and interferon gamma regulate allergic airway inflammation and mucus production. The Journal of experimental medicine. 1999;190(9):1309-18.

198. Cho SH, Oh SY, Lane AP, Lee J, Oh MH, Lee S, et al. Regulation of nasal airway homeostasis and inflammation in mice by SHP-1 and Th2/Th1 signaling pathways. PLoS One. 2014;9(8):e103685.

199. Hong JY, Bentley JK, Chung Y, Lei J, Steenrod JM, Chen Q, et al. Neonatal rhinovirus induces mucous metaplasia and airways hyperresponsiveness through IL-25 and type 2 innate lymphoid cells. The Journal of allergy and clinical immunology. 2014;134(2):429-39.

200. Mitchell C, Provost K, Niu N, Homer R, Cohn L. IFN-γ Acts on the Airway Epithelium To Inhibit Local and Systemic Pathology in Allergic Airway Disease. The Journal of Immunology. 2011;187(7):3815-20.

201. Shieh YH, Huang HM, Wang CC, Lee CC, Fan CK, Lee YL. Zerumbone enhances the Th1 response and ameliorates ovalbumin-induced Th2 responses and airway inflammation in mice. International immunopharmacology. 2015;24(2):383-91.

202. Kotelkin A, Prikhod'ko EA, Cohen JI, Collins PL, Bukreyev A. Respiratory Syncytial Virus Infection Sensitizes Cells to Apoptosis Mediated by Tumor Necrosis Factor-Related Apoptosis-Inducing Ligand. Journal of Virology. 2003;77(17):9156-72.

203. Schroder K, Hertzog PJ, Ravasi T, Hume DA. Interferon-γ: an overview of signals, mechanisms and functions. Journal of Leukocyte Biology. 2004;75(2):163-89.

204. Kumar M, Behera AK, Matsuse H, Lockey RF, Mohapatra SS. Intranasal IFN-γ gene transfer protects BALB/c mice against respiratory syncytial virus infection. Vaccine. 1999;18(5–6):558-67.

205. Yamada Y, Matsumoto K, Hashimoto N, Saikusa M, Homma T, Yoshihara S, et al. Effect of Th1/Th2 Cytokine Pretreatment on RSV-Induced Gene Expression in Airway Epithelial Cells. International archives of allergy and immunology. 2011;154(3):185-94.

206. El Saleeby CM, Bush AJ, Harrison LM, Aitken JA, DeVincenzo JP. Respiratory Syncytial Virus Load, Viral Dynamics, and Disease Severity in Previously Healthy Naturally Infected Children. Journal of Infectious Diseases. 2011;204(7):996-1002.

207. Purnama C, Ng SL, Tetlak P, Setiagani YA, Kandasamy M, Baalasubramanian S, et al. Transient ablation of alveolar macrophages leads to massive pathology of influenza infection without affecting cellular adaptive immunity. European journal of immunology. 2014;44(7):2003-12.

208. Sercan Ö, Hämmerling GJ, Arnold B, Schüler T. Cutting Edge: Innate Immune Cells Contribute to the IFN-γ-Dependent Regulation of Antigen-Specific CD8+ T Cell Homeostasis. The Journal of Immunology. 2006;176(2):735-9.

209. Sercan Ö, Stoycheva D, Hämmerling GJ, Arnold B, Schüler T. IFN-γ Receptor Signaling Regulates Memory CD8+ T Cell Differentiation. The Journal of Immunology. 2010;184(6):2855-62.

210. Stoycheva D, Deiser K, Stärck L, Nishanth G, Schlüter D, Uckert W, et al. IFN-γ Regulates CD8+ Memory T Cell Differentiation and Survival in Response to Weak, but Not Strong, TCR Signals. The Journal of Immunology. 2015;194(2):553-9.

211. Glezen WP, Taber LH, Frank AL, Kasel JA. Risk of primary infection and reinfection with respiratory syncytial virus. Am J Dis Child. 1986;140(6):543-6.

212. Henderson FW, Collier AM, Clyde WA, Jr., Denny FW. Respiratory-syncytial-virus infections, reinfections and immunity. A prospective, longitudinal study in young children. N Engl J Med. 1979;300(10):530-4.

213. Dakhama A, Park J-W, Taube C, Joetham A, Balhorn A, Miyahara N, et al. The Enhancement or Prevention of Airway Hyperresponsiveness during Reinfection with Respiratory Syncytial Virus Is Critically Dependent on the Age at First Infection and IL-13 Production. The Journal of Immunology. 2005;175(3):1876-83.

214. Adkins B, Du RQ. Newborn mice develop balanced Th1/Th2 primary effector responses in vivo but are biased to Th2 secondary responses. J Immunol. 1998;160(9):4217-24.

215. Lee YM, Miyahara N, Takeda K, Prpich J, Oh A, Balhorn A, et al. IFN-gamma production during initial infection determines the outcome of reinfection with respiratory syncytial virus. Am J Respir Crit Care Med. 2008;177(2):208-18.

216. Harker J, Bukreyev A, Collins PL, Wang B, Openshaw PJ, Tregoning JS. Virally delivered cytokines alter the immune response to future lung infections. J Virol. 2007;81(23):13105-11.

217. Harker JA, Yamaguchi Y, Culley FJ, Tregoning JS, Openshaw PJ. Delayed sequelae of neonatal respiratory syncytial virus infection are dependent on cells of the innate immune system. J Virol. 2014;88(1):604-11.

218. Netea MG, Joosten LAB, Latz E, Mills KHG, Natoli G, Stunnenberg HG, et al. Trained immunity: A program of innate immune memory in health and disease. Science. 2016;352(6284):aaf1098.

219. Janssen WJ, Stefanski AL, Bochner BS, Evans CM. Control of lung defence by mucins and macrophages: ancient defence mechanisms with modern functions. The European respiratory journal. 2016;48(4):1201-14.

220. Desch AN, Randolph GJ, Murphy K, Gautier EL, Kedl RM, Lahoud MH, et al. CD103+ pulmonary dendritic cells preferentially acquire and present apoptotic cell-associated antigen. The Journal of experimental medicine. 2011;208(9):1789-97.

221. Bertrand P, Lay MK, Piedimonte G, Brockmann PE, Palavecino CE, Hernandez J, et al. Elevated IL-3 and IL-12p40 levels in the lower airway of infants with RSV-induced bronchiolitis correlate with recurrent wheezing. Cytokine. 2015;76(2):417-23.

222. Asquith KL, Ramshaw HS, Hansbro PM, Beagley KW, Lopez AF, Foster PS. The IL-3/IL-5/GM-CSF Common β Receptor Plays a Pivotal Role in the Regulation of Th2 Immunity and Allergic Airway Inflammation. The Journal of Immunology. 2008;180(2):1199-206.

223. Koch S, Sopel N, Finotto S. Th9 and other IL-9-producing cells in allergic asthma. Seminars in Immunopathology. 2017;39(1):55-68.

224. Rignault-Bricard R, Machavoine F, Mecheri S, Hermine O, Schneider E, Dy M, et al. IL-3–producing basophils are required to exacerbate airway hyperresponsiveness in a murine inflammatory model. Allergy. 2018;73(12):2342-51.

225. Hall CB, Long CE, Schnabel KC. Respiratory syncytial virus infections in previously healthy working adults. Clinical infectious diseases : an official publication of the Infectious Diseases Society of America. 2001;33(6):792-6.

226. Alwan WH, Record FM, Openshaw PJ. CD4+ T cells clear virus but augment disease in mice infected with respiratory syncytial virus. Comparison with the effects of CD8+ T cells. Clinical and experimental immunology. 1992;88(3):527-36.

227. Tregoning JS, Wang BL, McDonald JU, Yamaguchi Y, Harker JA, Goritzka M, et al. Neonatal antibody responses are attenuated by interferon-γ produced by NK and T cells during RSV infection. Proceedings of the National Academy of Sciences. 2013;110(14):5576-81.

228. Matsuura H, Sakaue M, Subbaramaiah K, Kamitani H, Eling TE, Dannenberg AJ, et al. Regulation of cyclooxygenase-2 by interferon gamma and transforming growth factor alpha in normal human epidermal keratinocytes and squamous carcinoma cells. Role of mitogen-activated protein kinases. The Journal of biological chemistry. 1999;274(41):29138-48.

229. Li H, Edin ML, Bradbury JA, Graves JP, DeGraff LM, Gruzdev A, et al. Cyclooxygenase-2 inhibits T helper cell type 9 differentiation during allergic lung inflammation via down-regulation of IL-17RB. Am J Respir Crit Care Med. 2013;187(8):812-22.

230. Kurtz J. Specific memory within innate immune systems. Trends in immunology. 2005;26(4):186-92.

231. Quintin J, Cheng SC, van der Meer JW, Netea MG. Innate immune memory: towards a better understanding of host defense mechanisms. Current opinion in immunology. 2014;29:1-7.

232. Yamaguchi Y, Harker JA, Wang B, Openshaw PJ, Tregoning JS, Culley FJ. Preexposure to CpG Protects against the Delayed Effects of Neonatal Respiratory Syncytial Virus Infection. Journal of Virology. 2012;86(19):10456-61.

233. Cheng SC, Quintin J, Cramer RA, Shepardson KM, Saeed S, Kumar V, et al. mTOR- and HIF-1alpha-mediated aerobic glycolysis as metabolic basis for trained immunity. Science. 2014;345(6204):1250684.

234. Cohen HB, Ward A, Hamidzadeh K, Ravid K, Mosser DM. IFN-gamma Prevents Adenosine Receptor (A2bR) Upregulation To Sustain the Macrophage Activation Response. J Immunol. 2015;195(8):3828-37.

235. MedImmune. SYNAGIS (palivizumab). In: MedImmune, editor. Gaithersburgh, MD1998 [Revised 03/2014].

236. Homaira N, Rawlinson W, Snelling TL, Jaffe A. Effectiveness of Palivizumab in Preventing RSV Hospitalization in High Risk Children: A Real-World Perspective. Int J Pediatr. 2014;2014:571609.

237. Sastre P, Melero JA, Garcia-Barreno B, Palomo C. Comparison of affinity chromatography and adsorption to vaccinia virus recombinant infected cells for depletion of antibodies directed against respiratory syncytial virus glycoproteins present in a human immunoglobulin preparation. J Med Virol. 2005;76(2):248-55.

238. Delgado MF, Coviello S, Monsalvo AC, Melendi GA, Hernandez JZ, Batalle JP, et al. Lack of antibody affinity maturation due to poor Toll-like receptor stimulation leads to enhanced respiratory syncytial virus disease. Nature medicine. 2009;15(1):34-41.

239. Graham BS. Vaccine development for respiratory syncytial virus. Current opinion in virology. 2017;23:107-12.

240. Polack FP, Teng MN, Collins PL, Prince GA, Exner M, Regele H, et al. A role for immune complexes in enhanced respiratory syncytial virus disease. The Journal of experimental medicine. 2002;196(6):859-65.

241. A Study to Evaluate the Safety, Tolerability and Immunogenicity of an Investigational RSV Vaccine Candidate (Ad26.RSV.preF) in Adults 18 to 50 Years of Age, and RSV-seropositive Toddlers 12 to 24 Months of Age.

242. De Gregorio E, Tritto E, Rappuoli R. Alum adjuvanticity: Unraveling a century old mystery. European journal of immunology. 2008;38(8):2068-71.

243. Sastry M, Zhang B, Chen M, Joyce MG, Kong WP, Chuang GY, et al. Adjuvants and the vaccine response to the DS-Cav1-stabilized fusion glycoprotein of respiratory syncytial virus. PLoS One. 2017;12(10):e0186854.

244. Wang Y, Rahman D, Lehner T. A Comparative Study of Stress-mediated Immunological Functions with the Adjuvanticity of Alum. Journal of Biological Chemistry. 2012;287(21):17152-60.

245. Connors M, Kulkarni AB, Firestone CY, Holmes KL, Morse HC, Sotnikov AV, et al. Pulmonary histopathology induced by respiratory syncytial virus (RSV) challenge of formalin-inactivated RSV-immunized BALB/c mice is abrogated by depletion of CD4+ T cells. Journal of Virology. 1992;66(12):7444-51.

246. Johnson TR, Rothenberg ME, Graham BS. Pulmonary eosinophilia requires interleukin-5, eotaxin-1, and CD4+ T cells in mice immunized with respiratory syncytial virus G glycoprotein. Journal of Leukocyte Biology. 2008;84(3):748-59.

247. Larena M, Prow NA, Hall RA, Petrovsky N, Lobigs M. JE-ADVAX vaccine protection against Japanese encephalitis virus mediated by memory B cells in the absence of CD8(+) T cells and pre-exposure neutralizing antibody. J Virol. 2013;87(8):4395-402.

248. Lobigs M, Pavy M, Hall RA, Lobigs P, Cooper P, Komiya T, et al. An inactivated Vero cell-grown Japanese encephalitis vaccine formulated with Advax, a novel inulin-based adjuvant, induces protective neutralizing antibody against homologous and heterologous flaviviruses. The Journal of general virology. 2010;91(Pt 6):1407-17.

249. Saade F, Honda-Okubo Y, Trec S, Petrovsky N. A novel hepatitis B vaccine containing Advax, a polysaccharide adjuvant derived from delta inulin, induces robust humoral and cellular immunity with minimal reactogenicity in preclinical testing. Vaccine. 2013;31(15):1999-2007.

250. Cristillo AD, Ferrari MG, Hudacik L, Lewis B, Galmin L, Bowen B, et al. Induction of mucosal and systemic antibody and T-cell responses following prime–boost immunization with novel adjuvanted human immunodeficiency virus-1-vaccine formulations. Journal of General Virology. 2011;92(1):128-40.

251. Honda-Okubo Y, Barnard D, Ong CH, Peng B-H, Tseng C-TK, Petrovsky N. Severe Acute Respiratory Syndrome-Associated Coronavirus Vaccines Formulated with Delta Inulin Adjuvants Provide Enhanced Protection while Ameliorating Lung Eosinophilic Immunopathology. Journal of Virology. 2015;89(6):2995-3007.

252. McPherson C, Chubet R, Holtz K, Honda-Okubo Y, Barnard D, Cox M, et al. Development of a SARS Coronavirus Vaccine from Recombinant Spike Protein Plus Delta Inulin Adjuvant. Methods Mol Biol. 2016;1403:269-84.

253. Petrovsky N, Larena M, Siddharthan V, Prow NA, Hall RA, Lobigs M, et al. An Inactivated Cell Culture Japanese Encephalitis Vaccine (JE-ADVAX) Formulated with Delta Inulin Adjuvant Provides Robust Heterologous Protection against West Nile Encephalitis via Cross-Protective Memory B Cells and Neutralizing Antibody. Journal of Virology. 2013;87(18):10324-33.

254. Rodriguez-Del Rio E, Marradi M, Calderon-Gonzalez R, Frande-Cabanes E, Penadés S, Petrovsky N, et al. A gold glyco-nanoparticle carrying a listeriolysin O peptide and formulated with Advax™ delta inulin adjuvant induces robust T-cell protection against listeria infection. Vaccine. 2015;33(12):1465-73.

255. Feinen B, Petrovsky N, Verma A, Merkel TJ. Advax-Adjuvanted Recombinant Protective Antigen Provides Protection against Inhalational Anthrax That Is Further Enhanced by Addition of Murabutide Adjuvant. Clinical and Vaccine Immunology. 2014;21(4):580-6.

256. Honda-Okubo Y, Saade F, Petrovsky N. Advax™, a polysaccharide adjuvant derived from delta inulin, provides improved influenza vaccine protection through broad-based enhancement of adaptive immune responses. Vaccine. 2012;30(36):5373-81.

257. Honda-Okubo Y, Ong CH, Petrovsky N. Advax Delta Inulin Adjuvant Overcomes Immune Immaturity In Neonatal Mice Thereby Allowing Single–Dose Influenza Vaccine Protection. Vaccine. 2015;33(38):4892-900.

258. Honda-Okubo Y, Kolpe A, Li L, Petrovsky N. A single immunization with inactivated H1N1 influenza vaccine formulated with delta inulin adjuvant (Advax) overcomes pregnancy-associated immune suppression and enhances passive neonatal protection. Vaccine. 2014;32(36):4651-9.

259. Bielefeldt-Ohmann H, Prow NA, Wang W, Tan CS, Coyle M, Douma A, et al. Safety and immunogenicity of a delta inulin-adjuvanted inactivated Japanese encephalitis virus vaccine in pregnant mares and foals. Veterinary Research. 2014;45(1):130.

260. Gordon DL, Sajkov D, Honda-Okubo Y, Wilks SH, Aban M, Barr IG, et al. Human Phase 1 trial of low-dose inactivated seasonal influenza vaccine formulated with Advax™ delta inulin adjuvant. Vaccine. 2016;34(33):3780-6.

261. Hess JA, Zhan B, Torigian AR, Patton JB, Petrovsky N, Zhan T, et al. The Immunomodulatory Role of Adjuvants in Vaccines Formulated with the Recombinant Antigens Ov-103 and Ov-RAL-2 against Onchocerca volvulus in Mice. PLOS Neglected Tropical Diseases. 2016;10(7):e0004797.

262. Healy CM, Rench MA, Baker CJ. Importance of timing of maternal combined tetanus, diphtheria, and acellular pertussis (Tdap) immunization and protection of young infants. Clinical infectious diseases : an official publication of the Infectious Diseases Society of America. 2013;56(4):539-44.

263. Kachikis A, Eckert LO, Englund J. Who's the Target: Mother or Baby? Viral Immunol. 2018;31(2):184-94.

264. Munoz FM, Bond NH, Maccato M, Pinell P, Hammill HA, Swamy GK, et al. Safety and immunogenicity of tetanus diphtheria and acellular pertussis (Tdap) immunization during pregnancy in mothers and infants: a randomized clinical trial. JAMA. 2014;311(17):1760-9.

265. Weibel RE, J. Stokes J, Mascoli CC, Leagus MB, Woodhour AF, Tytell AA, et al. Respiratory Virus Vaccines. American Review of Respiratory Disease. 1967;96(4):724-39.

266. Chin J, Magoffin RL, Shearer LA, Schieble JH, Lennette EH. Field evaluation of a respiratory syncytial virus vaccine and a trivalent parainfluenza virus vaccine in a pediatric population. Am J Epidemiol. 1969;89(4):449-63.

267. Lee Y-T, Kim K-H, Hwang HS, Lee Y, Kwon Y-M, Ko E-J, et al. Innate and adaptive cellular phenotypes contributing to pulmonary disease in mice after respiratory syncytial virus immunization and infection. Virology. 2015;485:36-46.

268. Prince GA, Curtis SJ, Yim KC, Porter DD. Vaccine-enhanced respiratory syncytial virus disease in cotton rats following immunization with Lot 100 or a newly prepared reference vaccine. Journal of General Virology. 2001;82(12):2881-8.

269. Jans J, Vissers M, Heldens JGM, de Jonge MI, Levy O, Ferwerda G. FC GAMMA RECEPTORS IN RESPIRATORY SYNCYTIAL VIRUS INFECTIONS: IMPLICATIONS FOR INNATE IMMUNITY. Reviews in medical virology. 2014;24(1):55-70.

270. Fu B, Wang F, Sun R, Ling B, Tian Z, Wei H. CD11b and CD27 reflect distinct population and functional specialization in human natural killer cells. Immunology. 2011;133(3):350-9.

271. Romee R, Foley B, Lenvik T, Wang Y, Zhang B, Ankarlo D, et al. NK cell CD16 surface expression and function is regulated by a disintegrin and metalloprotease-17 (ADAM17). Blood. 2013;121(18):3599.

272. Peruzzi G, Femnou L, Gil-Krzewska A, Borrego F, Weck J, Krzewski K, et al. Membrane-Type 6 Matrix Metalloproteinase Regulates the Activation-Induced Downmodulation of CD16 in Human Primary NK Cells. The Journal of Immunology. 2013;191(4):1883.

273. Goodier MR, Lusa C, Sherratt S, Rodriguez-Galan A, Behrens R, Riley EM. Sustained Immune Complex-Mediated Reduction in CD16 Expression after Vaccination Regulates NK Cell Function. Front Immunol. 2016;7:384.

274. Guilliams M, Bruhns P, Saeys Y, Hammad H, Lambrecht BN. The function of Fcgamma receptors in dendritic cells and macrophages. Nature reviews Immunology. 2014;14(2):94-108.

275. Schuurhuis DH, Ioan-Facsinay A, Nagelkerken B, van Schip JJ, Sedlik C, Melief CJ, et al. Antigen-antibody immune complexes empower dendritic cells to efficiently prime specific CD8+ CTL responses in vivo. J Immunol. 2002;168(5):2240-6.

276. Bjorck P, Beilhack A, Herman EI, Negrin RS, Engleman EG. Plasmacytoid dendritic cells take up opsonized antigen leading to CD4+ and CD8+ T cell activation in vivo. J Immunol. 2008;181(6):3811-7.

277. Walsh EE, Falsey AR. Age related differences in humoral immune response to respiratory syncytial virus infection in adults. J Med Virol. 2004;73(2):295-9.

278. Walsh EE, Falsey AR. Humoral and mucosal immunity in protection from natural respiratory syncytial virus infection in adults. The Journal of infectious diseases. 2004;190(2):373-8.

279. Piedra PA, Jewell AM, Cron SG, Atmar RL, Glezen WP. Correlates of immunity to respiratory syncytial virus (RSV) associated-hospitalization: establishment of minimum protective threshold levels of serum neutralizing antibodies. Vaccine. 2003;21(24):3479-82.

280. Falsey AR, Singh HK, Walsh EE. Serum antibody decay in adults following natural respiratory syncytial virus infection. Journal of Medical Virology. 2006;78(11):1493-7.

281. Hall CB, Walsh EE, Long CE, Schnabel KC. Immunity to and frequency of reinfection with respiratory syncytial virus. The Journal of infectious diseases. 1991;163(4):693-8.

282. Griffin MP, Khan AA, Esser MT, Jensen K, Takas T, Kankam MK, et al. Safety, Tolerability, and Pharmacokinetics of MEDI8897, the Respiratory Syncytial Virus Prefusion F-Targeting Monoclonal Antibody with an Extended Half-Life, in Healthy Adults. Antimicrobial Agents and Chemotherapy. 2017;61(3).

283. Mazur NI, Horsley N, Englund JA, Nederend M, Magaret A, Kumar A, et al. Breast milk prefusion F IgG as a correlate of protection against respiratory syncytial virus acute respiratory illness. The Journal of infectious diseases. 2018.

284. Englund JA. Passive protection against respiratory syncytial virus disease in infants: the role of maternal antibody. The Pediatric infectious disease journal. 1994;13(5):449-53.

285. Schneider-Ohrum K, Cayatte C, Bennett AS, Rajani GM, McTamney P, Nacel K, et al. Immunization with Low Doses of Recombinant Postfusion or Prefusion Respiratory Syncytial Virus F Primes for Vaccine-Enhanced Disease in the Cotton Rat Model Independently of the Presence of a Th1-Biasing (GLA-SE) or Th2-Biasing (Alum) Adjuvant. J Virol. 2017;91(8).

286. Wong TM, Petrovsky N, Bissel SJ, Wiley CA, Ross TM. Delta inulin-derived adjuvants that elicit Th1 phenotype following vaccination reduces respiratory syncytial virus lung titers without a reduction in lung immunopathology. Hum Vaccin Immunother. 2016;12(8):2096-105.

287. Tanaka H, Komai M, Nagao K, Ishizaki M, Kajiwara D, Takatsu K, et al. Role of Interleukin-5 and Eosinophils in Allergen-Induced Airway Remodeling in Mice. American Journal of Respiratory Cell and Molecular Biology. 2004;31(1):62-8.

288. Lopez AF, Sanderson CJ, Gamble JR, Campbell HD, Young IG, Vadas MA. Recombinant human interleukin 5 is a selective activator of human eosinophil function. The Journal of experimental medicine. 1988;167(1):219-24.

289. Humbles AA, Lloyd CM, McMillan SJ, Friend DS, Xanthou G, McKenna EE, et al. A Critical Role for Eosinophils in Allergic Airways Remodeling. Science. 2004;305(5691):1776.

290. Bagnasco D, Ferrando M, Varricchi G, Puggioni F, Passalacqua G, Canonica GW. Anti-Interleukin 5 (IL-5) and IL-5Ra Biological Drugs: Efficacy, Safety, and Future Perspectives in Severe Eosinophilic Asthma. Frontiers in Medicine. 2017;4(135).

291. Flood-Page P, Swenson C, Faiferman I, Matthews J, Williams M, Brannick L, et al. A study to evaluate safety and efficacy of mepolizumab in patients with moderate persistent asthma. Am J Respir Crit Care Med. 2007;176(11):1062-71.

292. Rothenberg ME, Owen WF, Jr., Silberstein DS, Woods J, Soberman RJ, Austen KF, et al. Human eosinophils have prolonged survival, enhanced functional properties, and become hypodense when exposed to human interleukin 3. J Clin Invest. 1988;81(6):1986-92.

293. Lopez AF, Williamson DJ, Gamble JR, Begley CG, Harlan JM, Klebanoff SJ, et al. Recombinant human granulocyte-macrophage colony-stimulating factor stimulates in vitro mature human neutrophil and eosinophil function, surface receptor expression, and survival. J Clin Invest. 1986;78(5):1220-8.

294. Wills-Karp M, Luyimbazi J, Xu X, Schofield B, Neben TY, Karp CL, et al. Interleukin-13: central mediator of allergic asthma. Science. 1998;282(5397):2258-61.

295. Stevens WW, Sun J, Castillo JP, Braciale TJ. Pulmonary Eosinophilia Is Attenuated by Early Responding CD8(+) Memory T Cells in a Murine Model of RSV Vaccine-Enhanced Disease. Viral Immunology. 2009;22(4):243-51.

296. Higgins D, Trujillo C, Keech C. Advances in RSV vaccine research and development - A global agenda. Vaccine. 2016;34(26):2870-5.

297. Stevens WW, Falsey AR, Braciale TJ. RSV 2007: recent advances in respiratory syncytial virus research. Viral Immunol. 2008;21(2):133-40.

298. Meissner HC, Rennels MB, Pickering LK, Hall CB. Risk of severe respiratory syncytial virus disease, identification of high risk infants and recommendations for prophylaxis with palivizumab. The Pediatric infectious disease journal. 2004;23(3):284-5.

299. Levy O. Innate immunity of the human newborn: distinct cytokine responses to LPS and other Toll-like receptor agonists. Journal of endotoxin research. 2005;11(2):113-6.

300. Rittirsch D, Flierl MA, Day DE, Nadeau BA, Zetoune FS, Sarma JV, et al. Cross-Talk between TLR4 and FcγReceptorIII (CD16) Pathways. PLOS Pathogens. 2009;5(6):e1000464.

301. Karsten CM, Pandey MK, Figge J, Kilchenstein R, Taylor PR, Rosas M, et al. Anti-inflammatory activity of IgG1 mediated by Fc galactosylation and association of FcγRIIB and dectin-1. Nature medicine. 2012;18:1401.

302. Yao Y, Jeyanathan M, Haddadi S, Barra NG, Vaseghi-Shanjani M, Damjanovic D, et al. Induction of Autonomous Memory Alveolar Macrophages Requires T Cell Help and Is Critical to Trained Immunity. Cell. 2018;175(6):1634-50.e17.